CHARACTERISATION OF LIGHTWEIGHT STAIRS AS STRUCTURE-BORNE SOUND SOURCES

Thesis submitted in accordance with the requirements of the University of Liverpool for the degree of Doctor of Philosophy

by

Jochen Martin Scheck

June 2011

ABSTRACT

CHARACTERISATION OF LIGHTWEIGHT STAIRS AS STRUCTURE-BORNE SOUND SOURCES

by

Jochen Martin Scheck

The work reported in this thesis addresses the problem of structure-borne sound transmission from impacts on lightweight stairs. The primary aim was to provide a laboratory method for characterisation of lightweight stairs as structure-borne sound sources, which will give input data for prediction of the sound transmission in heavyweight building situations. By treating the stair system, combined with impact source(s), as an active component, available methods for active sources could be adapted. The component powers of a timber staircase attached to a solid wall in a staircase test facility have been determined in-situ by use of a reciprocal method. It was shown that the force perpendicular to the wall surface is dominant, moments can be neglected. The force induced power can be predicted from contact free velocity and mobility or by the blocked force as stairs constitute high mobility sources in heavyweight buildings. A practical characterisation is proposed that is based on the reception plate method. It is demonstrated that real walls and floors can be used as reception plates along with a power calibration that circumvents problems in estimating the plate mass, mean squared velocity and total loss factor for non-isolated reception plates. The sound transmission is predicted using EN 12354 and it is confirmed that the prediction gives values within acceptable engineering accuracy. A deterministic model that accounts for the modal coupling of structure and room is used to predict the sound transmission at low frequencies. For the case considered, a major difficulty was found in the modelling of the wall vibration field, mainly due to the boundary conditions that do not correspond to idealised conditions, such as pinned or free edges.

ACKNOWLEDGEMENTS

I wish to express my sincere gratitude to Prof. Barry Gibbs and to Prof. Heinz-Martin Fischer who enabled this thesis study, took me through the work with encouragement, guidance and criticism and most important, personal kindness and trust in my capabilities to finish this work. They were much more than supervisors during the past years and I will always be grateful.

I am also grateful to the working group of TC 126, WG 7 for valuable discussions and constructive suggestions that gave a strong motivation.

Big thanks go to my colleagues in Stuttgart, Andreas Drechsler, Andreas Mayr, Martin Schneider, Thomas Alber, Christoph Fichtel, Roland Kurz, Thomas Möck, Moritz Späh, Emre Taskan, Robert Marin and Andreas Ruff who always gave help and support in a very enjoyable atmosphere. In particular Andreas Mayr offered a lot to share and the many fruitful discussions we had made the work even more enjoyable.

Thanks to Dr. Carl Hopkins and Dr. Gary Seiffert at the ARU of The University of Liverpool, who contributed to this work with knowledge, help and humour.

Thanks to all members of the international acoustic community, Stefan Schönwald, Albano Sousa, Matthew Robinson, Andy Elliot, Tomos Evans, Matthias Lievens (and many others) for valuable discussions and good times at congresses.

Also the support by Roland and Thomas Köcher from Treppenmeister GmbH and in particular Heinz Lammers and Gabi Brenner for realising the experimental set-ups in the staircase test facility is gratefully acknowledged.

Very special thanks go to Eva, the love of my life, my parents and all my friends.

CONTENTS

LIST OF SYMBOLS

GENERAL

A	Equivalent absorption area [m^2]
A_0	Reference absorption area; $A_0 = 10\,m^2$
A_{ref}	Reference equivalent absorption area; $A_{ref} = 10\,m^2$
C	Spectrum adaptation term
C_{tr}	Spectrum adaptation term for traffic noise
$\overline{C}_f$	Coupling function [-]
$D_{s,a,i}$	Adjustment term from structure-borne to airborne excitation for supporting building element i [dB]
E	Young's modulus of elasticity [N/m²]
E	Energy [J]
F	Force [N]
F_b	Blocked force [N]
$\tilde{F}^2$	Mean square force [N^2]
HMS	High mobility source
L	Sound pressure level from tapping machine excitation [dB re $2x10^{-5}$ Pa]
L_1	Sound pressure level in sending room [dB re $2x10^{-5}$ Pa]
L_2	Sound pressure level in sending room [dB re $2x10^{-5}$ Pa]
L_F	Force level [dB re 10^{-6} N]
L_n	Normalized impact sound pressure level [dB re $2x10^{-5}$ Pa]
$L_{n,v}$	Normalized impact sound pressure level from measurement of the spatial average velocity [dB re $2x10^{-5}$ Pa]

L_{ij}	Length of junction [m]
$L_{n,s,ij}$	Normalized sound pressure level in the receiving room due to a structure-borne sound source mounted to supporting building element i in the source room caused by sound transmission from element i to a radiating element j in the receiving room [dB re $2x10^{-5}$ Pa]
$L_{W,i,s}$	Installed structure-borne sound power level of the source at supporting element i [dB re 10^{-12} W]
ΔL_P	Difference in power level [dB]
LMS	Low mobility source
M	Moment [Nm]
P	Real part of power [W]
$P_{\text{rec.}}$	Reception plate power [W]
P_{infinite}	Infinite plate power [W]
R	Sound reduction index [dB]
R_w	Weighted sound reduction index [dB]
$R_w^{'}$	Weighted sound reduction index including flanking transmission [dB]
$R_{\text{i j,ref}}$	Flanking sound reduction index for transmission from element i in the source room to element j in the receiving room, with reference to the area, $S_{ref} = 10\ \text{m}^2$
S	Surface area [m²]
S_c	Source descriptor [W]
S_{i}	Area of the supporting building element i in the source room [m^2]
T_s	Structural reverberation time [s]

V	Volume [m^3]
W	Complex power [W]
Y	Mobility [m/Ns]
$Y_{rec.}$	Point mobility of reception plate [m/Ns]
$Y_{infinite}$	Infinite plate mobility [m/Ns]
$\overline{Y}_{rec.}$	Spatial average point mobility of reception plate [m/Ns]
$\overline{Y}_{build.}$	Spatial average point mobility of building element [m/Ns]
a	Acceleration [m/s^2]
c_0	Wave speed in air [m/s]
c_B	Bending wave speed [m/s]
c_L	Longitudinal wave speed [m/s]
f	Frequency [Hz]
h	Thickness [m]
j	Complex operator (j=$\sqrt{-1}$)
m	Mass of plate [kg]
m'	Surface mass [kg/m^2]
p	Sound pressure [Pa]
s	Standard deviation [dB]
v	Velocity [m/s]
$\overline{v}^2$	Spatial averaged mean square velocity [m^2/s^2]
v_{sf}	Source free velocity [m/s]
w	Angular velocity [rad/s]

α	Absorption coefficient [-]
η	Loss factor [-]
η_{ij}	Coupling loss factor from subsystem I to subsystem j [-]
μ	Poisson's ratio [-]
ρ	Density [kg/m³]
ρ_0	Density of air [kg/m^3]
σ	Radiation Efficiency [-]
τ	Transmission loss [-]
φ	Velocity transfer function [-]
ω	Angular frequency [rad/s]; $\omega = 2\pi f$
$\mathrm{Re}\{\ \}$	Real part of complex quantity
$\mathrm{Im}\{\ \}$	Imaginary part of complex quantity
$[\ ]$	Matrix
$\{\ \}$	Vector
$\lvert\ \rvert$	Magnitude
$\sum$	Sum operator

SUPER / SUBSCRIPTS

B	Bending
e	Excitation position
F	Force
M	Moment
R	Receiver
r	Response position
S	Source
i, j	Points
n, m	Components
t	Time
x	X-axis
y	Y-axis
z	Z-axis
*	Complex conjugate
T	Complex transpose

1 INTRODUCTION

1.1 BACKGROUND TO THE STUDY

Noise from sources like washing machines, fans, pumps, whirlpools, water installations and domestic appliances that is transmitted to other rooms in buildings is an increasing problem. In general, the number of structure-borne sound sources is steadily increasing, due to mechanical automatization of buildings. In many cases the dominant transmission path is structure-borne and these kinds of sources are termed vibro-acoustic as the perceived noise is initially caused by vibrations of the source. The resultant noise often has significant low frequency components, which are transmitted more efficiently than high frequency components. Passive building elements, such as lightweight stair systems, become active when excited by footfalls and thus can be considered in the same way as vibrating machines. The topic of this thesis study is such stair systems and how they transmit structure-borne sound power to supporting walls and on into adjacent rooms.

For the prediction of the airborne and impact sound transmission, standard models have been developed for heavyweight buildings [1], [2]. Recently, a part has been added for prediction of the structure-borne sound transmission [3]. The models are largely based on Statistical Energy Analysis (SEA) [4] and require the source strength as input data.

Analogous to the characterisation of airborne sound sources, where the source strength is represented by the airborne sound power, a structure-borne sound power is proposed for the characterisation of structure-borne sound sources and to serve as input data for prediction models.

The process of structure-borne sound transmission is more complicated than airborne sound transmission since the power transmission is a function of both source and receiver quantities. For the source, the quantities involve a measure of the activity and structural dynamics; for the receiver, the structural dynamics. Therefore, three quantities may be required, compared with one quantity for airborne sources. Calculations are complicated and data acquisition is more intensive as it requires elaborate experimental set-ups and measurement techniques. Exact methods for the characterisation of structure-borne sound sources have been proposed in previous years, e.g. [5]-[8]. Based on these methods, attempts have been made towards simplifications in order to provide practical methods of measurement and prediction

Recently a test procedure, termed the reception plate method, has been proposed [9]. The method is based on a power balance such that the power of the source under test can be obtained indirectly by measurement of the energy conserved in the plate and the power losses. The method has been successfully applied for the case of machines in heavyweight buildings where the source mobility is much greater than the receiver mobility [9], [10].

The structure-borne sound sources so far considered are small-sized active sources that generate vibrations due to an internal excitation mechanism. The kinds of sources that are addressed in this thesis are lightweight stairs that are actually passive building components that become active due to excitation by people walking on the stairs. The primary activity of this thesis study was to provide a laboratory method for characterisation of lightweight stairs as structure-borne sound sources which will give input data for prediction of the sound transmission in heavyweight building situations.

1.2 STATEMENT OF THE PROBLEM

Lightweight stairs are situated in multi-storey houses, apartment blocks and row houses. Often, the stairs are mounted on the separating walls in dwellings, which in most cases are heavyweight single- or double-leaf constructions. The impact noise transmission from people walking on stairs is a recognised problem [11]-[13]. However, at present there are no validated methods available to predict this form of sound transmission.

There are three challenges in seeking a structure-borne sound source characterisation for lightweight stairs. First, methods for a proper source characterisation are required. Stairs are passive structures that become active due to excitation by people walking on the stairs or due to impacts from standardised sources like the ISO tapping machine [14]. A characterisation must consider both the dynamic characteristics of the stairs and the characteristics of the (external) impact source.

Secondly, the impact sound transmission from vibrating stairs through the wall connections involves multiple contacts and degrees of freedoms. As each contact forms a lever, moment excitation is expected to be significant.

Thirdly, the impact sound transmission of lightweight stairs is expected to be significant at low frequencies (about 40 to 200 Hz) [11]-[13] where structures and rooms exhibit modal behaviour. Specific attention has to be given to the modal characteristics of both the partition wall and the receiving room.

1.3 AIMS OF THE STUDY

Manufacturers of lightweight stairs need a tool for the comparison of the acoustic quality of their products which will indicate the noisiness of a stair system when installed in a building. Noise control engineers require a method for the prediction of sound pressure levels of lightweight stairs in buildings in order to fulfil requirements regarding impact sound insulation. Thus a characterization of lightweight stairs as structure-borne sound sources with respect to a given impact excitation is needed. The method should be physically correct and preferably simple, giving reliable data within engineering accuracy that can be used as input data for prediction models.

1.4 METHODOLOGY

The stair system, with impact source(s), is treated as an active component, in a similar manner to that used for common sources of structure-borne sound like vibrating machines. The adaption of available methods for the characterisation is investigated on a common lightweight stair system situated in a staircase test facility.

The structure-borne power transmission from the excited stair to the supporting wall is investigated in-situ to establish the dominant components of excitation at the contacts, including forces perpendicular to the receiving surface and moments about axes parallel to the surface. One contact with the wall is considered, with the stair otherwise supported at the top and bottom on resilient layers.

The free velocities and mobilities at the stair contact point are measured with the stair separate from the building. Various impact sources are considered.

The stair wall is then treated as a reception plate and methods for a simplified characterisation are investigated.

Characteristic source quantities from the above methods are then used as input data for prediction models and compared with measured sound pressure levels.

1.5 THESIS OVERVIEW

This study commences in Chapter 2 by reviewing the theory of structure-borne sound transmission at the source and receiver interface. Previous approaches of characterising structure-borne sound sources are reviewed and underlying requirements are discussed.

In Chapter 3, lightweight stair systems are described, in particular a prefabricated wooden stair, used for this investigation. The environment for the investigation, a special staircase test facility is described. Preliminary results are reported and the vibration behaviour of the stair is investigated by means of experimental modal analysis.

In Chapter 4, a reciprocal method is investigated for the identification of the dominant components of excitation. The method is experimentally validated for the excitation of both an isolated reception plate and a stair wall. The problem of cross-coupling of components is discussed.

The dominant components of excitation at the stair/wall contact are identified in Chapter 5 for both a shaker source and a standard tapping machine, exciting the stair.

In Chapter 6, the independent characterisation of the vibrating stair by free velocity and mobility is described and validated by comparison with the in-situ measurement of the power transmission.

In Chapter 7, methods, using reception plates, are investigated. The steady-state power into walls and floors is analysed by means of a simplified

Statistical Energy Analysis (SEA) model. A transient SEA model is used to quantify the effect of energy flow between coupled plates on the loss factor measurement. Finally a power substitution method is proposed for the characterisation of sources when connected to non-isolated receiver plates.

In Chapter 8 building propagation models such as EN 12354 [1]-[2] and a modal approach [15] are used to predict sound pressure levels from impacted stairs. It is shown how laboratory data as obtained from the previous investigations can be transformed for such predictions. By comparison of predicted and measured impact sound pressure levels, the achievable accuracy is assessed and sources of uncertainty are highlighted.

Finally the main results of this study are summarised, concluding remarks are given and suggestions for further work are presented in Chapter 9.

1.6 REFERENCES

[1] EN 12354-1: Building acoustics – Estimation of acoustic performance of buildings from the performance of elements – Part 1: Airborne sound insulation between rooms, September 2000

[2] EN 12354-2: Building acoustics – Estimation of acoustic performance of buildings from the performance of elements – Part 2: Impact sound insulation between rooms, September 2000

[3] EN 12354-5: Building acoustics – Estimation of acoustic performance of buildings from the performance of elements – Part 5: Sounds levels due to the service equipment, October 2009

[4] Craik R. J. M.: Sound Transmission Through Buildings using Statistical Energy Analysis, Gower Publishing Limited, 1996

[5] Gibbs B. M., Petersson B. A. T.: Measurement and Characterisation of sources of structure-borne sound, Proceedings Internoise 1996, 1307-1312, 1996

[6] Petersson B. A. T., Gibbs B. M.: Towards a structure-borne sound source characterization, Applied Acoustics, Vol. 61 (3), 325-343, 2000

[7] Moorhouse A. T.: On the characteristic power of structure-borne sound sources, Journal of Sound and Vibration, Vol. 248 (3), 441-459, 2001

[8] Gibbs B. M., Qi N., Moorhouse A. T.: A practical characterisation for vibro-acoustic sources in buildings, Acta Acustica united with Acustica, Vol. 93 (1), 84-93, 2007

[9] Späh M. M, Gibbs B. M.: Reception plate method for characterisation of structure-borne sound sources in buildings: Assumptions and application, Applied Acoustics, Vol. 70 (2), 361-368, 2009

[10] Mayr A. R., Gibbs B. M., Fischer H.-M.: Consideration of vibration sources in buildings on a power basis, Proceedings ICSV13, Vienna, 2006

[11] Ertl, H.: Zur Verbesserung des Schallschutzes an Leichtbautreppen (On the improvement of the sound insulation of lightweight stairs), FBW Blätter, 1985

[12] Savage, J. E., Fothergill, L. C.: Reduction of noise nuisance from footsteps on stairs, Applied Acoustics, Volume 27 (2), 147-152, 1989

[13] Kurz, R., Schnelle, F.: Schallschutz von Montagetreppen (Sound insulation of assembled stairs), Fortschritte der Akustik, DAGA, Oldenburg, 2000

[14] EN ISO 140-7: Acoustics – measurement of sound insulation in buildings and of building elements. Part 7: field measurements of impact sound insulation of floors, December 1998

[15] Neves e Sousa, A.; Gibbs, B. M.: Low frequency impact sound transmission in dwellings through homogeneous concrete floors and floating floors, Applied Acoustics, Vol. 72, 177-189, 2011

2 BACKGROUND THEORY

2.1 INTRODUCTION

In this chapter the dynamic characteristics of a vibrating source into a receiver structure, required for complete evaluation of structure-borne sound power transmission, are described. Whilst the theory and approaches described have been applied to mechanical and water services in building, it will be shown that impacted lightweight stairs can be treated in the same way. The complexity of structure-borne sound transmission, especially when considering several components of excitation at each contact, is addressed. This leads to the identification of the quantities required for a complete source characterisation for stair systems.

Existing methods of source characterisation are described, with an emphasis on possible simplifications that may be required by building engineers and manufacturers. The application and limitations of such methods are described.

Special consideration is given to a reception plate method [1], which provides input data for a structure-borne sound propagation model for heavyweight buildings [2].

This points to methods for characterising impacted stairs as sound sources on a power basis and in particular to the development of laboratory methods which yield data transformable to predictions of resultant sound pressure in adjacent rooms.

2.1.1 Mobility

The vibrational response of a structure due to mechanical excitation is usually and throughout this thesis assumed linear which means that the ratio between response and excitation is independent of the strength of excitation.

Consider a force at one point, in one direction, and the structural response velocity at the same point and in the same direction. The complex ratio of velocity to force is termed force (driving) point mobility, usually referred to as point mobility [3].

$$Y_{v,F} = \frac{v}{F} \tag{2.1}$$

The inverse of the mobility is termed impedance. Mechanical mobility and impedance methods have been used for many years to study structural dynamics. A comprehensive overview on the origin in the field of electricity and development of mobility and impedance methods in structural dynamics is given in [4].

Structure-borne sound power transmission also results from moment excitation. The complex ratio of angular velocity to the applied moment is termed moment (driving) point mobility, usually referred to as moment mobility [3].

$$Y_{w,M} = \frac{w}{M} \tag{2.2}$$

In cases where the response position j differs from the excitation position i, the term transfer mobility is used and denoted by Y_{ij}. Additional superscripts describe the direction of excitation m and response n. Thus, a point mobility is denoted by Y_{ii}^{mm}, a cross-transfer mobility by Y_{ij}^{mn}. An example of cross-transfer mobility is an angular velocity at a remote position caused by a force excitation.

Mobility is in general a complex frequency dependent value, and depends on material properties, geometry, boundary conditions, and damping of the structure. Analytical formulae of the mobility of beams and plates are given in [5]. Semi-analytical approaches for plates with different boundary conditions are given in [6].

For more complicated structures, numerical methods, like the Finite Element Method (FEM), are used [7]. For such methods, detailed knowledge of the boundary conditions is required, which is not always available. Measurement is therefore the most reliable method in determination of mobilities.

Comprehensive studies on machine (source) mobilities have been reported in [8]-[11]. Accordingly, machine bases can be characterised as compact rigid sources, plate bases and flanged bases or as frames. At very low frequencies the mobility of all sources is mass controlled, followed by a stiffness controlled region up to the fundamental resonance. Above the fundamental resonance the mobility is resonance controlled. At higher frequencies the mobility tends towards the mobility of infinite or semi-infinite systems [3].

The transition frequencies, defining the frequency range for each form of behaviour are determined by the source structure's configuration. Also the magnitude of the mobility will be different for different source structures. It will be demonstrated later that, for timber stair systems, the primary region of interest, concerning the source, is resonance controlled.

2.1.2 Free velocity and blocked force

When in operation, mechanical installations generate vibrations which are caused by internal mechanisms such as rotations, pressure variations impacts or friction. The vibrations within the source are transmitted to the contact points with the receiver. For the case of timber stair systems, the internal mechanisms are human footfalls, which are time and spatially variant or standard impact sources, which can be treated as quasi-stationary sources at a known location. For both stairs and mechanical installations, measurement of the internal mechanisms is difficult or even impossible, since there can be multiple generating components within the source structure. Under the assumption that the excitation is linear and that internal mechanisms are unaffected by the actual contact conditions, the source can be regarded as a "black box" [13]. A description of the activity or strength of a source by measuring its collective response at the contacts as either the free velocity or the blocked force is straightforward. Free velocity and blocked force are related by the source mobility [14]:

$$F_b = \frac{v_{sf}}{Y_s} \tag{2.3}$$

The free velocity at the contacts is measured when the source is not connected to receiver structures, but otherwise is operating under normal conditions. For small and lightweight machines, the free velocity can be measured with the source elastically suspended. For large machines, it is practical to support them by elastic interlayers on sufficiently stiff foundations and measure the free velocity in-situ. Above the mass-spring resonance frequency of the isolation, the measured velocity approximates the free velocity [16]. Measurements procedures are described in [17].

For measurement of the blocked force, the source is connected to an inert receiver via force transducers. In general, the measurement of the blocked force is more difficult than the measurement of the free velocity. Insertion of force transducers can alter the normal mounting conditions whereas mounting of accelerometers is in general unproblematic.

There are however potential difficulties in ensuring normal operating conditions, when measuring free velocity. For machines, it can be difficult to reproduce operational load conditions (through drive belts, gears and other power trains) in the laboratory. Likewise, people, running up and down a resiliently isolated stair, may encounter problems.

2.1.3 Structure borne sound power

For the transmission process between source and receiver, the quantity of prime interest is the complex power. The term power represents the energy flow from a vibrating source through the contact points into the connected receiving structure. If the transmission is expressed on a power basis, then

the relative importance of force and moment excitation can be assessed as the problem of dimensional incompatibility is overcome. A source characterisation on a power basis allows structure-borne sound power to be directly compared with airborne sound power. For these reasons power is increasingly recognised as the appropriate quantity for source characterisation [13].

2.1.4 Contacts with single degree of freedom

For a single contact, single translational motion system, with harmonic force excitation, the complex power is given by the product of the injected force and the resulting velocity at the contact point [3]:

$$W = \frac{1}{2} F^* \cdot v \tag{2.4}$$

For moment excitation:

$$W = \frac{1}{2} M^* \cdot w \tag{2.5}$$

* denotes the complex conjugate.

The real part of the complex power $P = \mathrm{Re}\{W\}$ is usually termed the (net) active power as it is carried by waves which propagate into the receiver structure(s) and radiate to ambient systems such as fluid spaces. The imaginary part of the complex power is termed the reactive power that forms a near-field kinetic energy, which flows to and from the receiver over alternate quarter cycles of the oscillation, such that there is no net energy

flow over a cycle [3]. It does not give rise to noise problems but can contribute to material fatigue and mechanical damage near the contact locations.

The power introduced into a receiving structure can be expressed in terms of the dynamics of source and receiver structure [14], [15]:

$$W = \frac{1}{2} \frac{\left| v_{sf} \right|^2}{\left| Y_S + Y_R \right|^2} Y_R \tag{2.6}$$

With $\overline{v}_{sf}$ the complex source free velocity Y_S , Y_R the complex source and receiver mobility, respectively.

For two extreme conditions, (2.6) can be simplified, namely the so-called constant force and constant velocity source idealizations. If the mobility of the source is very high i.e. $\left| Y_S \right| >> \left| Y_R \right|$ then the power is given by:

$$W = \frac{1}{2} \frac{\left| v_{sf} \right|^2}{\left| Y_S \right|^2} Y_R \tag{2.7}$$

This is termed the force source idealisation, as $F_b = \frac{v_{sf}}{Y_s}$ is the blocked force (2.3). The single quantity is independent of the receiver mobility and relates to the source only. The installed power then is determined by the receiver mobility. This situation often occurs in heavyweight buildings.

To avoid confusion when discussing the relationship between forces and moments, the terminology high mobility source is preferred, rather than force source.

If the mobility of the source is very small i.e. $|Y_S| << |Y_R|$ then the power is given by:

$$W = \frac{1}{2} \frac{|v_{sf}|^2}{|Y_R|^2} Y_R \tag{2.8}$$

The source imposes a velocity at the attached structure which is unaffected by the structural dynamics of the receiver and therefore only this quantity is required to fully characterise the source. Therefore this case is often termed the velocity source idealisation. However, the term low mobility source is preferred. This situation has been shown to occur in lightweight buildings [18], [19].

In addition to the idealised situations, a matched mobility condition can occur [20] which is discussed in more detail in section 2.2.5.

2.1.5 Multi-point and multi-component sources

The case of single-point and single component excitation is rarely encountered in practice. For each contact up to 6 degrees of freedom, 3 translational and 3 rotational components in three directions, can contribute to the transmission. In addition, interactions between the translational and rotational components are possible.

For the evaluation of the total power, a full description of source free velocity and mobility, together with the receiver mobility, is required. The general

expression of the complex power for multi-point connections with multi component excitation is given e.g. by [13]:

$$W = \frac{1}{2}\{v_{sf}\}^T \left[Y_S + Y_R\right]^{-1^T} \left[Y_R\right]^T \left[Y_S^* + Y_R^*\right]^{-1} \{v_{sf}\}^* \qquad (2.9)$$

^{T} denotes the transpose.

Equation (2.9) represents the matrix formulation, based on the single point, single component expression in (2.6). The total power is obtained by summation of the complex products of forces and moments and their associated translational and rotational response. If a source has *N* contacts and *M* components of excitation (where *M* is less than or equal to 6), the source data contains *MN* frequency dependent free velocity spectra and (*MN* x *MN*) source mobility spectra.

Likewise, the full description of the receiver structure requires (*MN* x *MN*) mobility spectra. The necessary total number of spectra of each mobility matrix can be reduced by invoking reciprocity [22]. The principle of reciprocity is that, for a linear and passive system, the transfer functions between different contacts are equal, when the position and direction or components of excitation are interchanged [23]. Accordingly, the mobility matrices are symmetrical about the leading diagonal.

It will be shown later that although lightweight stairs, connected to party walls, can be treated as single point sources, it is still necessary to initially consider more than one component of excitation.

2.2 METHODS FOR SOURCE CHARACTERISATION

A practical source characterisation should allow the following [20], [22]:

- Comparison of different sources
- Comparison of sources within set limits
- Quantification of improvement of low noise source designs
- Provision of data for building propagation models

Ideally, a source characterisation yields an independent measure of the source strength, as a single frequency dependent value that can be used to predict the installed structure-borne sound power in buildings. Any simplification on the source characterisation is likely to lead to inaccuracies, which however, may not be excessively large. A suitable method must offer an acceptable trade off between simplicity and accuracy.

In [22] seven possible methods for structure-borne sound source characterisation are discussed. Not all of them conform to the requirements given above or are relevant to the case study reported in this thesis. The most developed proposals are described briefly in the following.

2.2.1 Standard building situation

The standard building situation method was proposed in the early nineties [24]. More recent information can be found e.g. in [25]. The method has been developed for acoustical testing of water supply and waste water installations according to EN ISO 3822 [26] and EN 14366 [27]. It involves a standard building in which the source under test is mounted on the

separating wall of two adjoining rooms. With the source in operation the sound pressure is measured in the receiver room.

A comparison and ranking of different sources is straightforward. It appears to offer a way forward for testing stair systems, one reason being that stairs generally are viewed as integral parts of buildings. However, the rank order might be different with the same source installed in a different building and one defined building situation will not be representative of the whole range possible. In addition, the normalised sound pressure levels in the standard building are not likely to be the same in real buildings and therefore comparisons with legal requirements become tenuous. A source which meets certain legal requirements in the laboratory might fail in the installed condition. Although the procedure yields a single frequency dependent value, the data cannot be used for prediction models.

For the present study, the question of economic cost was raised by industrial collaborators. A dedicated test building was considered less attractive than a smaller and more flexible test space, which could be incorporated into a general work area.

2.2.2 Free velocity

As outlined in section 2.1.2 the source free velocity can be measured without much difficulty but forms only a subset of the necessary data, as prediction of the power transmission also requires the source mobility in the general case (2.6). In addition the free velocity is not a singular-value when several contacts and components of excitation are considered. Whilst it

provides a full source description for the low mobility source condition, described in section 2.1.4, this installation situation seldom if ever occurs in buildings [18], [19]. However, free velocity data was acquired and used throughout this study.

2.2.3 Blocked force

The blocked force provides a full source description for the high mobility source condition described in 2.1.4 provided that there is no contribution of moments. In EN 12354-2 [28] the blocked force of the standard tapping machine, calculated according to [3], is used to predict the impact sound transmission between rooms through ceilings. For other sources the blocked force can be obtained from measurements that require the connection to an inert receiver. For direct measurement a connection via force transducers is required which can alter the normal mounting conditions. As the blocked force is related to the source free velocity and mobility it can also be obtained indirectly from measurement of source free velocity and mobility (section 2.1.4). For the high mobility source condition the blocked force can be measured in-situ using reciprocal methods [29], [30] that do not require the installation of force transducers. It will be outlined later in this thesis how the blocked force can be estimated from measurement of the installed power and the receiver mobility.

2.2.4 Equivalent force

The equivalent force method reduces the excitation of a source with multiple contacts and components of excitation to a single equivalent force, also termed pseudo-force. The basic principle is that by excitation of a structure with the equivalent force the same power is introduced as for the real source. For the determination, direct and reciprocal measurements exist that yield the equivalent force as a single value [32], [33].

A basic assumption is that the source is a high mobility source, relative to the receiver structure. For a combined force and moment excitation, this must be ensured for each contact point and this is elaborate and time consuming. As the structure-borne sound power incident is dependent on the receiver mobility (2.6), different source locations yield different equivalent forces which contradicts the requirements of an independent source characterisation. The representation of moment excitation by a force excitation is theoretically not justified, especially when the source is placed near the boundaries of plate structures where the magnitude of force and moment mobility can differ greatly [34].

Attempts have been made to circumvent the problem of uncertainty in the evaluation of an equivalent force by considering several equivalent forces at different positions and then averaging [33]. Also, it has been suggested that moment excitation can be represented by equivalent moments [35]. However, the dimensional incompatibility of forces and moments remains as a problem.

By considering the components of excitation on a power basis the effect of force and moment excitation can be compared and summed. In [36] the source power has been examined by multiplication of equivalent forces with the associated real part of the receiver mobility. In general, there has been an increasing consensus that sources should be characterised on a power basis analogous to the characterisation of airborne sound sources.

2.2.5 Source descriptor and coupling function

A description of the source / receiver interaction on a power basis was proposed by Mondot and Petersson [14]. By multiplication of the numerator and denominator in equation (2.6) with the complex conjugate of the source mobility Y_S^* the power can be expressed into two terms: one dependent on the source and the other on the coupling between source and receiver. The first term is denoted source descriptor:

$$S_c = \frac{1}{2}\frac{\left|v_{sf}\right|^2}{Y_S^*} \tag{2.10}$$

The source descriptor has the dimension of power and is a measure of the source strength. It can be seen as the equivalent complex power needed to obtain the free velocity at the contacts of the source. The source descriptor has been used to rank sources in terms of their ability to deliver power [37].

The transmitted power into a receiver is a fraction of the source descriptor, determined by the second term denoted coupling function:

$$C_f = \frac{Y_S^* Y_R}{\left|Y_S + Y_R\right|^2} \tag{2.11}$$

The coupling function highlights the degree of mobility matching between source and receiver and thus describes the efficiency of the dynamic coupling. It illustrates how the dynamic properties of source and receiver would "filter" the transmission at the interface. For each contact point it can be seen as the transfer function of a one input one output system for which the input is the source descriptor and the output the complex power transmitted.

The product of source descriptor and coupling function is the complex structure-borne power, equivalent to equation (2.6):

$$W = S_c C_f \tag{2.12}$$

A dimensionless power can be calculated by normalization of the structure-borne power to the magnitude of the source descriptor to give insight into the result of various source / receiver mobility ratios, including the phase relationship [14], [20]. This is illustrated in Figure 1 for the magnitude of the complex power and in Figure 2 for the active power as the real part of the complex power.

Maximum power transmission occurs for mobility matching e.g. when the magnitude of the source and receiver mobility is equal. Then the phase relationship is essential. The phase of a point mobility is always distributed within $-\pi/2$ (pure mass) and $+\pi/2$ (pure spring). For equal phase of the source and receiver mobilities, the power into the receiver takes a minimum.

For a given magnitude ratio, the maximum power is obtained for the largest phase difference (in absolute value). However, a phase difference of π is physically impossible, as it corresponds to undamped structures.

When the mobilities are largely different in magnitude, the magnitude of the power is low. For that case the mobilities are called unmatched and the transmission is essentially independent of the mobility phase relationship. This corresponds to the high mobility and low mobility source approximations that are also illustrated in the Figures. In the matched condition, the power transmission can be very high, depending on the phase relationship. On a logarithmic scale, the power functions are symmetrical about the mobility ratio of unity. This implies that the complete system is reciprocal, i.e. the source can be regarded as the receiver and vice versa.

An extension of the source descriptor and coupling function concept to multiple contacts and components of excitation was presented by Moorhouse [20]. In addition the terminologies "mirror power", "characteristic power" (CP) and "maximum available power" (MAP) were introduced.

The "mirror power" is the power which is introduced into a receiver structure being a mirror of the passive source structure, i.e. $Y_R = Y_S$.

$$W(Y_R = Y_S) = \frac{1}{8}\frac{|v_{sf}|^2}{Y_S^*} \tag{2.13}$$

The maximum power occurs when the source and receiver mobilities are complex conjugate pair, i.e. $Y_R = Y_S^*$ (Figure 2.1).

$$W(Y_R = Y_S^*) = \frac{1}{2}\left|v_{sf}\right|^2 \cdot \frac{Y_S^*}{\left[2\,\mathrm{Re}\{Y_S\}\right]^2} \tag{2.14}$$

The real part is of particular interest as it represents the active power being transmitted and is thus termed "maximum available power":

$$\mathrm{Re}\{W(Y_R = Y_S^*)\} = \frac{1}{8}\frac{\left|v_{sf}\right|^2}{\mathrm{Re}\{Y_S\}} \tag{2.15}$$

The "characteristic power" is the same as the source descriptor for the one component case. It is obtained when the force is equal to the blocked force and the velocity is equal to the free velocity. In Figure 2.2 it is the value at the intersection of the high- and low mobility source (HMS and LMS) approximations and is four times the mirror power given by:

$$W(f = f_b, v = v_{sf}) = \frac{1}{2}\frac{\left|v_{sf}\right|^2}{Y_S^*} \tag{2.16}$$

Analogous expressions are given in [20] for the general case of multiple contacts and degrees of freedom.

The concept of source descriptor and coupling function gives helpful insight into general effects on the structure-borne sound transmission. However, for sources with multiple points and components of excitation, the same amount of data is necessary as described in section 2.1.5.

None of the methods discussed so far enable a source characterisation, which is physically correct and practical at the same time. Special interest is now given to the reception plate method.

2.2.6 Characteristic reception plate power

The use of a reception plate [22] for the characterisation of structure-borne sound sources is based on an energetic balance. The power gained by a reception plate is stored as reverberant bending wave energy and is assumed equal to the total emission of a source connected to it. In turn, the power gained by the plate is the bending wave energy loss according to [3]:

$$P_{\text{in}} = \omega E \eta \tag{2.17}$$

Where η is the total loss factor of the plate. The bending wave energy conserved in the plate equals the product of plate mass and spatial average velocity in the far field:

$$E = m\overline{\tilde{v}}^2 \tag{2.18}$$

The bending wave energy loss is controlled by the total loss factor. The total is the result of radiation, material damping and vibration energy transmission into attached structures.

Analogous to the measurement of airborne sound power in reverberation chambers [39] this method also is termed the reverberant plate method [40].

There have been several proposals, using a resiliently supported reception plate, for the characterisation of structure-borne sound sources, e.g. [22], with the following requirements:

- sufficiently high modal density (diffuse vibration field)
- low damping

- plate mobility similar to typical installation conditions

High mobility reception plate

A perforated thin reception plate was developed by an ISO standardisation group [38] for a draft standard [39] to yield the equivalent "strength" of the source under test. The requirement of a sufficiently high modal density and practical aspects concerning the plate size led to a perforated metal plate with dimensions 2 m by 1 m, and a thickness of 1 mm. The perforations were to reduce airborne excitation. The sources to be considered were small and lightweight electrical or mechanical devices like ventilators, pumps, valves etc. These devices are compact and can be termed low mobility, according to 2.1.4 and by implication, this reception plate yields an approximation of the free source velocity. Similar reception plates were tested by other research groups and laboratories.

The method has not been taken forward to a standard and the work was suspended. The major reason for this was a lack of indication how the source data obtained could be used for prediction of installed power and thence the resultant sound pressure in adjacent rooms. Again, the laboratory mobility condition will not in general correspond to installed conditions. Indeed, a device that constitutes a low mobility source in the laboratory might become a high mobility source when installed in a building.

Concrete reception plate

In recent considerations of a working group (CEN/TC 126/WG7 AHG1) also reported in the thesis work by Späh [41]-[43], the idea of using a reception plate for the characterisation of structure-borne sound sources was revisited. The use of the source data to be measured was clearly defined as to provide input for building propagation models like EN 12354-5 [2]. At present, the prediction model is limited to homogenous massive building constructions. By determination of the mobilities of typical sources in buildings and comparison with wall and floor mobilities it was found that the high mobility source approximation applies.

A prototype horizontal concrete reception plate of 100 mm thickness was initially constructed in order to fulfil the requirements mentioned above. Finally a prototype test rig consisting of three mutually perpendicular concrete plates was constructed.

A simple algorithm was proposed for evaluation of a characteristic reception plate power that takes into account the plate mobility and enables comparison of sources measured in different laboratories by a singular frequency dependent value [44]. For prediction models the characteristic reception plate power is then transformed into the installed power in a building. The reception plate method has been validated for a whirlpool bath and has recently been proposed as a standard 15657 [1].

In this thesis work, the reception plate method was applied to stairs as sound sources and compared to other methods.

2.3 SUMMARY

The background theory of structure-borne sound transmission has been presented and the challenges to the characterisation of structure-borne sound sources highlighted.

Existing and previously proposed approaches were described and assessed with respect to the requirements of an adequate characterisation.

It is proposed that an appropriate source characterisation should be on a power basis as the injected power is the primary quantity of interest regarding the prediction of structure-borne sound transmission. On a power basis the contribution of forces and moments can be directly compared.

In the remainder of this thesis, the free velocity method, the blocked force method, the reception plate method and the source descriptor will be adapted to characterise stairs as sound sources in buildings, with the aim of providing a practical laboratory method or methods.

2.4 REFERENCES

[1] EN 15657-1: Acoustic properties of building elements and of buildings - Laboratory measurement of airborne and structure borne sound from building equipment - Part 1: Simplified cases where the equipment mobilities are much higher than the receiver mobilities, taking whirlpool baths as an example, 2009

[2] EN 12354-5: Building acoustics – Estimation of acoustic performance of buildings from the performance of elements – Part 5: Sounds levels due to the service equipment, October 2009

[3] Cremer, L., Heckl, M., Petersson B.A.T.: Structure-borne sound, Springer Verlag, Berlin, 2005

[4] Gardonio P., Brennan M. J.: On the origins and development of mobility and impedance methods in structural dynamics, J. Sound and Vibration, Vol. 249, 557-573, 2002

[5] Heckl M.: Compendium of impedance formulas, Report No. 774, Bolt Beranek and Newman Inc., Cambridge, Massachusetts, 1961

[6] Gardonio P., Brennan M. J.: Mobility and impedance methods in structural dynamics, Advanced Applications in Acoustics, Noise and Vibration, edited by Fahy F. and Walker J., E&FN Spon Press, London, 2004, Chapter 9

[7] Hopkins, C.: Sound Insulation, Butterworth-Heinemann, 2007

[8] Petersson B. A. T., Plunt J.: Structure-borne sound transmission from machinery to foundations, Report 80-19, Department of Building Acoustics, Chalmers University of Technology, Sweden, 1980

[9] Moorhouse A. T., Gibbs B. M.: Prediction of the structure-borne noise emission of machines: development of a methodology, Journal of Sound and Vibration, Vol. 167(2), 223-237, 1993

[10] Petersson B. A. T., Gibbs B. M.: Some common characteristics of multi-Point and component structure-borne sound sources, Proceedings Internoise 1996, 1319-1324, 1996

[11] Gibbs B. M., Moorhouse A. T.: Case studies of machine bases as structure-borne sound sources in buildings, Journal of Sound and Vibration, Vol. 4 (3), 125-133, 1999

[12] Pinnington, R. J.: Vibrational power transmission to a seating of a vibration isolated motor. Journal of Sound and Vibration, Vol. 118 (3), page 515-530, 1987

[13] Gibbs B. M.: Towards a practical characterisation for sources of structure-borne sound, Proc. 8th international conference on recent advances in structural dynamics, Southampton, 1-22, 2003

[14] Mondot J. M., Petersson B. A. T.: Characterization of structure-borne sound sources: The source descriptor and the coupling function, Journal of Sound and Vibration, Vol. 114 (3), 507-518, 1987

[15] Fulford R. A.: Structure-borne sound power and source characterisation in multi-point-connected systems, PhD Thesis of The University of Liverpool, 1995

[16] Moorhouse A. T., Gibbs B. M.: Measurement of structure-borne sound emission from resiliently mounted machines in situ, J. Sound and Vibration, Vol. 180 (1), 143-161, 1995

[17] ISO 9611: Acoustics - Characterisation of sources of structure-borne sound with respect to sound radiation from connected structures - Measurement of velocity at the contact points of machinery when resiliently mounted, British Standard, 1996

[18] White, M.F., Liasjø, K.H.: Measurement of mobility and damping of floors, Journal of Sound and Vibration, Vol. 81 (4), 535-547, 1982

[19] Mayr, A. R.: Vibroacoustic sources in lightweight buildings, PhD Thesis of The University of Liverpool, 2009

[20] Moorhouse A. T.: On the characteristic power of structure-borne sound sources, J. Sound and Vibration, Vol. 248 (3), 441-459, 2001

[21] Petersson B. A. T., Gibbs B. M.: Towards a structure-borne sound source characterization, Applied Acoustics, Vol. 61 (3), 325-343, 2000

[22] Wolde T. T., Gadefelt G. R.: Development of standard measurement methods for structure-borne sound emission, Noise Control Engineering Journal, Vol. 28 (1), 5-14, 1987

[23] Fahy F. J.: The reciprocity principle and applications in vibro-acoustics, Proceedings of the Institute of Acoustics, 1-20, 1990

[24] Stromski, K., Fuchs, H.V., Voigtsberger, C.A.: Zur Messung von Geräuschen der Wasser-Installation (On the measurement of noise by water installations). Fortschritte der Akustik, DAGA 1984

[25] Villot M.: Characterization of building equipment, Applied Acoustics, Vol. 61, 273-283, 2000

[26] EN ISO 3822: Acoustics - Laboratory tests on noise emission from appliances and equipment used in water supply installations, CEN, 1997

[27] EN 14366: Laboratory measurement of noise from waste water installations, CEN, 2004

[28] EN 12354-2: Building acoustics – Estimation of acoustic performance of buildings from the performance of elements – Part 2: Impact sound insulation between rooms, September 2000

[29] Yap, S. H., Gibbs, B. M.: Structure-Borne Sound Transmission from Machines in Buildings, Part 1: Indirect Measurement of Force at the Machine - Receiver Interface of a Single and Multi - Point Connected System by a Reciprocal Method, Journal of Sound and Vibration, 1998

[30] Yap, S. H., Gibbs, B. M.: Structure-Borne Sound Transmission from Machines in Buildings, Part 2: Indirect Measurement of Force and Moment at the Machine - Receiver Interface of a Single Point

Connected System by a Reciprocal Method, Journal of Sound and Vibration, 1998

[31] Wolde T. T., Verheij J. W.: Practical quantities for the characterisation of structure-borne sound sources, Proceedings Internoise 1988, 449-454, 1988

[32] Janssens M. H. A., Verheij J. W.: A pseudo-forces methodology to be used in characterization of structure-borne sound sources, Applied Acoustics, Vol. 61, 285-308, 2000

[33] Ohlrich M., Crone A.: An equivalent force description of gear-box sources applied in prediction of structural vibration in wind turbines, Proceedings Internoise 1988, 479-484, 1988

[34] Moorhouse A. T., Gibbs B. M.: The relative contributions of forces and moments in structure-borne sound power emission from machines, Proceedings Internoise 1994, 645-648, 1994

[35] Vercammen M. L. S., Heringa P. H.: Characterising structure-borne sound from domestic appliances, Applied Acoustics, Vol. 28, 105-117, 1989

[36] Ohlrich M., Larsen C.: Surface and terminal source power for characterization of vibration sources at audible frequencies, Proceedings Internoise 1994, 633-636, 1994

[37] Moorhouse A. T., Mondot J. M., Gibbs B. M.: Source descriptors for structure-borne sound sources, Proceedings ICSV 5, Adelaide, 1997

[38] ISO/TC43/SC1/WG22 N99: Acoustics: Characterisation of structure-borne sound with respect to the airborne sound radiated of connected structures. Measurement of the average vibration velocity of a thin reception plate to which the source is connected, 1993

[39] ISO 3741: Acoustics - Determination of sound power levels of noise sources using sound pressure - Precision methods for reverberation rooms, ISO, 1999

[40] Davis E. B.: Characterization of structure-borne noise sources using a reverberant or anechoic plate, Proceedings Internoise 2006, Hawaii, 2006

[41] Späh M. M.: Characterisation of structure-borne sound sources in buildings, PhD Thesis of The University of Liverpool, 2006

[42] Späh, M. M.; Gibbs, B.M.: Reception plate method for characterisation of structure-borne sound sources in buildings: Installed power and sound pressure from laboratory data, Applied Acoustics, 70 (11-12), 1431-1439, 2009

[43] Späh, M. M.; Gibbs, B.M.: Reception plate method for characterisation of structure-borne sound sources in buildings: Assumptions and application, Applied Acoustics, 70 (11-12), 361-368, 2009

[44] Scheck, J.; Chamaoun, M.; Gibbs, B.M., Fischer H.-M.: Preparation of a round robin on the reception plate method to characterise structure-borne sound sources in buildings, Internoise, Lisbon, 2010

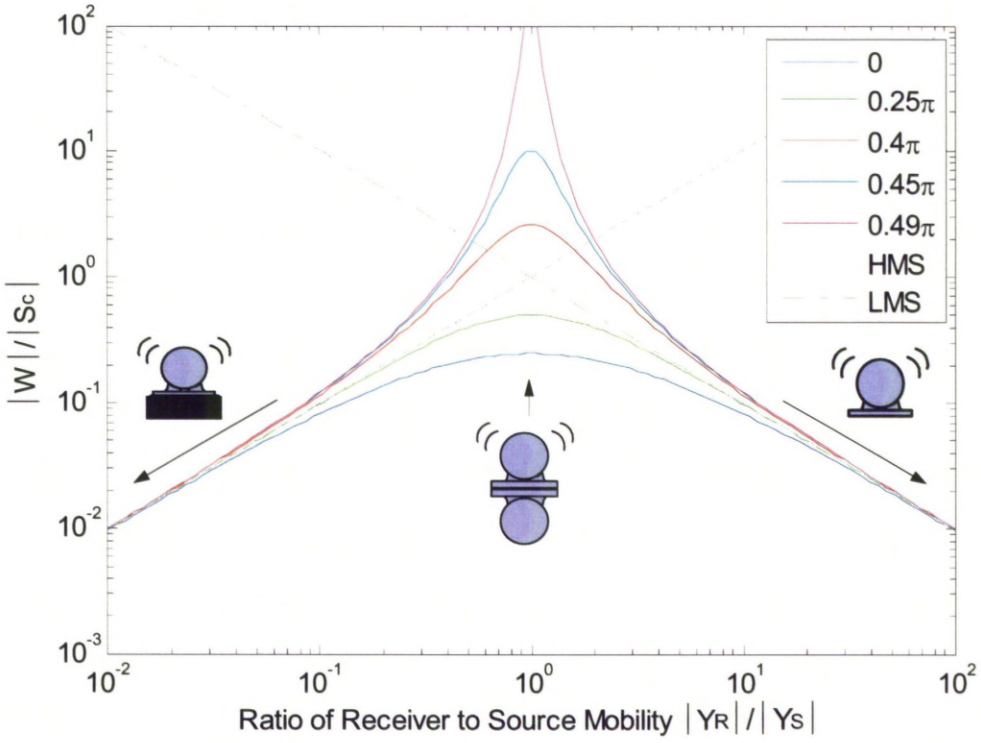

Figure 2.1: Magnitude of the power as a function of source-receiver mobility ratio, for various phase differences, after [14], [20]

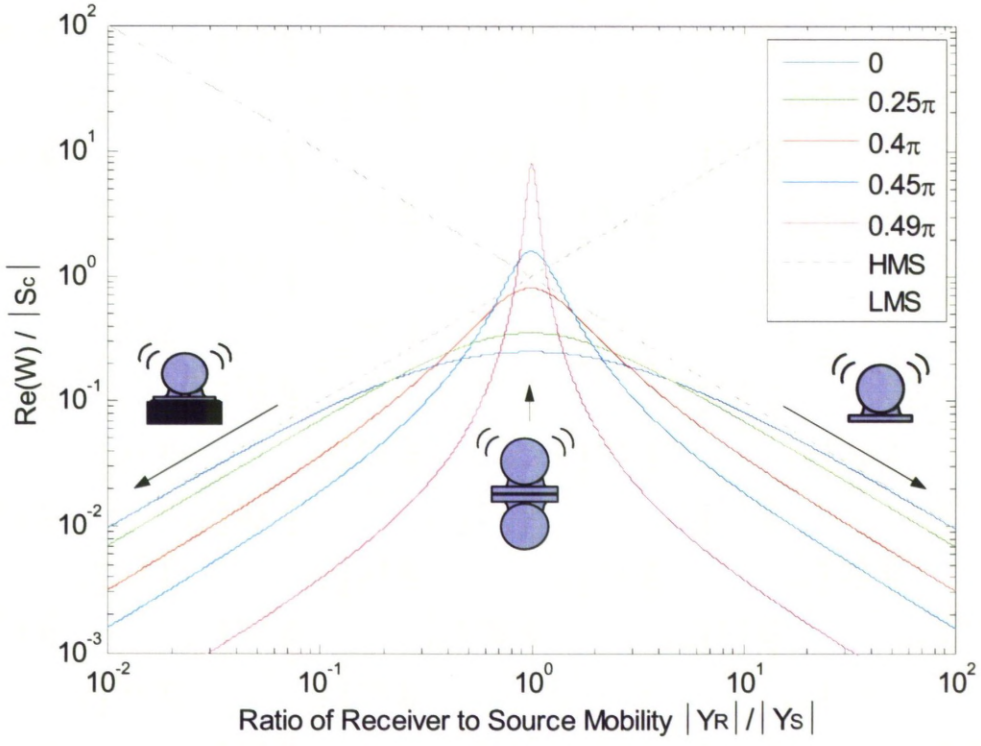

Figure 2.2: Real part of the power as a function of source-receiver mobility ratio, for various phase differences, after [20]

3 LIGHTWEIGHT STAIR SYSTEMS

3.1 INTRODUCTION

Lightweight stairs are situated in multi-storey houses, apartment blocks and row houses to connect floors at different levels. Usually the stairs are fixed to walls and supported on the upper and lower floors. In Germany, the walls often separate dwellings and in most cases are of heavyweight single-leaf or double-leaf construction. The floors/ceilings are usually of concrete. When walking on the stair, vibrations are transmitted through the contacts and structure-borne sound is transmitted into adjacent rooms.

Although impact noise transmission from lightweight stairs is still recognised as a problem [1]-[3], the focus of many architects and manufacturers is still on stability only. The situation is reflected in ETAG 008 [4] "Guideline for European Technical Approval of Prefabricated Stair Kits" where it is stated that protection against noise is "not relevant" and "where sound insulation or sound absorption is called for, the insulation is applied afterwards and is not part of the prefabricated kit".

The contacts with buildings are illustrated in Figure 3.1. For high stability, the string boards are often mounted directly to the wall using screws and the supports are without isolation. In this case, the sound transmission from the string board into the wall, and the resultant radiation, are generally dominant [1], [3].

Full contact of the string board to the wall is mostly avoided in newer stair systems, in order to reduce sound transmission. However, the string board must be fixed through one rigid wall connection to the wall for sufficient stability [4].

There is a large variety of stair systems available, concerning materials: timber, steel, plastic and combinations, geometry: straight stairs, spiral stairs, contacts: number, type etc. Previous investigations have shown that the type of staircase has a major effect on the sound transmission [1]-[3]. For this thesis study, a lightweight timber staircase was investigated. This stair system is now described in detail, along with preliminary investigations.

3.2 STAIRCASE TEST FACILITY

Driven by the need for good acoustic performance of their products, manufacturers of stair systems are investing in appropriate test facilities. The test facility described was constructed in 2001 [5] to enable acoustic measurements in building-like situations but under controlled laboratory conditions. The general requirements are according to ISO 140 [6]. A vertical section and a ground plan of the 1st level are shown in Figure 3.2. The area, used for experimental investigations, is highlighted. The source room SR-LO contains the stair under test and SR/ER-O is the receiving room.

The facility is of heavyweight construction and erected on isolation material to provide isolation from the ground plate. The permanent walls are of 24 cm CaSi with density 2000 kg/m^3, all permanent ceilings are of 18 cm

concrete with density 2300 kg/m^3. To prevent flanking transmission, the facility is divided into three separate areas by a 60 mm cavity.

Source rooms are situated in the left and right sections, the receiving rooms are in the central section. Ceilings in the source rooms contain 3,01 m x 1,20 m apertures for the installation of the stairs. The separating walls are interchangeable and are erected inside a concrete frame. In this investigation, the stair support wall was plastered 24 cm CaSi, density 2000 kg/m^3, similar to the outer walls. This construction is typical for separating walls in multi-storey houses in Germany.

The sound reduction index was measured according to ISO 140-3 [7], from the level difference between source and receiving room, and the receiving room reverberation time:

$$R = L_1 - L_2 + 10\lg\frac{S}{A} \tag{3.1}$$

The result is shown in Figure 3.3 along with the single-rated values according to ISO 717-1 [8]. The rated sound reduction index $R_w(C;C_{tr}) = 55(-1;-5)\,dB$.

3.3 INVESTIGATED STAIR SYSTEM

Experimental investigations were carried out on a straight wooden staircase with string board as illustrated in Figure 3.4. The stair has 14 steps each connected to the string board by two bolts encased in rubber. On the

opposite side, the steps are rigidly connected to bars that are screwed into the load bearing handrail.

In normal installations the stair is fixed to the floor (or floating floor) and ceiling. For this investigation, resilient layers were inserted as illustrated in Figure 3.5 to ensure that sound transmission is through the wall contact only.

For resilient layers, the static load at the floor/ceiling contacts was measured, without wall contacts, using force transducers as illustrated in Figure 3.6. The static load lies between 572 N and 763 N and the total stair mass is about 250 kg. A PUR foam (Sylomer) was used for isolation to yield a resonance frequency below 20 Hz. This was still stiff enough to allow safe walking on the stair.

Usually the string board is fixed to the wall using screws and a wall plug that is not specified by the manufacturer. For the present investigations a rigid point connection was considered in order to keep the system as simple as possible.

The wall contact was a thread anchor and a threaded rod that was screwed into a wall plug, as illustrated in Figure 3.7, before installation. To ensure that there is no tension on the screw by the static load of the stair, it was pushed to the wall after the hole in the wall was filled with hybrid mortar. After the mortar was dry, the connection could be loosened and fastened in ways necessary for the intended investigations. Counter nuts were used at both sides of the string board and also at the wall surface, fastened with a

torque of 35 Nm. The wall contact is shown in Figure 3.8 with and without the stair connected.

3.4 PRELIMINARY INVESTIGATIONS

For preliminary comparison of different set-ups, the normalised impact sound pressure level was measured for the frequency range from 50 Hz – 5 kHz, following the procedure according to ISO 140-6 [9]:

$$L_n = L - 10\lg\frac{A}{A_0} \tag{3.2}$$

Single-rated values were evaluated according to ISO 717-2 [10].

For most measurements, the tapping machine was located on step 8 near the wall contact. The sound pressure was recorded by a rotating microphone (Figure 3.9).

During the preliminary investigations, the contacts were modified several times e.g. by altering the distance between string-board and wall and replacing floor supports. These changes resulted in changes in the impact sound transmission, indeed, there were differences for nominally similar set-ups as will be outlined in section 3.4.3.

3.4.1 Direct and flanking transmission

The normalized impact sound pressure level was determined from airborne sound measurement and from measurement of the spatial average velocity on the wall (12 sampling positions) according to [9]:

$$L_{n,v} = L_v + 10\lg\sigma + 10\lg\frac{S}{A_0} + 6\,dB \tag{3.3}$$

The radiation efficiency is not known in detail and was set to 1 for all frequencies. This assumption holds above the critical frequency which is at 107 Hz.

Results are compared in Figure 3.10. In the frequency range above 200 Hz the agreement is within ± 1 dB. By this is confirmed that the sound pressure in the receiving room results from radiation of the separating wall; flanking transmission is not significant. Deviations below 250 Hz are expected because the radiation efficiency below the critical frequency is less than unity.

3.4.2 Structure-borne and airborne sound transmission

During excitation by the tapping machine, airborne sound is radiated by the stair into the source room. This component of the source room pressure is transmitted into the receiver room. The contribution of airborne sound transmission was investigated by removing the screwed wall contact.

Results are shown in Figure 3.11. For the connected stair, structure-borne sound transmission is dominant and airborne sound transmission can be neglected. This holds, except for 630 Hz, where the difference is 3 dB, indicating that structure-borne and airborne excitation of the wall is of the same order of magnitude, when the stair is connected. The high airborne sound transmission at 630 Hz was thought to be strong radiation of the string board in vicinity of the critical frequency.

3.4.3 Repeatability

The repeatability of impact sound pressure measurements was obtained with the screwed wall contact and the stair otherwise supported by resilient layers. Between each of the measurements, the set-up was altered by, for example, exchanging the floor supports and changing the distance to the wall. In Figure 3.12, seven single measurement results are compared. In Figure 3.13 are shown mean value, standard deviation and range. In the frequency range up to 200 Hz, the range is 5 dB, the standard deviation is about 2 dB. For 200 Hz < f < 3150 Hz, the range is 2 - 4 dB, the standard deviation is 1 dB. At higher frequencies, the variations increase due to an insufficient signal noise ratio. The single-rated values $L_{n,w}$ = 45 - 47 dB. These discrepancies result from modifications of the contact conditions, of joints in the stair assembly and of the contact conditions to wall and ceiling.

3.4.4 Transmission through wall contact and ceilings

The resilient supports at floor and ceiling were replaced by wooden pieces of the same size. This was to check if the transmission through the ceilings into the wall is important, for the worst case of rigid connection, often encountered in buildings. The measurements were without wall contact; the transmission is then through the rigid ceiling contacts and includes airborne excitation of the wall. Results are shown in Figure 3.14, in comparison to the main set-up and the fully isolated stair (no wall contact, isolated from the ceiling). Except for 200 Hz < f < 315 Hz, the impact sound pressure level, for the main set-up, is greater by 3 dB, indicating that the dominant transmission is through the wall contact, even when other contacts are rigid.

3.4.5 Location of excitation

A walking person will excite all steps, one after each other. Therefore, the effect of location of excitation was investigated. The tapping machine was located on each of the 14 steps. The variation of the impact sound pressure levels is shown in Figure 3.15. Up to 200 Hz, the range is 8 dB, the standard deviation is 3 dB. For 200 Hz < f < 3150 Hz, the range is 5 - 7 dB, the standard deviation is 2 dB. Again, at higher frequencies the range increases due to an insufficient signal noise ratio. The single-rated values $L_{n,w}$ = 44 - 47 dB with a mean value of $L_{n,w}$ = 46 dB. A likely reason for the dependence of the sound transmission on the source location is modal behaviour of the stair. This is described in detail in section 3.5.

3.4.6 Distance between string board and wall

The distance of string board and wall was to be set to 50 mm. This allowed access for attachment of accelerometers between string board and wall as required for the in-situ determination of the component powers (Chapter 4 and 5). In practice, the distance is usually smaller. Therefore, the effect of distance on sound transmission was considered. The case of the string board in full contact with the wall was also considered.

Results are shown in Figure 3.16. With a 20 mm distance, there is little difference (1-2 dB) compared to the 50 mm distance. The differences are of the same order of magnitude as for the repeatability. The sound transmission increases by about 10 dB with the string board in contact with the wall. The single-rated value $L_{n,w}$ = 57 dB is 10 dB higher as for the point connected string board.

3.4.7 Measurement bandwidth

The normalized impact sound pressure level is the target quantity, regarding legal requirements on sound insulation. Measurements have to be recorded in the frequency range 50 Hz – 5 kHz. The frequency spectrum exhibits significant peaks at 63 Hz, 125 Hz, 630 Hz and 1 kHz. However, the energy is concentrated in the low frequency range 50 Hz – 125 Hz. Above 1 kHz, a strong decrease is observed (e.g. Figure 3.15).

Besides the normative requirements an important criterion is the subjective annoyance caused to inhabitants by people walking on the stairs or worse,

children jumping on the stairs. It is well known that the tapping machine does not properly represent these forms of excitation [11]-[13]. In general, low frequencies are underrated and high frequencies overrated in the evaluation of the impact sound insulation, involving the standard tapping machine, and current rating procedures [10] and normative requirements e.g. [16]. Accordingly, inhabitants often remain annoyed by footfall noise, even if the floors exhibit an acceptable rating as defined by EN ISO 717-2 [10]. This has been observed for lightweight floor constructions [17] and it has been concluded that the current rating method is not appropriate for the assessment of floor impact sound insulation from a psychoacoustic point of view [13].

Psychoacoustic studies have shown that the loudness according to Zwicker [18] is suited for rating floor impact sounds [13]. Loudness is the quality of a sound that is primarily a psychological correlate of physical strength (amplitude). More formally, it is defined as "that attribute of auditory sensation in terms of which sounds can be ordered on a scale extending from quiet to loud" [19]. The unit of perceived loudness is sone as proposed by Stevens [20].

Investigations on lightweight stairs indicated that this also applies for stair impact sounds [21]. The psychoacoustic parameters roughness and sharpness are insignificant regarding the annoyance, but fluctuation strength might be important. Binaural measurements of stair impact sound from a walking person have been performed using an artificial head as illustrated in Figure 3.17. The walking process down the stair was recorded

in the room centre and in a corner. The footwear of the walker (weight: 80 kg, height: 1,87 m) is illustrated in Figure 3.18.

In Figure 3.19 the time-varying loudness is shown. Each impact is represented by a peak, between the peaks the loudness decays almost to background noise level (the walking impact frequency was about 1,5 Hz). For excitation of the individual steps similar values of typically 5 sone are observed except for step 1 which exhibits a loudness of 8.5 sone. A systematic difference of the impact sound pressure level between step 1 and the other steps was not observed and was thus thought to result from a stronger excitation by the walker.

In Figure 3.20 is displayed the time varying specific loudness (loudness per frequency/bark) for the frequency range up to 1 kHz e.g. up to 8.5 bark. The bark scale and the frequency scale are related according to Zwicker [22]. Up to 1 kHz the relation is almost linear; the first bark includes frequencies from 0-100 Hz, the second bark from 100-200 Hz and so on.

The highest values of typically 0.6 sone / bark are observed in the 1^{st} bark equivalent to the frequency range up to 100 Hz. In the 5^{th} bark / at 500 Hz the specific loudness is reduced by a factor 3. At higher frequencies, the sound transmission is insignificant in terms of subjective annoyance.

It is known that the footwear has a strong effect on the excitation by walking persons. Harder shoes generate high frequency components, to be considered. However, even with hard heeled shoes the sound transmission above 1 kHz can be assumed to be insignificant [21].

3.5 ANALYSIS OF THE VIBRATION BEHAVIOUR

To get an insight into the dynamic behaviour of the stair, an experimental modal analysis was conducted. Grid points were positioned at all steps, the handrail and the string board as illustrated in Figure 3.21. An instrumented hammer was used for transfer mobility measurements (Chapter 4). Accelerometers were placed on a central step (the 8th step from the floor), near the contact point and also on the edge of the 5th step (Figure 3.22).

The average transfer mobilities to the reference positions from excitation at 258 grid points are shown in Figure 3.23. The curves exhibit sharp resonance peaks that indicate modal behaviour throughout the whole frequency range up to 3200 Hz. In Figure 3.24 are illustrated the corresponding vibration shapes at distinct resonances, representing local stair modes. Due to reciprocity, the mode shapes result from excitation at the reference positions at step 8 and 5. In the frequency range below 100 Hz, the vibration of the stair is determined by beam modes of the handrail (35 Hz, 47 Hz, 77 Hz) and string board (67 Hz). The vibration strength at a particular frequency is therefore strongly dependent on the position of the excited step. The excitation of steps, situated at antinodes of the handrail / string board, causes significant vibration of the whole stair assembly. In contrast, excitation of steps at nodal positions, results in reduced vibration. For example the strong vibration of the stair at 77 Hz only occurs for excitation at step 5 since step 8 is situated at a nodal point of the corresponding handrail beam mode. In the frequency range above 100 Hz the vibration of the single steps is determined by plate modes. The first plate mode occurs at 106 Hz as was found from a separate modal analysis of a

step as illustrated in Figure 3.25. The handrail behaves as "deliverer" of vibration energy within the stair-system. At frequencies where step plate modes and handrail beam modes coincide (99 Hz), the vibration of the whole stair is strong. At frequencies where no handrail beam modes occur, the excitation energy is mainly contained in the directly excited step (e.g. 106 Hz, 166 Hz). This is also the case if the hand-rail has a beam mode, but the excited step is situated at a node (e.g. step 8 at 302 Hz, 622 Hz).

In general, the beam modes of the string board determine the motion at the contact. The contact motion is significant if the contact and the excited step are situated at an anti-node of the string board (67 Hz). In the case of the excited step at a node of the string board, there can still be motion at the contact, due to energy transmission through handrail modes.

3.6 DISCUSSION

So far it has been shown that stairs are complicated vibration systems, characterised by well separated and weakly damped modes of vibration. A prediction, using FE-models or analytical approaches [23], of the motion at the contact points with the receiving structures (walls, floors) from knowledge of the construction details appears difficult or even impossible.

In addition there is interaction of external excitation sources as human footfall and the tapping machine due to mobility matching. In Figure 3.26 the stair mobility near the centre of step 8 is compared to the mass mobility of a 500 g hammer of the standard tapping machine and an average walker mobility according to [24].

Within most of the frequency range the hammer and walker mobilities are of the same order of magnitude as the stair mobility. At particular frequencies, there is mobility matching and force or velocity source approximations are not valid. This makes the prediction of the contact force difficult [25], [26] even if the stair mobility is known. Therefore the mobility of both, walker and stair would have to be considered and moreover the contact history and eventual non-linearities would have to be integrated in a model for prediction of the contact force [24].

By treating the stair and impact source as one source system, the above difficulties are circumvented. The combined source can be characterised in terms of activity and mobility at the contacts with the receiver.

3.7 SUMMARY

The sound transmission of a timber staircase, situated in a staircase test facility, has been measured for excitation with the standard tapping machine and for a walking person. The structure-borne sound transmission is through one rigid wall contact and radiation of the separating wall and significant in the frequency range up to 1 kHz.

The vibration behaviour of the stair is complex and not easily predictable. In addition the interaction of impact source and stair is complicated due to mobility matching. By treating the stair and impact source as one source system, the characterisation of the stair as sound source reduces to the measurement of the activity and mobility at the contact. A precondition, for

this approach, is the determination of the dominant component(s) of excitation, which will be outlined in the following chapter.

3.8 REFERENCES

[1] Ertl, H.: Zur Verbesserung des Schallschutzes an Leichtbautreppen (On the improvement of the sound insulation of lightweight stairs), FBW Blätter, 1985

[2] Savage, J. E., Fothergill, L. C.: Reduction of noise nuisance from footsteps on stairs, Applied Acoustics, Volume 27 (Issue 2), 147-152, 1989

[3] Kurz, Roland, Schnelle, Frank: Schallschutz von Montagetreppen (Sound insulation of assembled stairs), Fortschritte der Akustik, DAGA, Oldenburg, 2000

[4] ETAG 008: Guideline for European Technical approval of prefabricated stair kits, EOTA Brussels, January 2002

[5] Möck, T.: Schalltechnisches Verhalten von Montagetreppen – Ein neuer Treppenprüfstand für Prüfung, Forschung und Entwicklung (A new staircase test facility for testing, research and development), DAGA, Hamburg, 2001

[6] EN ISO 140-1: Acoustics - Measurement of sound insulation in buildings and of building elements - Requirements for laboratory test facilities with suppressed flanking transmission, March 1998

[7] EN ISO 140-3: Acoustics. Measurement of sound insulation in buildings and of building elements. Laboratory measurement of airborne sound insulation of building elements, December 1995

[8] EN ISO 717-1: Acoustics. Rating of sound insulation in buildings and of building elements. Airborne sound insulation, September 1997

[9] EN ISO 140-6: Measurement of sound insulation in buildings and of building elements – part 6: laboratory measurements of impact sound insulation of floors, December 1998

[10] EN ISO 717-2: Acoustics. Rating of sound insulation in buildings and of building elements. Impact sound insulation, September 1997

[11] Gösele, K.: Zur Dämmung von Gehgeräuschen („On the damping of walking noise"), Gesundheits-Ingenieur, Heft 1, 1959

[12] Watters, B. G.: Impact-Noise Characteristics of Female Hard-Heeled Foot Traffic, Journal of the Acoustical Society of America, 4, 619-630, 1965

[13] Tachibana, H., Yano, H., Kiyoko, Y.: Laboratory experiments on loudness of floor impact sounds, Proceedings of Inter-Noise 93, 941-944, Leuven, Belgium, 1993

[14] Scholl, W.; Maysenhölder, W.: Impact sound insulation of timber floors: Interaction between source, floor coverings and load bearing floor, Building Acoustics, Vol. 6 (1), 43-61, 1999

[15] Scholl, W.: Impact sound insulation: The standard tapping machine shall learn to walk, Building Acoustics, 8 (4), 245-256, 2001

[16] DIN 4109: Schallschutz im Hochbau - Anforderungen und Nachweise („Sound insulation in buildings – requirements and verification"), November 1989

[17] Hammer, P.; Nilsson, E. (1997): On subjective grading of impact sound transmission through lightweight floor structures, Proceedings of Inter-Noise 97, 755 - 758, Budapest, Hungary, 1997

[18] ISO 532: Acoustics; Method for calculating loudness level, Juli 1975

[19] American National Standards Institute: American national psychoacoustical terminology, American Standards Association, 1973

[20] Stevens, S.: A scale for the measurement of the psychological magnitude: loudness. Psychological Review 43 Nr. 5, 405-416, APA Journals, 1936

[21] Drechsler, A., Fischer, H.-M.: Psychoacoustic studies on the evaluation of impact sound of lightweight stairs, CFA/DAGA, Strasbourg, 2004

[22] Zwicker, E.: Subdivision of the audible frequency range into critical bands, The Journal of the Acoustical Society of America, 33, 1961

[23] Rosenhouse, G., Ertel, H.: Theoretical Models for Investigation of Sound Transmission through Isolation Layers in Staircase Systems, Applied Acoustics 16, 51-66, 1983

[24] Lievens, M., Brunskog, J.: Model of a person walking as structure borne sound source, 19th International Congress on Acoustics, Madrid, Spain, 2007

[25] Brunskog, J., Hammer, P.: The interaction between the ISO tapping machine and lightweight floors, Acta Acustica, Vol. 89 (2), 296-308, 2003

[26] Rabold, A. et al.: Modelling the excitation force of a standard tapping machine on lightweight floor structures, Building Acoustics Vol. 17, 2010

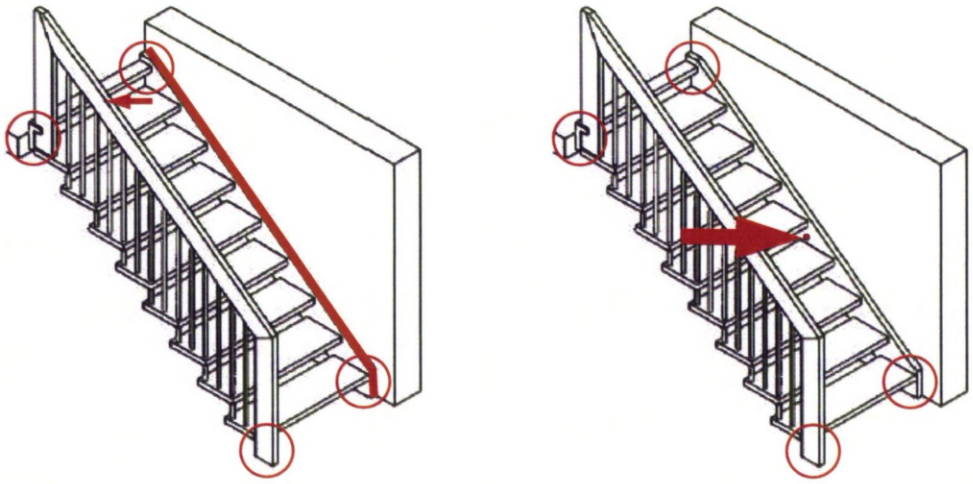

Figure 3.1: Contact points of lightweight stair systems with the building: left: string-board directly connected to wall; right: string board distanced from wall with point connection

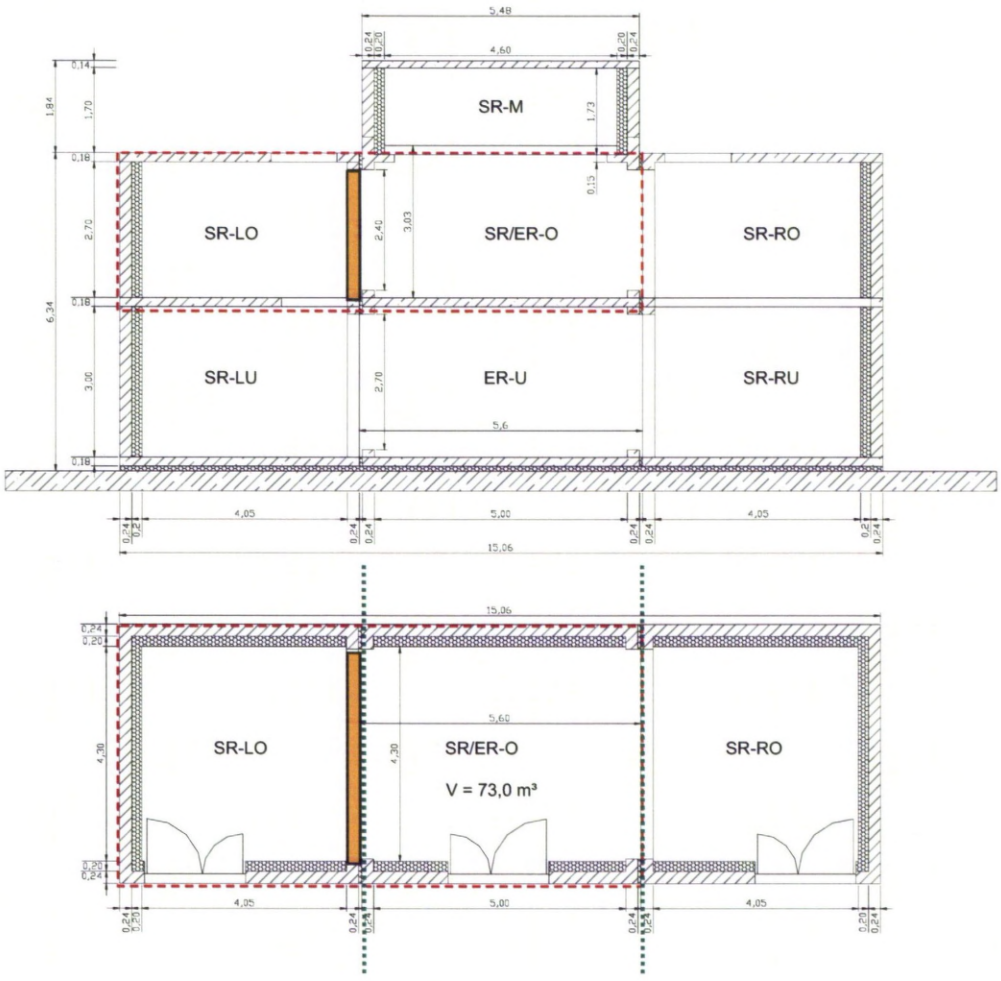

Figure 3.2: Staircase test facility: vertical section and ground plan of the 1st level used for investigations

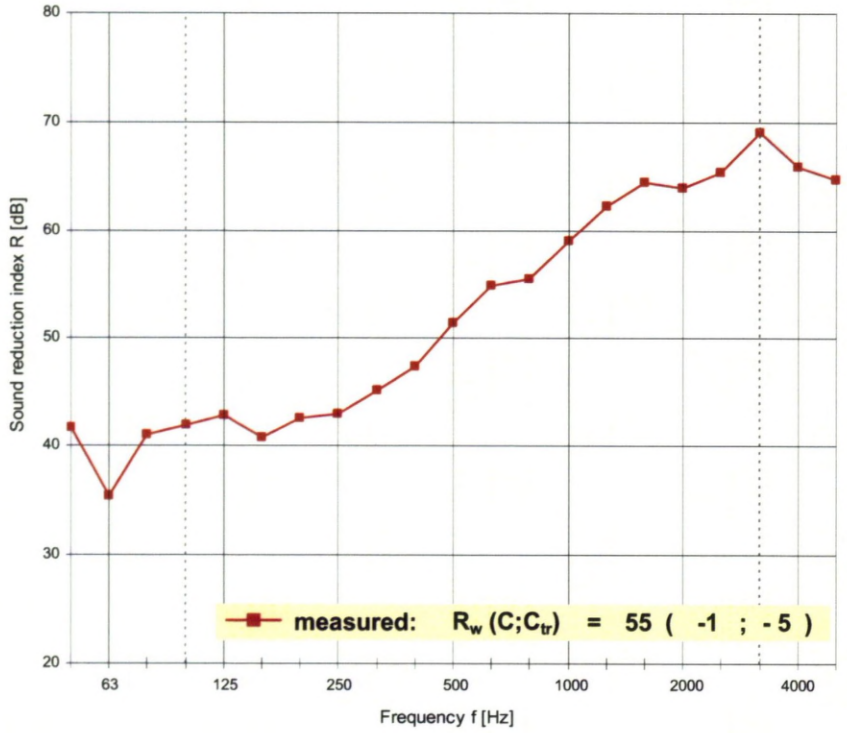

Figure 3.3: Sound reduction index of the stair wall, measured according to ISO 140-3 [7]

Figure 3.4: Investigated stair system: straight timber stair with string board.

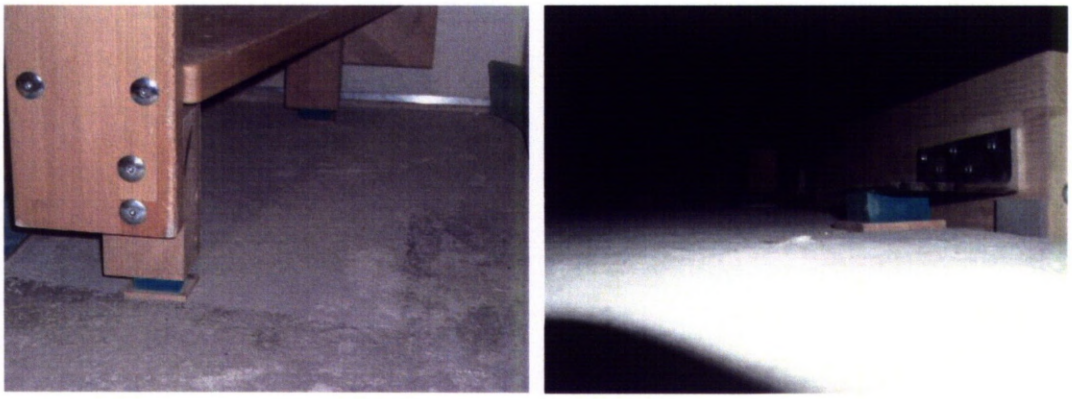

Figure 3.5: Stair supported on floor and ceiling: Main set-up with resilient layers

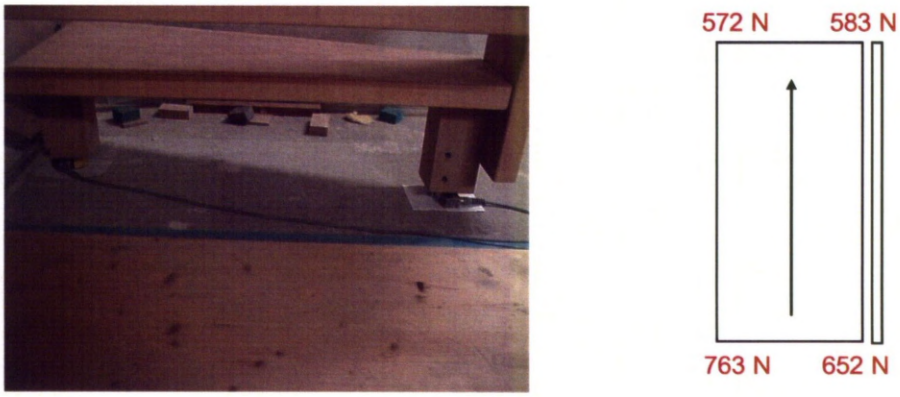

Figure 3.6: Static load at the contacts with floor and ceiling and results (the arrow denotes walking direction)

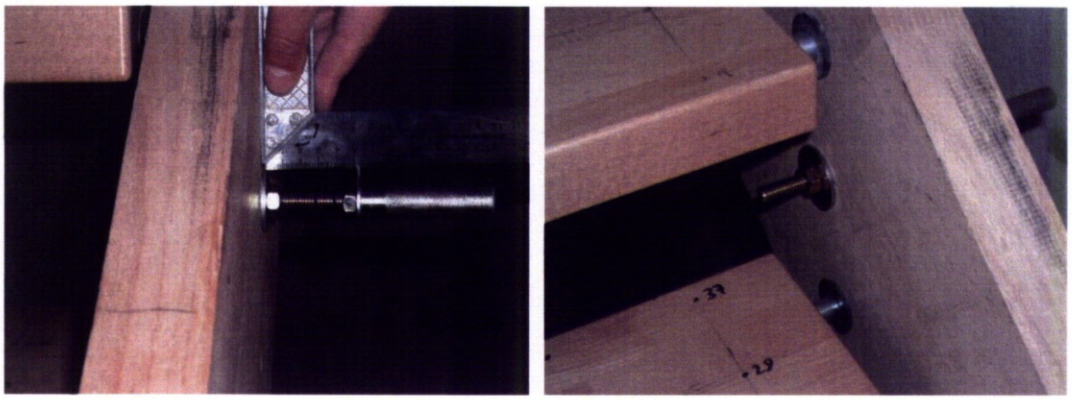

Figure 3.7: Wall plug to ensure rigid connection before installation

Figure 3.8: Left: Wall plug after installation; Right: Main set-up with 5 cm distance between string board and wall

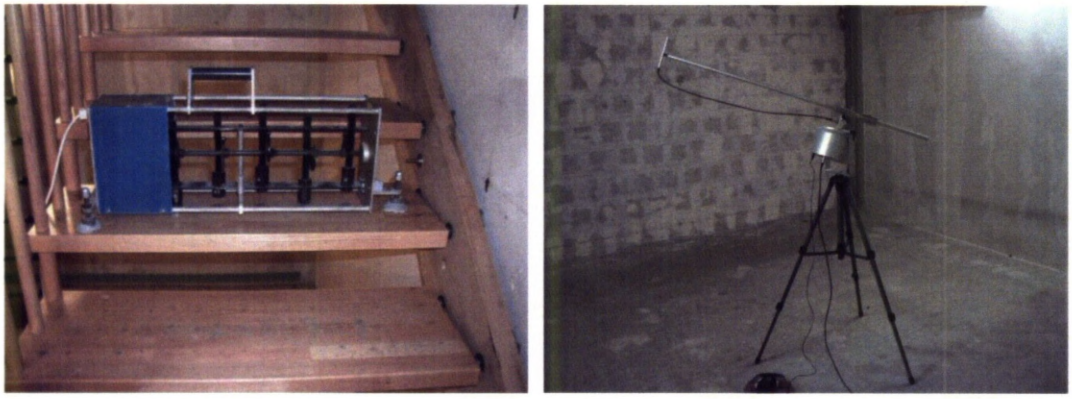

Figure 3.9: Measurement of impact sound pressure level: tapping machine on step 8 and recording of sound pressure level in the receiver room

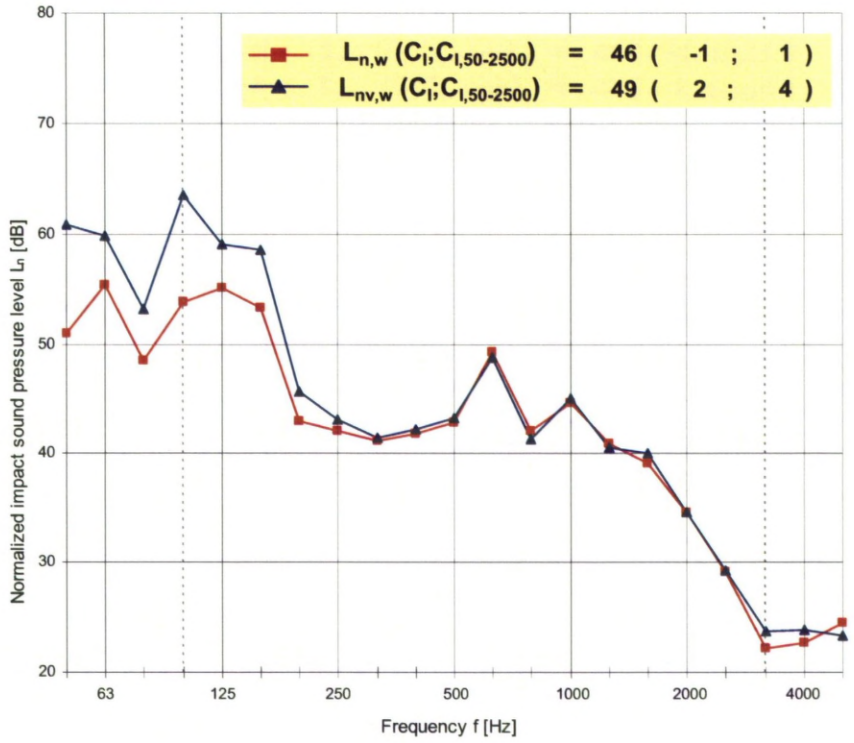

Figure 3.10: Normalised impact sound pressure level from sound pressure (red) and wall velocity (blue)

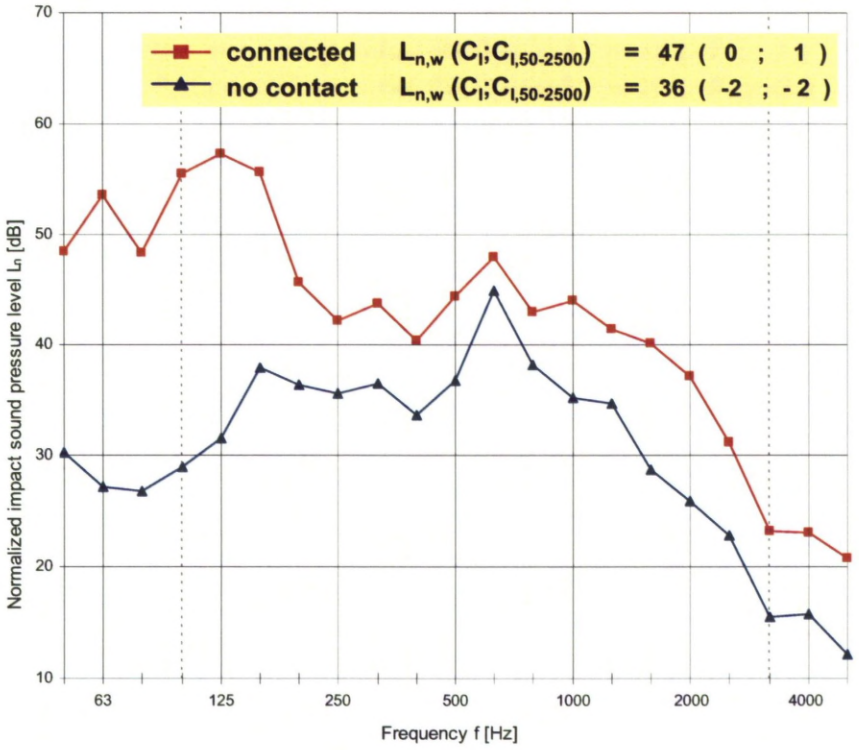

Figure 3.11: Structure-borne (red) and airborne (blue) sound transmission

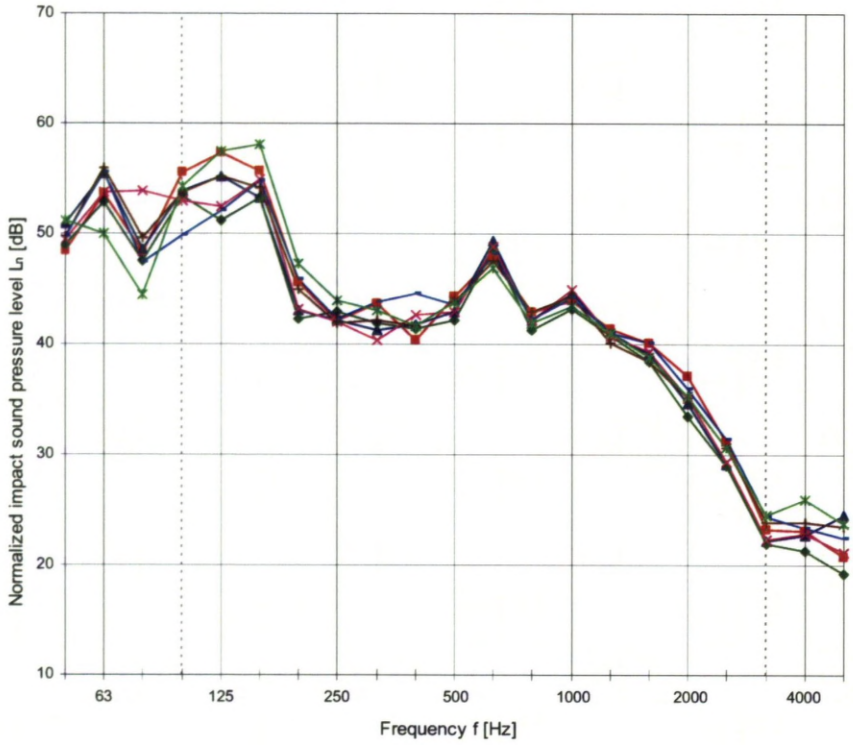

Figure 3.12: Repeatability of main set-up – single measurements

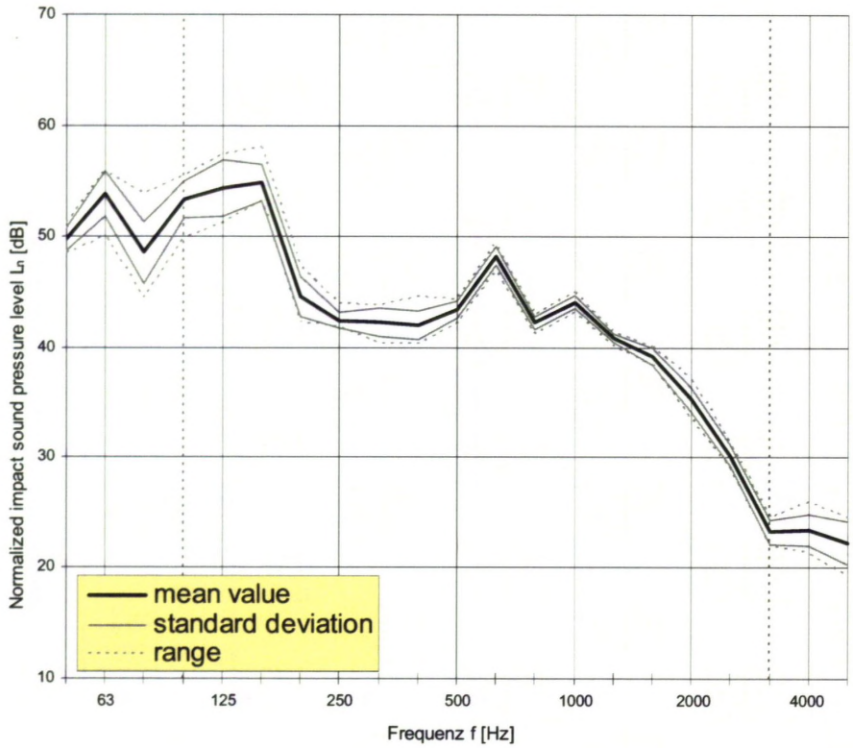

Figure 3.13: Repeatability of main set-up – mean value, standard deviation and range

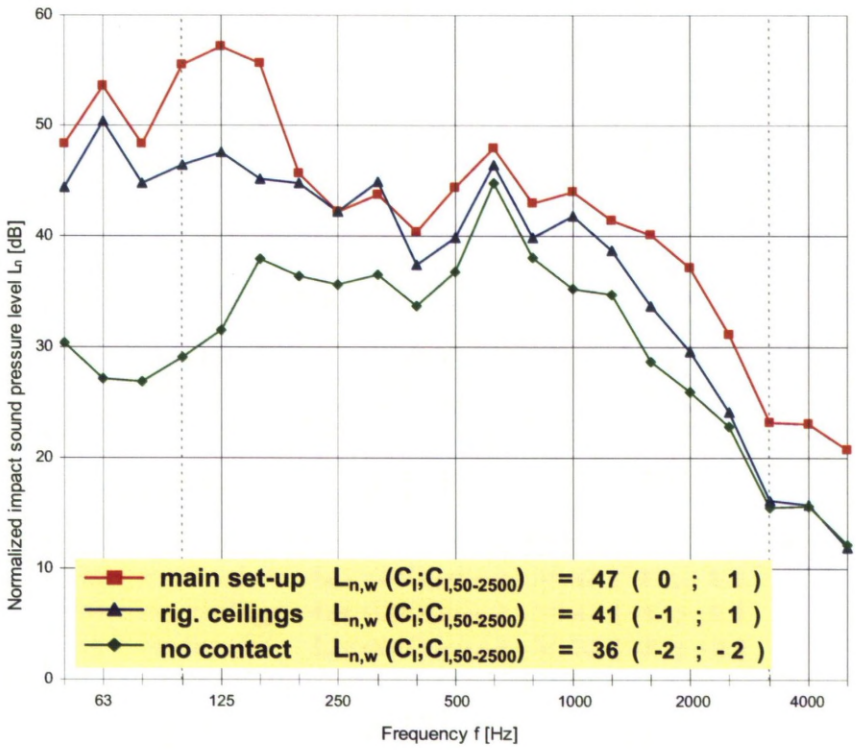

Figure 3.14: Stair isolated from ceilings and rigid wall contact (red), rigidly supported without wall contact (blue) and fully isolated (green)

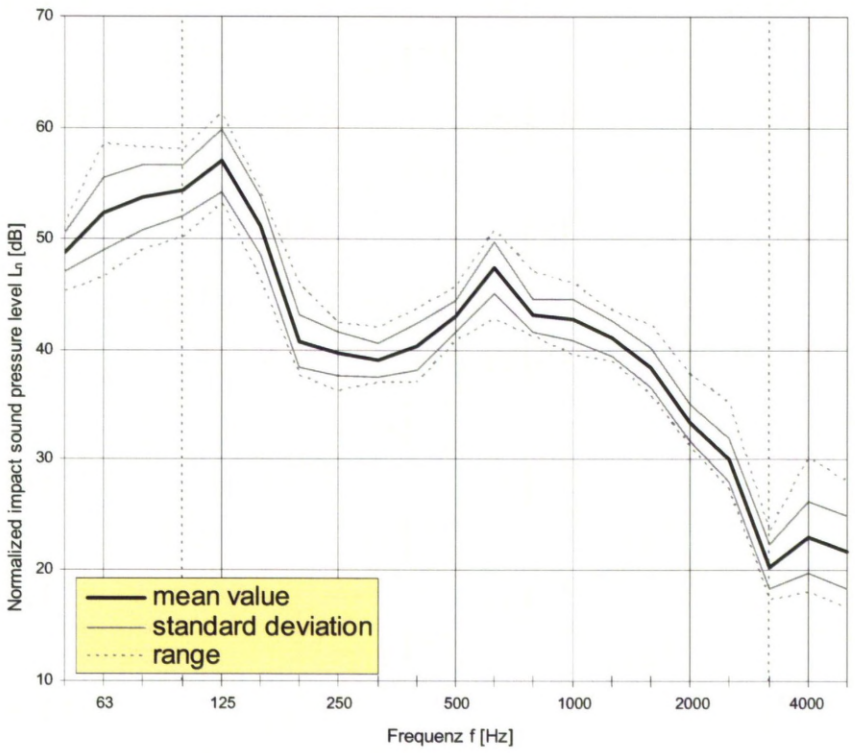

Figure 3.15: Location of tapping machine on steps 1 to 14 – mean value, standard deviation and maximum spread

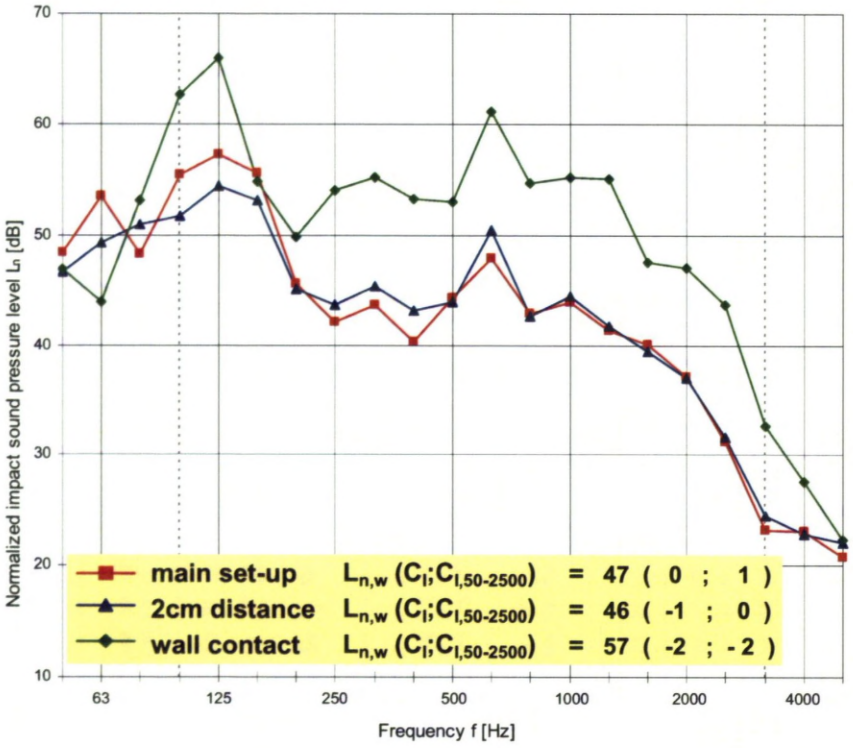

Figure 3.16: Distance of string board to wall: 5 cm (red), 2 cm (blue) and string board with wall contact

Figure 3.17: Artificial head for psychoacoustic measurements

Figure 3.18: Left: corner-position of artificial head; Right: human walker wearing sneakers with rubber soles

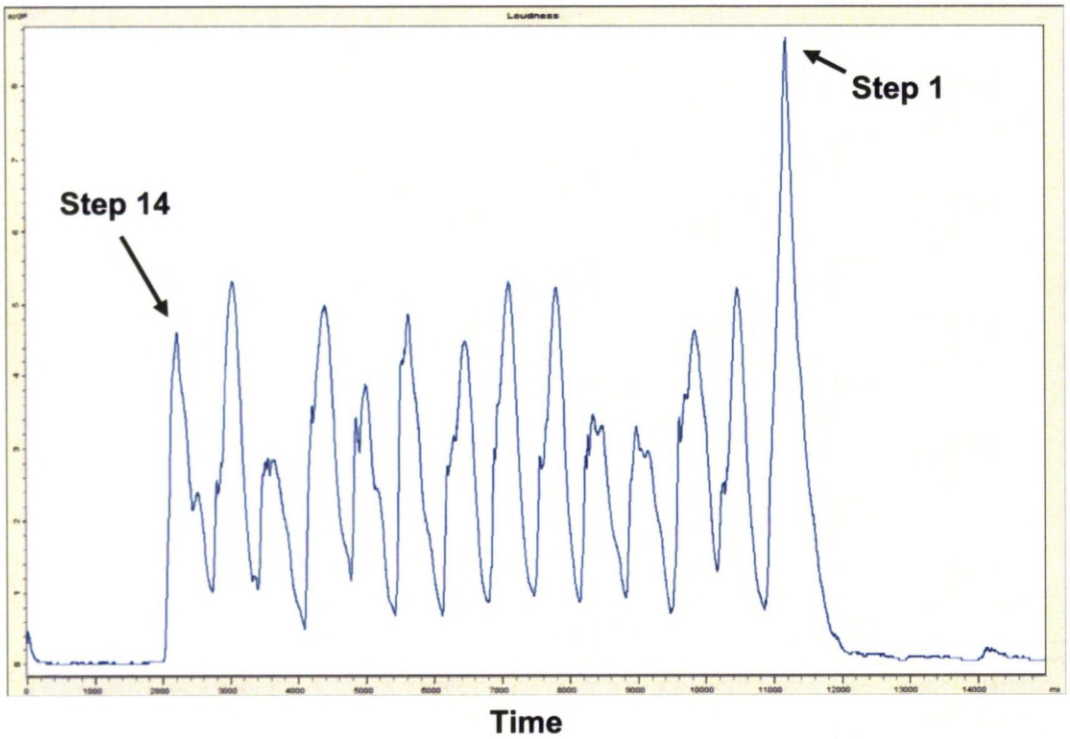

Figure 3.19: Time varying loudness of a person walking down the stair; x-axis: 0 – 15 s; y-axis: 0 – 8.8 sone

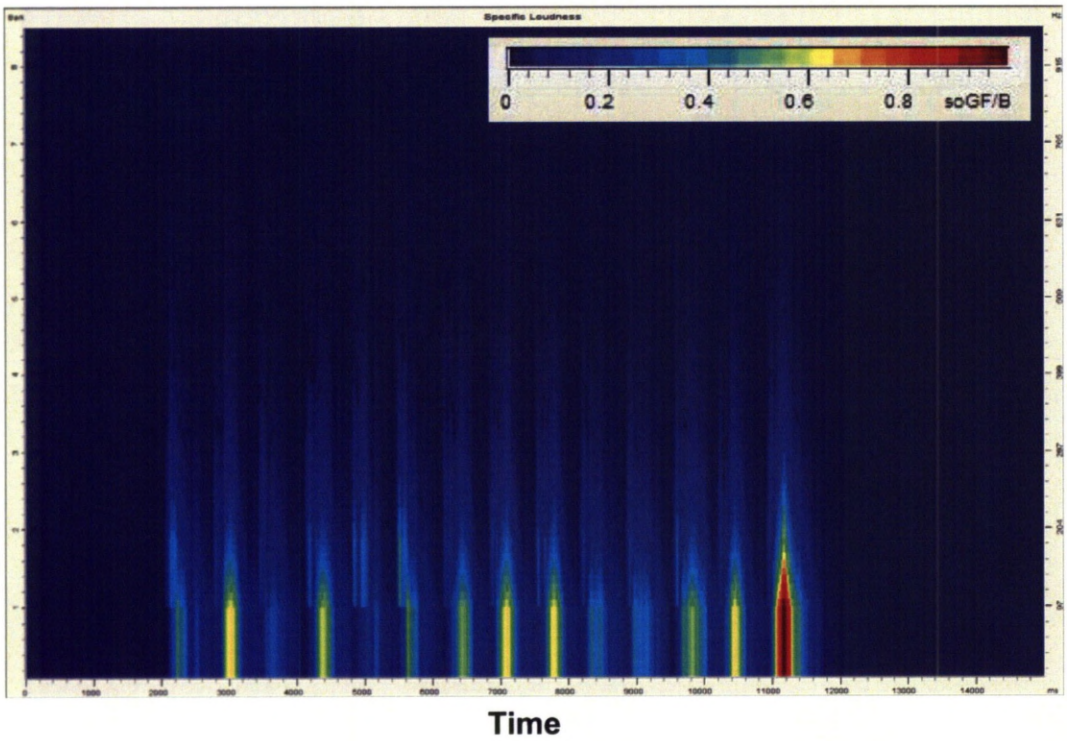

Figure 3.20: Time varying specific loudness: x-axis: 0 – 15 s; left y-axis: 0 – 8.5 bark; right y-axis: 0 – 1 kHz

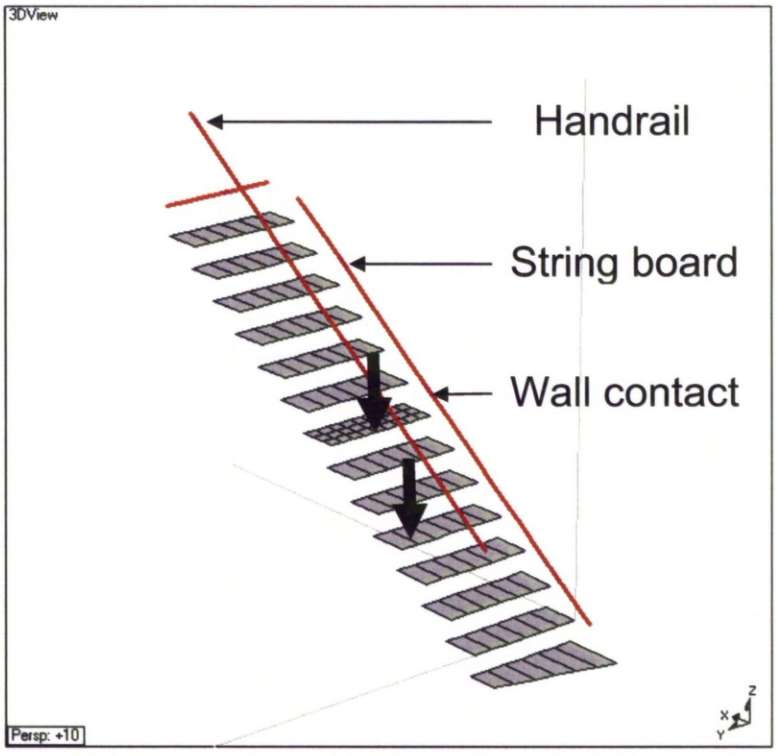

Figure 3.21: Investigated components, sampling positions and reference positions (arrows) on stair for experimental modal analysis

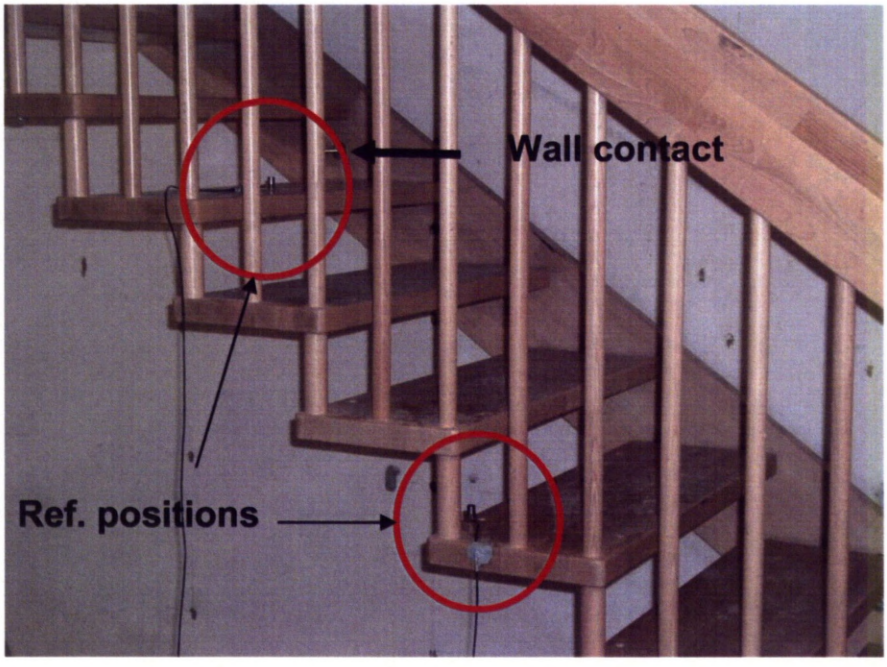

Figure 3.22: Reference positions on step 8 and 5 for experimental modal analysis

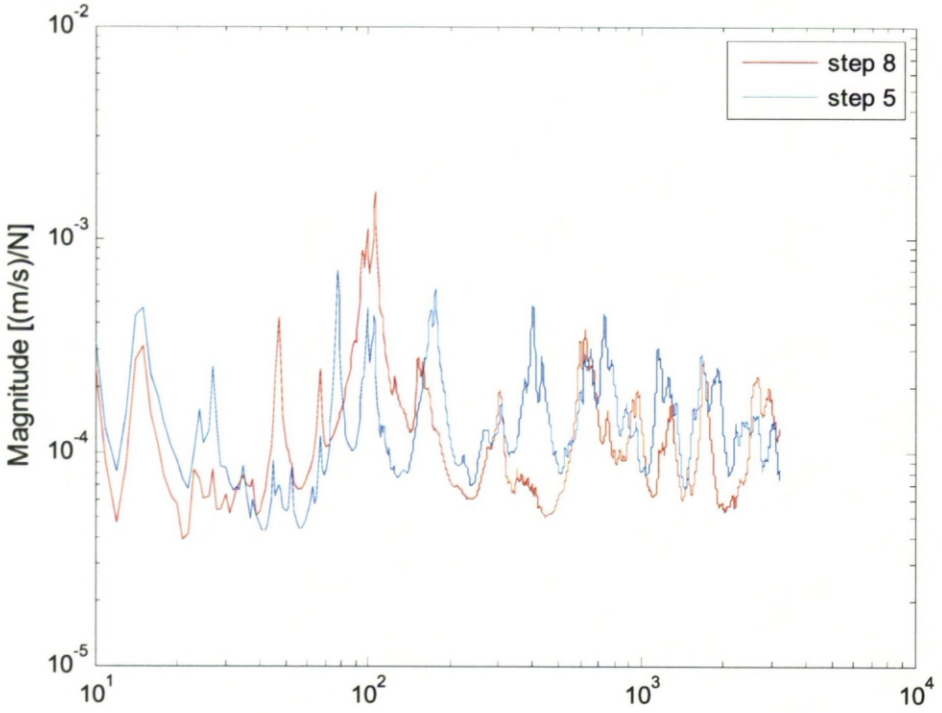

Figure 3.23: Average transfer mobility to reference positions on step 8 and step 5 from experimental modal analysis

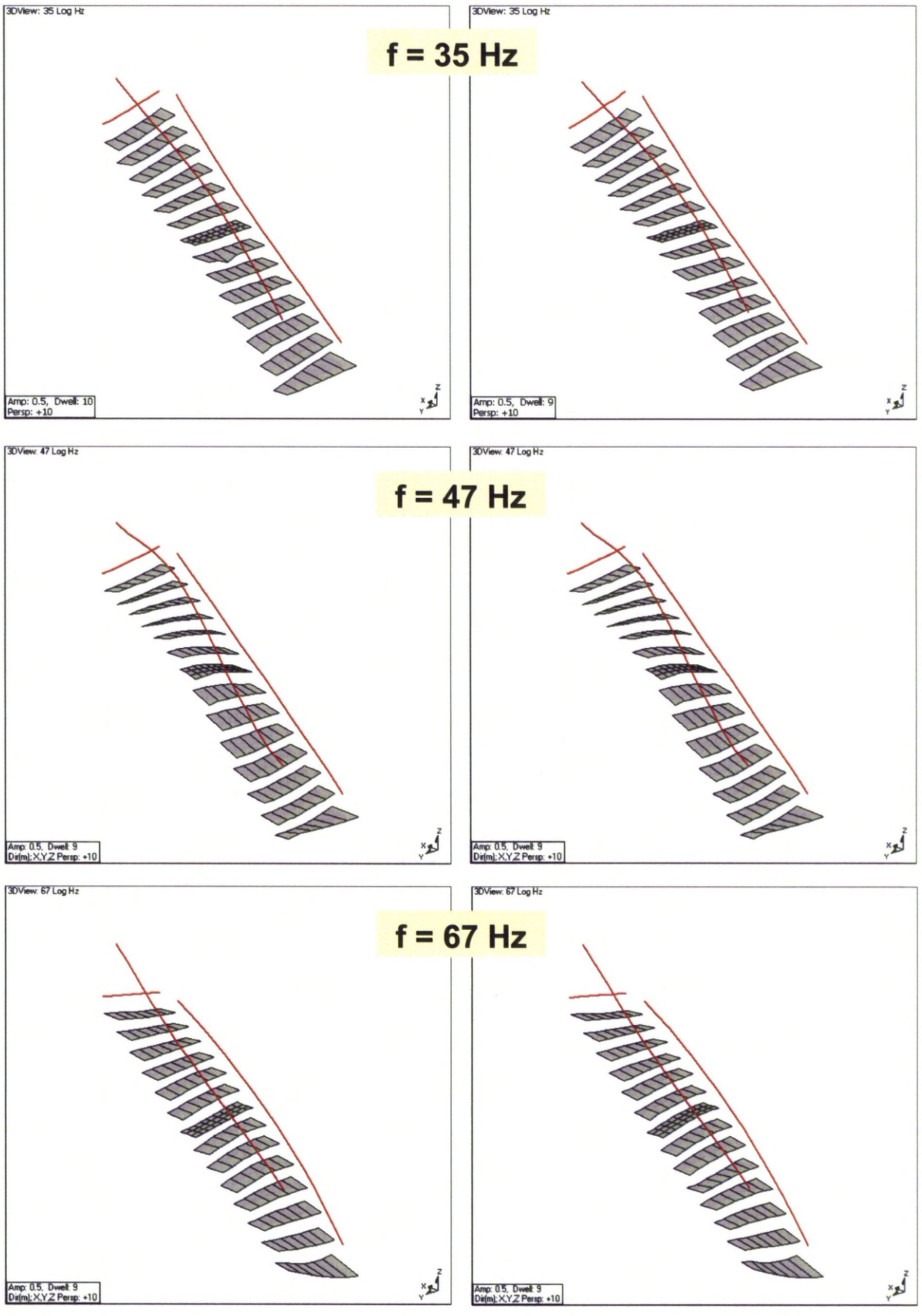
3DView: 35 Log Hz
f = 35 Hz
Amp: 0.5, Dwell: 10
Persp: +10
3DView: 35 Log Hz
Amp: 0.5, Dwell: 9
Persp: +10
3DView: 47 Log Hz
f = 47 Hz
Amp: 0.5, Dwell: 9
Dir(m): X,Y,Z Persp: +10
3DView: 47 Log Hz
Amp: 0.5, Dwell: 9
Dir(m): X,Y,Z Persp: +10
3DView: 67 Log Hz
f = 67 Hz
Amp: 0.5, Dwell: 9
Dir(m): X,Y,Z Persp: +10
3DView: 67 Log Hz
Amp: 0.5, Dwell: 9
Dir(m): X,Y,Z Persp: +10

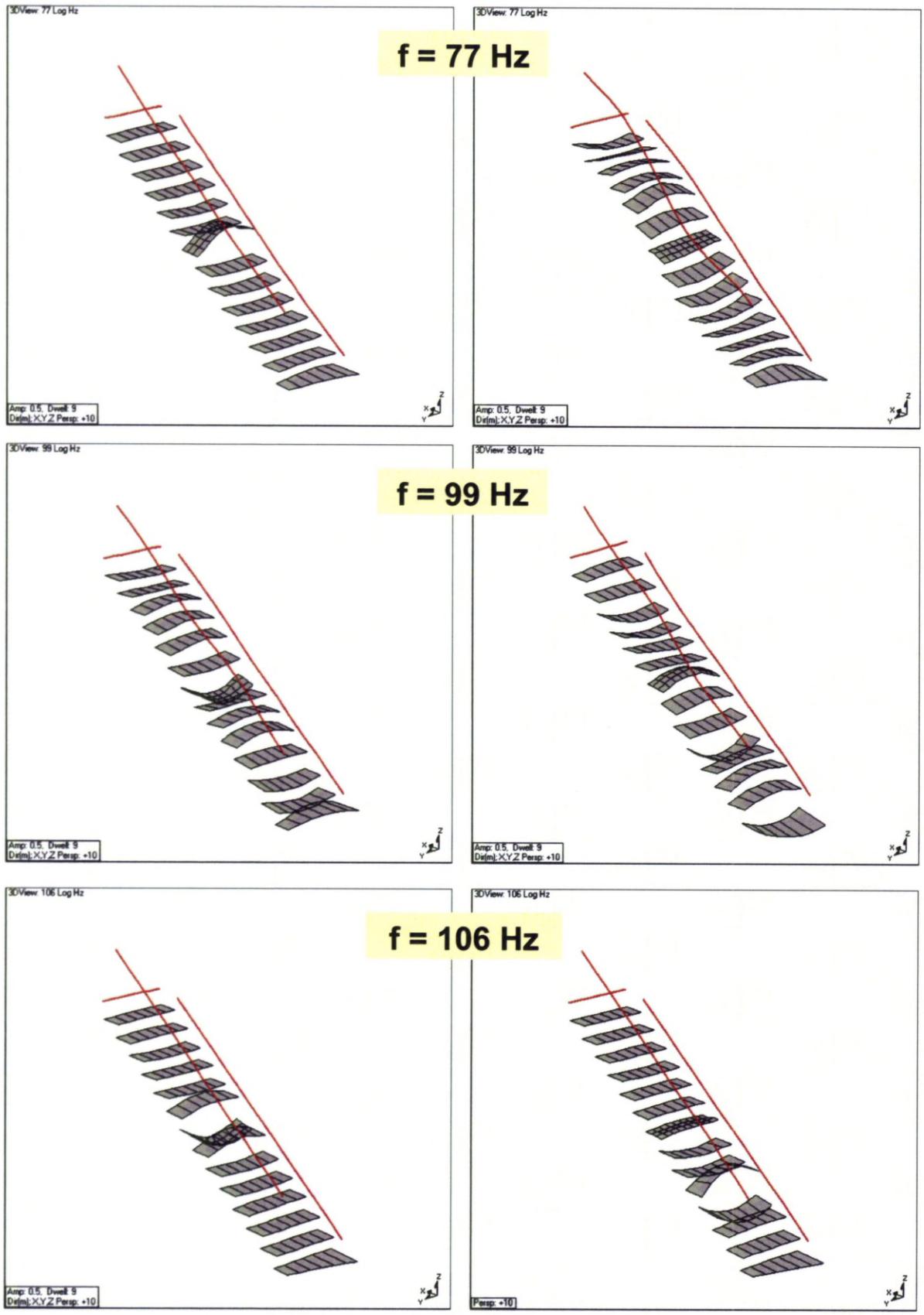
3DView: 77 Log Hz
f = 77 Hz
3DView: 77 Log Hz
Amp: 0.5, Dwell: 9
Dir(m): X,Y,Z Persp: +10
Amp: 0.5, Dwell: 9
Dir(m): X,Y,Z Persp: +10
3DView: 99 Log Hz
f = 99 Hz
3DView: 99 Log Hz
Amp: 0.5, Dwell: 9
Dir(m): X,Y,Z Persp: +10
Amp: 0.5, Dwell: 9
Dir(m): X,Y,Z Persp: +10
3DView: 106 Log Hz
f = 106 Hz
3DView: 106 Log Hz
Amp: 0.5, Dwell: 9
Dir(m): X,Y,Z Persp: +10
Persp: +10

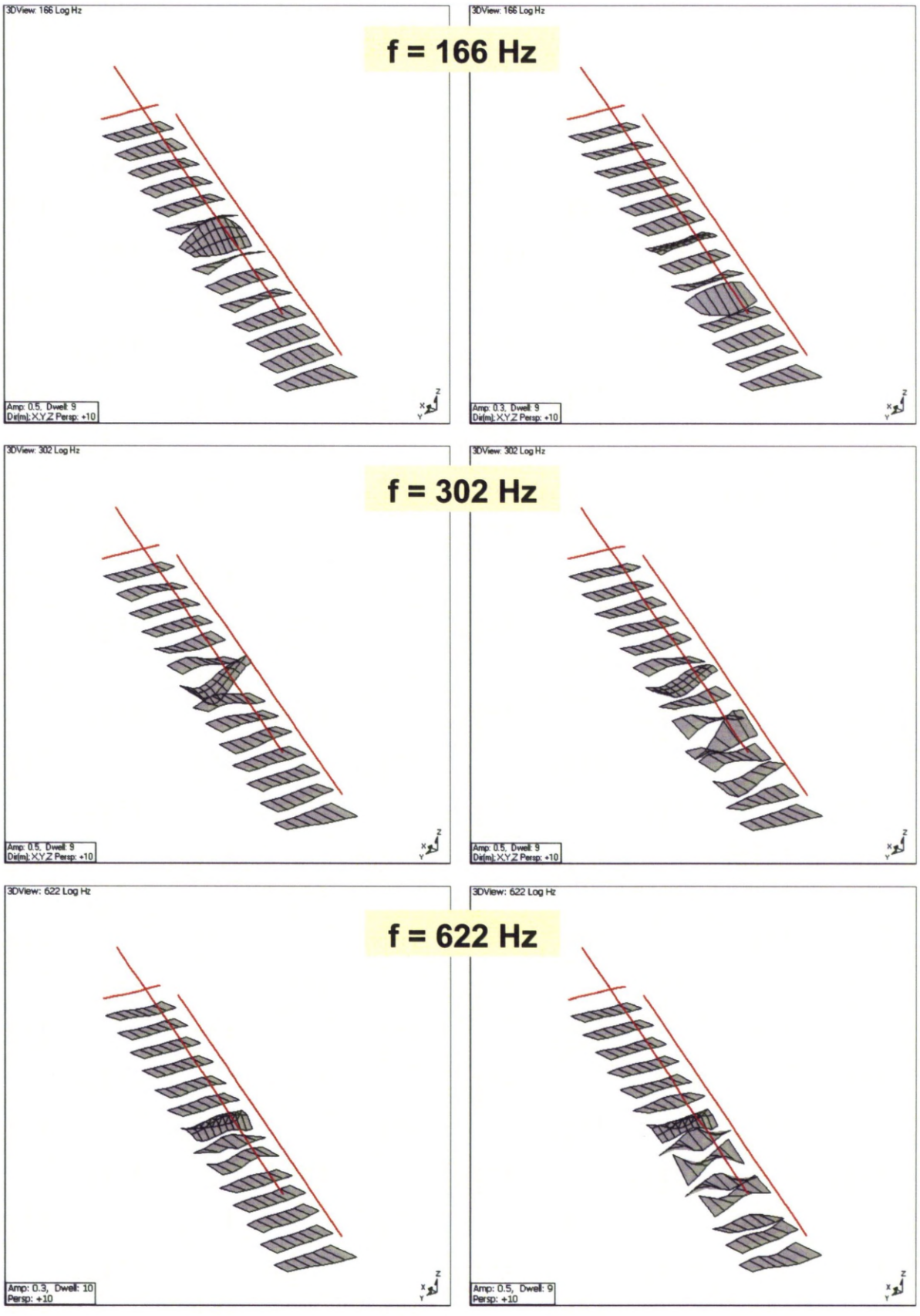

Figure 3.24: Stair mode shapes from experimental modal analysis

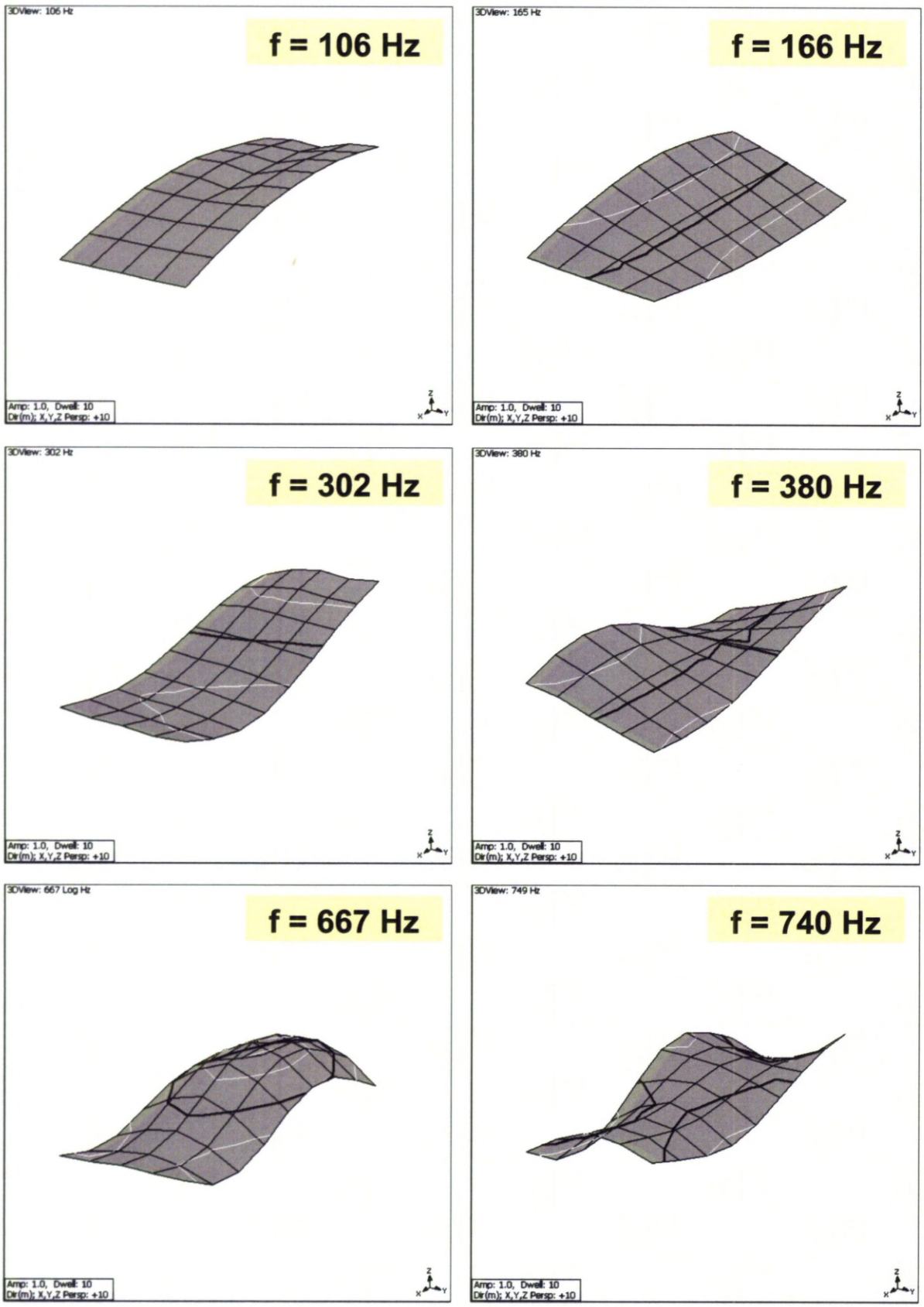

Figure 3.25: Step 8 mode shapes from experimental modal analysis

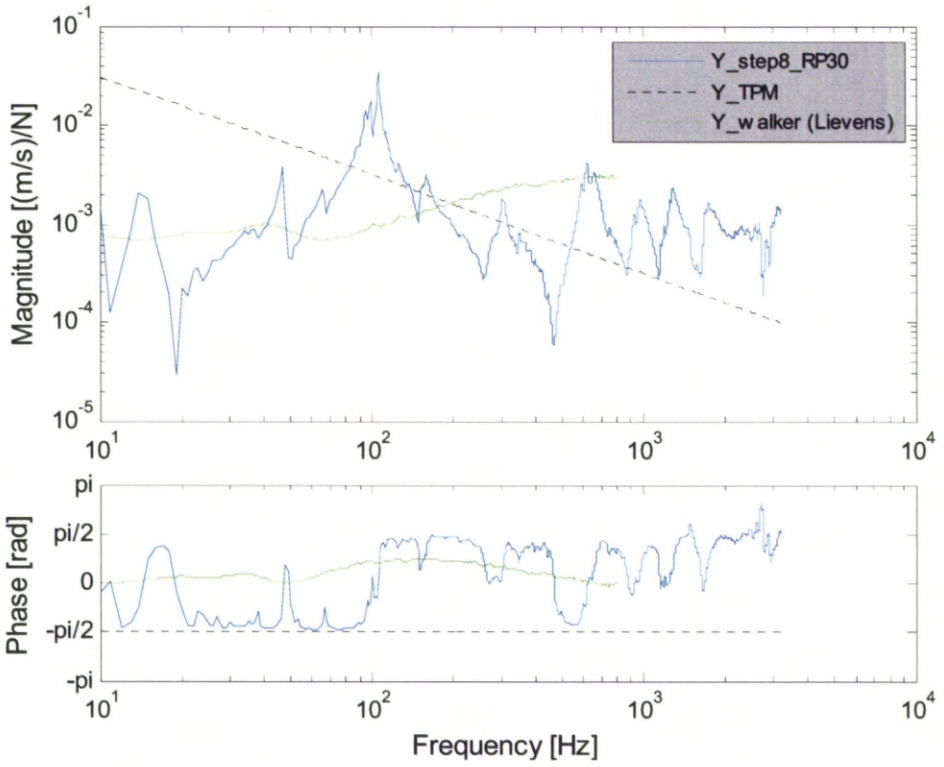

Figure 3.26: Point mobility near the centre of step 8 (blue), mass mobility of a 500 g hammer (black) of the tapping machine and walker mobility (green) according to [24]

4 COMPONENTS OF EXCITATION BY INDIRECT MEASUREMENT

4.1 INTRODUCTION

In total six components of excitation can contribute to the excitation of receiving structures by structure-borne sound sources. Knowledge of the respective contributions of forces and moments is essential in order to reduce noise problems e.g. by isolation of the contacts and for providing input data for prediction models. As the structure-borne sound transmission is generally dependent on the structural dynamics of the source and the receiver, the contributions of the individual components can vary, depending on the actual coupling condition. Hence an experimental investigation of the in-situ power provides a foundation to the understanding of and solution to the problem. If a particular situation is representative then, importantly, simplifications to the characterisation of structure-borne sound sources can be deduced from case studies, such as in the identification of the dominant component(s) of excitation.

Direct measurement of the component power transmission is difficult or even impossible because of practical problems in registering forces and moments directly.

In this chapter a reciprocal method [1]-[3] is developed which yields the power through each excitation point and component by means of an indirect

approach where problems in registering forces and moments directly are circumvented.

The reciprocal measurement of the components and respective powers was experimentally investigated on an isolated reception plate and on a real wall represented by the laboratory stair wall. The method could be validated for the determination of the dominant force component of a shaker source which is the basis for the determination of the component power flow of a vibrating lightweight stair in Chapter 5.

4.2 THEORY AND PREVIOUS APPLICATIONS OF RECIPROCITY IN VIBRO-ACOUSTICS

The reciprocity principle states that the response of a linear system to a time-harmonic disturbance that is applied at some point by an external agent is invariant with respect to exchange of the points of input and observed response [4]. The general prerequisite of reciprocity relations is that the product of the variables to be interchanged yields the power. In the literature this is often termed the principle of mutual energy [5].

Acoustic reciprocity was first considered by Helmholtz 1860 regarding sound transmission through pipes [6]. A general theory of reciprocity for vibrating systems was formulated by Rayleigh [7], [4] in 1873 in succession to the earlier work by Helmholtz. Lyamshev published a formal proof of these assumptions in 1959 [8] and stated that any (linear) vibrating structure can be incorporated in the reciprocal system. This paved the way for many of the modern applications of the principle to vibroacoustic problems. Before

that, the most important and recognised application was the calibration of electro-acoustical transducers like microphones.

A general derivation of the principle from four-pole theory was given by ten Wolde in 1973 [9]. The field of application, as used by Wolde and Verheij, was sound transmission in ships [10]-[12]. Thus most of the studies were confined to the vibro-acoustical reciprocity involving sound radiation of vibrating structures. An example for vibro-acoustical reciprocity for elastic structures excited by point force, after [13], is illustrated below:

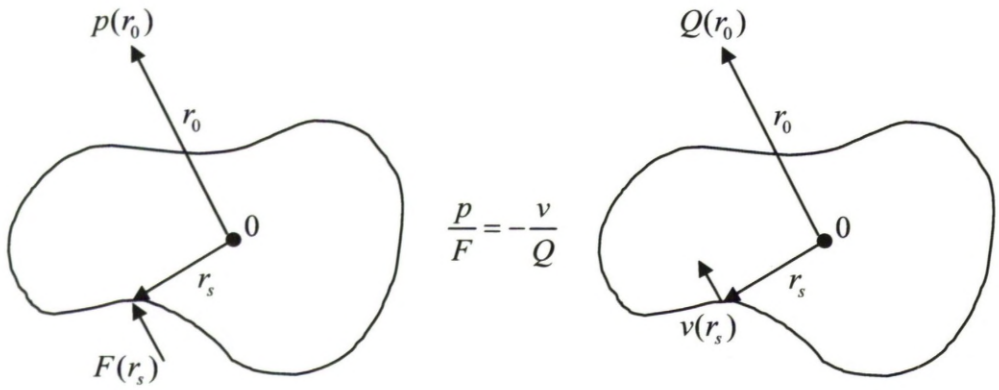

The ratio of sound pressure to applied force is equal in magnitude and opposite in sign to the ratio of acoustically induced response velocity in the force direction to the volume velocity (source strength) of the source.

By use of reciprocity principles, difficulties in the measurement of transfer functions, such as results from difficulties in separation and identification of excitation components, can be overcome. An illustrative example is the measurement of the sound transmission from a position on a machinery seating on a ship to a distant location in the water [10]. In the reciprocal

measurement the direct generation of forces is not required but replaced by the generation of an acoustic sound field and measurement of the velocities at the position of interest using triaxial accelerometers. It is an interesting fact that sufficiently high input levels were achieved by use of explosives.

A comprehensive review of the development of reciprocal methods, with applications to vehicle acoustics and to sound source identification at complex vibrating structures, is given by Fahy 1995 [11] and supplemented by more practical applications in 2003 [13]. Based on Rayleigh's work, he derived reciprocity for dipole sources and confirmed the validity of the principle for vibrating fluid-structure boundaries. It was concluded that a prime aim of further research should be to establish the accuracy and reliability of reciprocal measurement techniques. In the above example an obvious experimental difficulty is the generation and precise measurement of an omni-directional volume velocity.

Within recent decades an increasingly important field of application of reciprocal methods has been in the quantification of sound paths e.g. in vehicles [14], and the characterization of noise sources [15] which is also the purpose in this thesis. The vibrational reciprocity principles are given by Rayleigh [4] as follows:

Type 1

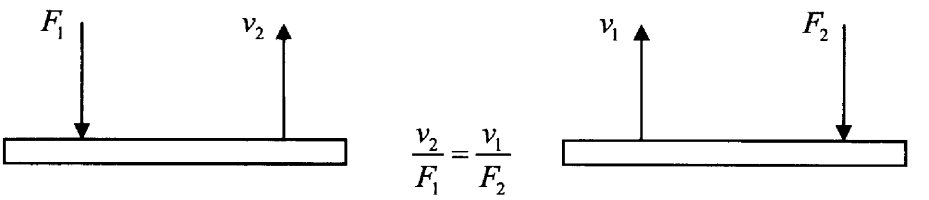

The ratio of velocity at a point 2, generated by a force at point 1, is equal to the ratio of the velocity at point 1 resulting from a force at point 2. The source and receiver positions are interchangeable in the measurement of transfer mobilities.

Type 2

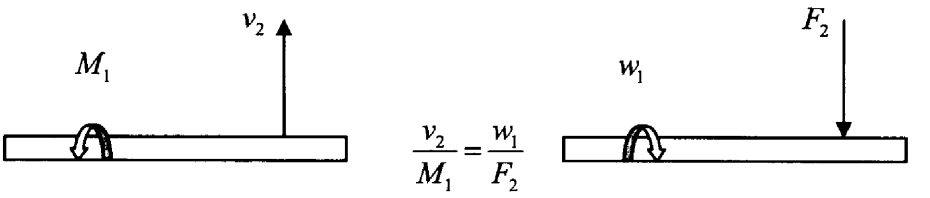

The ratio of translational velocity at a point 2, generated by a moment at point 1, is equal to the ratio of the angular velocity at point 1, generated by a force at point 2.

It will be demonstrated that by use of these two reciprocity principles practical measurement difficulties in the determination of contact forces and moments are avoided.

4.3 APPLICATION TO SINGLE AND MULTIPLE POINT/COMPONENT SOURCES

4.3.1 Coordinate system

In total six components of excitation and response, three translations and three rotations, can contribute to the structure-borne sound transmission. In Figure 4.1 is shown the Cartesian coordinate system as used for the measurements, indicating positive and negative directions. The origin was set to the lower left corner. F_x, F_y, F_z and v_x, v_y, v_z are the forces and velocities whereas M_x, M_y, M_z and w_x, w_y, w_z are the moments and angular velocities.

4.3.2 Single point and component of excitation

In the simplest case a structure-borne sound source is connected to a supporting structure via a single point and exhibits only a translational force F_e. Under action of this force the translational response velocity at the contact point e is v_e. The active power transmitted through the contact is given by the real part of the cross spectrum of force and velocity [1].

$$P_{F_{e,z}} = \frac{1}{2}\mathrm{Re}\left\{F_{e,z} \cdot v_{e,z}^{*}\right\} \tag{4.1}$$

This requires the installation of an intervening force transducer which can be difficult or even impossible. In addition, the installation of a force transducer can change the contact condition. In contrast, measurement of the contact

velocity is not a practical problem. By use of a matched accelerometer pair the contact velocity can be approximated by averaging the velocities around the contact.

Consider an arbitrary point r remote from the excitation point. The translational response velocity at this point is v_r.

$$P_{F_{e,z}} = \frac{1}{2}\mathrm{Re}\left\{\frac{F_{e,z} \cdot v_{e,z}^{*} \cdot v_{r,z}}{v_{r,z}}\right\} \tag{4.2}$$

The ratio of contact force and velocity at the remote point is termed the transfer mobility between the contact and the remote position. The power transmitted through the contact can then be expressed as:

$$P_{F_{e,z}} = \frac{1}{2}\mathrm{Re}\left\{Y_{v_{r,z}F_{e,z}}^{-1} \cdot v_{e,z}^{*} \cdot v_{r,z}\right\} \tag{4.3}$$

By use of reciprocity principle Type 1 the transfer mobility can be measured in the opposite direction by excitation of the remote point and registration of the velocity at the contact point.

$$P_{F_{e,z}} = \frac{1}{2}\mathrm{Re}\left\{Y_{v_{e,z}F_{r,z}}^{-1} \cdot v_{e,z}^{*} \cdot v_{r,z}\right\} \tag{4.4}$$

This re-arrangement converts the problem of direct force measurement to transfer mobility and velocity cross-spectrum measurements. Transfer mobilities can easily be measured using a calibrated hammer and a pair of matched accelerometers. Equally the measurement of the velocity cross-spectrum is unproblematic.

The contact force is obtained from the transfer mobility and the velocity spectrum at the remote point with the structure-borne sound source in operation.

$$F_{e,z} = Y^{-1}_{v_{e,z}F_{r,z}} \cdot \left| v_{r,z} \right| \tag{4.5}$$

By use of the auto spectrum of the remote point velocity the force is yielded as complex value with phase reference to the remote point.

4.3.3 Multiple points and components of excitation

Sources of structure-borne sound often have more than one contact point and the excitation is not restricted to the perpendicular force. Referring to the co-ordinate system in Figure 4.1 F_x, F_y and M_z are termed the in-plane components. Previous investigations on a variety of practical sources, such as fans [1] - [3], whirlpools [17] - [19], and bathroom ceramics [20], [21] indicate that the power of in-plane components are at least one order of magnitude below the dominant component and can thus be neglected.

Consequently the following expansion of the reciprocal method is restricted to the perpendicular force F_z and two moments M_x and M_y.

Consider the combined force and moment excitations at a single contact, each resulting in a translational and rotational response in the corresponding directions. The net active power is then given as the sum of the component powers.

$$P = \frac{1}{2}\mathrm{Re}\left\{ F_{e,z} \cdot v^*_{e,z} + M_{e,x} \cdot w^*_{e,x} + M_{e,y} \cdot w^*_{e,y} \right\} \tag{4.6}$$

Three remote points r_1, r_2, r_3 are now required for a solvable linear equation system. The translational velocities at the remote points with the source in operation result from a superposition of all components.

$$\begin{Bmatrix} v_{r1,z} \\ v_{r2,z} \\ v_{r3,z} \end{Bmatrix} = \begin{bmatrix} Y_{v_{r1,z}F_{e,z}} & Y_{v_{r1,z}M_{e,x}} & Y_{v_{r1,z}M_{e,y}} \\ Y_{v_{r2,z}F_{e,z}} & Y_{v_{r2,z}M_{e,x}} & Y_{v_{r2,z}M_{e,y}} \\ Y_{v_{r3,z}F_{e,z}} & Y_{v_{r3,z}M_{e,x}} & Y_{v_{r3,z}M_{e,y}} \end{bmatrix} \cdot \begin{Bmatrix} F_{e,z} \\ M_{e,x} \\ M_{e,y} \end{Bmatrix} \tag{4.7}$$

The second and third rows of the transfer mobility matrix contain cross-transfer terms which would normally require a moment excitation at the contact point. By virtue of reciprocity the moment cross-transfer mobilities can be replaced by its associated force cross-transfer mobilities referring to reciprocity principle Type 2. The second and third columns are replaced by reciprocal equivalents and the components of excitation are then obtained from inversion of the transfer mobility matrix.

$$\begin{Bmatrix} F_{e,z} \\ M_{e,x} \\ M_{e,y} \end{Bmatrix} = \begin{bmatrix} Y_{v_{e,z}F_{r1,z}} & Y_{w_{e,x}F_{r1,z}} & Y_{w_{e,y}F_{r1,z}} \\ Y_{v_{e,z}F_{r2,z}} & Y_{w_{e,x}F_{r2,z}} & Y_{w_{e,y}F_{r2,z}} \\ Y_{v_{e,z}F_{r3,z}} & Y_{w_{e,x}F_{r3,z}} & Y_{w_{e,y}F_{r3,z}} \end{bmatrix}^{-1} \cdot \begin{Bmatrix} v_{r1,z} \\ v_{r2,z} \\ v_{r3,z} \end{Bmatrix} \tag{4.8}$$

In order to obtain the phase relationship between the excitation components, remote point r_1 is selected as reference. In principle any remote point or component can be chosen as reference. For numerical and practical convenience a translational response perpendicular to the receiving structure is preferred. With the structure-borne sound source in operation the velocity transfer functions between r_1, r_2, r_3 are determined. The components are then obtained as complex values, phase linked to r_1.

$$\begin{Bmatrix} F_{e,z} \\ M_{e,x} \\ M_{e,y} \end{Bmatrix} = \begin{bmatrix} Y_{v_{e,z}F_{r1,z}} & Y_{w_{e,x}F_{r1,z}} & Y_{w_{e,y}F_{r1,z}} \\ Y_{v_{e,z}F_{r2,z}} & Y_{w_{e,x}F_{r2,z}} & Y_{w_{e,y}F_{r2,z}} \\ Y_{v_{e,z}F_{r3,z}} & Y_{w_{e,x}F_{r3,z}} & Y_{w_{e,y}F_{r3,z}} \end{bmatrix}^{-1} \cdot \begin{Bmatrix} 1 \\ \varphi(v_{r1,z}, v_{r2,z}) \\ \varphi(v_{r1,z}, v_{r3,z}) \end{Bmatrix} \cdot \left| v_{r1,z} \right| \tag{4.9}$$

The velocities at the contact point also can be obtained as complex values, phase linked to r_1 from velocity transfer functions.

$$\begin{Bmatrix} v_{e,z} \\ w_{e,x} \\ w_{e,y} \end{Bmatrix} = \begin{Bmatrix} \varphi(v_{r1,z}, v_{e,z}) \\ \varphi(v_{r1,z}, w_{e,x}) \\ \varphi(v_{r1,z}, w_{e,y}) \end{Bmatrix} \cdot \left| v_{r1,z} \right| \tag{4.10}$$

Accordingly, the component powers can be expressed as:

$$\begin{aligned} P_{F_{e,z}} &= \frac{1}{2} \mathrm{Re}\left\{ F_{e,z} \cdot \left| v_{r1,z} \right| \cdot \varphi^*(v_{r1,z}, v_{e,z}) \right\} \\ P_{M_{e,x}} &= \frac{1}{2} \mathrm{Re}\left\{ M_{e,x} \cdot \left| v_{r1,z} \right| \cdot \varphi^*(v_{r1,z}, w_{e,x}) \right\} \\ P_{M_{e,y}} &= \frac{1}{2} \mathrm{Re}\left\{ M_{e,y} \cdot \left| v_{r1,z} \right| \cdot \varphi^*(v_{r1,z}, w_{e,y}) \right\} \end{aligned} \tag{4.11}$$

The total active power can also be written as [1]:

$$P = \frac{1}{2} \mathrm{Re}\left\{ \left| v_{r1,z} \right|^2 \cdot \left\{ \varphi^*(v_{r1,z}, v_{e,z}) \varphi^*(v_{r1,z}, w_{e,x}) \varphi^*(v_{r1,z}, w_{e,y}) \right\} \cdot \left[Y_r \right]^{-1} \cdot \begin{Bmatrix} 1 \\ \varphi(v_{r1,z}, v_{r2,z}) \\ \varphi(v_{r1,z}, v_{r3,z}) \end{Bmatrix} \right\}$$

(4.12)

In the general case m degrees of freedom and n contact points can be considered. This will require m x n remote points and result in a $(m \times n)^2$ mobility matrix. The method lends itself to the use of over-sampling, where additional remote points can be considered to give second, third, etc. estimates of the contact force and moments. By averaging of components

the accuracy can be improved especially when remote positions are on nodal points.

4.4 MOBILITY MEASUREMENT

Methods for mobility measurement can be divided into two types: contacting and non contacting [22]. The first involves connection of an exciter to the structure [23]. Electromagnetic shakers are commonly used as exciters. The shaker can either be driven with a stationary signal, random noise or swept sine, or with a transient signal, a pulse or chirp, to give a broadband frequency response function. The second type includes devices which are either out of contact throughout the vibration (such as provided by a non-contacting electromagnet) or which are only in contact for a short period, while the excitation is being applied, such as a blow by an impact hammer [24]. In both cases the measurement involves a force transducer. As long as the structure under investigation behaves linearly, both methods in principle yield the same result.

Using an instrumented hammer is more convenient than the use of electromagnetic shakers since it is much easier to change the location of an applied force. In addition less equipment is required. A disadvantage is that the accuracy of results is dependent upon the consistency of the operator's technique. There are difficulties in avoiding unwanted excitation by other components not under consideration.

In this study, mobility measurements mainly involved impulse excitation. An impact hammer type 8202 with piezoelectric force transducer 8200

(Brüel&Kjaer) was used with a steel tip to provide a broadband excitation. Each measurement was obtained as an average of four hammer hits.

Stationary excitation was employed for comparison and the validation of reciprocity. Moreover the comparison provided an additional check of calibration. An electromagnetic inertial shaker of type IV 45 (Gearing & Watson), with a force vector of 50 N, was used whenever stationary excitation was required. A piezoelectric force transducer of type 9331 (Kistler) was inserted between shaker and test structure.

The shaker source also was used for comparison of different methods of estimating the power into receiving structures. The shaker power could be measured directly and thus constitutes the real imparted power within the limits of experimental error. This value was used as a benchmark for assessment of the accuracy of the indirect methods, including the reciprocal method.

4.4.1 Instrumentation and measurement procedure

For experimental investigations, a PULSE system (Brüel&Kjaer), with four input channels, was used in combination with a conditioning amplifier of type Nexus (Brüel&Kjaer). Generally input channel 1 was used to measure force and channels 2, 3 and 4 to measure acceleration which was converted into velocity by mathematical integration in the PULSE software. The input channels 3 and 4 of the PULSE Frontend are phase matched within 0,2° and were thus used for determination of the rotational components by the finite difference method using a pair of matched accelerometers. The

frequency range was generally 0 – 3200 / 6400 Hz with a resolution of 1 Hz. Results presented in 3rd octave bands were obtained from conversion of the narrow band values. In terms of power the conversion into 3rd octave bands was performed by summing up the narrow band values within the upper and lower frequency band limits taking only positive real parts into account. Most evaluations were performed with the software MatLab.

4.4.2 Calibration

Accelerometers were calibrated using a standard calibrator of type 4294 (Brüel&Kjaer) with a calibration frequency of 159,2 Hz and 10 m/s^2 acceleration amplitude e.g. 10 mm/s velocity amplitude. The matching of the accelerometers was checked by putting one accelerometer on top of the other (Figure 4.2).

In Figure 4.3 are shown the auto spectra of the measured velocities with a calibration signal of 10 mm/s. The peaks at distinct frequencies are thought to result from a rocking motion.

In Figure 4.4 are shown the magnitude and phase differences of the velocity transfer functions with reference to the accelerometer (channel 2) directly attached to the calibrator. Except at the very low frequencies the difference in magnitude is generally within ± 0.1 dB and that in phase is generally within ± 0.2°.

In contrast to accelerometers, there is no standard calibrator for force transducers available. In-situ calibration, after assembly of hammer/shaker

and force transducer, is necessary because the force output of the crystals will always be slightly different from that transmitted to the structure. This is because a fraction of the force detected by the crystals will be used to move the small amount of material between the crystals and the structure resulting in an apparent reduction of the sensitivity. Apart from that the system calibration indicates the directionality of the transducers which is not always known but required since incorrect adjustment will result in a phase error of 180°.

The standard calibration procedure involves excitation of a known rigid mass and simultaneous measurement of force and acceleration. From Newton's second law, the mobility of a pure mass is given by:

$$Y_{mass} = \frac{1}{j\omega m} \tag{4.13}$$

A freely suspended concrete block of 8 kg was used for calibration. In Figure 4.5 is shown the set-up for hammer excitation. A typical result for the measured mobility is shown in Figure 4.6. The measured magnitude and phase of the mobility agree with the known value within ± 5% and thus conform to the standard [24].

In Figure 4.7 is shown the set-up for mobility measurements with the shaker. To ensure a rigid contact a small aluminium indenter, with a threaded hole for attachment of the force transducer, was glued on the concrete block. To avoid excitation by moments, a thin drive rod (piano wire) was inserted. The same mounting technique was applied for the

experiments involving receiver plates when moment excitation was unwanted.

The shaker was driven with random noise. Time domain weighting of the signals using a Hanning window was applied. In Figure 4.8 is shown the measured and expected mobility. The agreement is satisfactory except in the frequency range above 2 kHz where the transmitted force is too low to give a sufficient signal to noise ratio in the response acceleration.

4.4.3 Transfer mobility measurement

The accuracy of the reciprocal method is dependent on the agreement between directly and reciprocally measured transfer mobilities. In practice the agreement is strongly dependent on the "quality" of the measurement.

As direct access to the contact points of source and receiver is not possible in the mounted condition the velocity at the contact point is approximated as the average of two accelerometer signals at equal distance around the contact according to:

$$v_{e,z} = 0.5\left(v_{x2,z} + v_{x1,z}\right) = 0.5\left(v_{y2,z} + v_{y1,z}\right) \tag{4.14}$$

Consequently the transfer mobility from a fixed reference position to the contact point is obtained as average of the respective transfer mobilities:

$$Y_{v_{e,z}F_{r,z}} = 0.5\left(Y_{v_{x2,z}F_{r,z}} + Y_{v_{x1,z}F_{r,z}}\right) \tag{4.15}$$

4.4.4 Cross-transfer mobility measurement

The experimental determination of cross-transfer mobilities involves the measurement of rotational acceleration. Besides the use of rotational accelerometers a widely accepted technique is based on the finite difference principle [5]. This involves a pair of matched accelerometers situated in equal distance around the contact point which is the same arrangement as for the previously described transfer mobility measurement. Direct access to the contact point is again not required which is an apparent advantage compared to the measurement with a rotational accelerometer.

Consider a rotation around the contact point e in x-direction (Figure 4.1). The angular velocity is:

$$w_{e,x} = \dot{\varphi}_{e,x} = \frac{\partial \varphi_{e,x}}{\partial t} \tag{4.16}$$

For small angles φ:

$$\tan \varphi_{e,x} = \frac{\partial \xi_{e,z}}{\partial y} \approx \varphi_{e,x} \tag{4.17}$$

Thus:

$$w_{e,x} = \frac{\partial}{\partial t}\left(\frac{\partial \xi_{e,z}}{\partial y}\right) = \frac{\partial v_{e,z}}{\partial y} \approx \frac{1}{y2 - y1}\left(v_{y2,z} - v_{y1,z}\right) \tag{4.18}$$

The optimal distance between the two accelerometers is determined by the governing bending wavelength on the receiving structure. The distance must be significantly smaller than the bending wavelength which sets an upper frequency limit of applicability for a given distance. At low frequencies

the bending wavelength is large and the variation of the translational velocity with distance is relatively small. A too small distance therefore leads to a subtraction of similar values which tends to result in large errors. A compromise is suggested by [5] as a distance of 1/10 to 1/20 of the bending wavelength. In the present investigations an accelerometer distance of 10 cm was chosen as approximately one tenth of the bending wavelength at 1 kHz on the investigated receiver plates.

A direct experimental verification of the reciprocity relationship e.g. $Y_{w_{e,x}F_{r,z}} = Y_{v_{r,z}M_{e,x}}$ could not be performed in absence of a useful moment source. However, the validity of reciprocity in terms of cross-transfer mobility measurement as well as the accuracy of measurement has been confirmed experimentally in [1].

4.5 SHAKER SOURCE ON ISOLATED RECEPTION PLATE

For the validation of the reciprocal method, a shaker with force transducer was first connected to an isolated reception plate (10 cm reinforced concrete, density 2300 kg/m^3). This kind of plates is currently used in laboratories for the simplified characterisation of structure-borne sound sources using the reception plate method [17]-[19]. As such the dynamic characteristics of this plate are well understood from previous investigations. By knowledge of the vibration behaviour it was possible to keep away from nodal lines. Due to the isolation the plate vibrates as a free plate and by placing the shaker near a corner (Figure 4.9) the excitation of all plate modes was ensured in the frequency range of interest. The shaker was connected to the plate directly without inserting a piano wire. On the one hand this was due to practical difficulties on the other hand a (small) contribution of moments was affected. The excitation (e) and response positions (r_1, r_2, r_3) are indicated in Figure 4.10.

The simple shaker source had the advantage that the force perpendicular to the plate and thus the associated power could be measured directly and compared with the estimates obtained from the reciprocal method. The force and power measurements are unbiased by airborne radiation since the shaker behaved as a poor sound radiator and there is no significant transmission via flanking paths. The excitation strength could be controlled and adjusted to the dynamic characteristics of the excited structure such that the response velocity was well above background noise. In order to provide a broadband excitation the shaker was driven with random noise.

4.5.1 Direct force and power measurement

The power transmitted by a force perpendicular to the receiving plate through a single contact equals the real part of the cross-spectrum of translational force and velocity at the contact point (4.1). Using a shaker source and stationary excitation the measurement set-up is actually the same as for point mobility measurements the only difference is the post-processing of the signals. Thus the mobility calibration as described in 4.4.2. is also meaningful in terms of a power calibration.

In the application of the reciprocal method, measurements were recorded in sequence as a maximum of four channels was available (seven channels would have been required for the simultaneous measurement of 3 components and one contact point). Thus it was necessary to ensure that the excitation was constant during the measurements and the force was monitored for drift throughout the measurements.

In Figure 4.11 is shown the force spectra for excitation of the isolated reception plate as single values and as the mean value. Also indicated is the maximum deviation. The variation is within 0.5 dB and the force is well represented by the mean value. The variation in force is reasonably flat within the frequency range 30 Hz - 2 kHz. The peaks around 20 Hz and 4 kHz are attributed to the construction of the shaker (e.g. suspension of the coil) and the coupling with the receiver. The resonance frequencies however are not critical, except for the drop-off at high frequencies. In Figure 4.12 is shown the directly measured power as mean value and single measurements and the maximum deviation of all measurements. The

variation of the power is within 0.5 dB in the frequency range up to 1 kHz and increases at higher frequencies. Well above the second resonance peak the force is too small such that the velocity at the contact is biased by background noise and thus the evaluated power is discounted.

4.5.2 Prediction of the plate mobility

For high mobility sources the transmitted power is proportional to the magnitude of force squared and the receiver mobility at the contact point [5]. As the shaker constitutes a high mobility source, for excitation of the reception plate, the power in Figure 4.12 is composed of the blocked force in Figure 4.11 and the mobility at the shaker contact. The latter is shown in Figure 4.13 along with the predicted mobility using a modal summation approach described in [29]. In the frequency range from 30 Hz – 2 kHz the effect of structural modes on the transmission is apparent. Peaks in the power result from peaks in the (measured) mobility.

The receiver mobility of plate structures are normally not measured before the installation of structure-borne sound sources in buildings. Therefore, a predicted value is required in order to obtain the structure-borne power and thence the transmission and radiation into receiver rooms. The predicted point mobility was obtained using data from the literature [25] (c_L = 3400 m/s, μ = 0.2, ρ = 2500 kg/m^3) and the measured total loss factor. Measurement and prediction are in good agreement which is promising.

4.5.3 Direct and reciprocal transfer mobility

In Figure 4.14 is shown a typical result for the directly (with shaker excitation) and reciprocally (with hammer excitation) measured transfer mobility on the horizontal reception plate with the reference point r_1. Figure 4.15 shows the respective magnitude and phase differences. In the frequency range 20 Hz - 1 kHz the difference in magnitude is generally within ± 2 dB. At higher frequencies the difference is greater. This is expected when the excitation or response position is at a nodal line. If for example the excitation is at a node then the resulting velocity will be zero irrespective of the force magnitude. As the forces, obtained by the shaker and hammer, differ by a factor of about 1000, large discrepancies are expected for the respective mobilities at antiresonances. Similarly discrepancies will also arise when the response transducer is at a nodal line. Another reason for the increasing difference with frequency is that the area of excitation is different for hammer and shaker this becomes a controlling factor at higher frequencies, due to local deformation effects. This is described in the literature as the local stiffness effect [27], [28]. Furthermore at high frequencies the distance of the accelerometers, which was 100 mm in this experiment, approaches the governing wavelength, causing aliasing [1]. For the same reason even small variations in the excitation position that are inevitable regarding the hammer excitation tend to result in increased errors at high frequencies. This is confirmed by the coherence, an example measurement is shown in Figure 4.16. At high frequencies the coherence is significantly greater for shaker excitation than for hammer excitation.

4.5.4 Perpendicular force and force-induced power

The initial measurements and evaluations were performed under the assumption of a single point and component of excitation represented by the perpendicular force F_z as outlined in Chapter 4.3.2. Hence the measurements comprised only one transfer mobility measurement and velocity transfer function with the reference point being r_1. The force is obtained from inversion of a 1x1 mobility matrix containing the reciprocally measured transfer mobility (4.5).

Figure 4.17 shows the comparison with the directly measured force and that obtained from reciprocal measurement of the transfer mobility. The difference (obtained by 10lg) in the two estimates of the force mirrors that of the transfer mobility measurement (Figure 4.18).

In Figure 4.19 are shown the respective force induced powers and in Figure 4.20 the differences as narrow band values and 3rd octave bands. The reciprocally measured force induced power is generally in good agreement with the direct measurement. At single frequencies differences of up to 10 dB occur due to the 1 Hz frequency resolution. The 3rd octave band values agree within ± 2 dB.

At certain frequencies there are discontinuities in the narrow band values of reciprocal force. Discontinuities[1] in the power indicate negative real parts

[1] The conspicuous points in the graphs represent values at single frequencies which are displayed bold because of poor compatibility of the MatLab software and Microsoft Word.

which can be interpreted as negative powers (out of the reception plate). This is partly the result of experimental error. As the method relies on the complex spectra of the transfer mobility and velocity transfer function, any discrepancy can cause an inversion of sign of the power during computation. For the pure force excitation, of a high mobility source such as might be possible by the shaker connected via a thin piano wire, the power transmitted is given by (4.19).

$$P = \frac{1}{2} \cdot |F|^2 \cdot \mathrm{Re}\left\{ Y_{v_{e,z}F_{e,z}} \right\} \tag{4.19}$$

As the force squared is not complex, negative powers can only result from negative real parts in the point mobility. In the reciprocal method the point mobility is computed from the transfer mobility and velocity transfer function to the reference point, where

$$Y_{v_{e,z}F_{e,z}} = Y_{v_{e,z}F_{r,z}} \cdot \varphi(v_{r,z}, v_{e,z}) \tag{4.20}$$

In Figure 4.21 are shown the real parts of the directly and reciprocally measured point mobility. The negative real parts in the reciprocal transfer mobility mainly correspond to those in the reciprocal power curve in Figure 4.19. From this it can be concluded that experimental errors in the complex transfer function measurements primarily cause the gaps in the power curve. The discrepancy in force is more conspicuous than in power. This is probably due to the fact that the cross-spectrum in the power expression includes the cross-correlation in the velocity transfer functions and is thus less sensitive to random error.

In addition to experimental error, negative powers may result when the structure is being energised by excitation components other than those under consideration. In the case considered only the force component is assumed. However a contribution of moments M_x and M_y could arise from the stiff connection of the shaker and supposed that the shaker is not performing a pure translational motion. Furthermore a contribution of F_z, M_x, M_y was assumed a priori for the sound transmission from lightweight stairs. Therefore those components also comprised the validation of the reciprocal method in a second experiment as follows.

4.5.5 Moments and moment-induced powers

For the evaluation of 3 components, 9 complex transfer / cross-transfer mobilities and 5 complex velocity transfer functions were recorded again for remote points r_1, r_2, r_3 and r_1 as reference point. As previously, inversion of the transfer mobility matrix yielded the complex components of excitation.

In Figure 4.22 the reciprocal estimate of the force is compared with the direct measurement. In the frequency range up to 1,6 kHz the agreement is generally within ± 2 dB. The deviations are less compared with the one - component assumption (Figure 4.17). For the one component assumption, it was shown that the deviation of the reciprocally obtained force can be attributed to inaccuracies in the reciprocally measured transfer mobility. For the three-component assumption, this interpretation is not so obvious since the accuracy of the force determination also depends on the accuracy of the cross-transfer mobility measurement. However as the force is dominant it is

expected that the accuracy of the measured transfer mobilities determines that of the force determination. The better agreement of force for the three component assumption could then be referred to an averaging effect as three transfer mobilities are involved here instead of one in the previous evaluation.

The component powers and the directly measured force induced power are shown in Figure 4.23 as narrow band values and in Figure 4.24 in 3rd octave bands. In Figure 4.25 are shown the respective level differences.

The reciprocally measured force induced power is generally in good agreement with the direct measurement and the (apparent) moment induced powers are generally 10-20 dB below the force induced power. The moment induced power curves are less continuous which is expected for a non-dominant component.

In comparison to the one component assumption the reciprocal force power curve is less smooth and has more gaps that occur primarily at antiresonances. The agreement in 3rd octave band is again within ± 2 dB.

To give insight into the consequence of experimental error, the reciprocally measured transfer mobilities $Y_{v_{e,z}F_{r,z}}$ in the first column of the mobility matrix were replaced by directly measured values. This means that the transfer mobilities $Y_{v_{e,z}F_{r,z}}$ and the transmissibilities between the remote points $\varphi(v_{r1,z}, v_{r2,z})$ and $\varphi(v_{r1,z}, v_{r3,z})$ result from the same measurement and thus phase errors are significantly reduced in the evaluation of the force component and respective power. The remaining elements in the mobility

matrix and velocity transfer functions were the same as in the previous evaluation. Figure 4.26 shows the component powers using these unbiased transfer mobilities. The force induced power is now a continuous line due to the absence of negative real parts. The moment induced powers are more continuous and the values are significantly less than those in Figure 4.23, with less fluctuation.

The peaks in the moment induced powers correspond to the peaks in the force induced power, which in turn correspond to plate modes. This is expected since strong rotation can only occur at structural resonances. However, it is not clear if the moment induced powers result from the presence of a real moment or from cross-coupling of force and angular velocity. This is discussed in detail in Chapter 4.7.

In Figure 4.27 are shown the powers, corresponding to those in Figure 4.26, as 3rd octave band values. The reciprocal force estimate is now in almost perfect agreement as can be seen more clearly in Figure 4.28. The moment induced powers are 20-40 dB below.

4.5.6 Discussion

For excitation of an isolated reception plate by a shaker source, the reciprocal measurement of the force component and associated power was successful both for the one component and the three component assumption. In both cases, the force is the dominant component of excitation, giving good agreement with the directly measured value.

However, it has been demonstrated that small experimental errors in the reciprocal determination of the transfer mobilities can result in large errors in the evaluation of the force component in narrow bands. It is likely that the effect of experimental error is generally greater in the determination of moments as the finite difference method involves the subtraction of two signals. At low frequencies, where the bending wavelength is large compared to the distance between the matched accelerometers, the two signals are nearly equal. The effect of inaccurate cross-mobility determination could however not be investigated as clean values could not be measured in absence of a proper moment source.

For the assumption of three components of excitation, it was demonstrated that experimental errors in the reciprocal transfer mobilities also affect the evaluation of moments and in the case considered yielded an over-estimate of the moment induced powers. However, conversion of narrow band data into 3^{rd} octave band powers indicates the general unimportance of moments.

In the evaluation of the component powers the major source of error is thought to be that in the determination of the components as this involves an inversion of the mobility matrix.

Referring to the reciprocal determination of the force component it is shown that the quality of the results is strongly dependent on the initial assumption of the components, which should be considered. In other words, an assumption of ultimately unimportant components reduces the accuracy of determination of the dominant component(s).

4.6 SHAKER SOURCE ON STAIR WALL

A similar set of measurements was conducted on a real wall with the edges bonded into the flanking walls and ceilings. The wall is situated in a staircase test facility and performs as reference wall for acoustic tests in combination with lightweight stairs as introduced in Chapter 3. The wall construction (24 cm CaSi, 2000 kg/m^3) is typical of separating walls in multi-storey houses in Germany.

The excitation (e) and response positions (r_1, r_2, r_3) are shown in Figure 4.29. The experimental set-up is shown in Figure 4.30. For the excitation of the stair wall a piano wire was inserted to minimise the contribution of moments. The reference position was r_2.

Similar to the previous investigations on the reception plate, the initial evaluation assumed one component only, the force perpendicular to the wall surface. Only small differences in force and force induced power, were observed between the one-component and three-component assumptions. Therefore the following results and discussions are restricted to the three-component assumption, as this is more relevant to the subsequent investigations on the component power flow from a vibrating stair.

4.6.1 Direct and reciprocal transfer mobility

In Figure 4.31 is shown a typical result for the directly and reciprocally measured transfer mobility on the stair wall between e and r_2. Figure 4.32 shows the respective magnitude and phase differences. The differences are

considerably larger than for the isolated concrete plate, described in Chapter 4.5.4. This is probably the result from inhomogenities in the brickwork. In the frequency range up to 1 kHz the difference in magnitude is generally within ± 3 dB. The high deviations at some frequencies are thought to result from excitation at nodes and local effects due to imperfect bonding and loosened bricks. Above 1 kHz the mobility, obtained with shaker excitation shows an increase, likely caused by insufficient signal/noise.

Despite the discrepancies encountered, it can be stated that the reciprocal measurement of mobility also holds for the stair-wall system. The agreement is satisfactory up to 1 kHz which is the frequency range of interest in this thesis work.

4.6.2 Perpendicular force and force-induced power

In Figure 4.33 is shown the directly and reciprocally measured shaker force. The force spectrum is different from the one for excitation of the isolated reception plate due to a re-configuration of the shaker some time between the two measurements and the different coupling condition which is now via a piano wire.

There is a maximum at 780 Hz followed by one at 910 Hz and a sharp drop-off at higher frequencies. Consequently the signal noise ratio above 1 kHz is insufficient. In the frequency range 40 – 1000 Hz the agreement with the directly measured force is generally within ± 3 dB. The reciprocal value provides only a small overestimate.

The reciprocally and directly measured force induced power is presented in Figure 4.34. In Figure 4.35 are shown the respective level differences in 3rd octave bands. The agreement is within ± 2 dB but with positively bias due to an overestimate by the reciprocal method.

4.6.3 Moments and moment induced powers

In Figure 4.36 and Figure 4.37 are shown the component powers in narrow bands and 3rd octave bands. The moment induced powers are generally well below the force induced power except between 600-700 Hz where the moment excitation assumes importance.

Again, the elements of the first column of the transfer mobility matrix were replaced by the directly measured transfer mobilities and results are shown in Figure 4.38, Figure 4.39 and Figure 4.40. Again, there is no significant contribution from moments. The apparent high values in the moment induced powers for the initial evaluation result from experimental errors in the reciprocal transfer function measurements. The overestimation of moment contributions in the initial evaluation is more apparent for the stair wall than for the isolated reception plate. This can be attributed to lower signal/noise as a consequence of the lower mobility of the stair wall.

Despite the overestimation of the moment induced powers in the initial evaluation the force component could clearly be identified as the dominant component of excitation in all cases.

Referring to the actual results it is expected that the evaluation would as well yield a moment and respective power with reasonable accuracy if it were the dominant component of excitation. This could however not be verified in absence of a useful moment source.

4.7 THE CROSS-MOBILITY PROBLEM

In this section, moment induced powers are re-interpreted with respect to cross-coupling of components.

4.7.1 Theory of cross power

The theory outlined in Chapter 4.3 is extended again referring to the simplest case of a single contact. For a single component of excitation the contact velocity is determined by that component only and the phase difference of force (moment) and translational (rotational) velocity must be in between $\pm \pi/2$. Consequently the power expressions for force and moment excitation in equations (4.21) and (4.22) must in theory always yield positive values.

$$P_F = \frac{1}{2}\mathrm{Re}\left\{F^* \cdot v\right\} \tag{4.21}$$

$$P_M = \frac{1}{2}\mathrm{Re}\left\{M^* \cdot w\right\} \tag{4.22}$$

For a combined force and moment excitation the contact velocity in a particular degree of freedom is generally determined by both components

due to cross-coupling between components. For clarity the contact velocities can be expressed as a function of mobilities:

$$v = F \cdot Y_{v\,F} + M \cdot Y_{v\,M} \tag{4.23}$$

$$w = M \cdot Y_{w\,M} + F \cdot Y_{w\,F} \tag{4.24}$$

Each velocity term includes contributions from both force and moment due to the presence of the cross-mobility. Provided that the prior assumption of components is correct e.g. all other components (F_x, F_y, M_z in the case considered) are truly negligible then the evaluation of the components is exact in theory since the mobility matrix is constructed from transfer and cross-transfer mobilities.

The reciprocal estimates of the component powers are obtained from the product of (complex) component and the (complex) contact velocity for the respective degree of freedom. The contact velocity can only be measured as sum of all excitation components. In the three-component case:

$$\begin{aligned} v_z &= F_z \cdot Y_{v_z F_z} + M_x \cdot Y_{v_z M_x} + M_y \cdot Y_{v_z M_y} \\ w_x &= M_x \cdot Y_{w_x M_x} + M_y \cdot Y_{w_x M_y} + F_z \cdot Y_{w_x F_z} \\ w_y &= M_y \cdot Y_{w_y M_y} + M_x \cdot Y_{w_y M_x} + F_z \cdot Y_{w_y F_z} \end{aligned} \tag{4.25}$$

The moment point cross mobilities can be replaced by their reciprocal equivalents (which is essential for the experimental evaluation).

$$\begin{aligned} Y_{v_z M_x} &= Y_{w_x F_z} \\ Y_{v_z M_y} &= Y_{w_y F_z} \end{aligned} \tag{4.26}$$

The component powers can be written as:

$$P_{F,z} = \frac{1}{2}\left|F_z\right|^2 \mathrm{Re}\left\{Y_{v_z F_z}\right\} + \frac{1}{2}\mathrm{Re}\left\{F_z^* \cdot M_x \cdot Y_{w_x F_z}\right\} + \frac{1}{2}\mathrm{Re}\left\{F_z^* \cdot M_y \cdot Y_{w_y F_z}\right\} \quad (4.27)$$

$$P_{M,x} = \frac{1}{2}\left|M_x\right|^2 \cdot \mathrm{Re}\left\{Y_{w_x M_x}\right\} + \frac{1}{2}\mathrm{Re}\left\{M_x^* \cdot F_z \cdot Y_{w_x F_z}\right\} + \frac{1}{2}\mathrm{Re}\left\{M_x^* \cdot M_y \cdot Y_{w_x M_y}\right\} \quad (4.28)$$

$$P_{M,y} = \frac{1}{2}\left|M_y\right|^2 \cdot \mathrm{Re}\left\{Y_{w_y M_y}\right\} + \frac{1}{2}\mathrm{Re}\left\{M_y^* \cdot F_z \cdot Y_{w_y F_z}\right\} + \frac{1}{2}\mathrm{Re}\left\{M_y^* \cdot M_x \cdot Y_{w_y M_x}\right\} \quad (4.29)$$

In these equations the first term represents the power due to a pure force or moment excitation. The second and third terms represent the power transmission due to the coupling of force and moment or two moments.

Due to the apparent effect of cross-coupling the force and moment induced powers cannot in general be treated as independent of each other and it is thus not possible to segregate and quantify the relative contribution of moments due to the pure and cross-mobility terms. There are special cases where the cross terms vanish, such during excitation of symmetrical modes of finite plates or excitation of an infinite plate, where the cross-mobility is zero. As such, the evaluation of the reciprocal method will in general yield "equivalent" component powers.

Consider a situation where the force component dominates the angular acceleration in one degree of freedom rather than the expected associated moment. Then the phase relationship between the moment and the angular velocity would be arbitrary since the latter is determined by the force only. In that condition, negative power flows will result from the computation at some frequencies. Accordingly the occurrence of negative real parts is more likely in the reciprocal power evaluation of unimportant components.

4.7.2 Cross power

The pure and cross-power terms were obtained directly for the shaker excitation of the isolated reception plate and also the stair wall and compared to the reciprocally measured component powers. The aim was to identify the dominant power term(s) and hence to judge the importance of pure force and moment excitation in the presence of cross-coupling of components.

The subsequent evaluation comprises directly measured transfer mobilities as this gives the most accurate approximation of the components and respective powers. For the evaluation of the cross-term powers in equations (4.27), (4.28), (4.29) the point-cross mobility $Y_{w_x F_z}$ is required in addition to the point mobility. To avoid a contribution of moments in the experimental determination the measurement was performed using the impact hammer.

For the force induced power all three terms in equation (4.27) could be evaluated and compared to the "total" force induced power measured reciprocally. The results for excitation of the isolated reception plate are shown in Figure 4.41. The first term in equation (4.27) which is the power due to a pure force excitation is almost equal to the total power. The cross power is generally more than 20 dB lower and thus can be ignored. The two cross-terms referring to moments M_x and M_y are of the same order of magnitude. This is not surprising considering that the rocking of the shaker is not expected to have a strong x- or y-direction. In addition the receptiveness of the plate is not expected to vary with the direction as the excitation position is near to an edge and the plate's dimensions are similar.

For the moment induced power only the second term in equation (4.28) and (4.29) could be evaluated and compared to the "total" moment induced power measured reciprocally. The results are shown in Figure 4.42 and Figure 4.43. The total moment induced power almost equals the cross power. Hence the evaluation of the pure term and the moment-moment cross-term would have yielded significantly smaller values. It further can be concluded that the reciprocally measured moment induced powers are dominated by cross-coupling of force and angular velocity and do not primarily result from the presence of strong 'pure' moments. The curves are not continuous and gaps also occur at some of the plate's resonance frequencies where strong rotations occur. Accordingly the negative real parts are not due to signal/noise problems but result from to the arbitrary phase relationship of moment and angular velocity, since again the latter is determined by the force and not by the respective moment.

A similar investigation was undertaken for the excitation of the stair wall. The results[2] are displayed in Figure 4.44, Figure 4.45 and Figure 4.46. As for the isolated reception plate the total force induced power almost equals the pure term and the moment induced powers are similar to the cross-term values. Accordingly it can be concluded that the apparent moment induced powers result from cross-coupling and not from the presence of strong moments.

---

[2] The conspicuous points in the graphs represent values at single frequencies which are displayed bold because of poor compatibility of the MatLab software and Microsoft Word.

4.7.3 Discussion

As a consequence of the a priori assumption of moments for the shaker excitation of the isolated reception plate and the stair wall the evaluation of the reciprocal method inevitably gives some value for the moments. As cross coupling is included in the evaluation of the components those are theoretically exact provided that no other components of excitation contribute. However the angular velocity around the contact can only be measured as sum of contributions of all excitation components.

In the cases considered only the force component is significant. In the presence of cross-coupling a pure force excitation also causes a rotation around the contact provided that the excitation is not exactly on a nodal line. Thus a non-zero angular velocity around the contact inevitably appears as a moment and thus a moment induced power by the evaluation of the reciprocal method. By separate evaluation of the pure and cross-term powers, it was demonstrated that cross-coupling of components determines the moment induced powers. Similarly a dominant moment can cause a non-zero translational velocity. Even if there was no significant force present a force induced power would thus result from the prior assumption of a force.

However, the measured power transmission due to cross-coupling of components is negligible relative to the pure force excitation. This might be the general case in the field of building acoustics but not necessarily for structures like thin (ribbed) plates in airplanes or vehicles.

4.8 SUMMARY

A reciprocal method for the in-situ measurement of forces and moments and their associated powers has been developed and experimentally investigated. The advantage of the method is that problems in installation of transducers between source and receiver are circumvented.

The component powers, resulting from a shaker source point connected to an isolated reception plate and also to a stair wall, were evaluated by reciprocal measurements. The components were the perpendicular force F_z and two moments M_x and M_y around axes in the plane of the receiving structure.

By use of directly measured transfer mobilities it was demonstrated that the moment induced powers were significantly overestimated as a result of (small) experimental errors in the reciprocal transfer mobility measurements.

Furthermore it was shown that the moment induced powers result from cross-coupling of force and angular velocity and not from the presence of real moments.

Despite the fact that it is not in principle possible to separate 'pure' from 'cross-term' components, the reciprocal method has been successfully used in establishing the hierarchy of components excitations and thus provides the basis for the investigation of the power flow from a vibrating lightweight stair.

4.9 REFERENCES

[1] Yap, S. H.: The role of moments and forces in structure-borne sound emission from machines in buildings, PhD Thesis at the University of Liverpool, 1988

[2] Yap, S. H., Gibbs, B. M.: Structure-Borne Sound Transmission from Machines in Buildings, Part 1: Indirect Measurement of Force at the Machine - Receiver Interface of a Single and Multi - Point Connected System by a Reciprocal Method, Journal of Sound and Vibration, 1998

[3] Yap, S. H., Gibbs, B. M.: Structure-Borne Sound Transmission from Machines in Buildings, Part 2: Indirect Measurement of Force and Moment at the Machine - Receiver Interface of a Single Point Connected System by a Reciprocal Method, Journal of Sound and Vibration, 1998

[4] J.W. Rayleigh: The theory of sound, Dover Publications (2^{nd} edition), 1945

[5] Cremer, L., Heckl, M., Petersson B.A.T.: Structure-borne sound, Springer Verlag, Berlin, 2005

[6] H. Helmholtz: Theory of airborne sound in pipes with open edges (Theorie des Luftschalls in Röhren mit offenen Enden), Crelle J. 57, 1860

[7] J. W. Rayleigh: Some general theorems relating to vibrations. Proc. Lond. Math. Soc. 4, 1873

[8] Lyamshev, L. M.: A question in connection with the principle of reciprocity in acoustics. Soviet Physics Doklady 4, 1959

[9] T. Ten Wolde: On the validity and application of reciprocity in acoustical, mechano-acoustical and other dynamic systems, Acustica, Vol. 28, 1973

[10] T. Ten Wolde, J. W. Verheij & H. F. Steenhoek: Reciprocity method for the measurement of mechano-acoustical transfer functions, Journal of Sound and Vibration, Vol. 42, 1975

[11] Fahy, F. J.: The vibro-acoustic reciprocity principle and applications to noise control, Acustica, Vol. 81, 1995

[12] J.W. Verheij: Multi-path sound transfer from resiliently mounted shipboard machinery, Technish Physische Dienst TNO-TH, Delft, 1982

[13] Fahy, F. J.: Some applications of the reciprocity principle in experimental vibroacoustics. Acoustical Physics, Vol. 49, 2003

[14] Gustafson, A. and Sturk, P. U.: Reciprocal measurement of mechano-acoustical transfer functions in vehicles, Department of Applied Acoustics, Chalmers University of Technology, Report E95-04, Gothenburg, 1995

[15] Verheij, J. W.: Inverse and reciprocity methods for machinery noise source characterisation and sound path quantification, Part 2: Transmission Paths, International Journal of Acoustics and Vibration, Vol. 2, 1997

[16] Verheij, J. W.: Inverse and reciprocity methods for machinery noise source characterisation and sound path quantification, Part 1: Sources, International Journal of Acoustics and Vibration, Vol. 2, 1997

[17] Späh, M. M.: Characterisation of structure-borne sound sources in buildings, PhD Thesis of The University of Liverpool, 2006.

[18] Späh, M. M.; Gibbs, B.M.: Reception plate method for characterisation of structure-borne sound sources in buildings: Installed power and sound pressure from laboratory data, Applied Acoustics, Vol. 70 (11-12), 1431-1439, 2009

[19] Späh, M. M.; Gibbs, B.M: Reception plate method for characterisation of structure-borne sound sources in buildings: Assumptions and application, Applied Acoustics, Vol. 70 (2), 361-368, 2009

[20] Alber, T. H.: Valves as sources of structure-borne sound, PhD Thesis of The University of Liverpool, 2006.

[21] Alber, T.H.; Gibbs B.M.; Fischer H.M.: Characterisation of valves as sound sources: Structure-borne sound, Applied Acoustics, Vol. 70 (5), 661-673, 2009

[22] Ewins, D. J.: Modal Testing: Theory, Practice and Application (2nd edition), Research Studies Press LTD, 2000

[23] ISO 7626-2: Measurements using single-point translation excitation with an attached vibration exciter, 1990

[24] ISO 7626-5: Experimental determination of mechanical mobility Part 5: Measurement using impact excitation with an exciter which is not attached to the structure, 1995

[25] Hopkins, C.: Sound Insulation, Butterworth-Heinemann, 2007

[26] ISO 9611: Acoustics – Characterization of sources of structure-borne sound with respect to sound radiation from connected structures – Measurement of velocity at the contact points of machinery when resiliently mounted, 1996

[27] Pinnington, R.J.: Approximate mobilities of built up structures, ISVR Technical Report No. 162, 1988

[28] Kihlman, T.; Simmons, C.: Structure-borne sound power input into low-mobile concrete plates, Report F 88-01, 1988

[29] Fahy, F. and Walker, J.: Advanced Applications in Acoustics, Noise and Vibration. E&FN Spon, London, 2004. Chapter 9: Mobility and impedance methods in structural dynamics

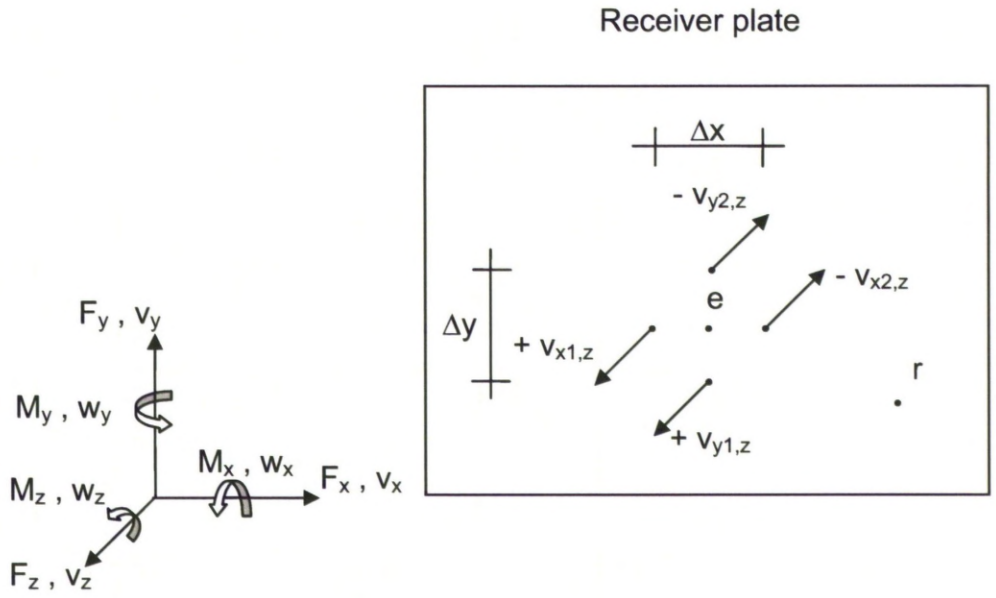

Figure 4.1: Coordinate system, arrows denote direction of motion (e = excitation position; r = reference position)

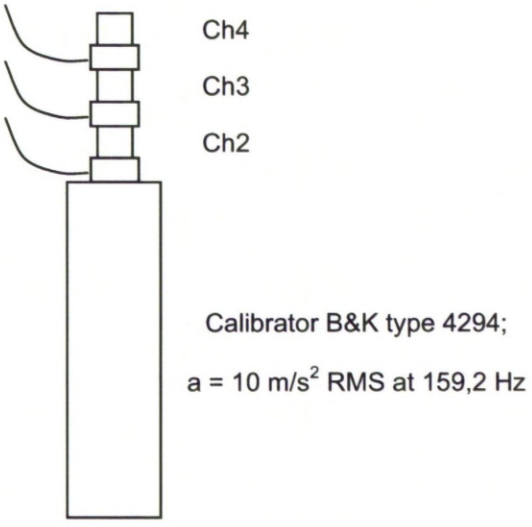

Figure 4.2: Set-up for check of mobility matching of accelerometers

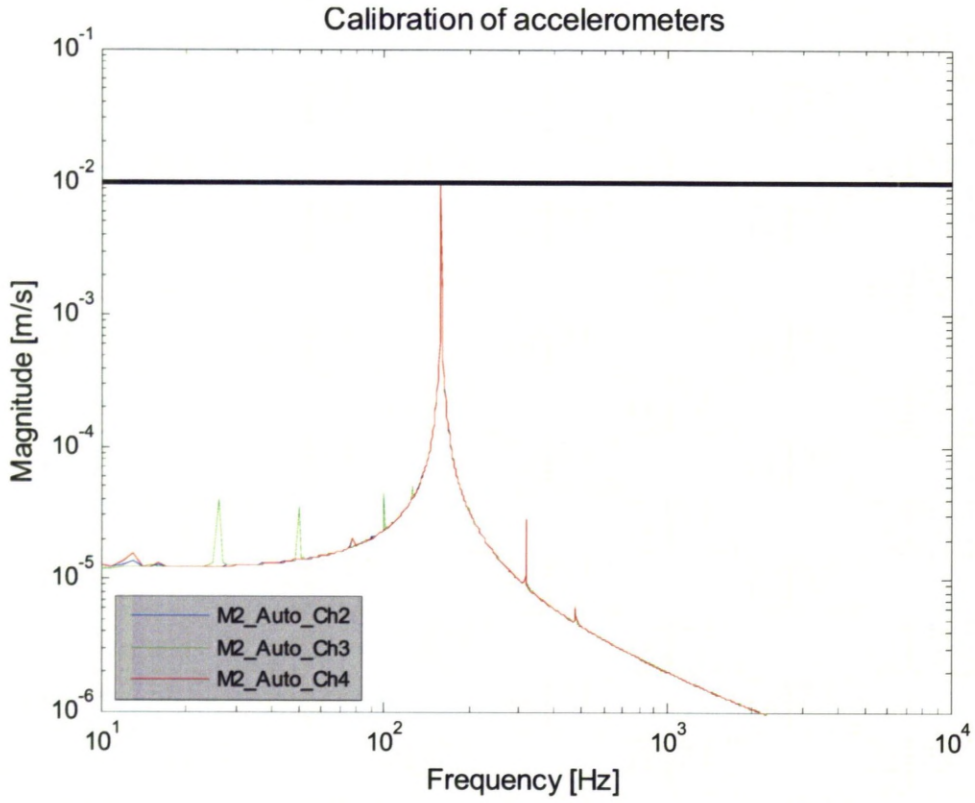

Figure 4.3: Calibration of accelerometers

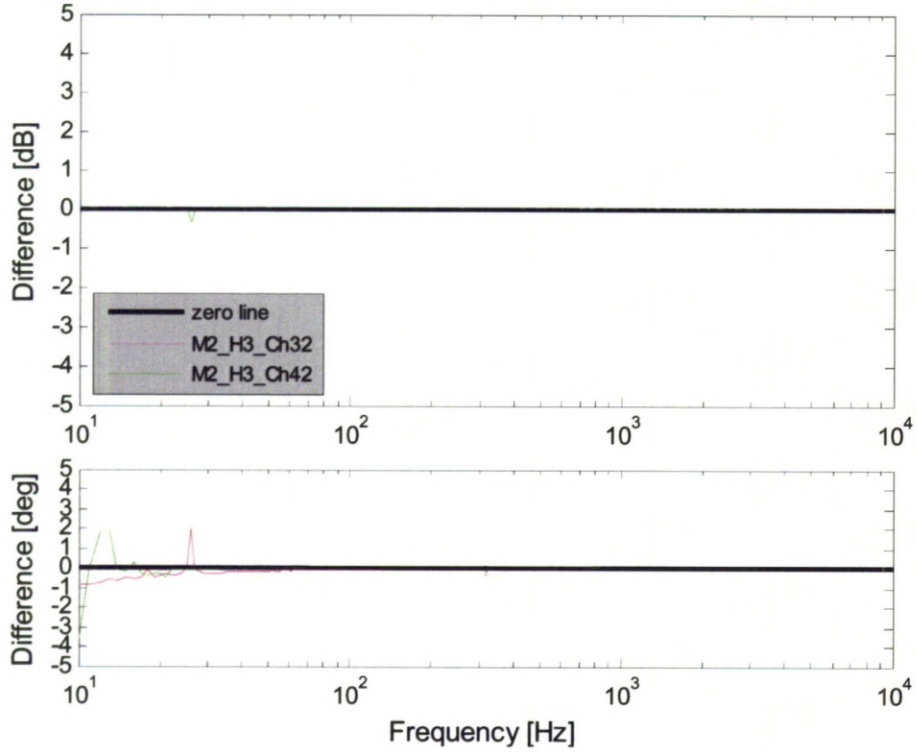

Figure 4.4: Matching of accelerometers: magnitude and phase difference of velocity transfer functions

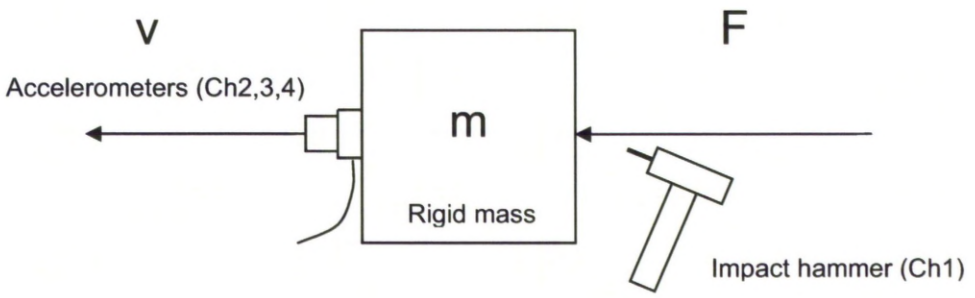

Figure 4.5: Calibration set-up for mobility measurements with impact hammer

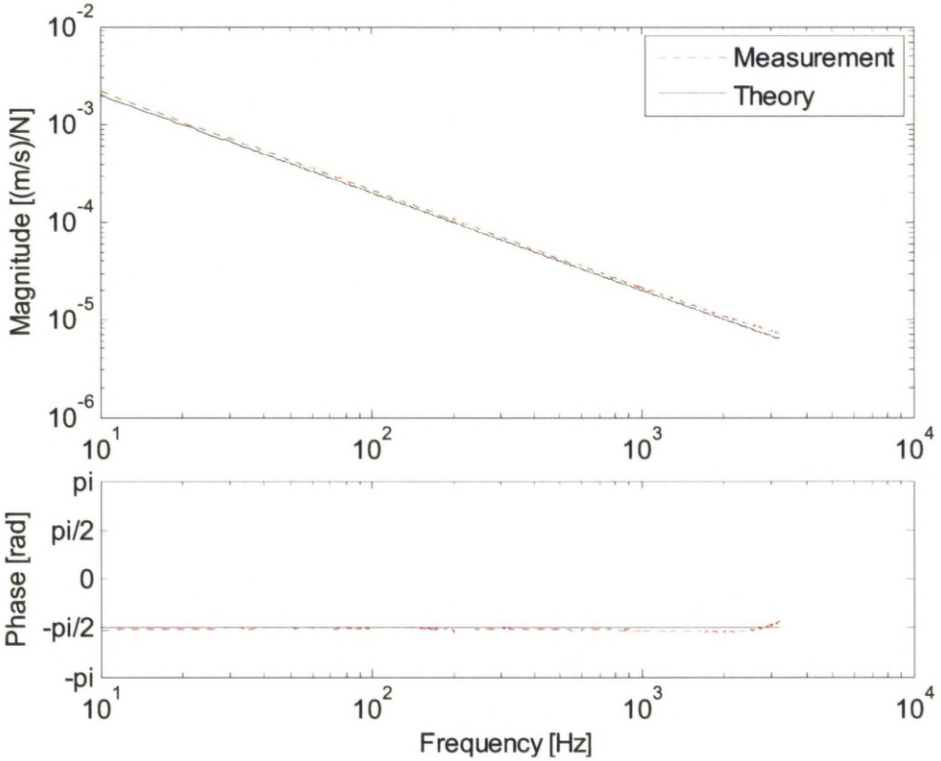

Figure 4.6: Mobility of concrete block – impact hammer excitation

Figure 4.7: Calibration set-up for mobility measurements with shaker

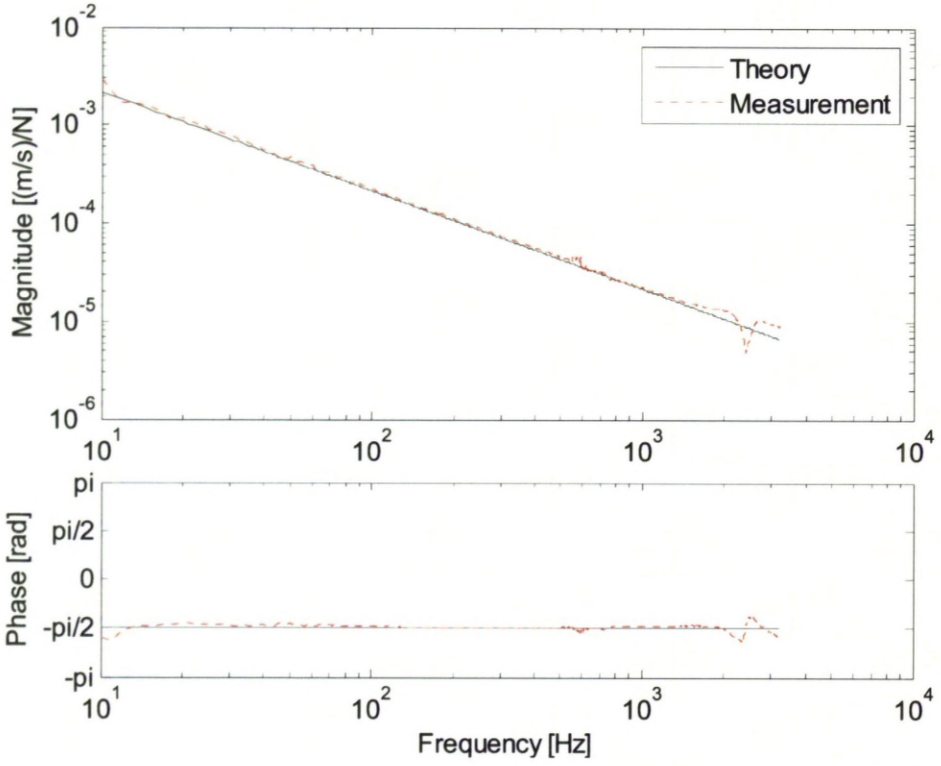

Figure 4.8: Mobility of concrete block – shaker excitation

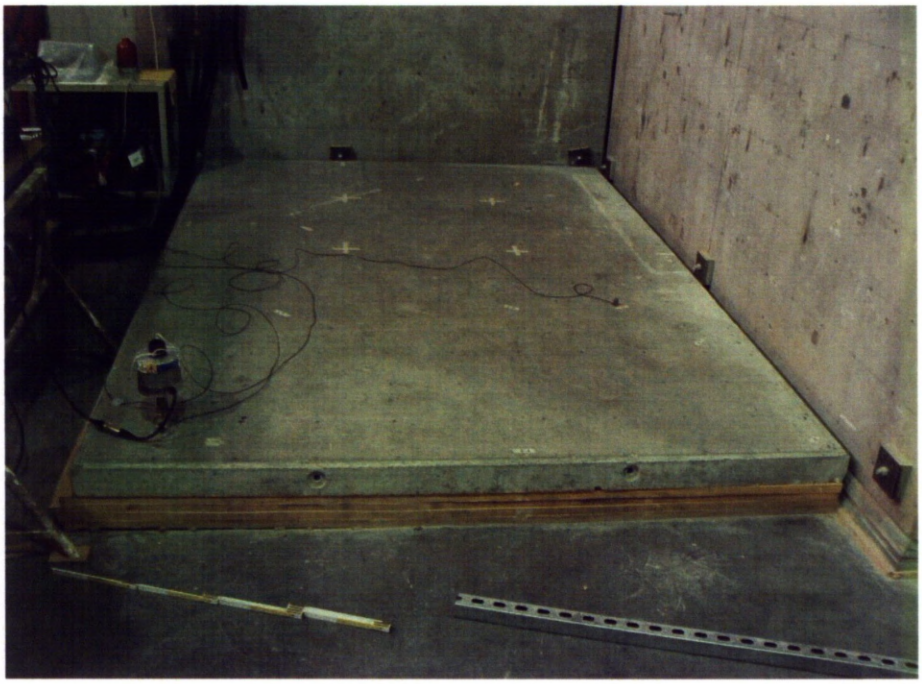

Figure 4.9: Set-up on horizontal reception plate for direct and reciprocal force and power measurement

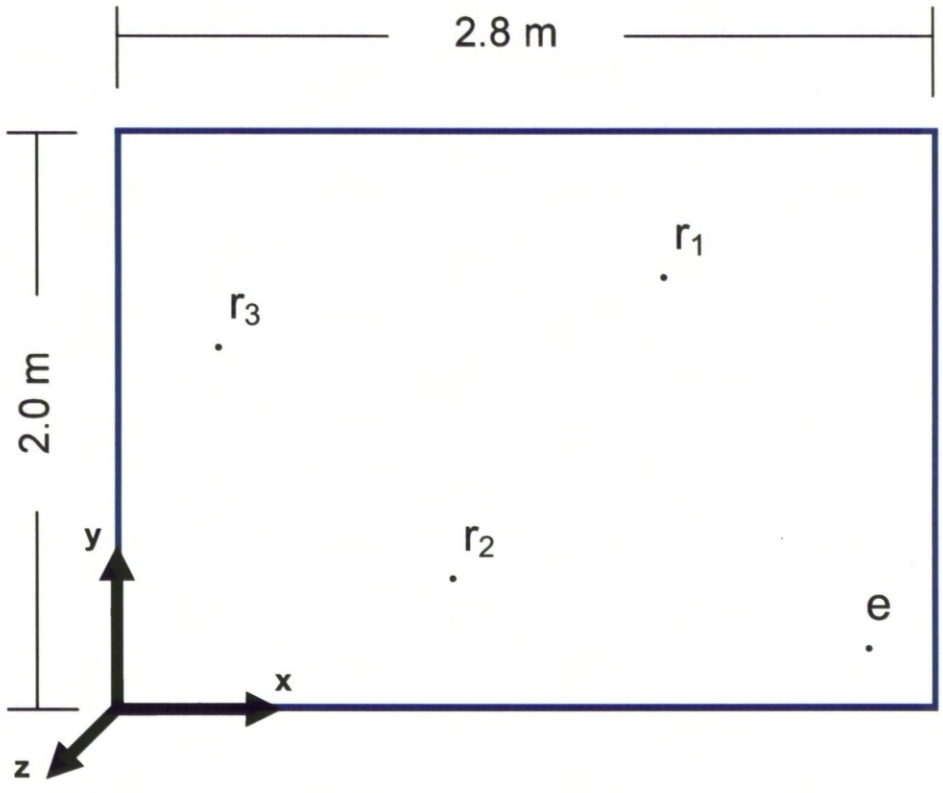

Figure 4.10: Excitation (e) and reference positions (r) on horizontal reception plate; e (2,60/1,80), r_1 (1,84/1,61), r_2 (1,07/0,55), r_3 (0,36/1,32)

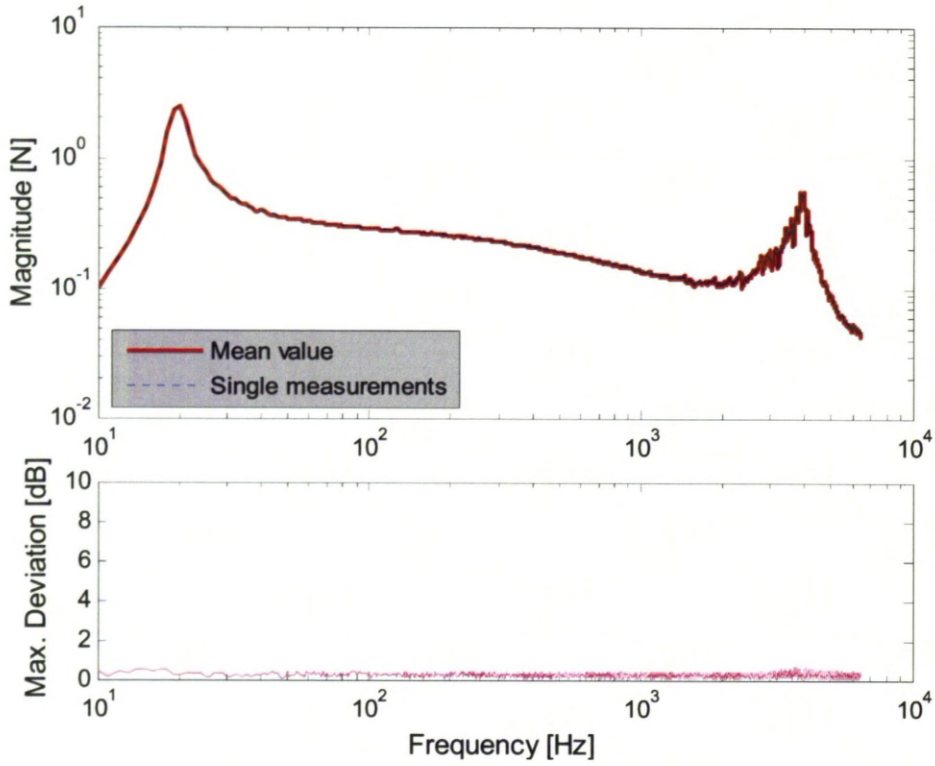

Figure 4.11: Isolated reception plate: shaker force direct

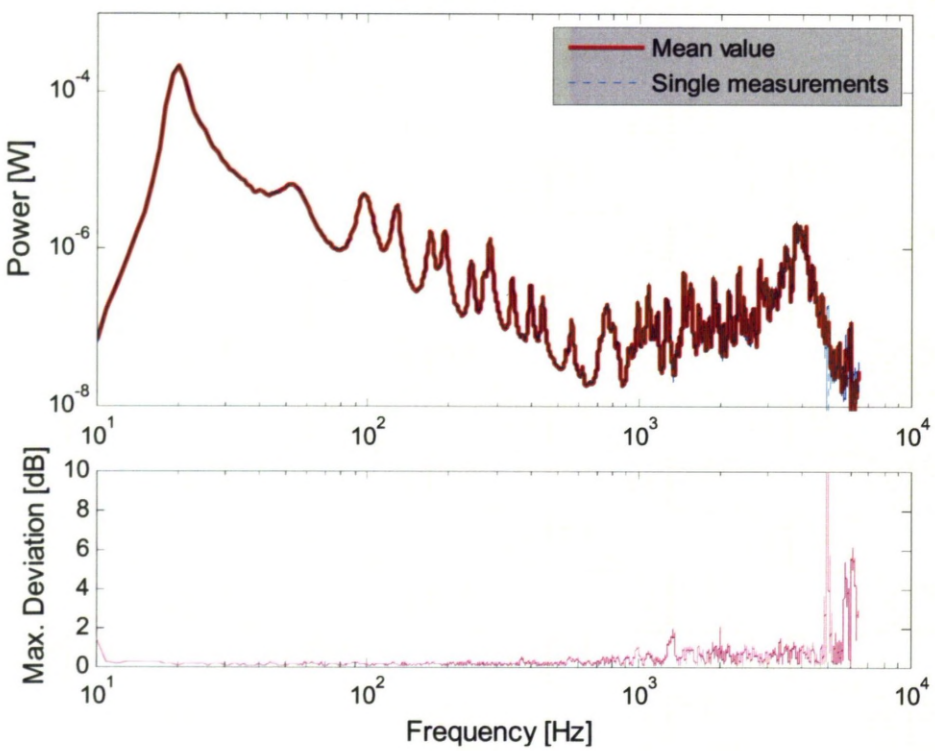

Figure 4.12: Isolated reception plate: shaker power direct

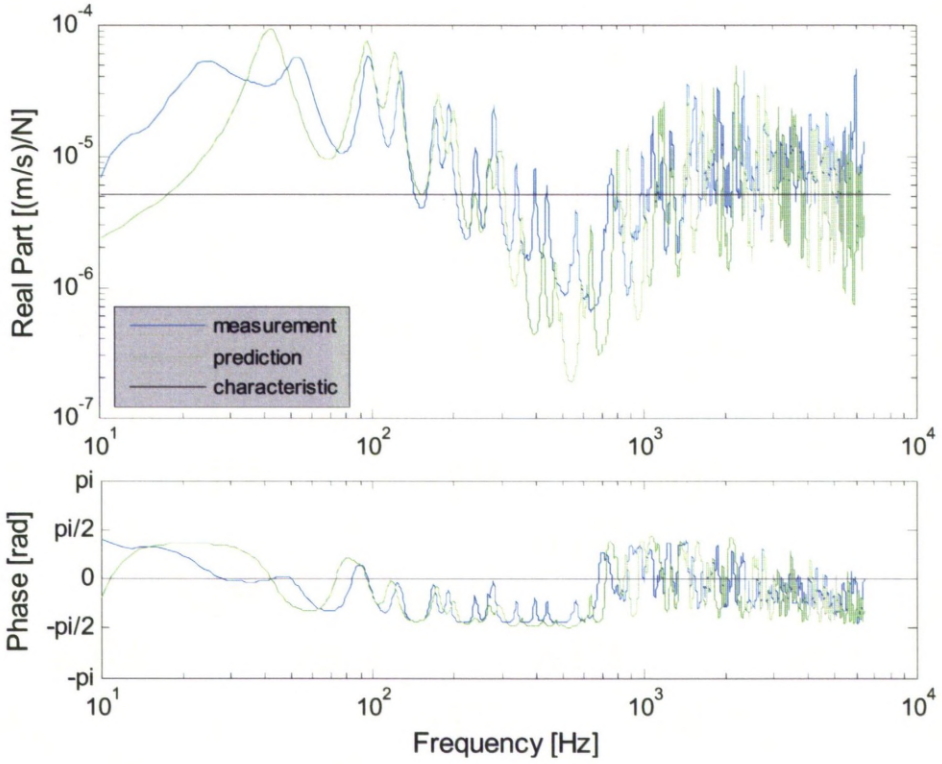

Figure 4.13: Isolated reception plate: point mobility at the shaker contact

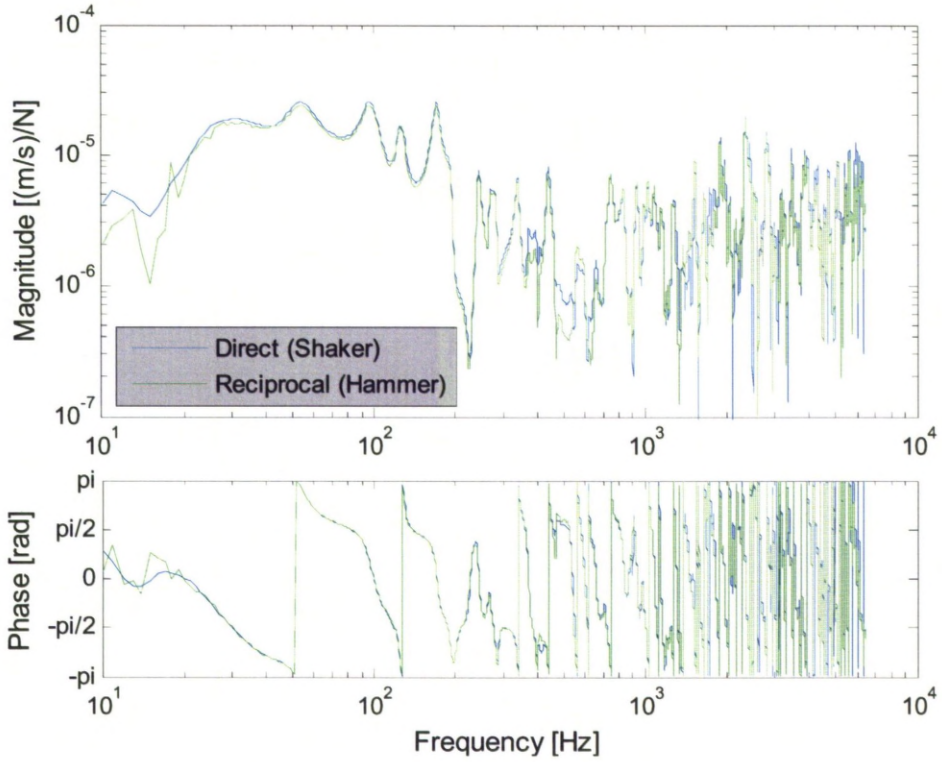

Figure 4.14: Isolated reception plate: transfer mobility direct (shaker) and reciprocal (impact hammer)

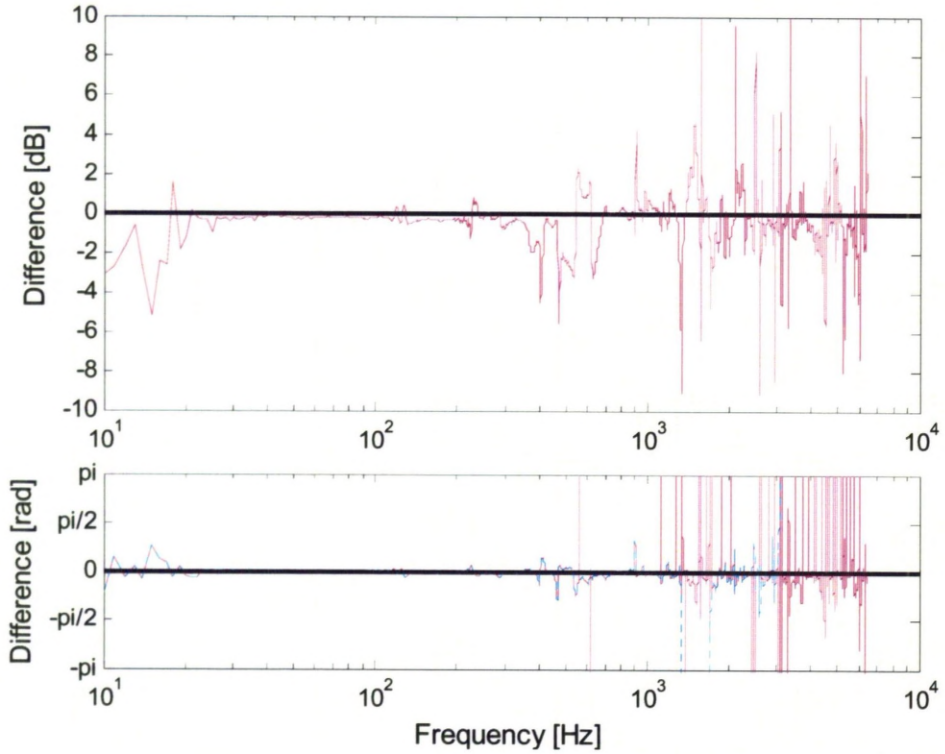

Figure 4.15: Isolated reception plate: Level and phase (wrapped and unwrapped) difference of transfer mobility direct and reciprocal

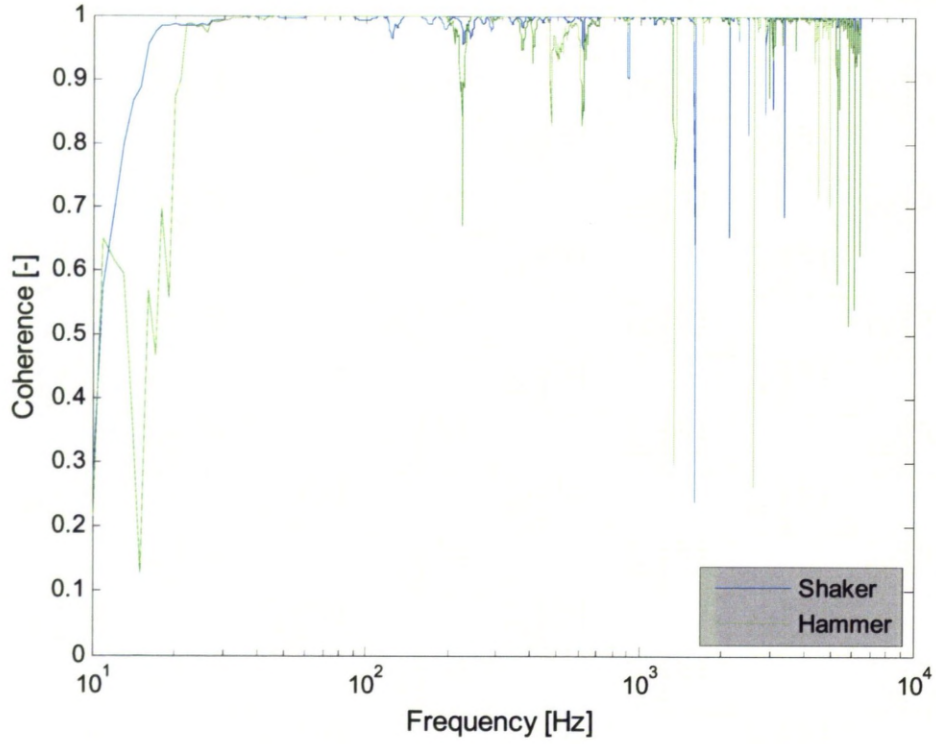

Figure 4.16: Isolated reception plate: coherence for transfer mobility (Figure 4.14) direct and reciprocal

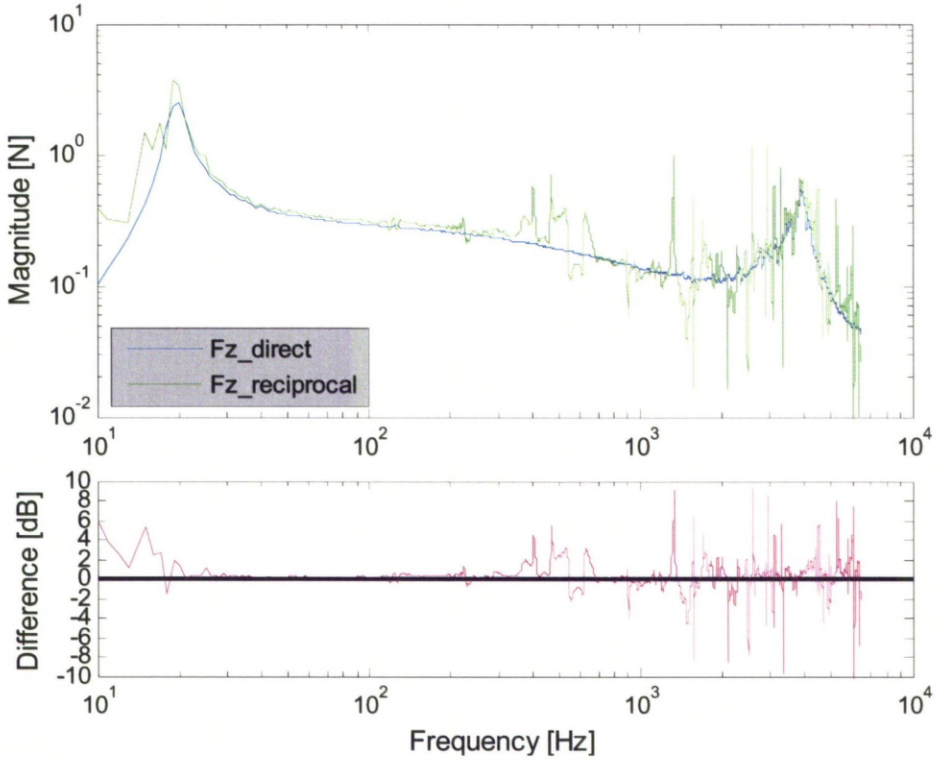

Figure 4.17: Isolated reception plate: force direct and reciprocal – one component assumption

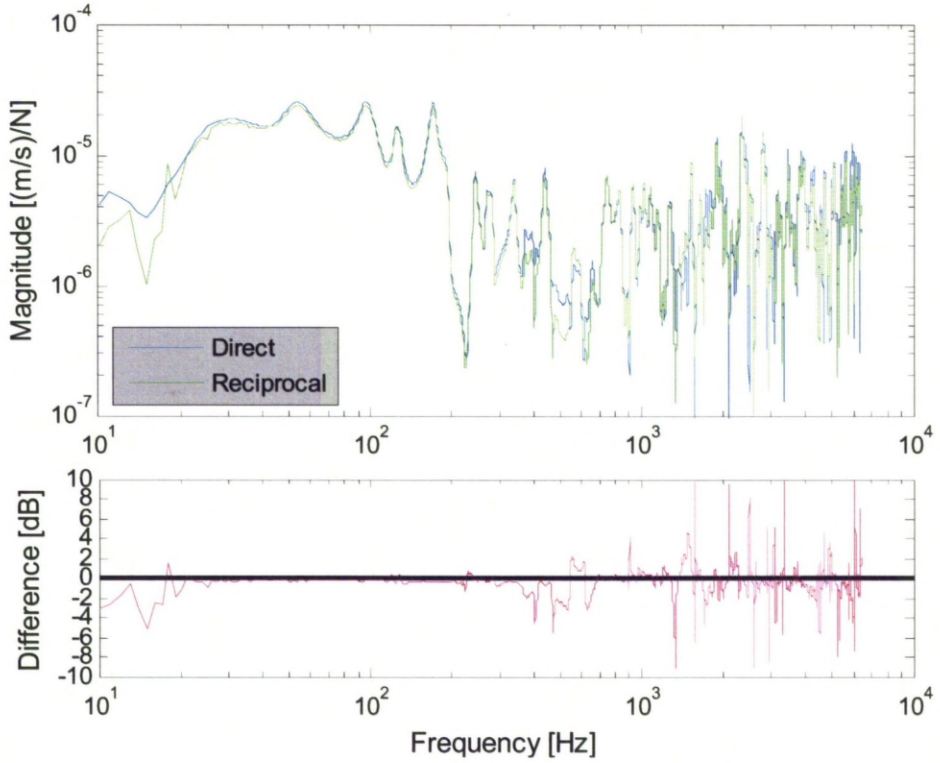

Figure 4.18: Isolated reception plate: transfer mobility direct (shaker) and reciprocal (impact hammer)

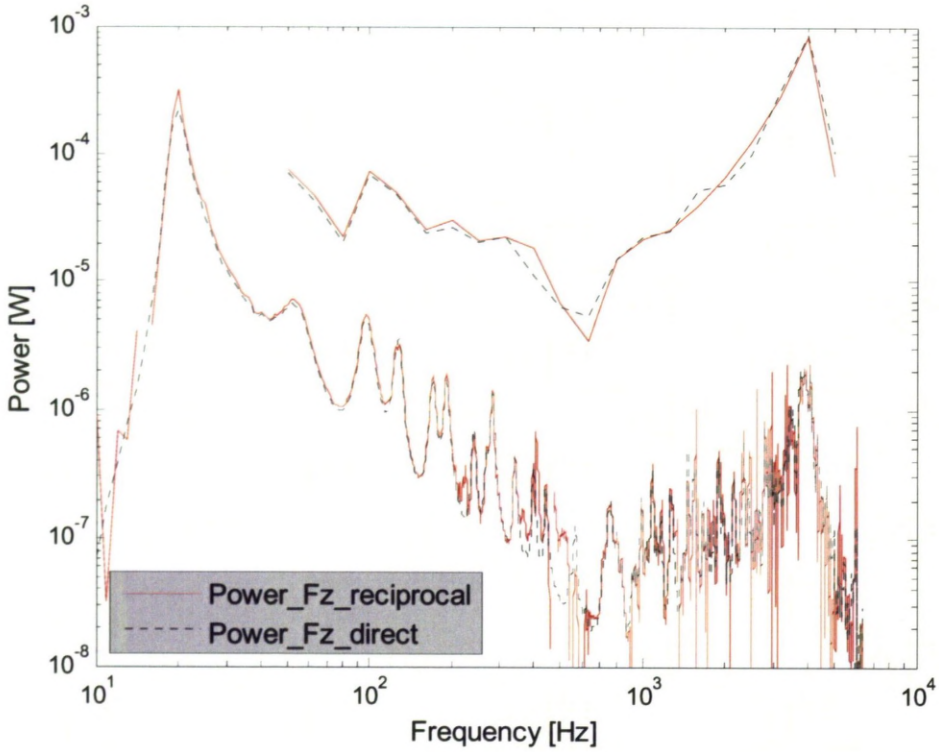

Figure 4.19: Isolated reception plate: force induced power direct and reciprocal – one component assumption

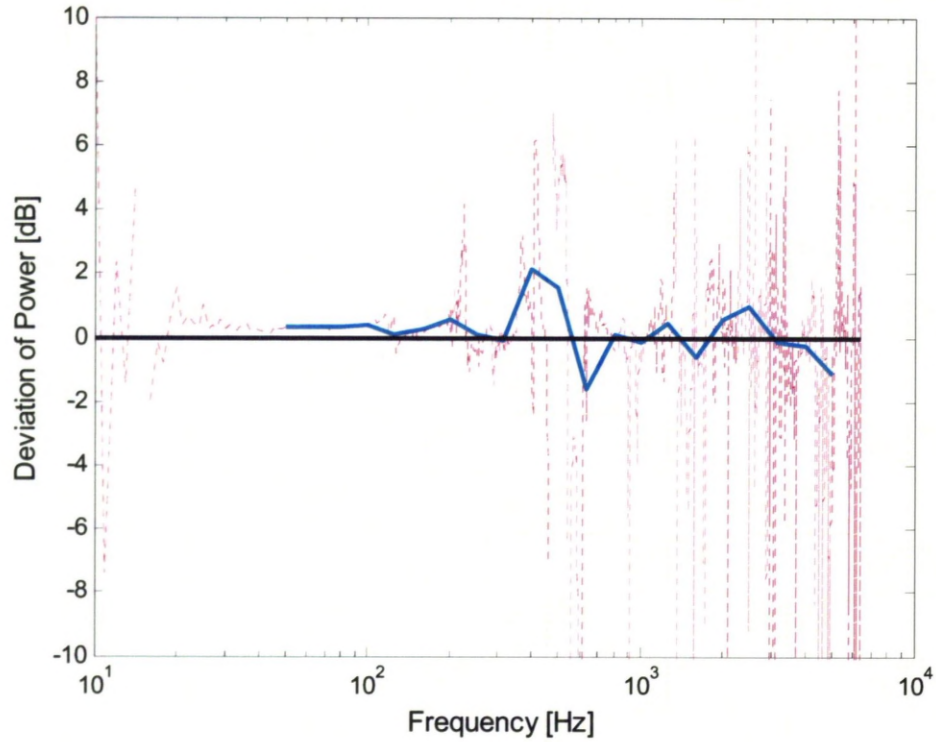

Figure 4.20: Isolated reception plate: deviation of force induced power direct and reciprocal – one component assumption

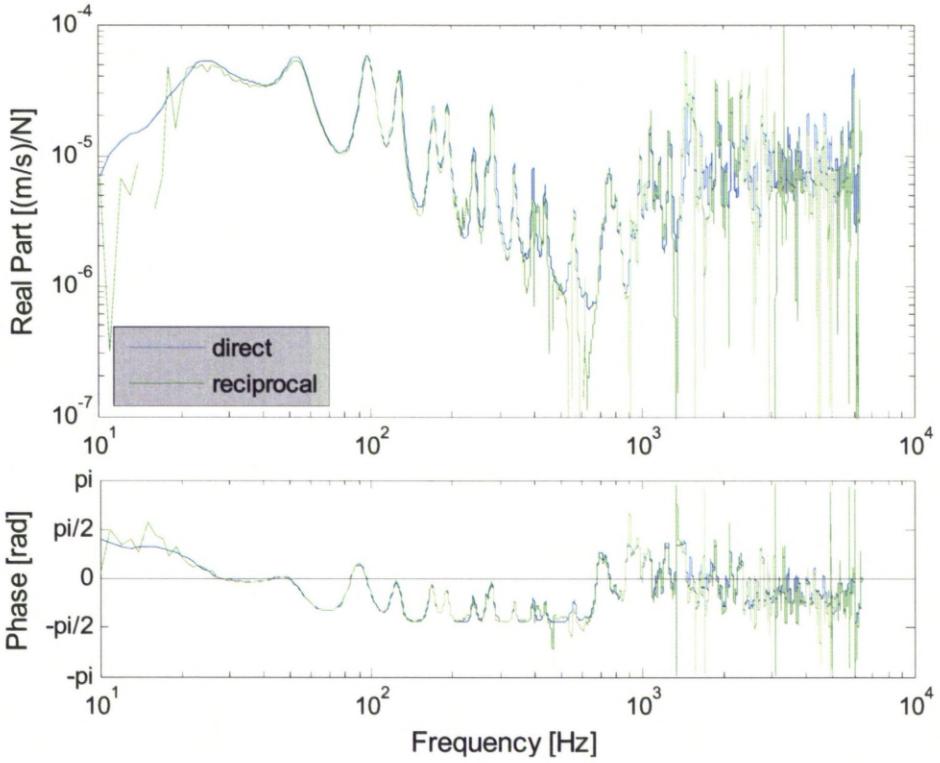

Figure 4.21: Isolated reception plate: Point mobility direct and reciprocal – one component assumption

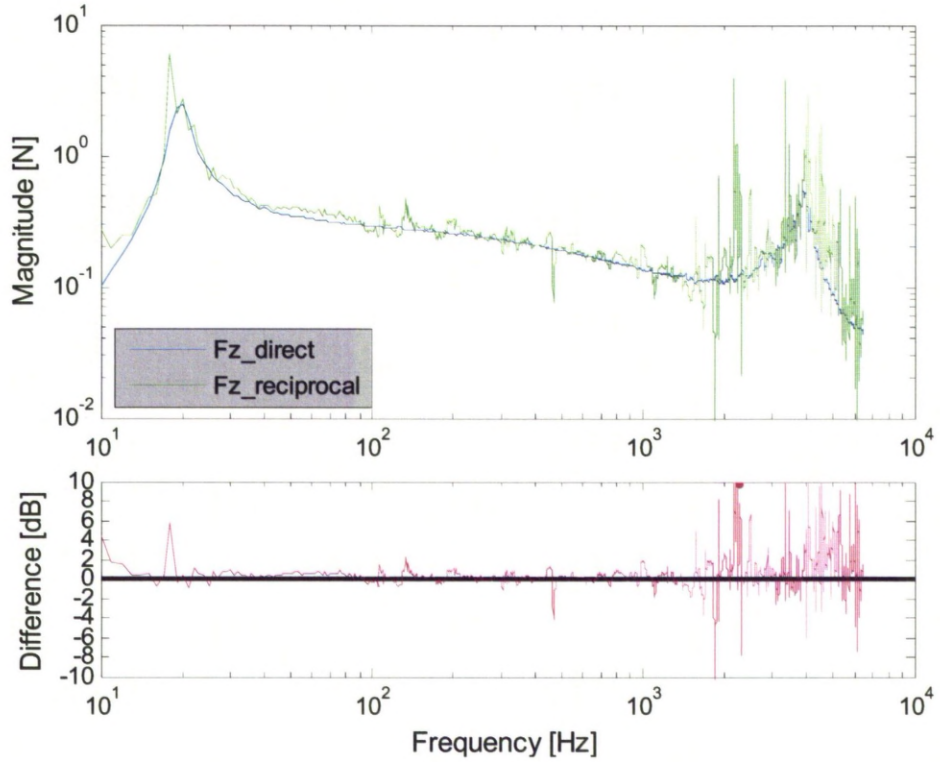

Figure 4.22: Isolated reception plate: Force direct and reciprocal – three component assumption

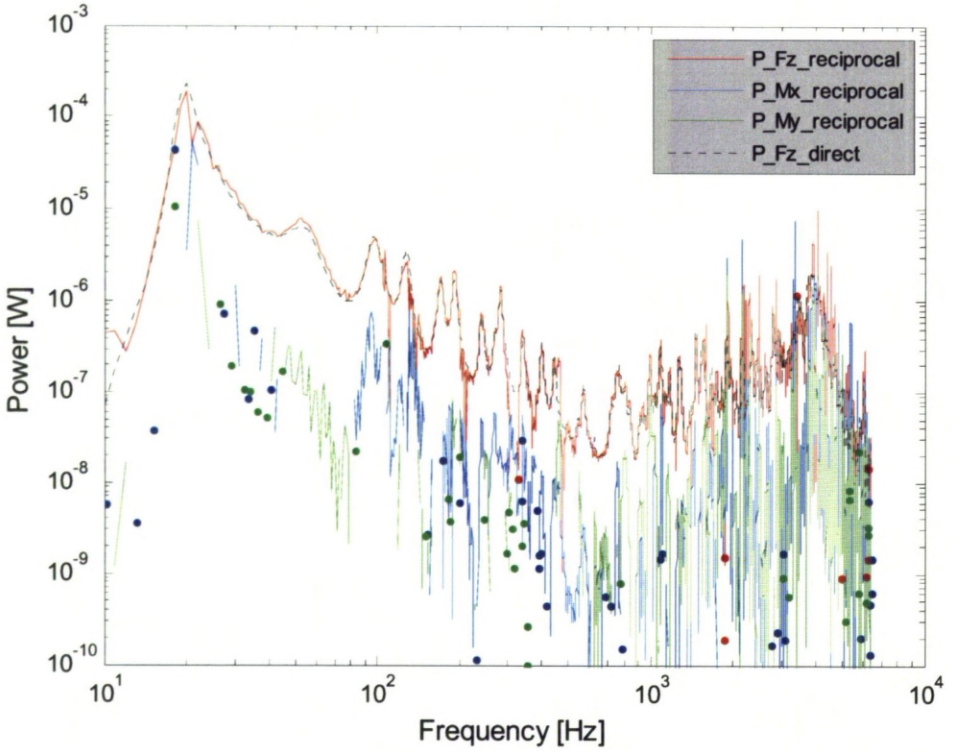

Figure 4.23: Isolated reception plate: component powers from reciprocal method – three component assumption

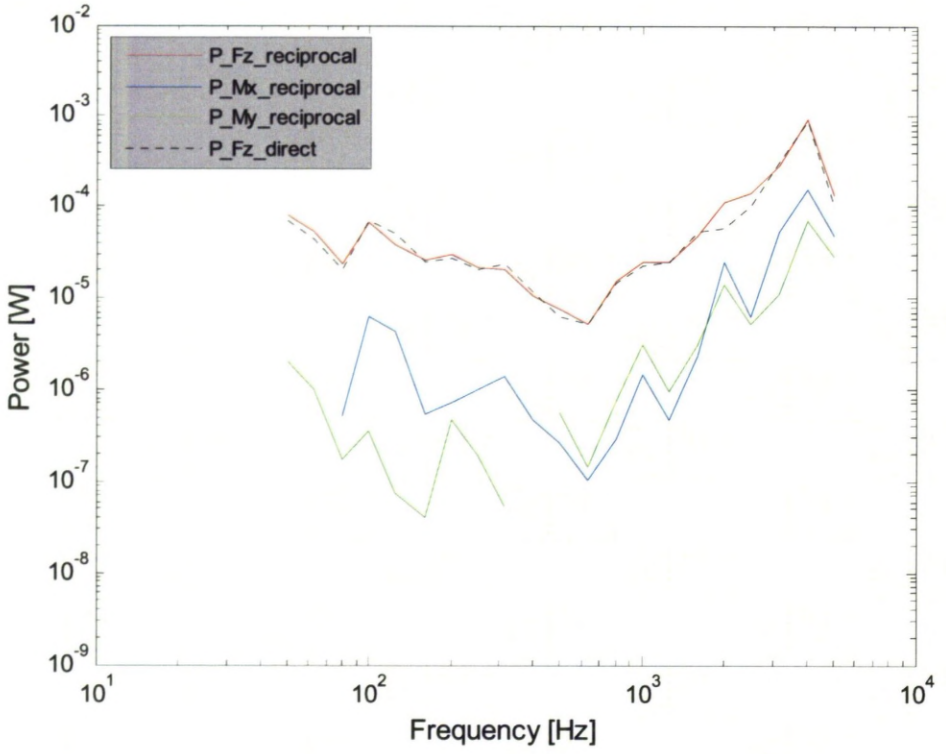

Figure 4.24: Isolated reception plate: component powers from reciprocal method in 3rd octave bands – three component assumption

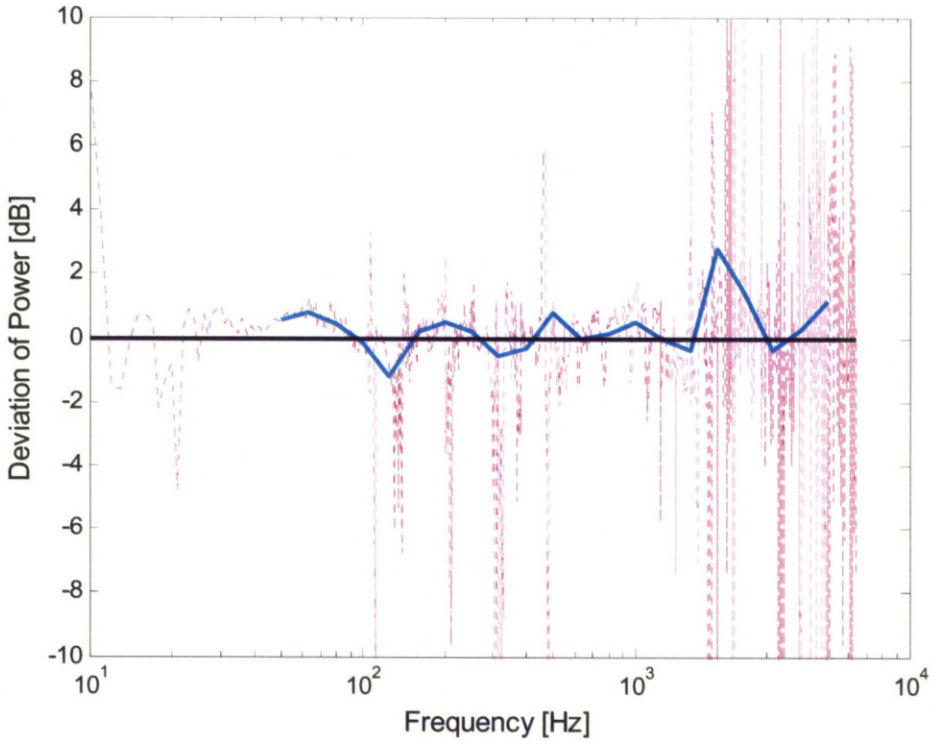

Figure 4.25: Isolated reception plate: deviation of force induced power direct and reciprocal – three component assumption

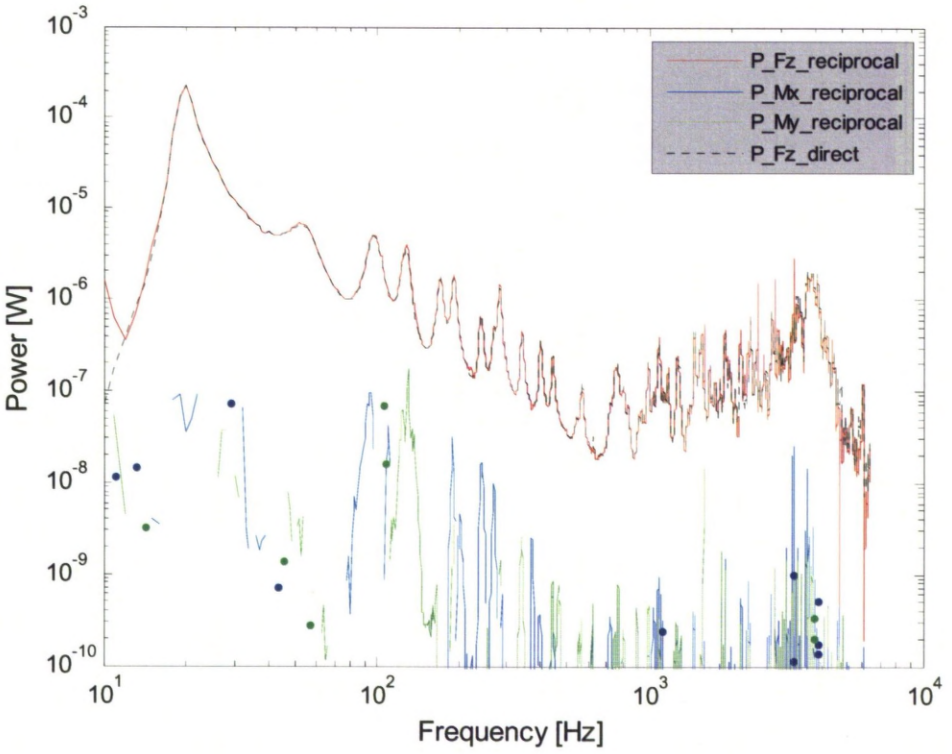

Figure 4.26: Isolated reception plate: Component powers from reciprocal method using directly measured transfer mobilities

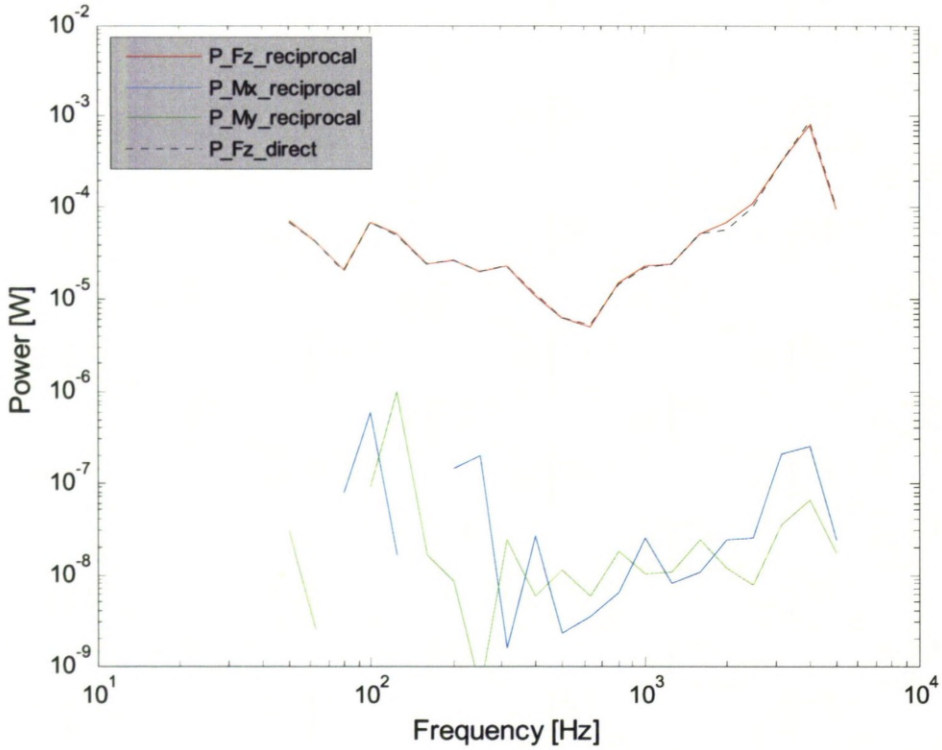

Figure 4.27: Isolated reception plate: component powers from reciprocal method using directly measured transfer mobilities

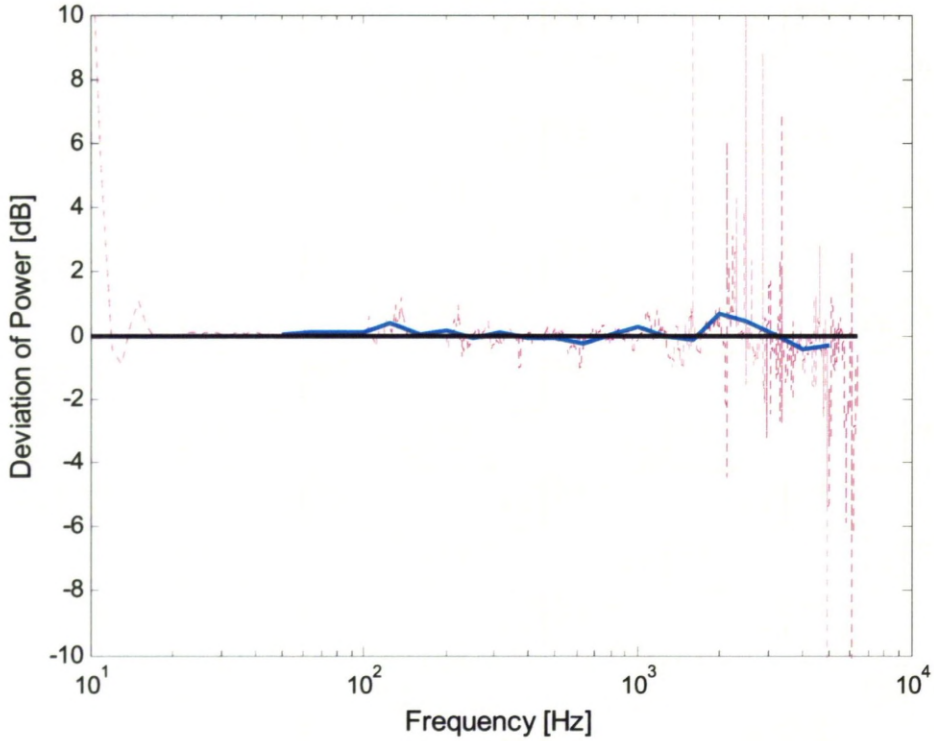

Figure 4.28: Isolated rec. plate: deviation of force induced power direct and reciprocal using directly measured transfer mobilities

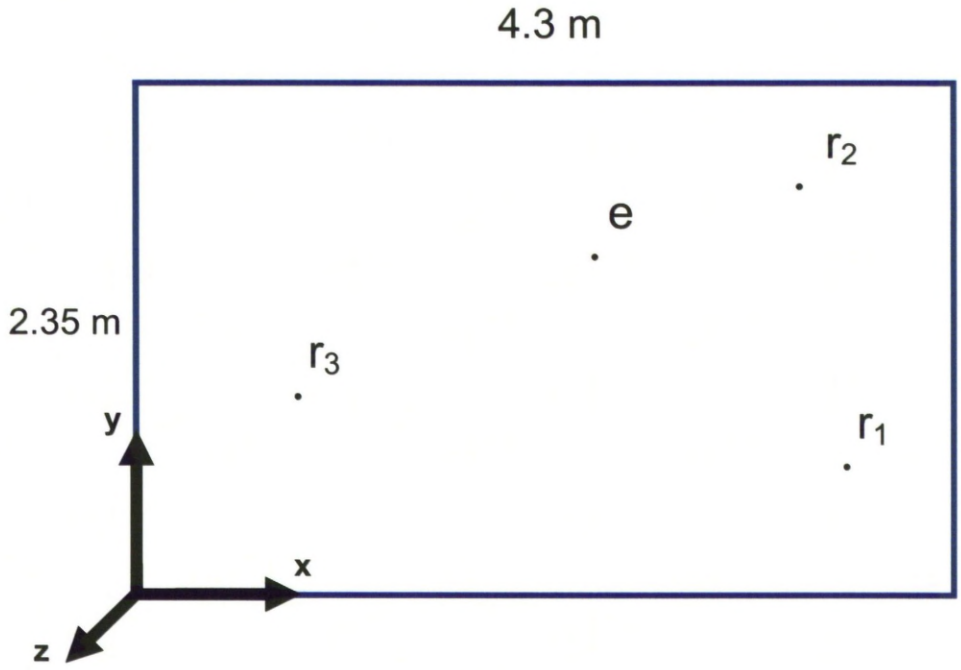

Figure 4.29: Excitation (e) and reference points (r) on stair wall; e (2,60/1,80), r_1 (1,84/1,61), r_2 (1,07/0,55), r_3 (0,36/1,32)

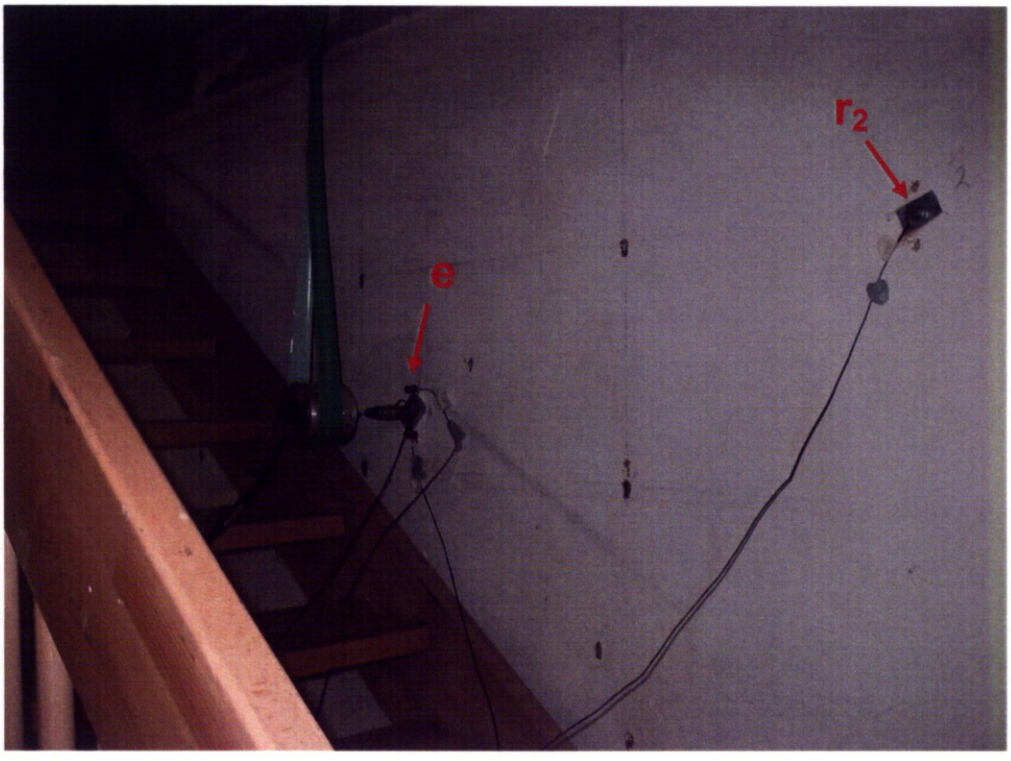

Figure 4.30: Set-up on stair wall for direct and reciprocal force and power measurement

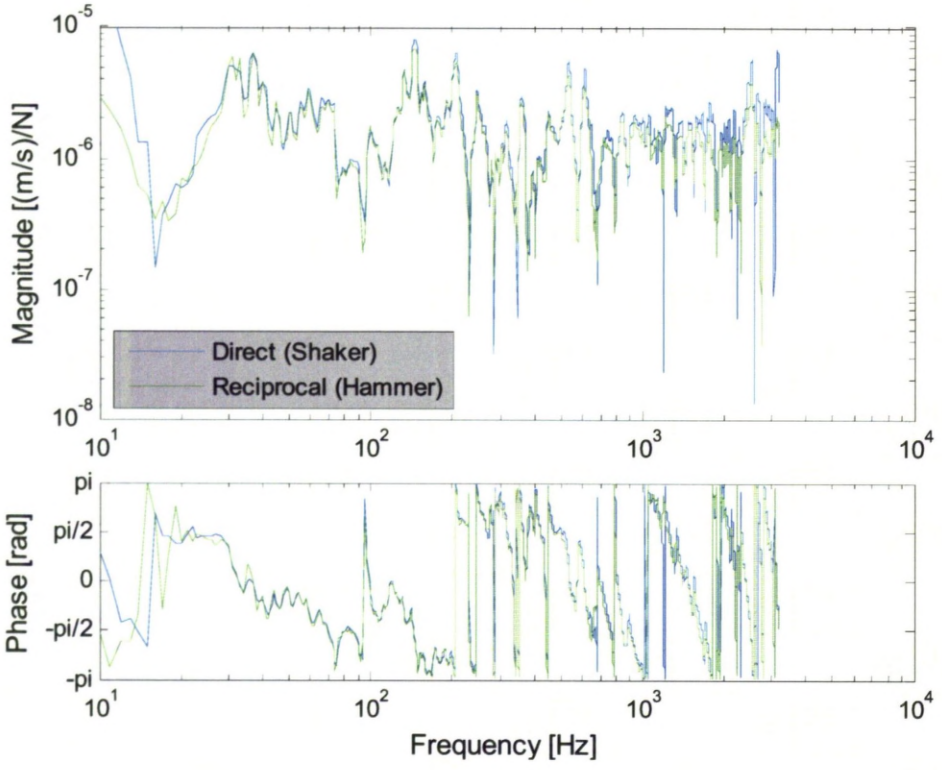

Figure 4.31: Stair wall: transfer mobility direct (shaker) and reciprocal (impact hammer)

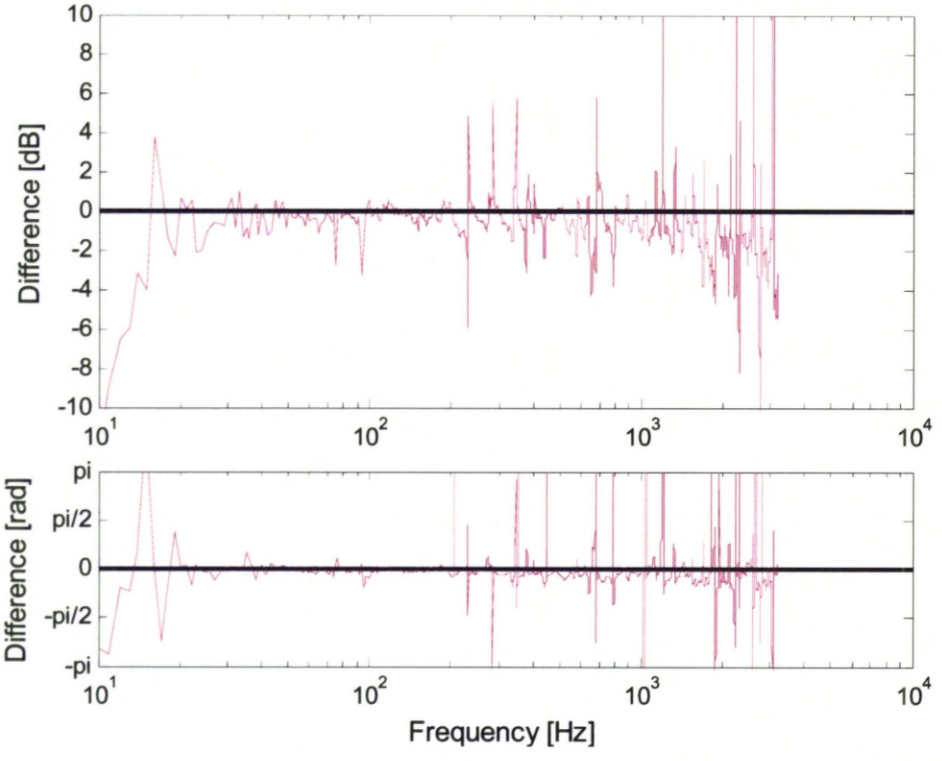

Figure 4.32: Stair wall: level and phase difference of transfer mobility (Figure 4.31) direct and reciprocal

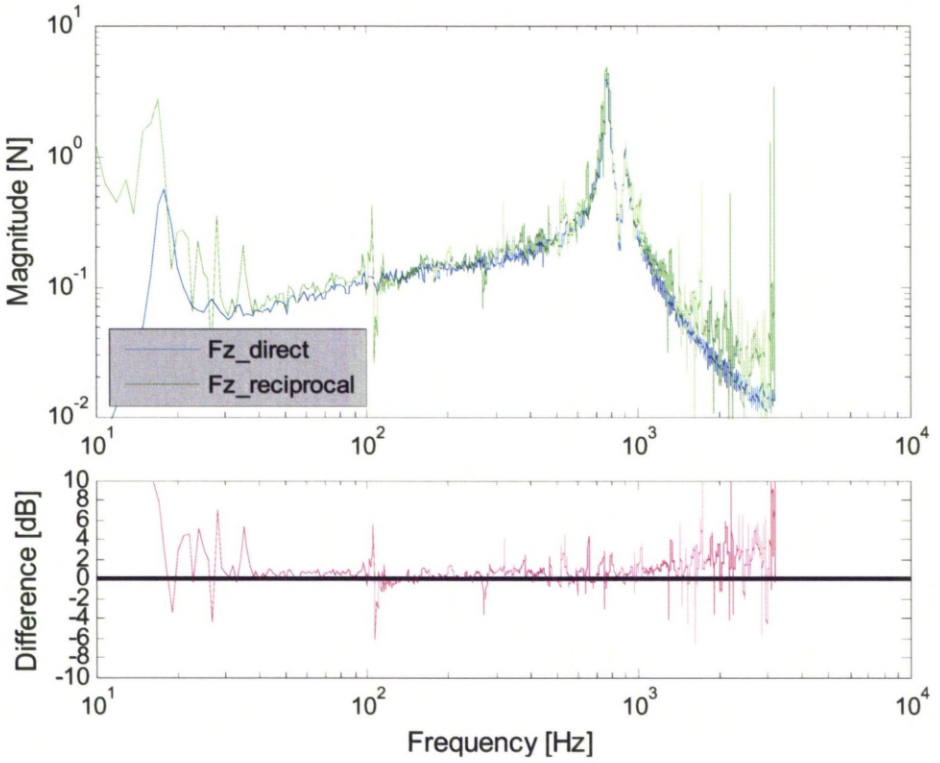

Figure 4.33: Stair wall: force direct and reciprocal

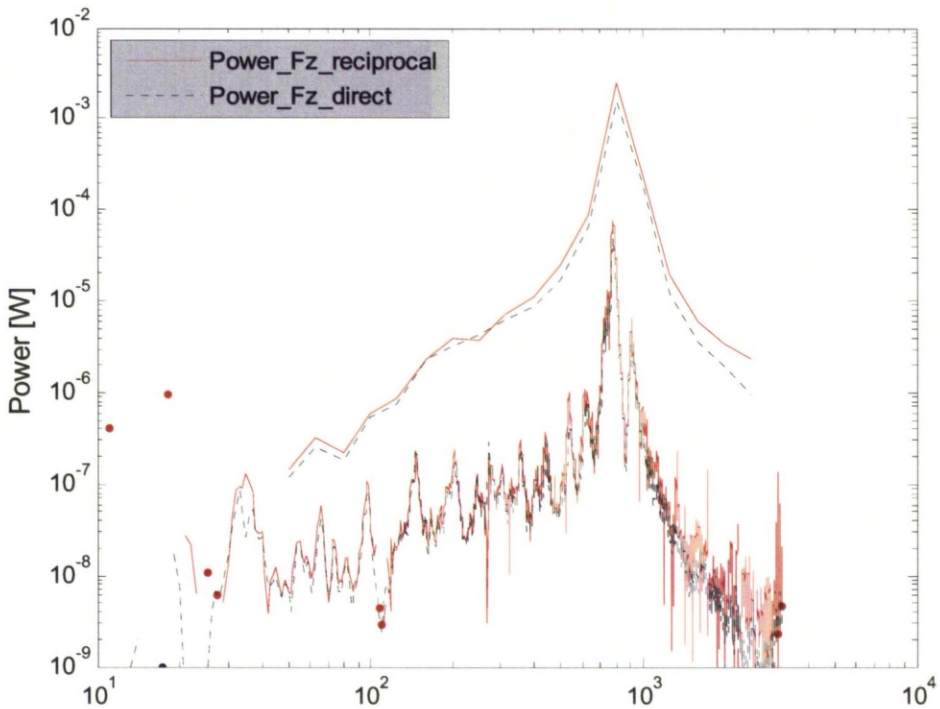

Figure 4.34: Stair wall: force induced power direct and reciprocal

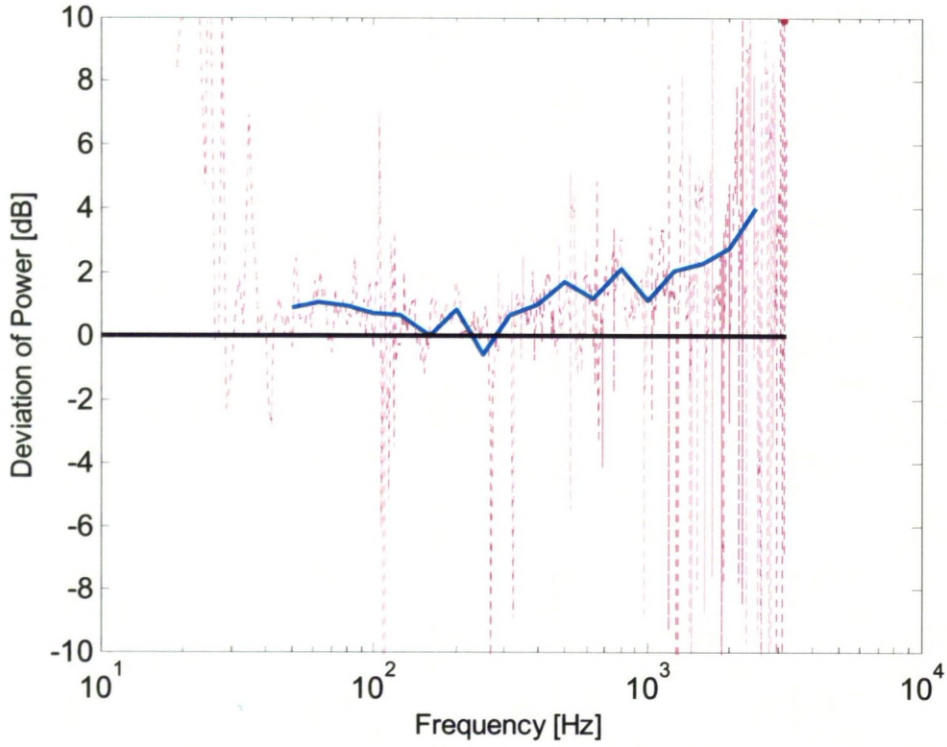

Figure 4.35: Stair wall: deviation of force induced power direct and reciprocal

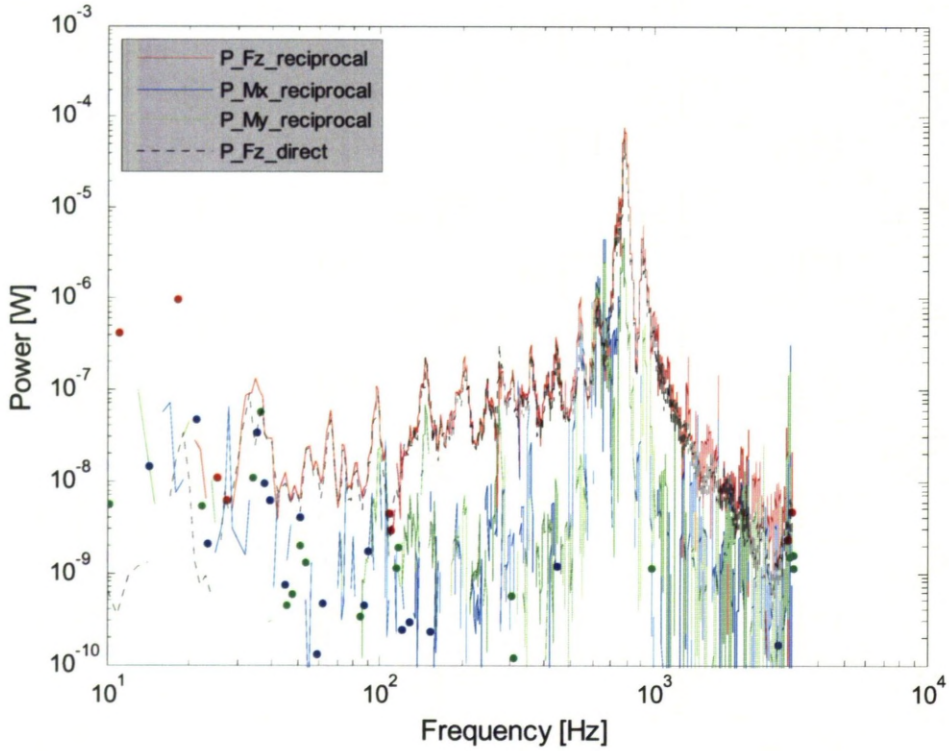

Figure 4.36: Stair wall: component powers from reciprocal method

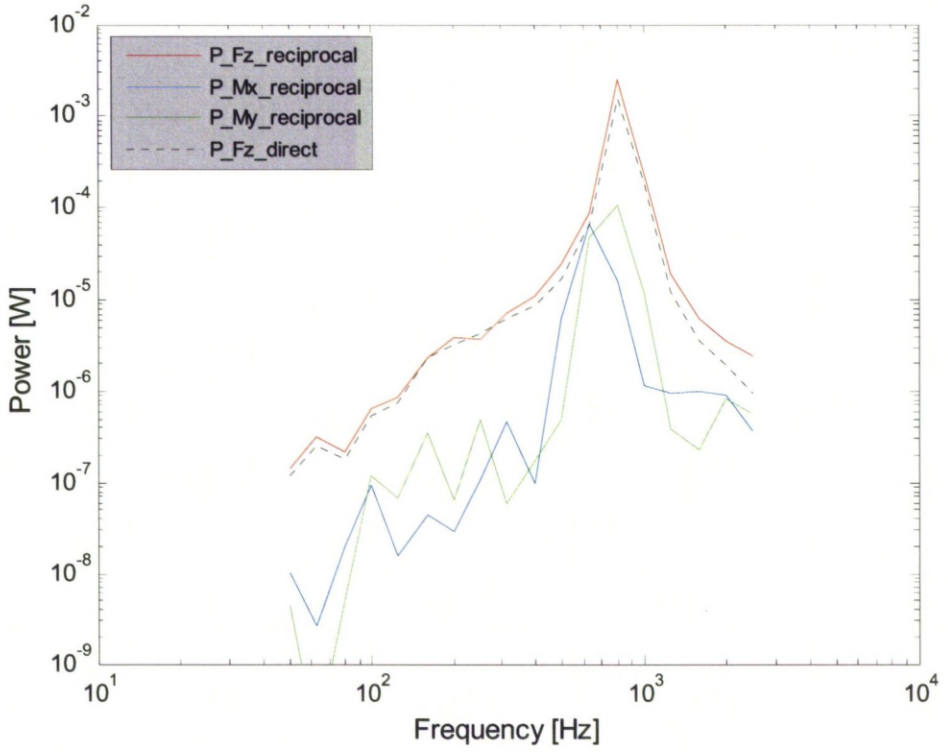

Figure 4.37: Stair wall: component powers from reciprocal method in 3rd octave bands

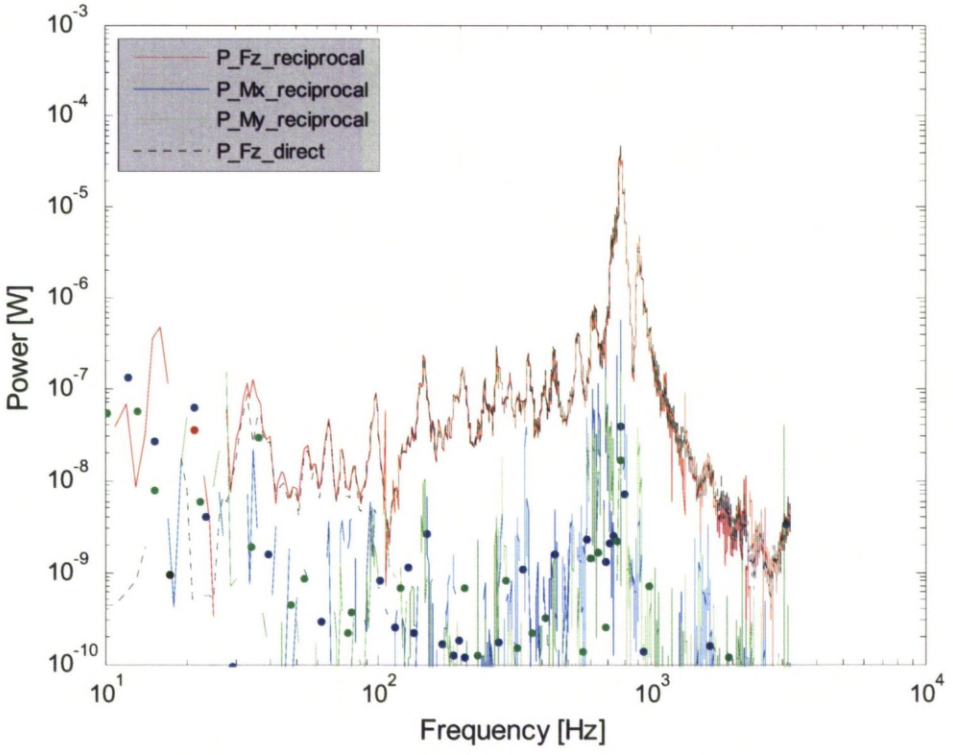

Figure 4.38: Stair wall: component powers from reciprocal method using directly measured transfer mobilities

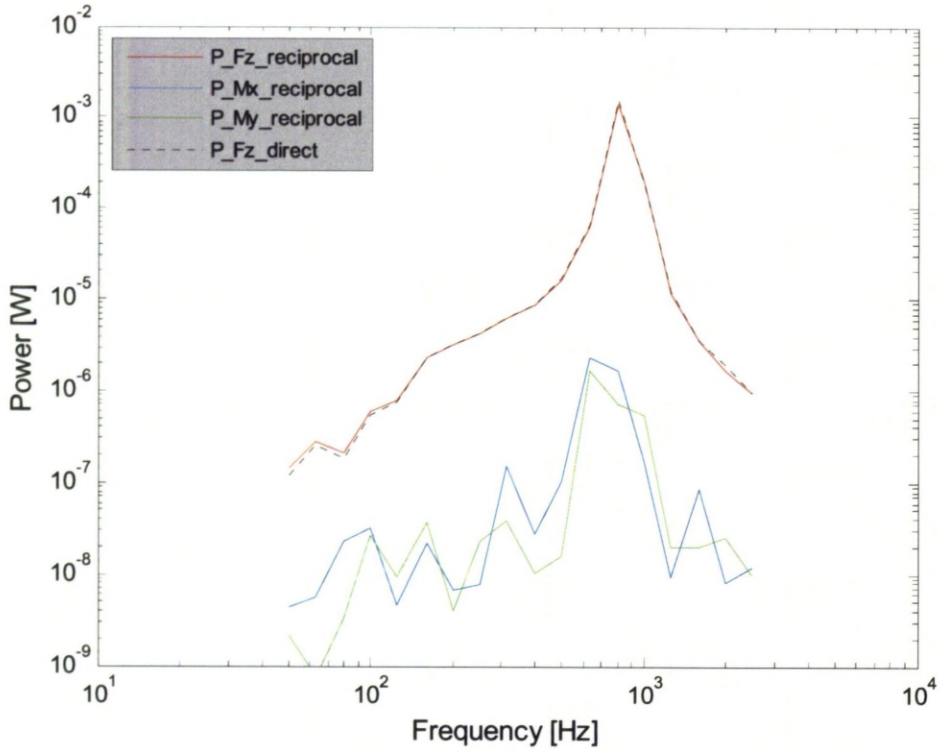

Figure 4.39: Stair wall: component powers from reciprocal method using directly measured transfer mobilities

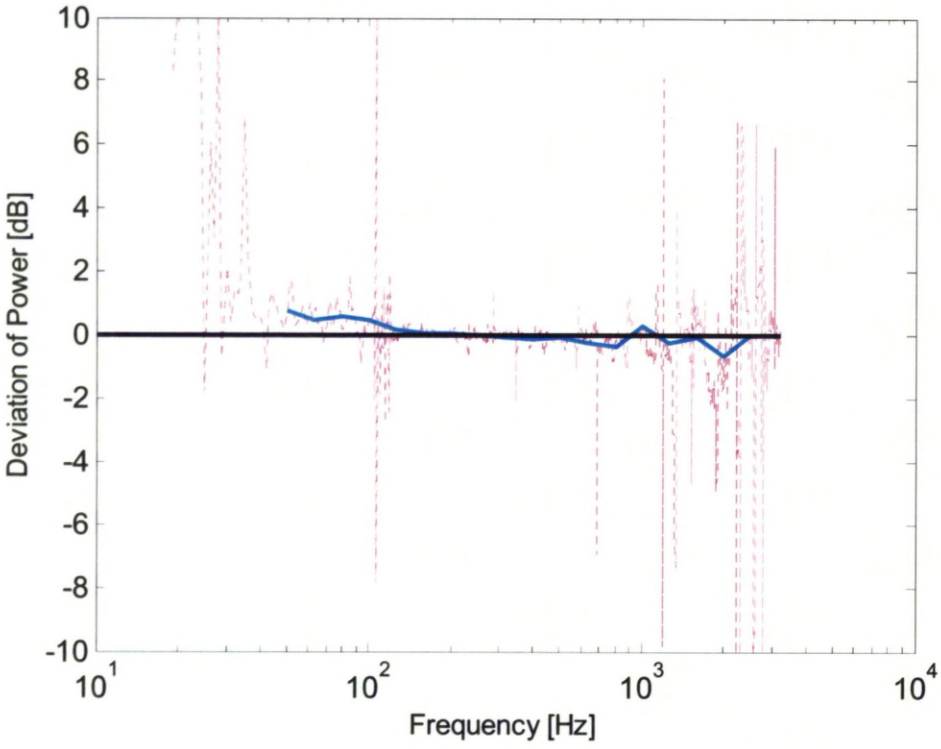

Figure 4.40: Stair wall: deviation of force induced power direct and reciprocal - directly measured transfer mobilities

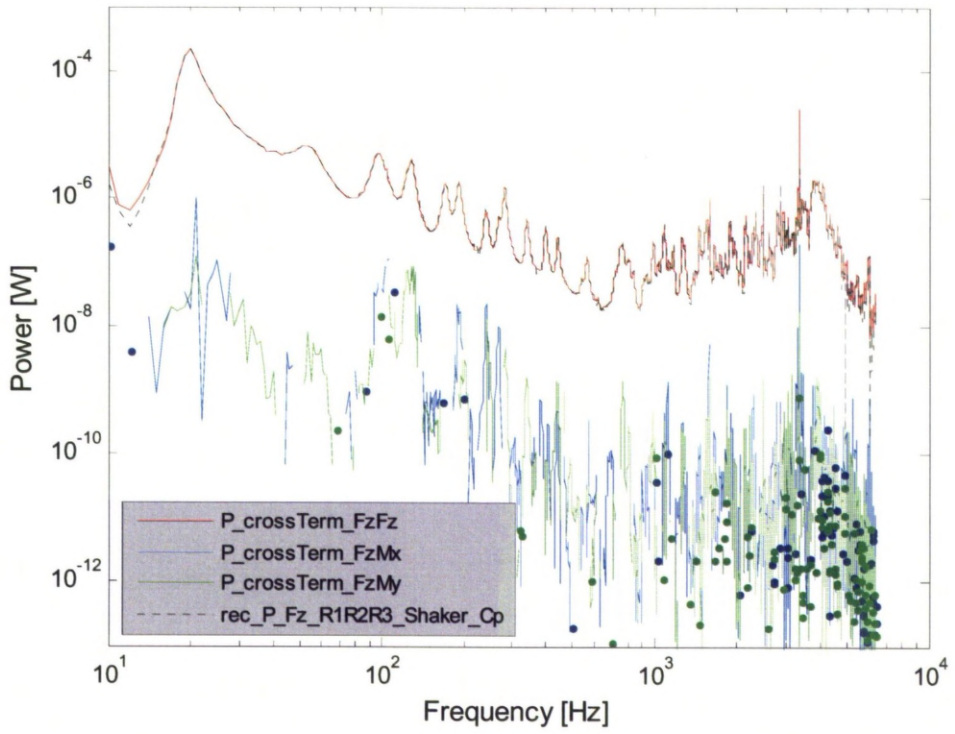

Figure 4.41: Isolated reception plate: Force induced power due to pure force and cross-coupling of components

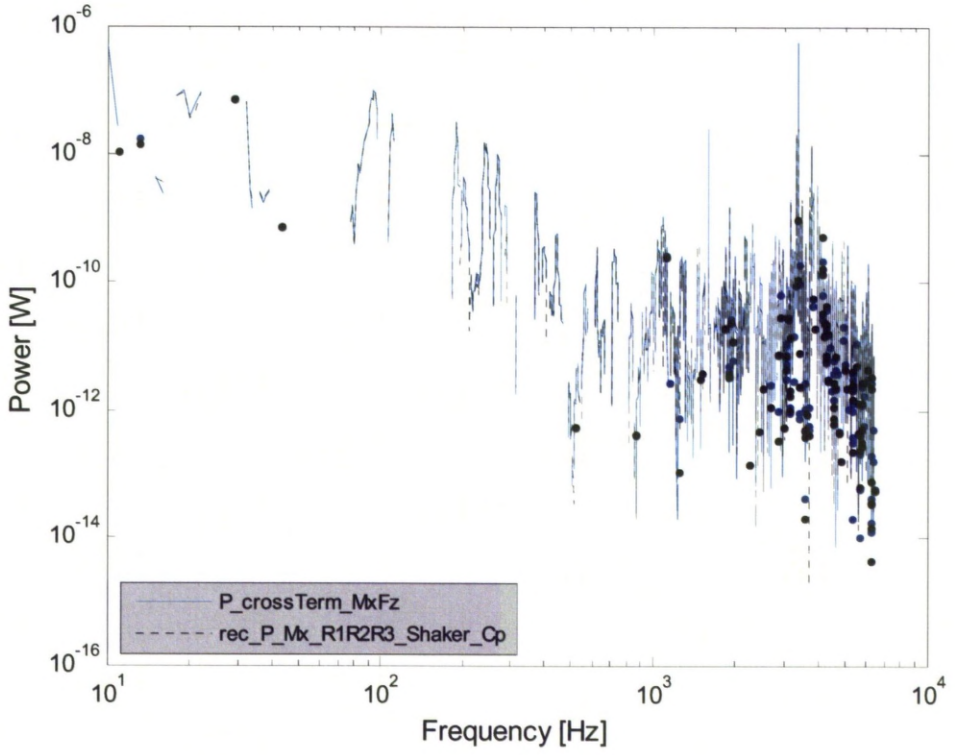

Figure 4.42: Isolated reception plate: Moment M_x induced power due to cross-coupling of moment and force

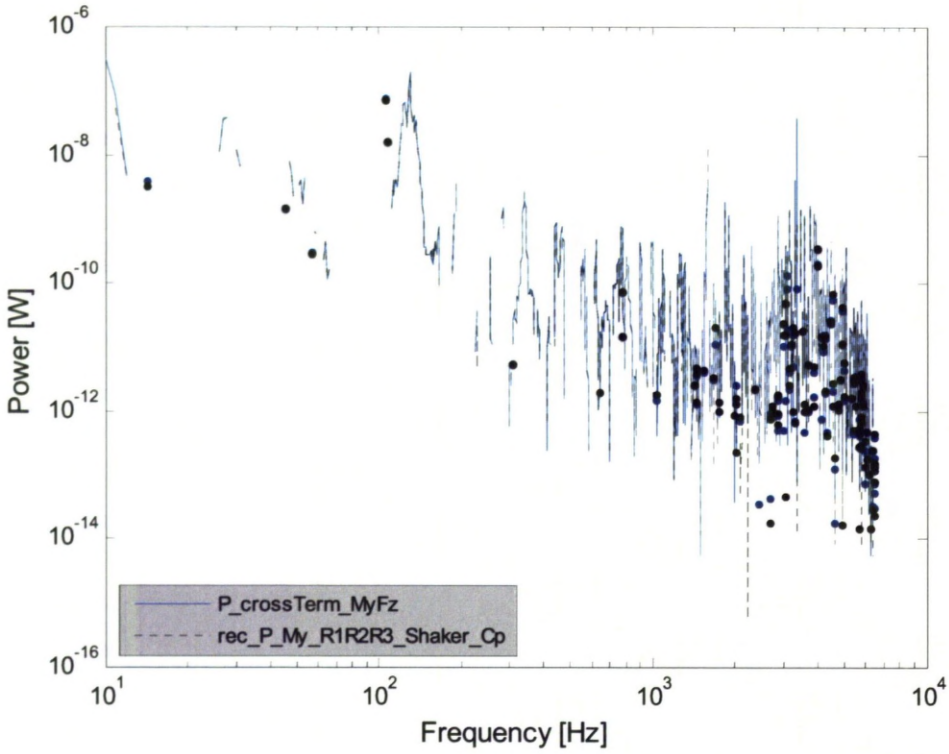

Figure 4.43: Isolated reception plate: Moment M_y induced power due to cross-coupling of moment and force

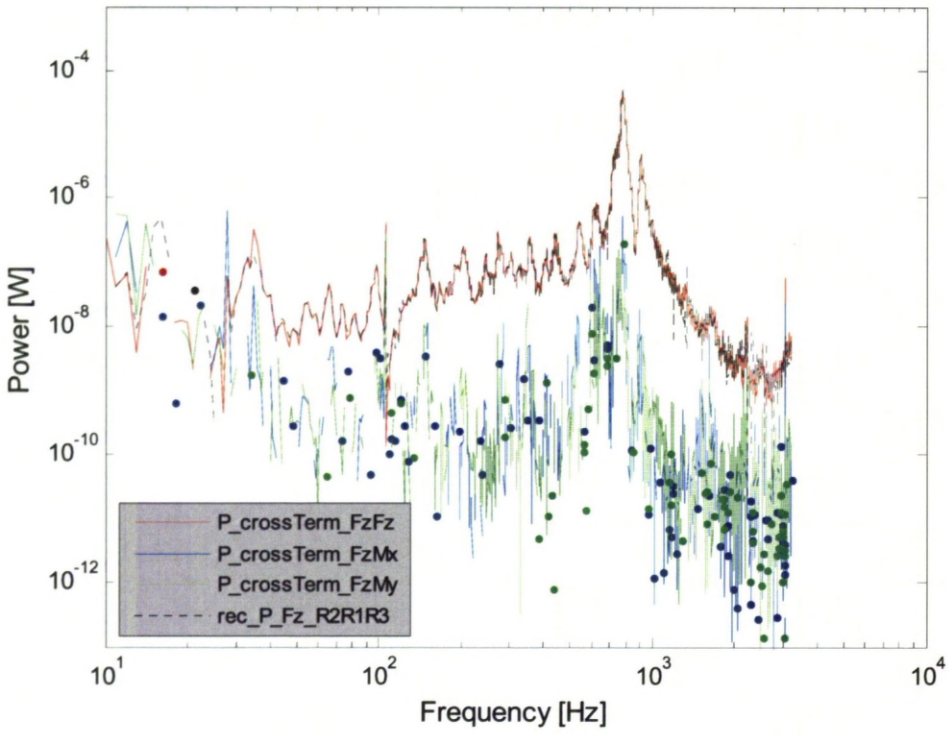

Figure 4.44: Stair wall: Force induced power due to pure force and cross-coupling of components

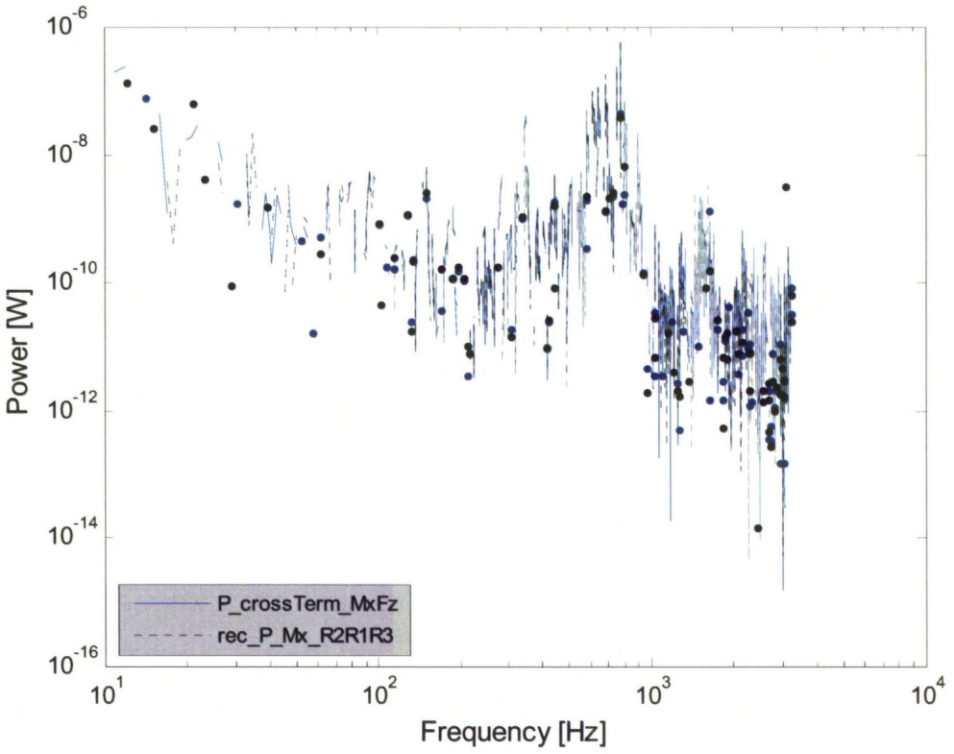

Figure 4.45: Stair wall: Moment M_x induced power due to cross-coupling of moment and force

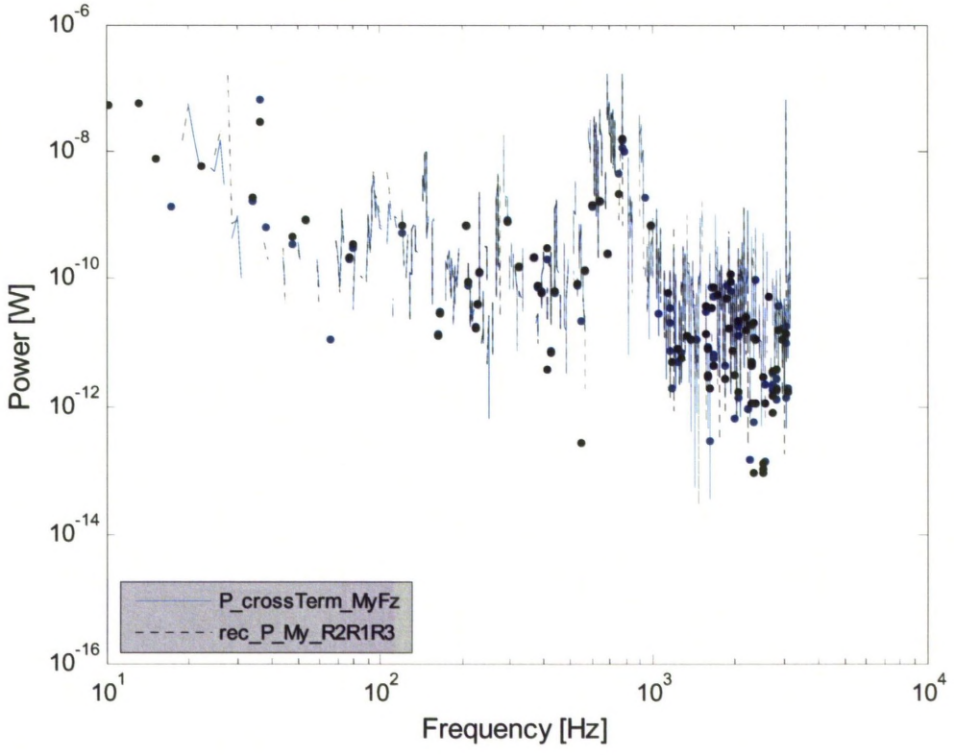

Figure 4.46: Stair wall: Moment M_y induced power due to cross-coupling of moment and force

5 IMPORTANT COMPONENTS OF EXCITATION

5.1 INTRODUCTION

The identification of the component of excitation from a vibrating lightweight stair into a supporting wall (Figure 5.1, Figure 5.2) was performed using the reciprocal method described in Chapter 4. The perpendicular force F_z and two moments M_x and M_y initially were assumed to contribute on the excitation of the wall. The in-plane components were neglected as a result of previous considerations outlined in Chapter 4. The aim was to identify the dominant component(s) of excitation in order to simplify the characterisation.

The stair was excited by a shaker, representing a stationary excitation, and alternatively by a standard tapping machine, representing a quasi-stationary excitation. The sound transmission through the wall contact resulting from excitation with the tapping machine is of particular importance regarding requirements on the impact sound insulation and hence for the prediction that is the main target of this thesis study.

The tapping machine was positioned on two different steps, to highlight the dependence of the stair vibrations on excitation position (Chapter 3.5). The wall excitation (e) and response positions (r_1, r_2, r_3) involved in the experiments are shown in Figure 5.2.

5.2 STAIR EXCITED BY SHAKER

The shaker was rigidly attached to the edge of step 8 (Figure 5.3) and driven with random noise to yield a steady-state and broadband excitation of the stair.

In Figure 5.5 are shown the component powers in narrow bands. The force perpendicular to the wall yields a power curve, which is generally continuous. This indicates that the wall is primarily energised by this component. In contrast, the moment induced power curves show discontinuities at several frequency intervals, indicating negative power flow[3]. In Figure 5.6 the moment induced powers are normalized with respect to the perpendicular force induced power and displayed on a 10 log scale. For most frequencies the force induced power is well above the moment induced powers. At frequencies above 1 kHz, the narrow-band values fluctuate about the zero line, indicating a general increase in the relative importance of moments with frequency. This is consistent with the theory of moment and force mobility of an infinite plate [1]. The force mobility is independent of frequency whereas the moment mobility increases with frequency. This finding also confirms the conclusions of others reported in [2]-[7].

In Figure 5.7 are shown the component powers in 3rd octave bands, and in Figure 5.8, the moment induced powers are normalized with respect to the

---

[3] The conspicuous points in the graphs represent values at single frequencies which are displayed bold because of poor compatibility of the MatLab software and Microsoft Word.

perpendicular force. Except in the mid frequency range about 300 Hz, the force induced power is equal to or greater than the moment induced powers. The force F_z is thus identified as the dominant component of excitation for excitation of the stair with the shaker.

5.3 STAIR EXCITED BY TAPPING MACHINE

The standard tapping machine is currently used for rating the impact sound transmission [8], [9]. Normative requirements refer to the normalized impact sound level, which is therefore the quantity of interest concerning predictions of the impact sound transmission [10]. In comparison with the shaker, the excitation by the tapping machine is not stationary but a sequence of impulses, and is often termed a quasi-stationary excitation. Moreover the excitation position is not at a single point but is a line array of five points at 100 mm spacing. It was initially assumed that the hierarchy of excitation components at the contact with the wall is dependent on the location of the exciter(s) of the stair. Accordingly, the components of excitation were obtained for the tapping machine positioned on two different steps. In both locations, the tapping machine was positioned along the long axis of the steps as shown in Figure 5.4.

In Figure 5.9 are shown the component powers in 3rd octave bands, with the normalised moment induced powers shown in Figure 5.10. Again, the force induced power is equal to or greater than the moment induced powers, except at 63 Hz and 315 Hz. The results are similar to the results for the shaker (Figure 5.7, Figure 5.8), regarding the peaks and dips, indicating that

that the hierarchy of components is not significantly dependent on the type or location of the stair excitation.

Figure 5.11 and Figure 5.12 correspond to the excitation of the stair with the tapping machine on step 5. Again, the force induced power is dominant at most frequencies, but with significant moment induced powers at 63 Hz and 315 Hz. This shows that the relative importance of moments varies with the stair excitation location, as could be expected from the analysis of the vibration behaviour of the stair (Chapter 3.5). Nevertheless, it can be assumed that the force is the dominant component of excitation, when an average is taken for excitations of all steps.

5.4 DISCUSSION

The excitation of the wall by the vibrating stair is generally through the force perpendicular to the wall surface. This may be surprising, since it has been shown in Chapter 3.5 that the stair is primarily set into bending vibrations. It might be expected that the screwed connection acts as a lever, generating a strong moment M_x especially at frequencies where the string board exhibits beam modes. A dominant excitation by moment M_x is indeed observed at the first bending resonance of the string board at 67 Hz, for excitation by the tapping machine but in general the moment excitation is not important. This means that despite the excitation by the stair being normal to the treads and parallel to the supporting wall, there is a significant vibration of the string board normal to the wall, which was not considered in the analysis of the vibration behaviour described in Chapter 3.5. It must also be kept in mind

that the receptiveness of the wall, expressed by the component mobilities, is significantly higher for force excitation perpendicular to the wall surface than it is for moment excitation, especially when the excitation is at a central position [1]. In previous investigations [2]-[4] it was demonstrated that the significance of moments increases when the source, such as an installed machine, is located close to a structural discontinuity, such as an edge of a receiving plate. However, the string boards of stairs are typically connected near the centre of walls [11].

Reciprocal measurements of the component powers could not be performed for human walkers because the excitation is not reproducible [12]-[14]. The measurements would need to be carried out in sequence due to the limited number of input channels (Chapter 4). The walking process might contain a force component in the walking direction which could alter the hierarchy of components and result a strong moment M_y. Although this was not considered further in this thesis study, the sound caused by human walkers on stairs is suggested as a future research topic.

A question arises of if and when an assumed perpendicular force only can provide a practical source characterisation for stairs, even when moments are present and significant. The concept of the equivalent force has been discussed in the literature [15]-[17] and offered as a source characterisation [18].

In Figure 5.13 are shown the reciprocally estimated contact forces for two locations of the footsteps machine on the stair. Again, the contact force is strongly dependent on the location of the excitation and an average value

over all steps might provide a practical and robust measure of source activity.

In Figure 5.14 are contained three estimates of the structure-borne power from the stair into the wall, using the reciprocal method described in Chapter 4. The first consists of the sum of the three component powers (4.6); the second is of the force induced power only (4.4); the third is obtained from assuming that the wall response is due only to the reciprocally obtained single component, the force with equation (4.19). The third value follows the assumption that the reciprocal determination of the force is accurate but there are uncertainties in the force induced power due to cross-coupling (Chapter 4.7). The second estimate underestimates the total power at 200 Hz to 315 Hz, which corresponds to significant moments, see Figure 5.7. However, the third estimate agrees with first estimate over most of the frequency range of interest.

A similar conclusion can be drawn from Figure 5.15, for a footsteps machine on step 8, and from Figure 5.16 for a footsteps machine on step 5.

5.5 SUMMARY

The force perpendicular to the wall is the dominant component in the case considered although moments have shown importance at particular frequencies. This finding allows a significant simplification regarding the simplified prediction of the sound transmission since only the translational component perpendicular to the wall has to be taken into account.

This offers a way forward to a practical characterisation. In Chapter 6, the free velocity method is explored where only the component of vibration perpendicular to the stair running board is measured, along with the component source and receiver mobilities

5.6 REFERENCES

[1] Cremer, L., Heckl, M., Petersson B.A.T.: Structure-borne sound, Springer Verlag, Berlin, 2005

[2] Yap, S. H.: The role of moments and forces in structure-borne sound emission from machines in buildings, PhD Thesis at the University of Liverpool, 1988

[3] Yap, S. H., Gibbs, B. M.: Structure-Borne Sound Transmission from Machines in Buildings, Part 1: Indirect Measurement of Force at the Machine - Receiver Interface of a Single and Multi - Point Connected System by a Reciprocal Method, Journal of Sound and Vibration, 1998

[4] Yap, S. H., Gibbs, B. M.: Structure-Borne Sound Transmission from Machines in Buildings, Part 2: Indirect Measurement of Force and Moment at the Machine - Receiver Interface of a Single Point Connected System by a Reciprocal Method, Journal of Sound and Vibration, 1998

[5] Späh, M. M.: Characterisation of structure-borne sound sources in buildings, PhD Thesis of The University of Liverpool, 2006

[6] Späh, M. M.; Gibbs, B.M.: Reception plate method for characterisation of structure-borne sound sources in buildings: Installed power and sound pressure from laboratory data, Applied Acoustics, Vol. 70 (11-12), 1431-1439, 2009

[7] Späh, M. M.; Gibbs, B.M.: Reception plate method for characterisation of structure-borne sound sources in buildings: Assumptions and application, Applied Acoustics, Vol. 70 (2), 361-368, 2009

[8] EN ISO 140-7: Acoustics – measurement of sound insulation in buildings and of building elements. Part 7: field measurements of impact sound insulation of floors, December 1998

[9] ISO 717-2: Acoustics – Rating of sound insulation in buildings and of building elements. Part 2: Impact sound insulation, December 1996

[10] EN 12354-2: Building acoustics – Estimation of acoustic performance of buildings from the performance of elements – Part 2: Impact sound insulation between rooms, September 2000

[11] ETAG 008: Guideline for European Technical approval of prefabricated stair kits, EOTA Brussels, January 2002

[12] Scholl, W.: Impact sound insulation: The standard tapping machine shall learn to walk, Building Acoustics, 2001

[13] Lievens, M.: Model of a Person walking as a Structure - Borne Sound Source, 19th International Congress on Acoustics, Madrid, Spain, 2007

[14] Racic, V.; Pavic, A.; Brownjohn, J.M.W: Experimental identification and analytical modelling of human walking forces: Literature review, Journal of Sound and Vibration, 2009

[15] Ohlrich, M. and Larson, C.: Surface and Terminal Source Power for Characterization of Vibration Sources at Audible Frequencies, Proceedings of Inter-Noise 1994, page 633-636, 1994

[16] Ohlrich, M.: Terminal Source Power for Predicting Structureborne Sound Transmission from a Main Gearbox to a Helicopter Fuselage, Proceedings of Inter-Noise 1995, 555-558, 1995

[17] Ohlrich, M.: The Use of Surface Power for Characterization of Structure-borne Sound Sources of low Modal Density, Proceedings of Inter-Noise 1996, 1313-1318, 1996

[18] Ten Wolde, T.; Gadefelt, G. R.: Development of standard measurement methods for structure-borne sound emission, Noise Control Engineering Journal 28 (1), 5-14, 1987

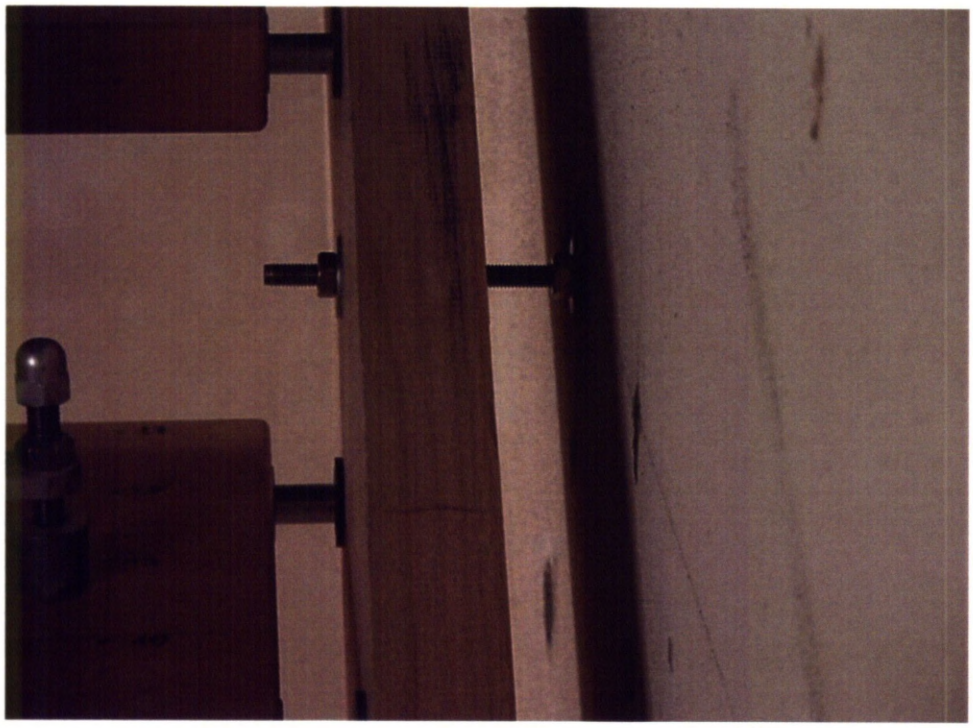

Figure 5.1: Wall contact for in-situ measurement of the component power transmission of a vibrating lightweight stair

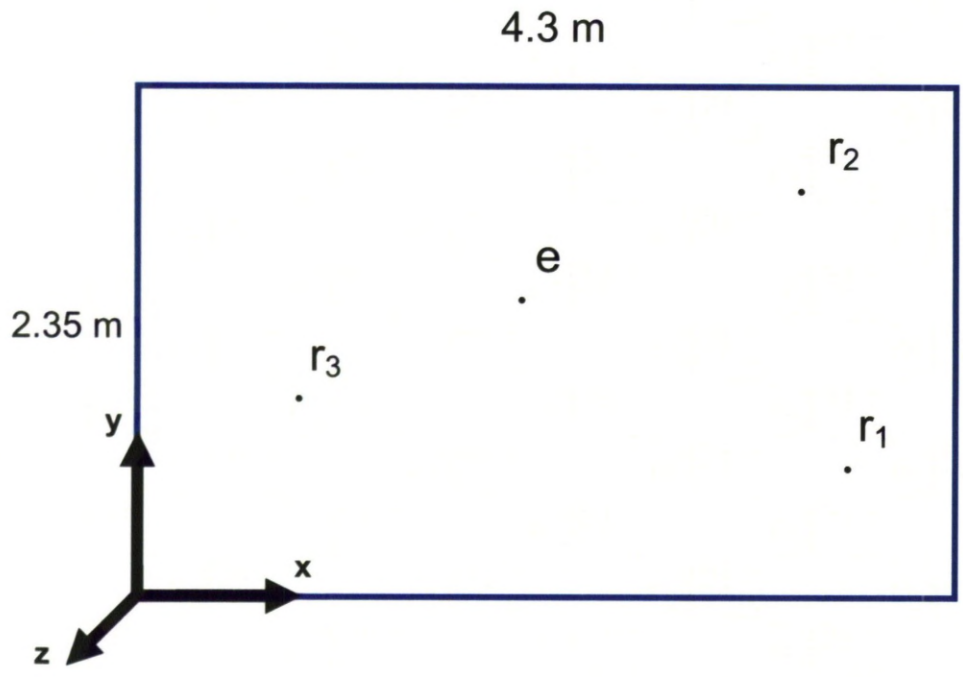

Figure 5.2: Excitation (e) and reference points (r) on stair wall; e (2,33/1,57), r_1 (1,84/1,61), r_2 (1,07/0,55), r_3 (0,36/1,32)

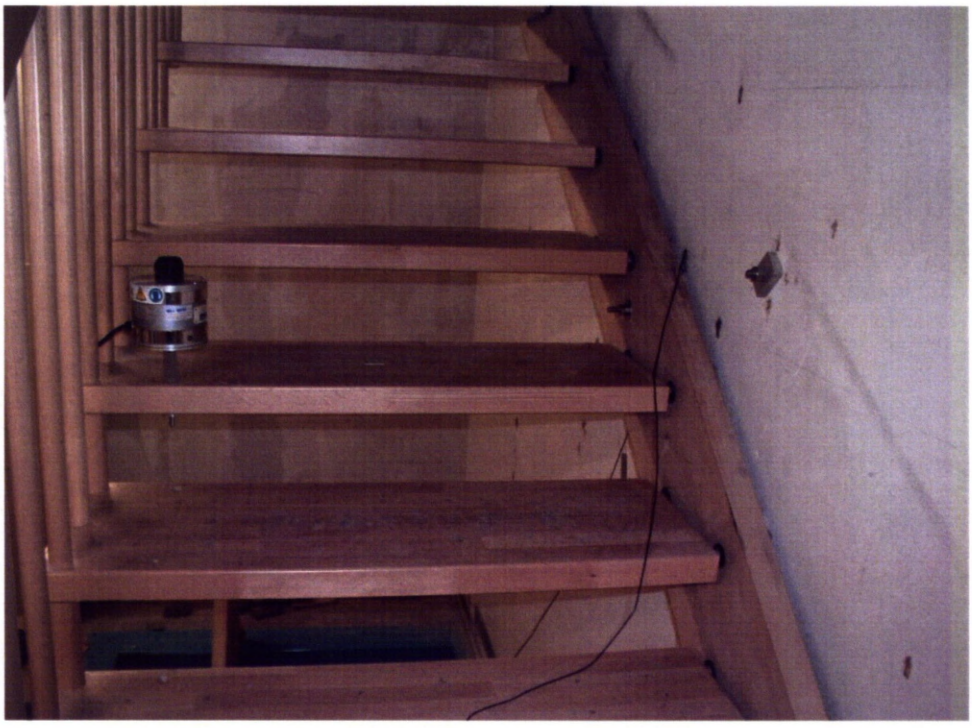

Figure 5.3: Set-up on stair wall for direct and reciprocal force and power measurement – shaker attached to step 8

Figure 5.4: Set-up on stair wall for direct and reciprocal force and power measurement – tapping machine on step 8

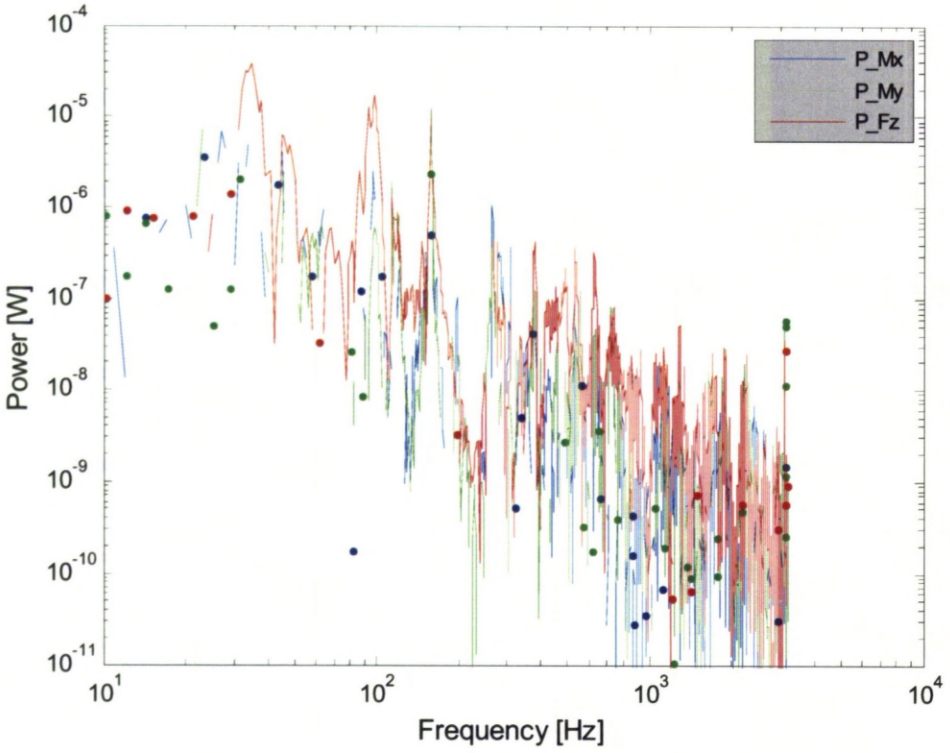

Figure 5.5: Stair excited by shaker on step 8: component powers from reciprocal method

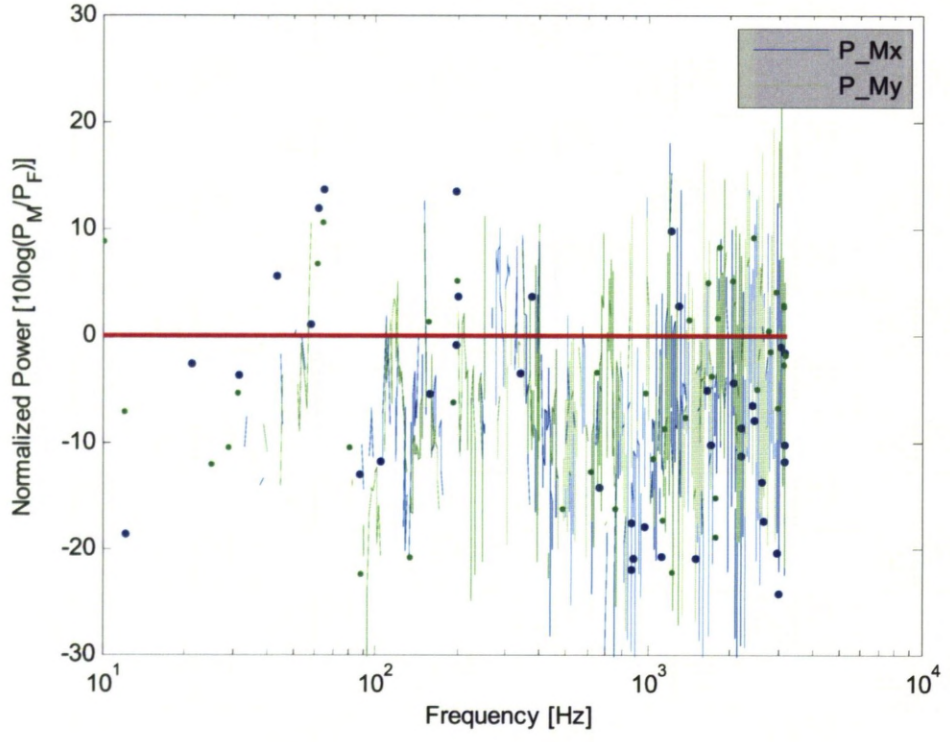

Figure 5.6: Stair excited by shaker on step 8: component powers from reciprocal method normalized to F_z

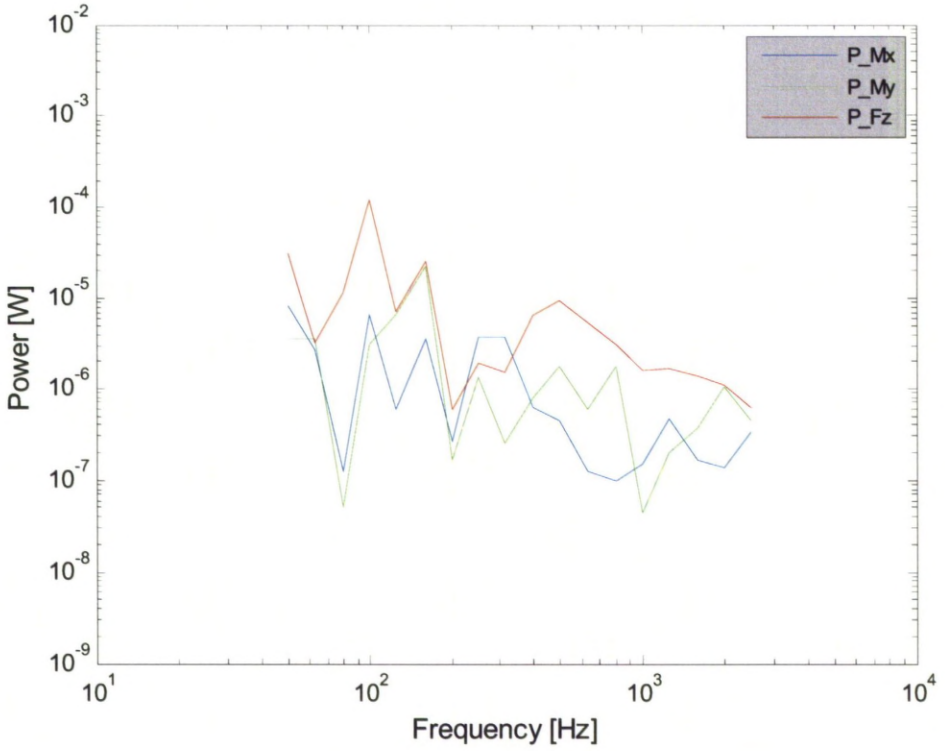

Figure 5.7: Stair excited by shaker on step 8: component powers from reciprocal method in 3rd octave bands

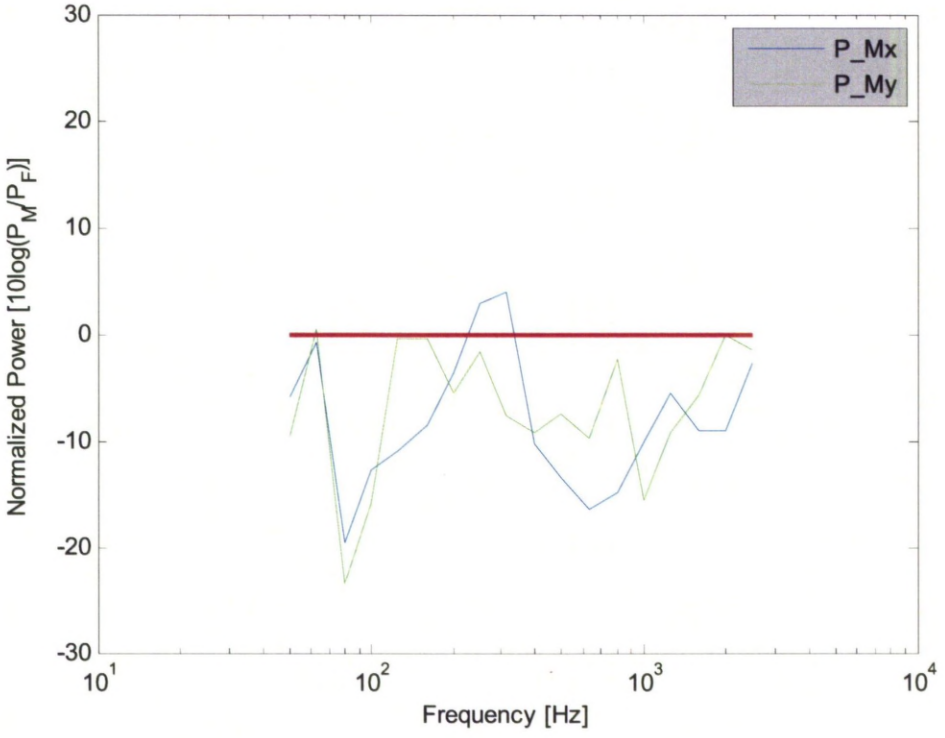

Figure 5.8: Stair excited by shaker on step 8: component powers from reciprocal method normalized to F_z in 3rd octave bands

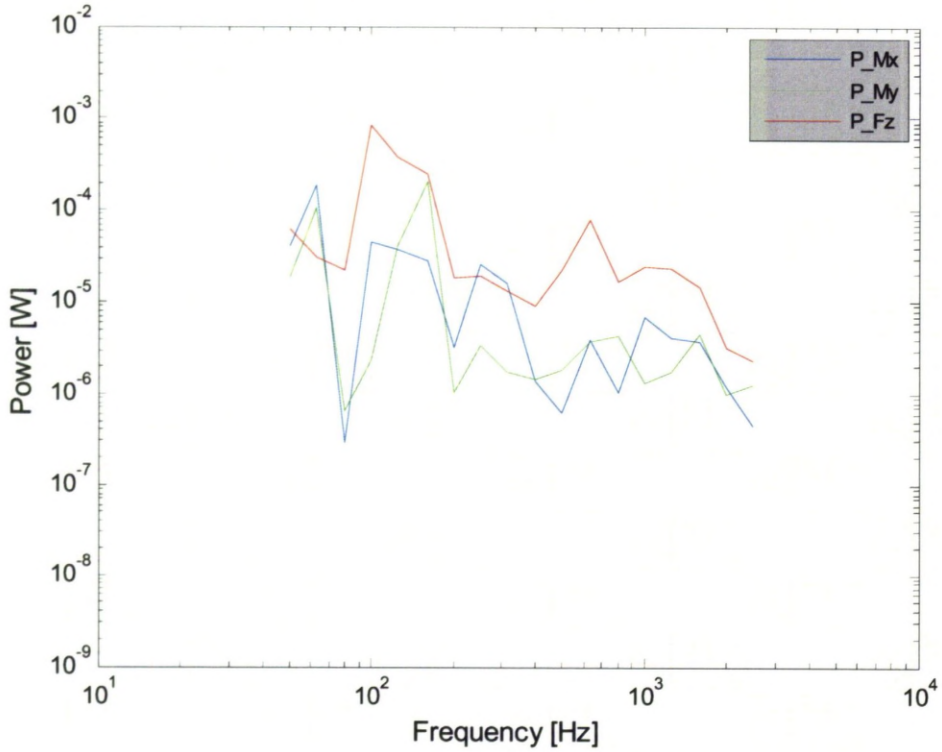

Figure 5.9: Stair excited by tapping machine on step 8: component powers from reciprocal method in 3rd octave bands

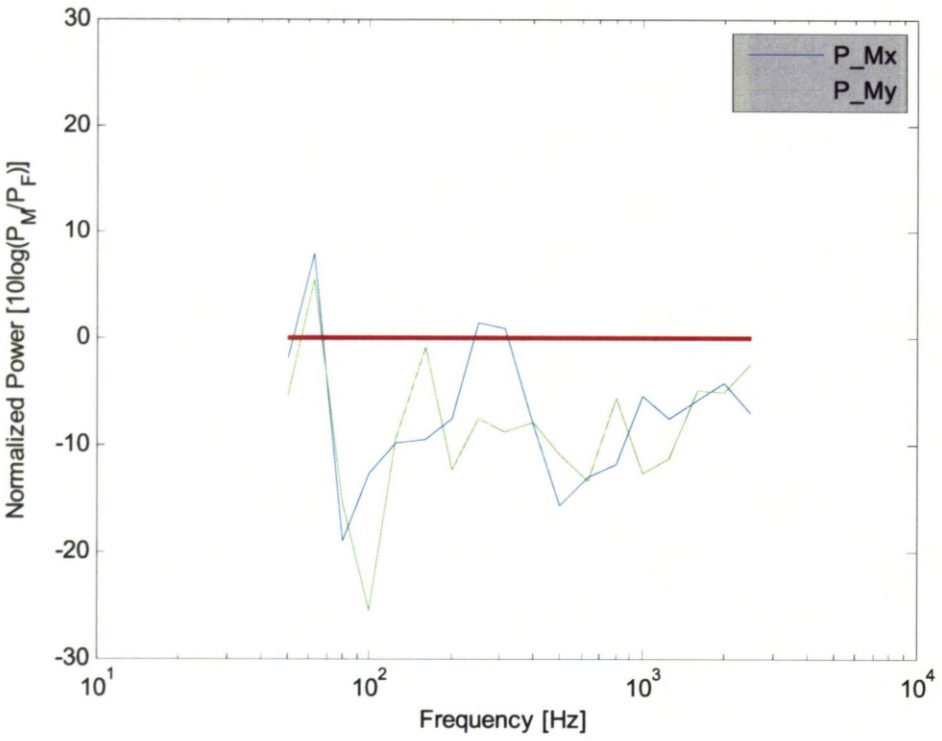

Figure 5.10: Stair excited by tapping machine on step 8: component powers from reciprocal method normalized to F_z

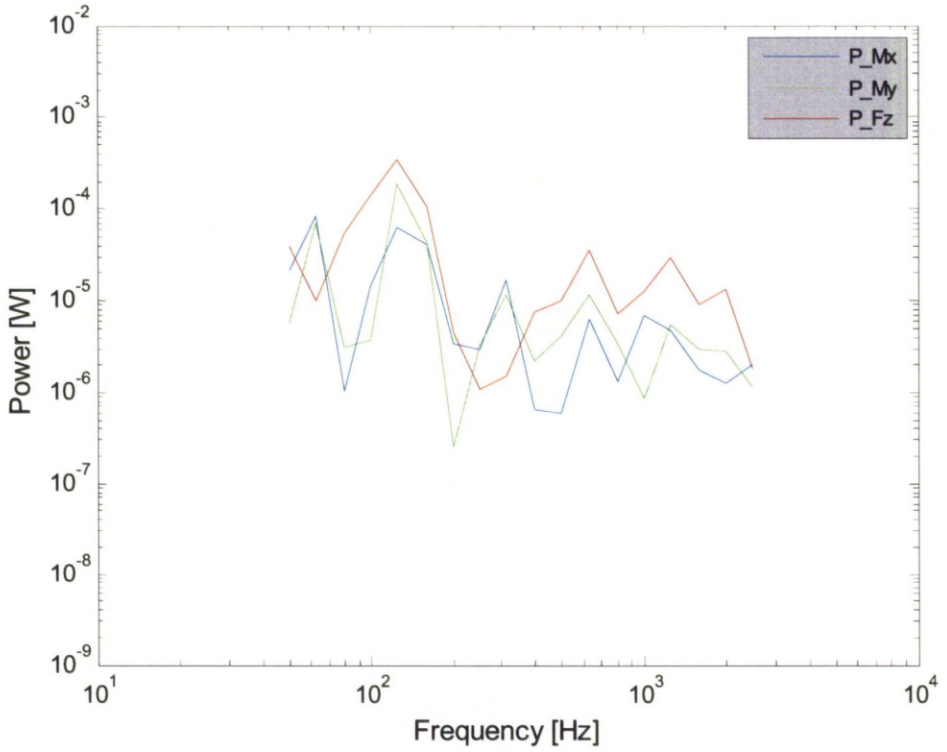

Figure 5.11: Stair excited by tapping machine on step 5: component powers from reciprocal method in 3rd octave bands

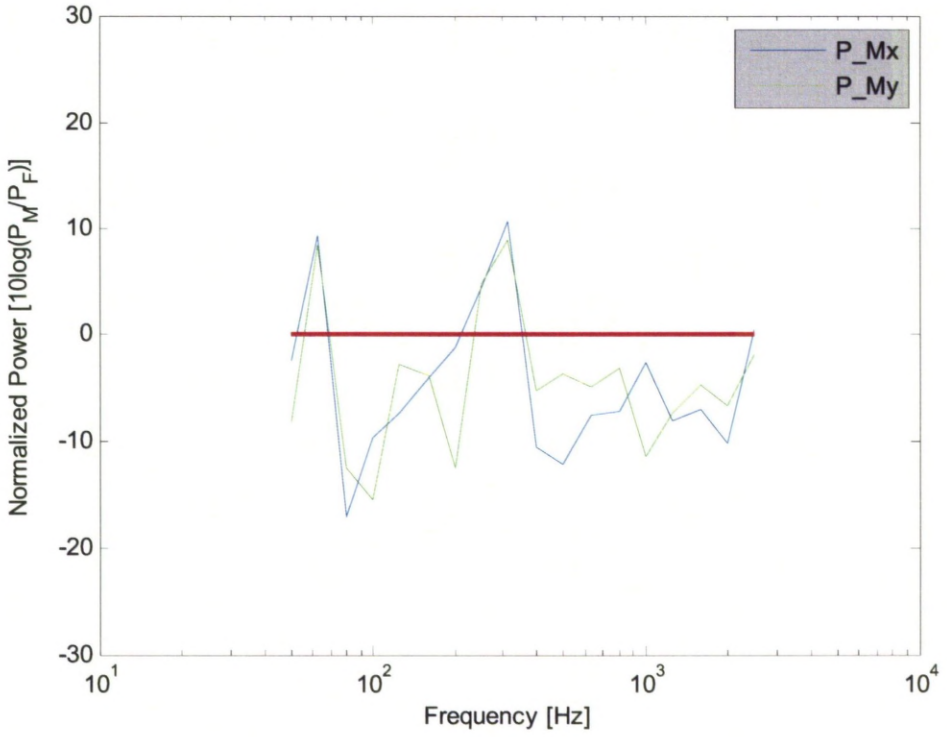

Figure 5.12: Stair excited by tapping machine on step 5: component powers from reciprocal method normalized to F_z

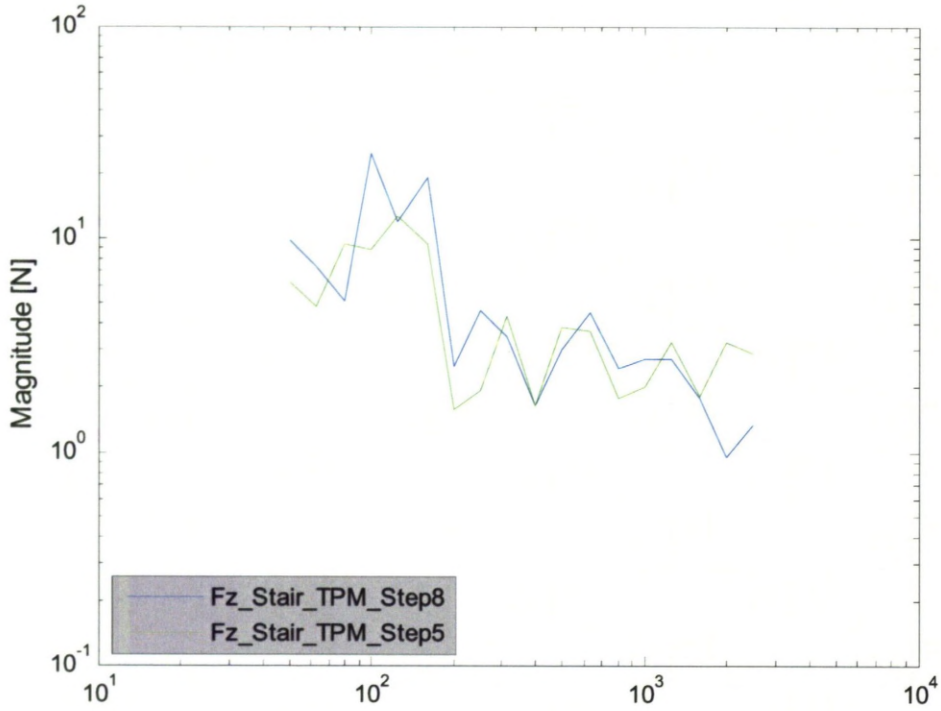

Figure 5.13: Wall contact forces for the excitation of the stair with the tapping machine

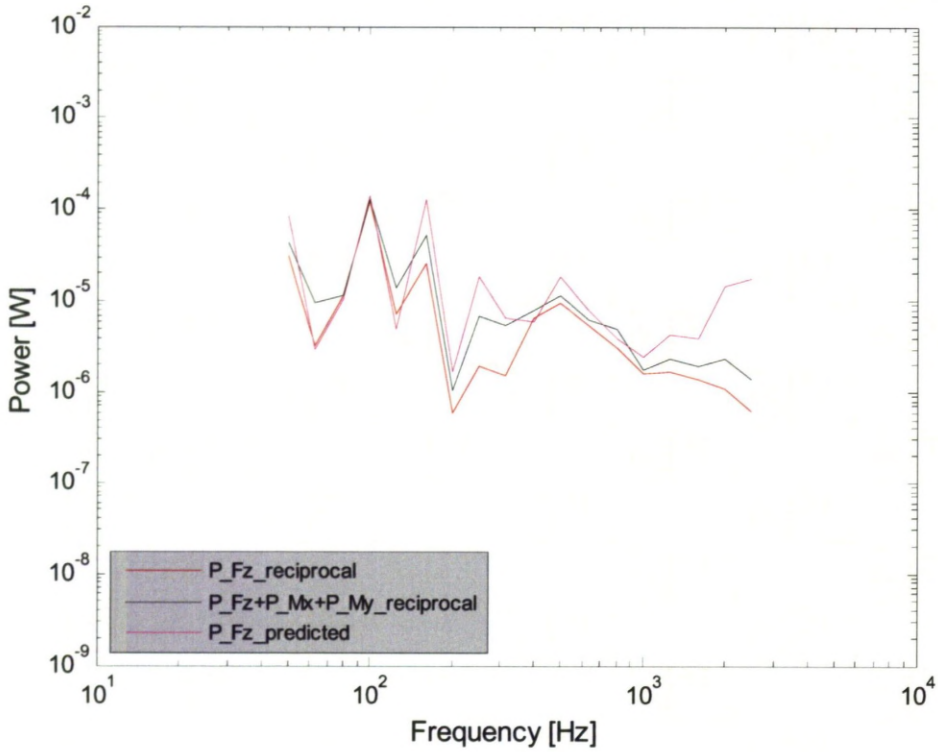

Figure 5.14: Stair excited by shaker on step 8: power predicted from reciprocal force and wall mobility; sum of component powers

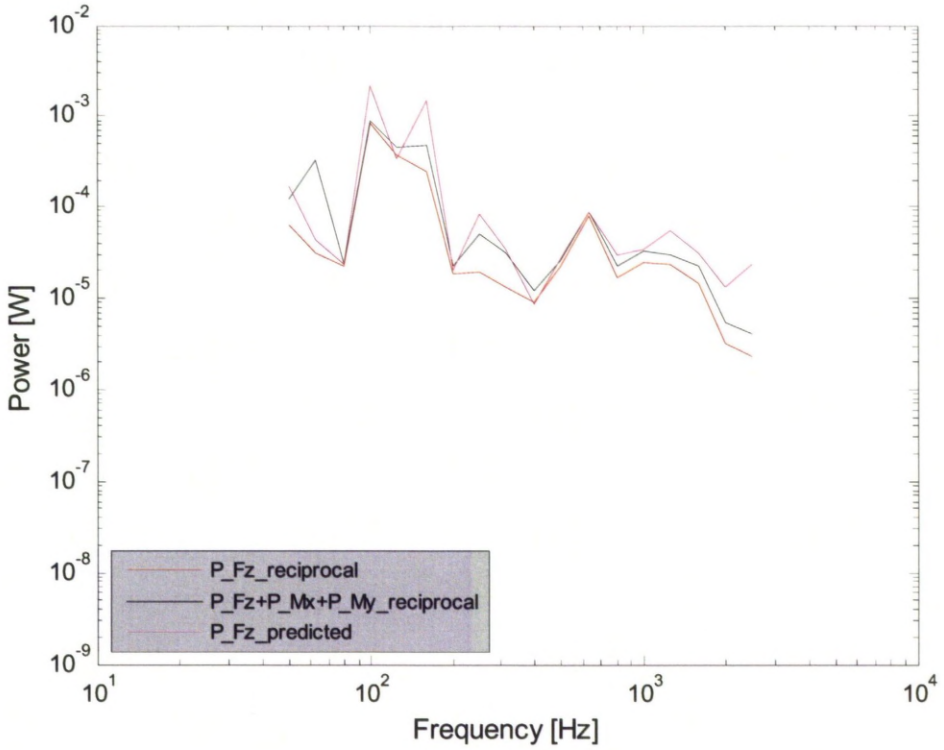

Figure 5.15: Stair excited by tpm on step 8: power predicted from reciprocal force and wall mobility; sum of component powers

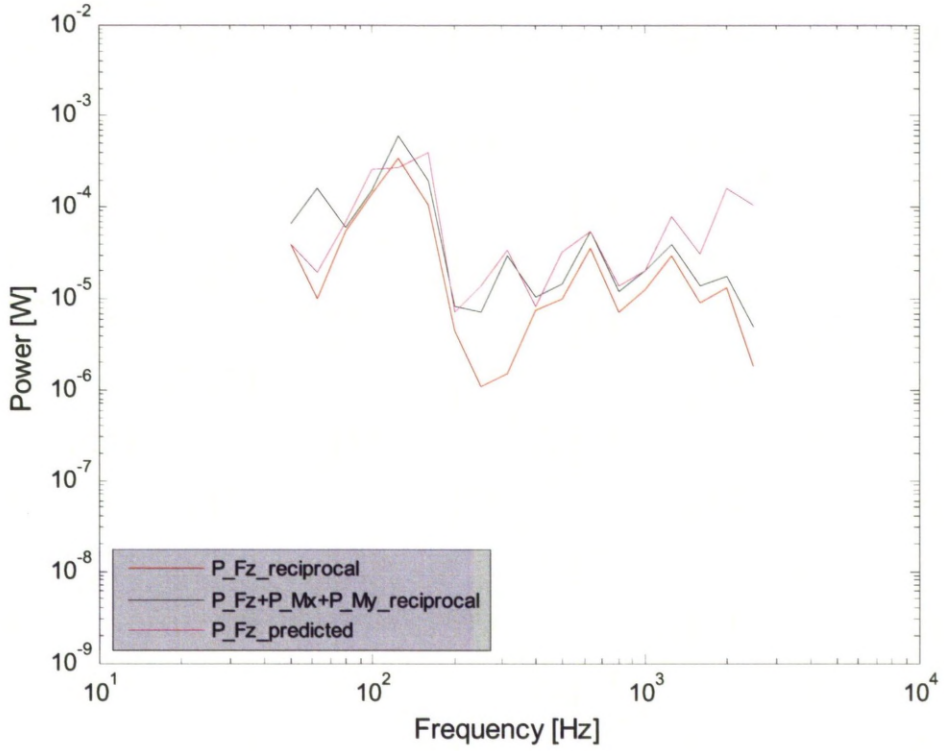

Figure 5.16: Stair excited by tpm on step 5: power predicted from reciprocal force and wall mobility; sum of component powers

6 CHARACTERISATION BY FREE VELOCITY AND MOBILITY

6.1 INTRODUCTION

The characterisation of a vibrating lightweight stair as a structure-borne sound source was performed by reference to the free velocity and mobility at the contact with the supporting wall. Following from the conclusions of Chapter 5, the characterisation was simplified by considering only the translational component perpendicular to the wall. As in the previous investigations, the stair was excited by a shaker, representing a stationary excitation, and alternatively by a standard tapping machine, representing a quasi-stationary excitation.

The structure-borne power into a receiving wall was predicted from source free velocity and source and receiver mobilities and compared to the measured in-situ power (Chapter 5).

6.2 MEASUREMENT SET-UP

The experimental set-up according to [1] is shown in Figure 6.1 and Figure 6.2. The stair was removed from the wall to access the contact point. The screw was cut according to the distance between the string board and wall in the mounted condition. The resilient supports (Figure 3.5) had a mass-

spring resonance below 20 Hz such that the measurement of the free velocity in the frequency range from 50 Hz upwards was ensured.

To enable measurement of the translational (and rotational) free velocity and the contact mobility, an aluminium indenter was used (Figure 6.2). Previously, measurement of the point mobility of the aluminium indenter showed it to be resonance free in the frequency range up to 5 kHz (not shown).

6.3 MOBILITY

The stair and wall contact (point force) mobilities are shown in Figure 6.4. Also shown is the indenter mobility. The combined mobility of stair and indenter is given by:

$$\frac{1}{Y_{stair+indenter}} = \frac{1}{Y_{stair}} + \frac{1}{Y_{indenter}} \tag{6.1}$$

To judge the influence of mass-loading the stair mobility without indenter was calculated by subtraction of the indenter mobility. The result is also shown in Figure 6.4. In the relevant frequency range up to ca. 1 kHz mass loading by the indenter can be neglected except for a stair resonance at ca. 750 Hz. At higher frequencies the combined mobility partly exceeds the indenter mobility which can be referred to errors in the mobility measurement of the stair, probably due to local stiffness effects.

The (combined) stair mobility exhibits resonant behaviour except in the frequency range 125 Hz - 300 Hz where spring-like behaviour is observed.

In this region, the phase is + $\pi/2$. The point mobility of the wall shows typical plate behaviour with the fundamental mode at about 33 Hz. A detailed analysis of the vibration behaviour of the wall is described in Chapter 8.3.3. The stair mobility is of the order of 10^{-4} m/s and that of the wall is of the order of 10^{-6} m/s. The level difference therefore is generally 20 dB (Figure 6.5). Mobility matching occurs only near the fundamental (1,1) wall mode at 33 Hz. In general the stair constitutes a high-mobility source.

6.4 FREE VELOCITY

The free velocity at the stair contact was measured using the aluminium indenter used in the mobility measurement. The results are shown in Figure 6.6 for shaker and tapping machine excitation on step 8.

The free velocity exhibits a first strong resonance peak around 20 Hz, with additional peaks, of decreasing amplitude, with increased frequency.

The free velocity is shown as one third octave values in Figure 6.7. For excitation with the tapping machine, the spectrum displays values between 10^{-3} – 10^{-4} m/s and a maximum level difference of 18 dB. For shaker excitation the spectrum displays fluctuations about an average value of 10^{-4} with a maximum level difference of 27 dB. The higher frequency dependence for shaker excitation can be referred to the vibration shapes of the stair (Chapter 3.5).

A question arises concerning the expected free velocity spectrum for human footfall excitation. In principle the procedure is similarly applicable. However

a practical difficulty might be to ensure sufficient stability for walking without changing the dynamic characteristics of the stair. The free velocity could be recorded as an average value for excitation of all steps. A major difficulty that has not yet been overcome is that walking is not reproducible and is strongly dependent on the individual walker's characteristics [2]-[4]. Therefore a unique characterisation of vibrating stairs excited by a walking person is in principle not possible.

6.5 SOURCE DESCRIPTOR

So far, the stair has been described in terms of free velocity and source mobility. Both are required if the stair is to be characterised on a power basis. The source descriptor proposed by Mondot and Petersson [5] offers an independent source characterisation (Chapter 2.2.5). It is an expression of the ability of the stair to generate power. The source quantities, free velocity and source mobility, are required in the following form:

$$S = \frac{1}{2}\frac{\left|v_{sf}\right|^2}{Y_s^*} \tag{6.2}$$

The source descriptor can be interpreted as the maximum power possible from the stair. The real part of the source descriptor is of particular interest as it represents the maximum available net active power, the installed power is some value below this. In [6] the single-point formulation by Mondot and Petersson is extended to multiple contacts. Here the complex source descriptor is termed characteristic power (CP) and the maximum

available power (MAP) is introduced as the real part of the source descriptor.

In Figure 6.8 is shown the real part of the source descriptor (MAP) for the stair excited by shaker and tapping machine in narrow bands. For some frequencies the curves show gaps indicating negative real parts. This is unphysical and can be referred to errors in the measured source mobility. In Figure 6.9 is shown the maximum available power in 3rd octave bands. For excitation with the tapping machine the values are generally 10 dB higher than for shaker excitation representing higher source strength. This gives an example how the source descriptor could be used for ranking stairs in terms of the source strength. Here the parameter is the excitation and the location of the excitation. The source descriptor could similarly be used to quantify the effect of structural modifications on stair systems or to compare stairs with each other or with other sources of structure-borne sound.

The source descriptor enables a full characterisation on a power basis. In the case considered it could alternatively have been used for ranking the components of excitation e.g. forces and moments, which has been done by in-situ measurement as outlined in the previous Chapter.

Finally the source descriptor provides the basis for the calculation of the installed power which is the desired quantity.

6.6 INSTALLED POWER

In addition to the source free velocity and mobility the prediction of the installed power i.e., that into the supporting wall also requires knowledge of the real part of the receiver (wall) mobility. The installed power is given by:

$$P = \frac{1}{2} \frac{\left|v_{sf}\right|^2}{\left|Y_s + Y_R\right|} \cdot \mathrm{Re}\left\{Y_R\right\} \tag{6.3}$$

By use of the source descriptor equation (6.3) is rearranged such that the coupling conditions are comprised in the coupling function [5] or a coupling factor [6].

$$P = \frac{1}{2} \mathrm{Re}\left\{ \frac{\left|v_{sf}\right|^2}{Y_s^*} \frac{Y_s^* \cdot Y_R}{\left|Y_s + Y_R\right|^2} \right\} \tag{6.4}$$

The power, predicted from equation (6.3) and by reciprocal measurement (Chapter 4 and 5), is compared in Figure 6.10 and Figure 6.11 for shaker excitation and in Figure 6.12 and Figure 6.13 for excitation of the stair with the tapping machine. The maximum available power (real part of blue curve in Figure 6.9) is given as reference. In Figure 6.14 are shown the level differences of the power for prediction and in-situ measurement.

The agreement of predicted and in-situ measured power is generally within +/- 3 dB in the relevant frequency range up to 1 kHz. At higher frequencies the predicted power consistently underestimates the in-situ measured power.

The installed power is 10-20 dB below the maximum available power which is due to the large mobility mismatch of stair and wall (Figure 6.4, Figure 6.5) [6]. The maximum available power could rather be encountered when the stair is attached to a lightweight wall where the order of point mobilities is typically 10^{-3} m/Ns [7].

6.7 BLOCKED FORCE

In the case considered the stair constitutes a high-mobility source and thus the blocked force alternatively can be used to characterise the stair system as the installed power is given by the square of the blocked force and the receiver mobility (4.19). It can be assumed that this holds true for other lightweight stair systems (e.g. steel-wood constructions) in heavyweight buildings since the variations in mass are not significant and also the variation of wall mobilities tends to be small due to requirements on the sound insulation of separating walls.

In Figure 6.15 the blocked force and the in-situ force were computed from the source free velocity for excitation of the stair with the tapping machine and source mobility e.g. source and receiver mobilities (6.3). The in-situ force and the blocked force agree within ± 0.5 dB. Thus the blocked force can be used as input for the prediction of the sound transmission in buildings according to 12354-2 [8] as will be outlined in Chapter 8.

6.8 DISCUSSION

The characterisation of stairs by free velocity and mobility yields an independent source characterisation and provides the basis for the calculation of power delivered when installed at arbitrary walls. For heavyweight walls the characterisation can be simplified to the blocked force without a lack of accuracy for the prediction of the installed power.

The source activity of the stair strongly depends on the location of the excitation. This effect could be considered e.g. by means of averaging the free velocities to be measured over all steps.

There are often practical difficulties in the measurement of free velocity [12]. In the case considered, the stair must be moved away from the wall and the contact point(s) must be defined properly. Problems concerning stability might be encountered when a characterisation for a walking person is desired. So far it has been shown that the characterisation for excitation with the tapping machine is practically unproblematic which provides the basis for the prediction of the normalized impact sound pressure level.

6.9 SUMMARY

The force induced power by a vibrating stair can be predicted from contact free velocity and mobility as has been demonstrated for a stationary and a quasi-stationary excitation. By treating stairs and excitation (tapping machine or walking human) as one system, stair systems can be

characterised in the same way as common sources of structure-borne sound such as mechanical installations [9]-[11].

The characterisation is however complicated, even for one component of excitation, if several contacts are considered. In Chapter 7, the reception plate method is explored, to circumvent the detailed description of multiple contacts and degrees of freedom for a practical characterisation.

6.10 REFERENCES

[1] ISO 9611: Acoustics – Characterization of sources of structure-borne sound with respect to sound radiation from connected structures – Measurement of velocity at the contact points of machinery when resiliently mounted, 1996

[2] Scholl, W.: Impact sound insulation: The standard tapping machine shall learn to walk, Building Acoustics, 2001

[3] Lievens, M.: Model of a Person walking as a structure-borne sound source, International Congress on Acoustics, 2007

[4] Racic, V.; Pavic, A.; Brownjohn, J.M.W: Experimental identification and analytical modelling of human walking forces: Literature review, Journal of Sound and Vibration, 2009

[5] Mondot, Petersson: Characterisation of structure-borne sound sources: the source descriptor and the coupling function, Journal of sound and vibration 114, pp. 507-518, 1987

[6] Moorhouse, A. T.: On the characteristic power of structure-borne sound sources, Journal of Sound and Vibration, Vol. 248(3), 2001, page 441-459

[7] Mayr A. R.: Vibroacoustic sources in lightweight buildings, PhD Thesis of The University of Liverpool, 2009

[8] EN 12354-2: Building acoustics – Estimation of acoustic performance of buildings from the performance of elements – Part 2: Impact sound insulation between rooms, September 2000

[9] Späh M. M.: Characterisation of structure-borne sound sources in buildings, PhD Thesis of The University of Liverpool, 2006

[10] Alber T. H.: Valves as sources of structure-borne sound, PhD Thesis of The University of Liverpool, 2006.

[11] Gibbs B. M., Ning Qi, Moorhouse A.T. "A practical characterisation for vibro-acoustic sources in buildings", Acta Acustica united with Acustica, Vol. 93, 84-93, 2007

[12] Moorhouse, A.T, Elliot, A.S., Evans, T.A., "In situ measurement of the blocked force of structure-borne sound sources", Journal of sound and vibration 325, pp. 679–685, 2009

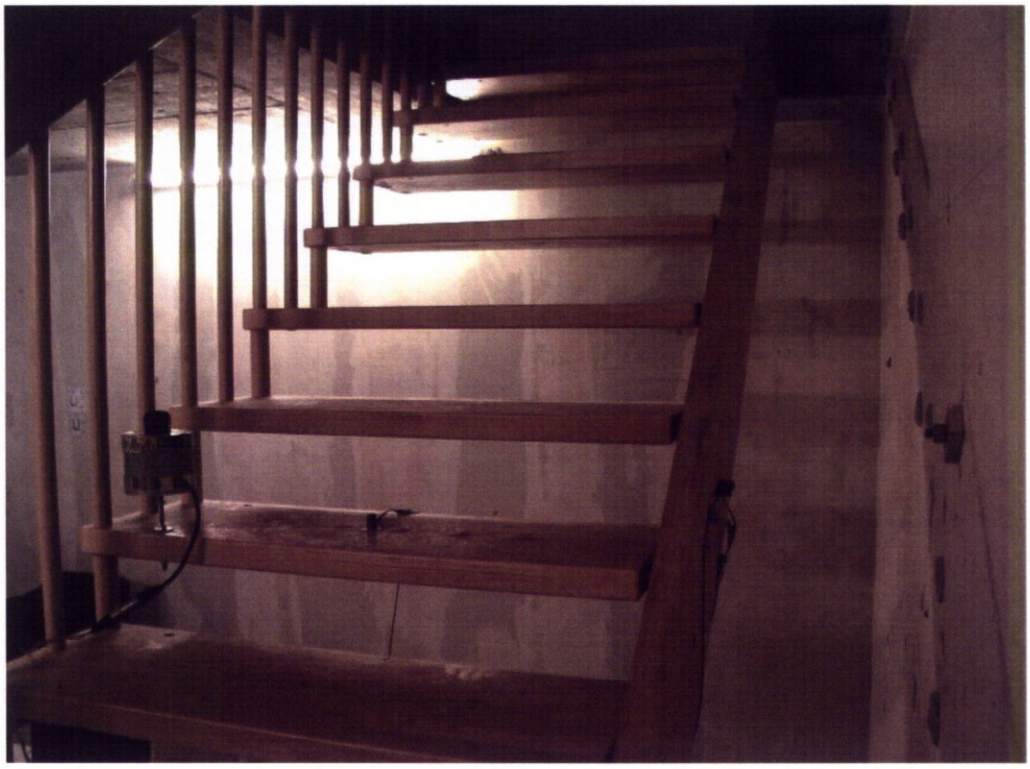

Figure 6.1: Set-up for free velocity and mobility measurement: Stair decoupled from the receiving wall and ceilings

Figure 6.2: Set-up for mobility measurement: Indenter on screw to enable measurement of velocity

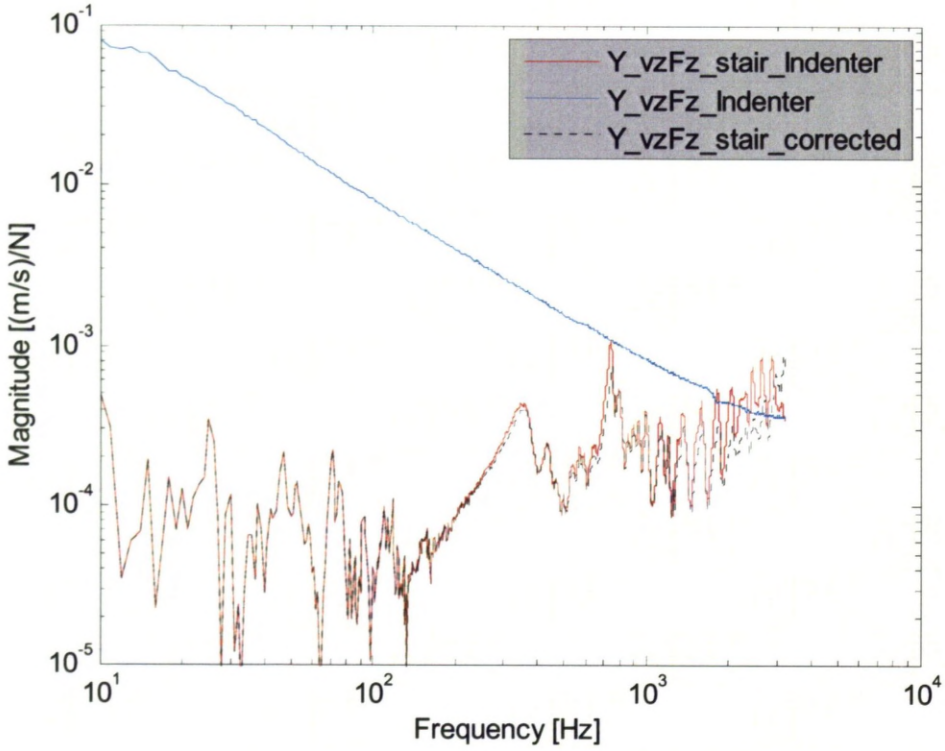

Figure 6.3: Stair and indenter point mobilities

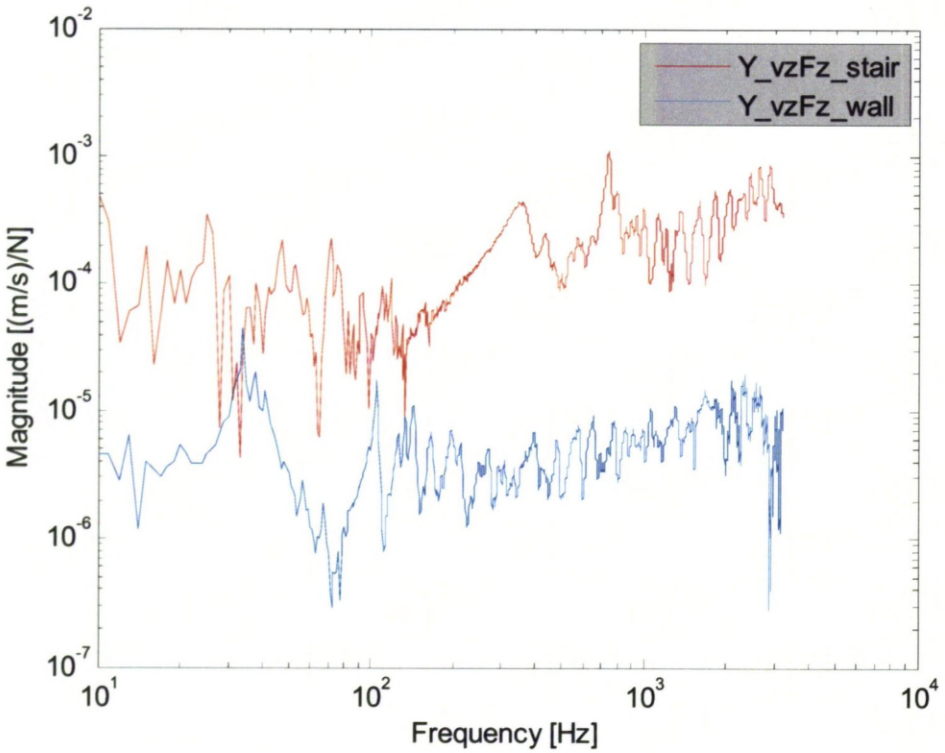

Figure 6.4: Stair and wall contact mobilities

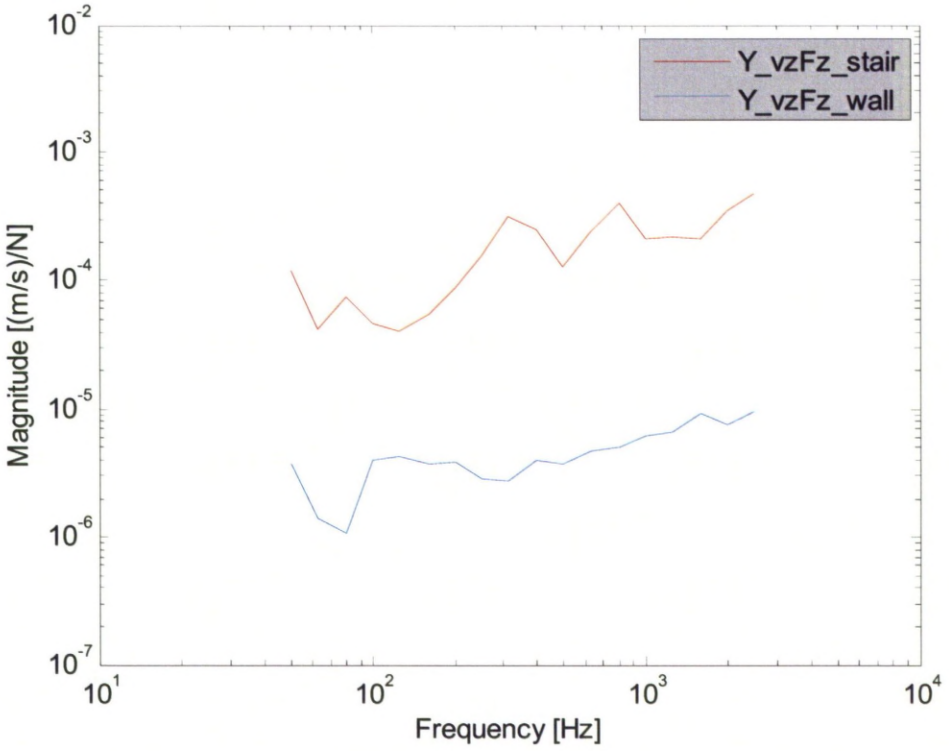

Figure 6.5: Stair and wall contact mobilities in 3rd octave bands

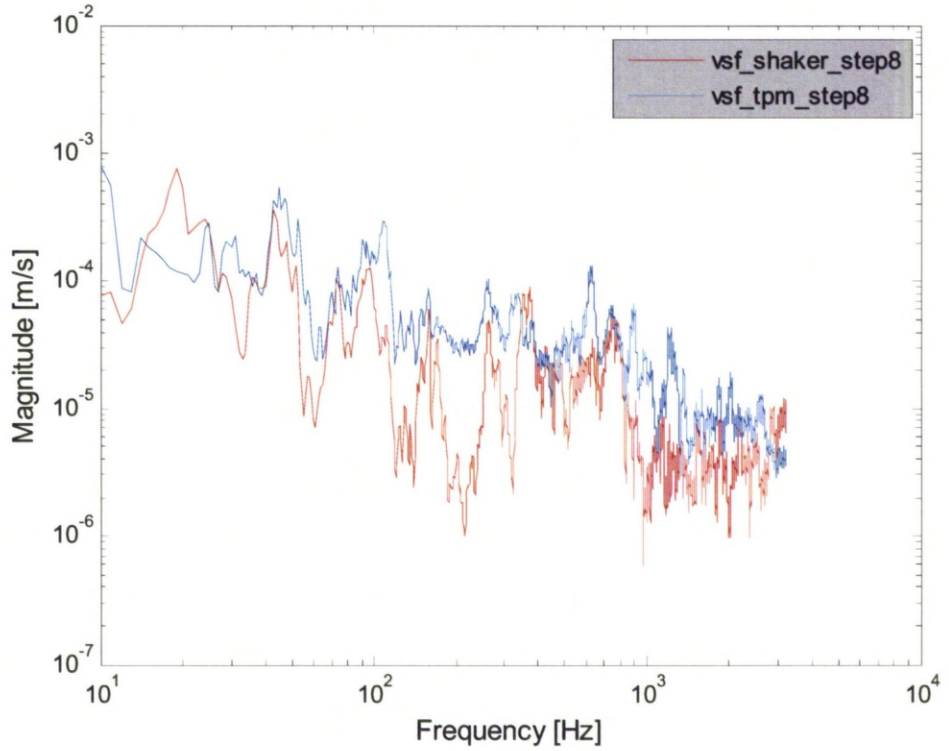

Figure 6.6: Free velocity at contact indenter with stair excited by shaker and tapping machine on step 8

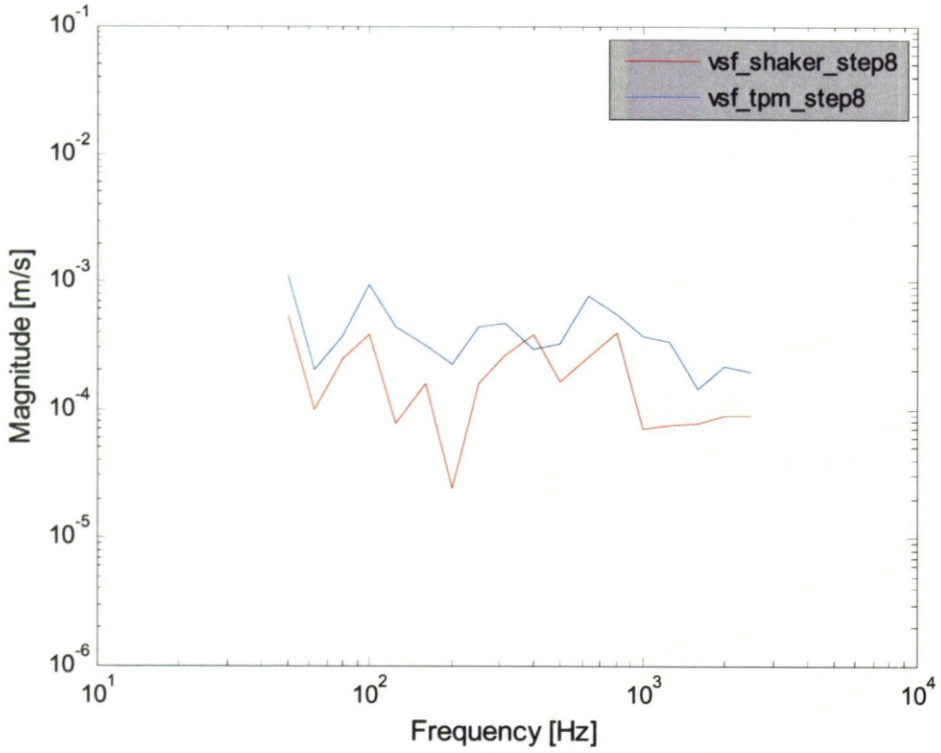

Figure 6.7: Free velocity at contact indenter with stair excited by shaker and tapping machine on step 8

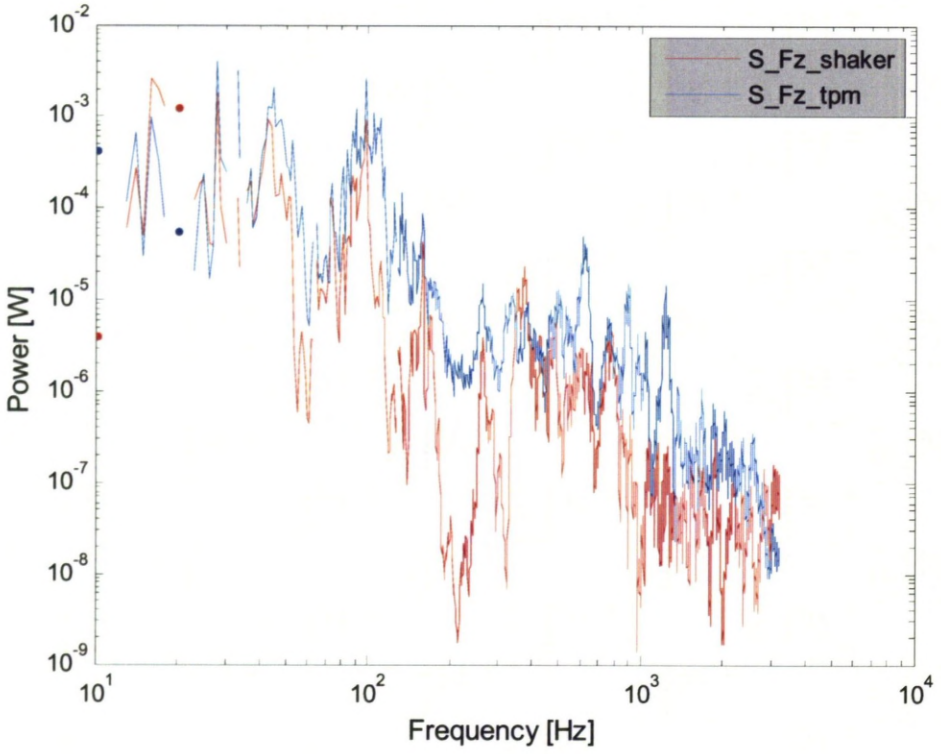

Figure 6.8: Real part of source descriptor of stair excited by shaker and tapping machine on step 8

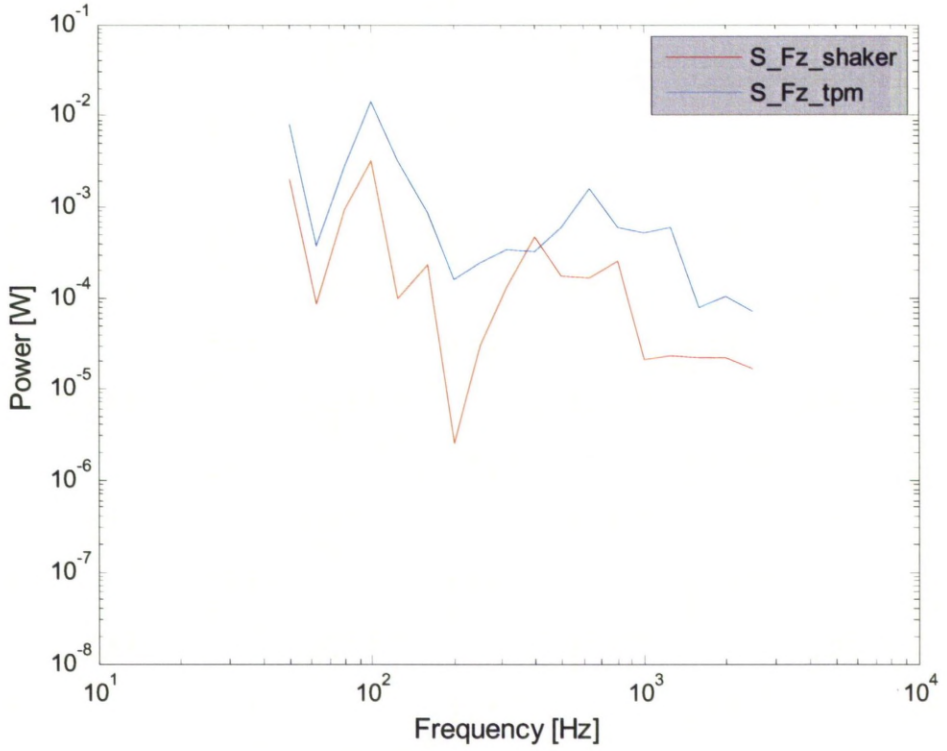

Figure 6.9: Real part of source descriptor of stair excited by shaker and tapping machine on step 8 in 3rd octave bands

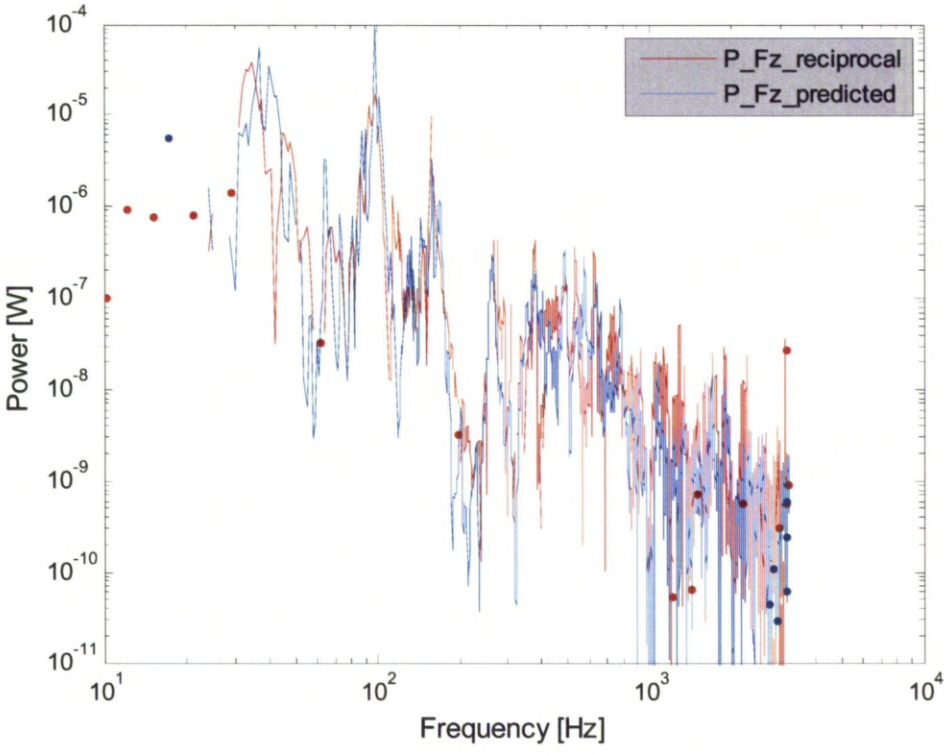

Figure 6.10: Power in-situ and predicted from free velocity and mobility for stair excited by shaker on step 8

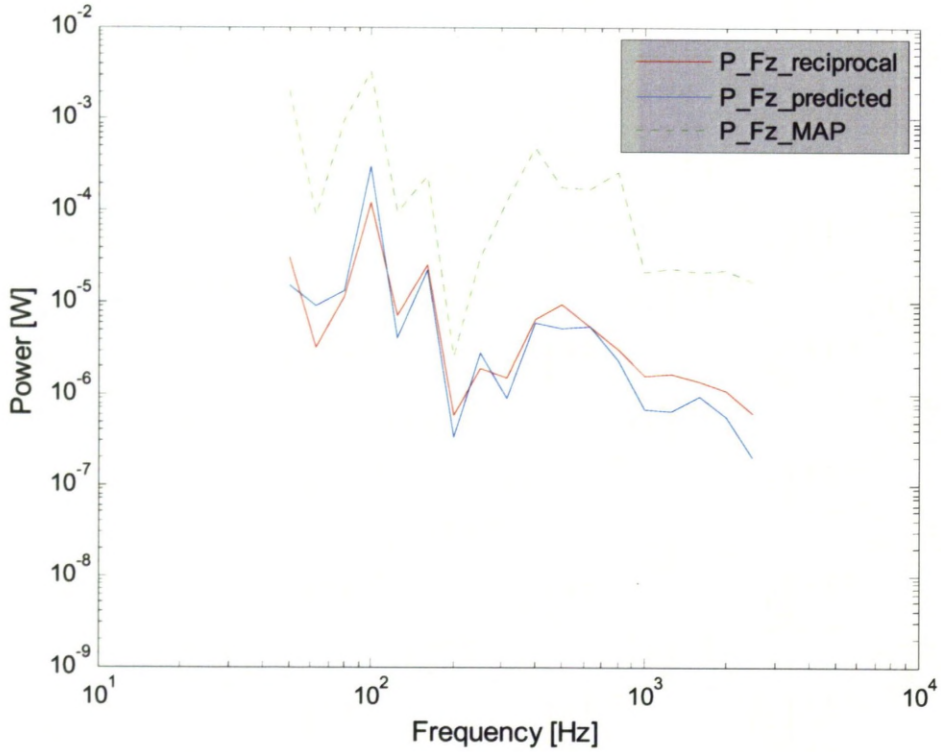

Figure 6.11: Power in-situ and predicted from free velocity and mobility for stair excited by shaker on step 8

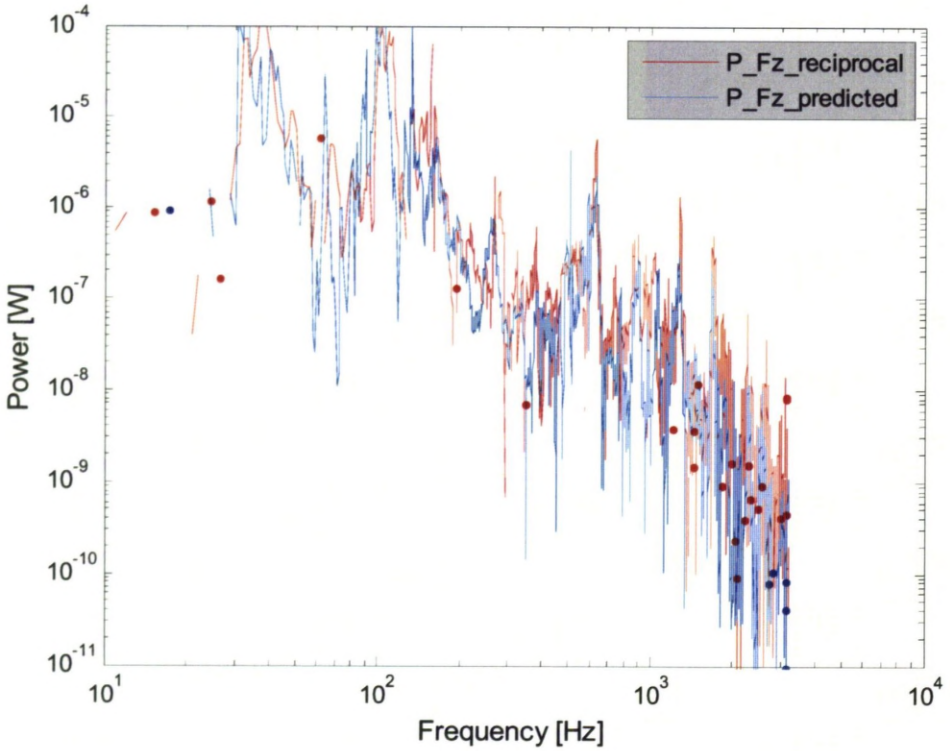

Figure 6.12: Power in-situ and predicted from free velocity and mobility for stair excited by tapping machine on step 8

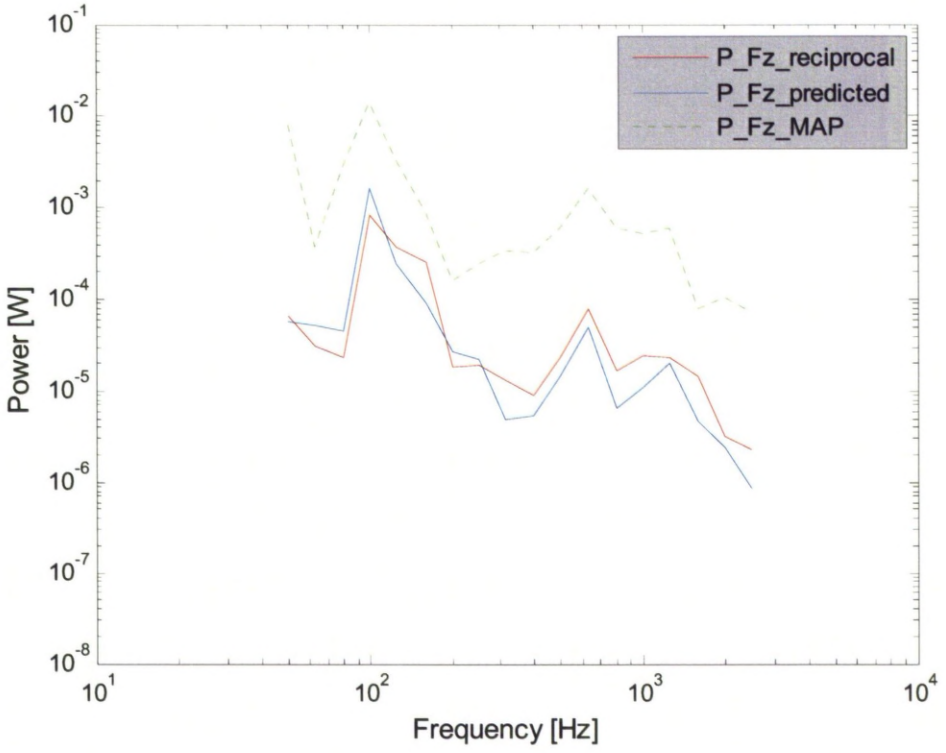

Figure 6.13: Power in-situ and predicted from free velocity and mobility for stair excited by tapping machine on step 8

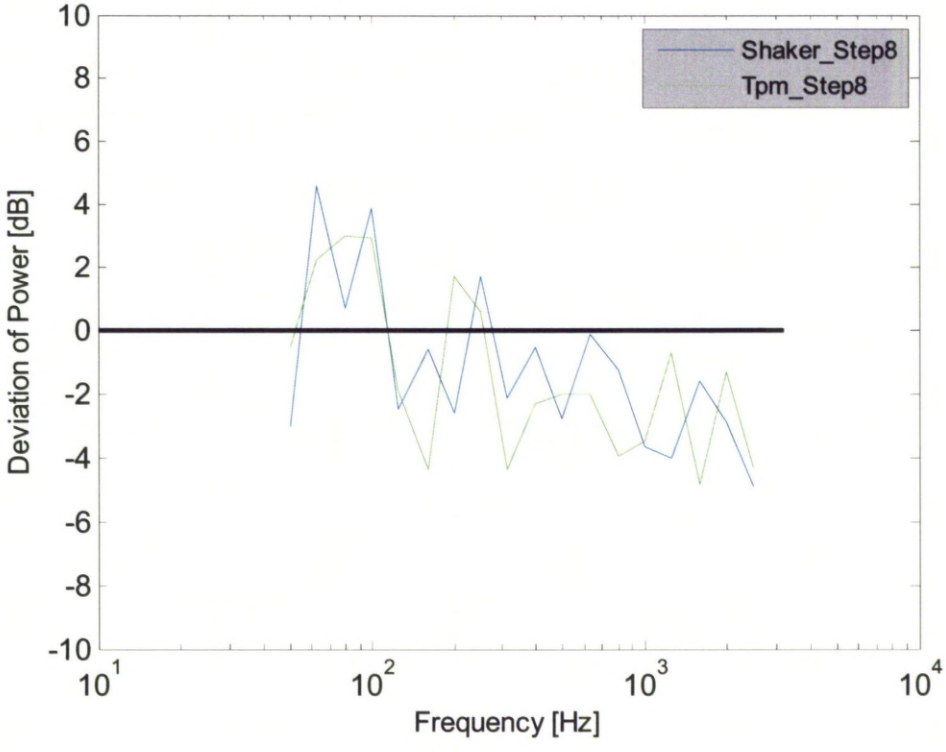

Figure 6.14: Level difference between power in-situ and predicted from free velocity and mobility for stair excited on step 8

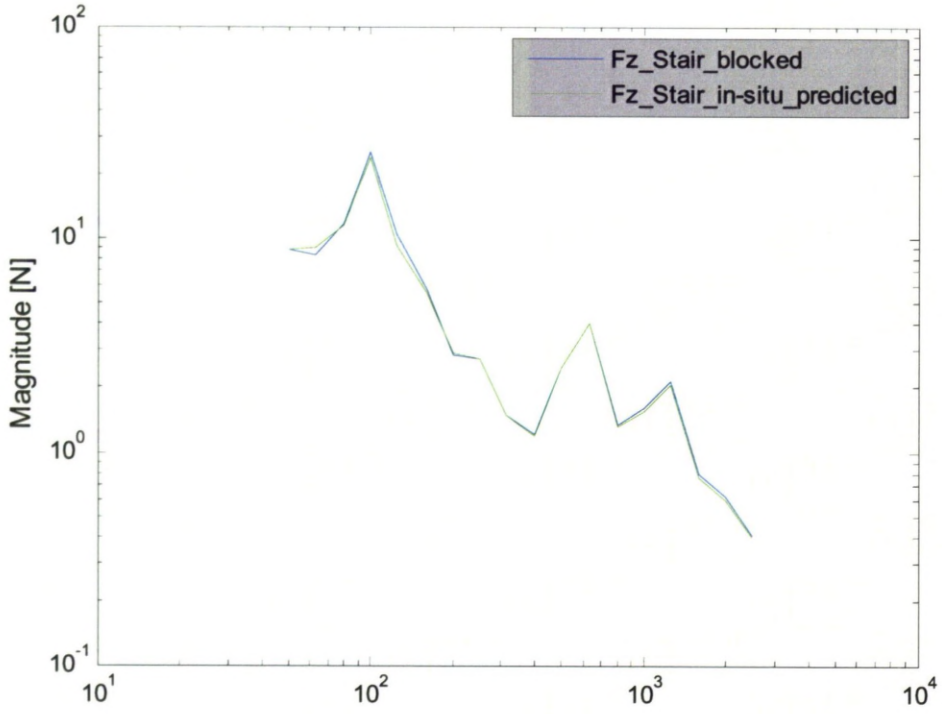

Figure 6.15: Blocked and in-situ force of stair excited by tapping machine on step 8

7 SOURCE CHARACTERISATION USING RECEPTION PLATES

7.1 INTRODUCTION

The use of reception plates, to obtain the structure-borne power in a laboratory, is investigated. The underlying theory of the reception plate method is described (the expressions in section 2.2.6 are repeated for completeness), also an experimental validation on an isolated reception plate system. Next the application of the reception plate method to real walls and floors is explored. This is of particular importance for this work because stairs cannot be easily connected to isolated plates. By means of analytical considerations and experiments, potential sources of error for the field application of the reception plate method are highlighted. Finally a power substitution method is proposed for the in-situ characterisation of vibrating stairs attached to real walls and floors.

7.2 ISOLATED RECEPTION PLATE

7.2.1 Power balance

The power gained by a freely suspended reception plate is assumed equal to the total emission of a source connected to it through multiple contacts

and components of excitation. In turn, the power gained by the plate is the bending wave energy loss according to [1]:

$$P_{in,i} = \omega E_i \eta_i \tag{7.1}$$

The bending wave energy conserved in the plate equals the product of plate mass and spatial average velocity over locations in the far field:

$$E_i = m_i \overline{\tilde{v}}_i^2 \tag{7.2}$$

The bending wave energy loss is controlled by the total loss factor.

7.2.2 Three dimensional test rig

A prototype reception plate has been developed by Späh [2]-[4], for the case of sources to be installed in heavy-weight buildings. The construction details were prepared by the ISO working group CEN/TC126/WG7 and adopted by EN 15657 [5]. The rig consists of three mutually, perpendicular concrete plates, each of 10 cm thickness (Figure 7.1) and a mass per unit area of ca. 230 kg/m^2. The three plates simulate a room-corner position and where the source is in contact with all three surfaces. The rig also is designed for measurement of sources in contact with vertical surfaces only, such as domestic boilers and in principle the stair system, which is object of this thesis study. The plate dimensions are 2.8 m x 2.0 m for the horizontal plate and 2.74 m x 1.95 m and 3.1 m x 2.21 m for the vertical plates. The plates are isolated from each other and from surrounding structures, using polyurethane foam (Sylomer HD 30/25).The isolation area was adjusted to realise a mass-spring resonance below 20 Hz. The isolation material also

provided additional losses, to account for typical energy losses in buildings and to ensure a sufficiently high modal overlap. The isolation material was positioned at the edges of the plates.

7.2.3 Loss factor measurement

The total loss factor of building elements is usually obtained from vibration decay measurements in 3rd octave bands and by evaluation of the integrated impulse response [7]. To avoid filtering problems (ringing of the band pass filter and smoothing caused by the averaging device) the reversed time technique generally is used [8]. Distortion only occurs at the initial part of the decay curve which therefore should be discarded. A difficulty lies in the identification of the part of the decay appropriate for calculating the reverberation time because the rate of decay of non-diffuse fields is not constant over the entire 60 dB range. Since the initial 20 dB decay determines the steady-state vibration level within 0.1 dB, an evaluation of T_{10}, T_{15} or T_{20} is recommended rather than T_{30} or T_{60} [9]. Normative instructions for the measurement of structural reverberation time are given in ISO 10848-1 [10]. Here the evaluation of T_{15} or T_{20} is specified. Furthermore specifications for the location and number of excitation and response positions are given.

Decay measurements were performed with a Norsonic 840 analyser and a Maximum Length Sequence (MLS) as signal. The shaker used was that described in Chapter 4.5. In Figure 7.2 the reversed integrated impulse

response of the horizontal reception plate is shown for one excitation and response position, for 50, 100, 250 and 1 kHz.

For the vertical log scale, the decay curves are almost straight lines and the calculation of the gradient is unproblematic. The loss factor was obtained by evaluation of a T_{20}, excluding the first 5 dB of the decay.

In Figure 7.3 is shown the reverberation time and in Figure 7.4 the corresponding loss factor for the horizontal plate, both as averages of at least 12 independent measurements, according to [10]. In Figure 7.3 are also shown the lowest measurable values for the conventional method and for the time reversed filtering technique [10], determined for digital 3rd octave filters. Due to efficient damping by the isolation material measured values are below the minima allowed by the conventional method and close to the minima for reversed time filtering. Therefore, only the latter was used for frequencies below 200 Hz.

The measured loss factor in Figure 7.4 is compared to the average total loss factor obtained from a survey of German masonry buildings [11] and British masonry buildings [12]. The loss factor is close to the average value in German buildings, which was the initial aim for the development of the reception plates. The high values obtained in the laboratory at low frequencies are advantageous because they compensate for the low modal density of the plate. Similar loss factors were recorded for the vertical plates and are not shown.

7.2.4 Velocity level difference

A requirement of the three-plate rig was that the powers from the source into each plate could be obtained and treated independently. Chapter 8 considers that each power forms the input to structural propagation models, which treat up to three transmission paths separately and then sum the contributions to give the resultant sound pressure in the room of interest. However, in order for this to be possible, the three laboratory reception plates must be isolated from each other such that there is no significant vibration transmission between them. This was confirmed by recording velocity levels on all three plates for excitation of one plate [2]. The level differences are of the order of at least 20 dB at 50 Hz increasing to 70 dB at 5 kHz. It has also been shown that when a water cistern was connected to both, the floor plate and the large vertical plate, that the level difference is still greater than 30 dB. A question arises if a stronger coupling by other sources might affect the isolation.

In this study, the horizontal plate and large vertical plate were rigidly coupled by two steel angles, screws and plugs as illustrated in Figure 7.5. This was thought to represent stronger coupling than likely to occur with typical sound sources in buildings. The steel angles were mounted at the plate edges at positions of high vibration amplitude when in the isolated condition. The horizontal plate was excited by a shaker at the same position and with the same gain settings as described in Chapter 4.5.

In Figure 7.6 are shown the velocity levels for the isolated and coupled condition and in Figure 7.7 the respective level differences. The velocity

levels on the excited horizontal plate are similar for both conditions. The small differences can be referred to a slight change in input mobility (Figure 7.8) and are similarly found in the directly measured power from the cross-spectrum of shaker force and contact velocity. In contrast the velocity levels on the vertical plate are about 30-40 dB higher in the coupled condition. From this it is seen that the coupling is reducing the isolation of the plates, but the velocity level difference is however still of the order of at least 10 dB. For most common sources it is unlikely that a stronger coupling between the plates would be realised. Accordingly, the coupling of the reception plates through sources connecting to more than one plate is in general unlikely to cause problems in the application of the method.

7.2.5 Calibration

For the purpose of this thesis work, calibration is defined as the comparison between measurements – one of known magnitude made with one device and the other made with a second device.

Therefore, to calibrate the reception plate, the power injected by the shaker was measured directly using the cross-spectral method described in Chapter 4.5.1) and compared with the power obtained from the reception plate method from (7.1). The plate response velocity was recorded as the average square velocity over 15 accelerometer positions (a minimum of 12 is recommended in [3]).The total loss factor was obtained from 12 independent measurements.

The set-up for excitation of the isolated small vertical plate is shown in Figure 7.9. In Figure 7.10 and Figure 7.11 is shown the reception plate power and the direct power as narrow-band and 3rd octave band values, respectively. The respective level differences are shown in Figure 7.12. The maximum deviation at the frequency resolution of 1 Hz is 5 dB. The agreement of 3rd octave band values is generally within ± 2 dB.

Results for the coupled situation are shown in Figure 7.13 and Figure 7.14. Except for the frequency range below 100 Hz, the agreement remains within ± 2 dB.

A similar experiment was performed with a massive stair landing as receiving plate with similar mass per unit area as the stair wall. The experimental set-up is illustrated in Figure 7.15. The landing is constructed of reinforced concrete with dimensions of 2,8 m x 1,3 m x 0,18 m and was resiliently supported by resilient pads (PUR-Elastomer elements) on the supporting walls. The theoretical mass spring resonance frequency is about 30 Hz. In contrast to the reception plates of the test rig the resilient pads did not provide significant additional damping. As a result, the value of modal overlap was 0.3, which was considerably smaller than that of the reception plates of the test rig [14].

In Figure 7.16 is shown the reception plate power and the direct power in 3rd octave bands; the respective level differences are presented in Figure 7.17. The agreement is generally within ± 2 dB with a maximum deviation of 4 dB at frequencies below 200 Hz.

7.2.6 Discussion

For isolated reception plates, the power imparted by the source is wholly contained by the reception plate and can be estimated with little difficulty. The plate mass can be estimated with good accuracy, likewise the mean squared velocity. The total loss factor also can be measured without difficulty by decay measurements as the identification of the evaluation range is unambiguous. It is observed that the reception plate method underestimates the power at the very low frequencies where the isolation from surrounding structures is less efficient.

7.3 WALLS AND FLOORS AS RECEPTION PLATES

A field characterisation of sources, using real walls and floors as reception plates, would be of practical benefit, for sources that cannot be easily moved to a laboratory. However, it was envisaged that there might be problems in identifying the physical boundaries of the plate and therefore of the total mass, and in confirming the total loss factor, where significant edge losses occur into the bonded associated building elements. In work reported by Späh, significant discrepancies between directly measured powers and reception plate estimates have been reported [2], [4]. There was agreement at the peaks in the powers but band averaging resulted in differences, which could not be ignored.

Initially, the reception plate method was applied to the stair wall similarly as described for the isolated reception plates. The shaker was attached to a

central position, as described in Chapter 4.6. The spatial average velocity was sampled at 14 arbitrary accelerometer positions excluding an area of 50 cm distance to the wall's edges and around the contact point. The total loss factor was determined from 12 independent decay measurements from evaluation of T_{20}.

In Figure 7.18 and Figure 7.19 is shown the direct power and the reception plate power in narrow bands and in 3rd octave bands, respectively. The associated level differences are given in Figure 7.20.

The peaks in both the narrow band powers, representing wall modes, are at the same frequencies. The peaks generally are of the same magnitudes but the dips are more accentuated in the reception plate power. This results in a level difference of 2-5 dB in 3rd octave bands. On average the reception plate method gives an underestimate of the power of about 3 dB.

An underestimation of the directly measured power was also observed in [2], [4] for shaker excitation of a concrete floor in a transmission suite. The discrepancies were of the order of 10 dB, which is considerably greater than for the present study.

The underestimation of the power by the reception plate method is related to the 'properties' of real floors and walls which differ from 'ideal' reception plates. In the next sections the single quantities in the reception plate power expression in (7.3) are investigated more detailed.

$$P = \omega \cdot m \cdot \tilde{v}^2 \cdot \eta \tag{7.3}$$

The stair wall is thereby the main object of investigation, in addition the situation analysed by Späh [2], [4] was revisited.

7.3.1 Dimensional and material considerations

The mass per area of the stair wall was calculated from the density of 1900 kg/m^3 and the thickness of 24 cm to 456 kg/m^2. The density was obtained from the nominal density class (RDK), which provides the range 1810 - 2000 kg/m^3.

The area of the wall was restricted to the area inside the concrete frame (length 4,30 m x height 2,35 m = 10,1 m^2) as it is assumed that the concrete frame and ceiling constitute the (non-moving) subsystem boundaries. The wall mass is given by the product of surface mass and area.

The Poisson's ratio was assumed to 0.2 according to [9]. Estimation of the Young's modulus is difficult especially for brickwork walls as the CaSi wall considered here. Thus, the quasi-longitudinal phase velocity was measured according to the flight of time method [9] and the Young's modulus was calculated from:

$$E = c_L^2 \cdot \rho \cdot (1 - \mu^2) \tag{7.4}$$

The result for the measurement of the longitudinal wave speed of the wall was 2374 m/s in the vertical direction and 2588 m/s in the horizontal direction. The average value used for the calculations is 2481 m/s which is similar to values found in the literature e.g. Hopkins: 2500 m/s [9] or ISO 12354: 2600 m/s [13]. This gives a Young's modulus of 11.2 GPa, which in

turn yields a value of the characteristic mobility (Chapter 8.2.1) of $1.6*10^{-6}$ m/sN. In Figure 7.21 is shown the measured mobility and the characteristic mobility in narrow bands and as 3rd octave band averages. The measured mobility exhibits strong resonances that represent modes of the stair wall and of adjacent structures. This will be analysed in more detail in Chapter 8.3.3. At frequencies above 1 kHz spring-like behaviour is indicated by the phase converging to a value of $+\pi/2$, again due to the local stiffness effect that is more evident than for excitation of the isolated reception plate (Figure 4.13). In the frequency range 100 Hz - 1 kHz the measured mobility is 3 dB more than the characteristic mobility.

If it was assumed that the discrepancy was due only to an incorrect estimate of density, then the density of the wall would have to be 400 kg/m^3. This is unrealistic as the measured airborne sound insulation of the wall is R_w = 55 dB (Chapter 3.2, Figure 3.2) which is expected for a density of 1900 kg/m^3 according to a prediction with EN 12354-1 [13] (section 8.2.1).

With a density of 400 kg/m^3, $R_w' = 35\,dB$ and therefore it is concluded that an incorrect wall mass is not the reason for the shift.

The discrepancy in the power is of the same order, but there is no obvious reason why the direct power measurement should be erroneous, since the same technique was successfully used for the isolated reception plate (Chapter 4). Therefore, questions remain regarding possible errors in the spatial sampling of plate velocity and in the estimate of total loss factor.

7.3.2 Sampling of spatial average velocity

The spatial average velocity was sampled at 14 arbitrary wall positions excluding an area of 50 cm distance to the wall's edges and around the contact point. In Figure 7.22 are shown the velocity levels and the standard deviation according to:

$$s_{\tilde{v}^2} = \left(\frac{1}{n-1} \sum_{i=1}^{n} (L_{v,i} - \bar{L}_v)^2 \right)^{\frac{1}{2}} \tag{7.5}$$

With

$$L_v = 10 \log \left(\frac{\tilde{v}^2}{v_{ref}^2} \right) \tag{7.6}$$

The maximum range is about 10 dB. The standard deviation is generally about 3 dB with a maximum of 5 dB at 100 Hz. In [3] the standard deviation was calculated for an isolated reception plate with free edges (the horizontal plate of the test rig) and excitation at a corner by use of a semi-numerical model [15]. For a sample size of 12 the predicted standard deviation is about 1 dB. From this a generally higher uncertainty can be expected and therefore a more careful sampling was conducted.

With the shaker attached to the contact point of stair and wall, the whole wall surface was scanned using a laser scanning vibrometer (Polytec). The set-up is illustrated in Figure 7.23. The shaker was attached in a similar manner as in the previous experiments but without the piano wire. This was done because it was found that the piano wire causes an unwanted resonance in the shaker system below 1 kHz. Without the piano wire this

resonance was shifted to 1,2 kHz and thus outside the frequency range of interest.

For direct power measurement the PULSE system was used in parallel with the laser vibrometer. The steady state condition was maintained by control of the shaker force. Both analysers had the same frequency range from 0 to 3200 Hz and resolution of 1 Hz. The scanning grid of 1100 points comprises the area inside the concrete frame including the edges as illustrated in Figure 7.24. Reflecting material was glued to the wall at the grid points.

Before scanning the wall surface the reciprocal method was applied as outlined in Chapter 4 assuming only a force F_z and compared to the direct power measurement. The result is shown in Figure 7.25 and Figure 7.26. In the frequency range up to 1 kHz the agreement is within $\pm$ 2 dB with a positive bias in the reciprocal power measurement. Deviations at high frequencies are due to an insufficient S/N ratio in the reciprocal measurement.

The same total loss factor was used as in the previous investigation (determined from 12 independent decay measurements and evaluation of T_{20}).

In Figure 7.27 is shown the direct power and the reception plate power in narrow bands and in Figure 7.28 in 3rd octave bands. The respective level differences are given in Figure 7.29.

The reception plate power underestimates the exact power. Again the difference in power is significantly lower at the peaks than at the dips. The

difference in 3rd octave bands is constant at 4 dB, with respect to frequency. This is the result of the spatial averaging that reduces the measurement uncertainty at wall resonances.

Consideration is now given to the possible discrepancy due to the fact that the stair wall is not isolated from surrounding building elements.

7.3.3 SEA model

In this section a simplified SEA model is described, which gives a general insight into the power balance of isolated and coupled (reception) plates.

If a source is attached to a wall or floor in a building, then the excited plate is connected to other plates (i.e. walls and floors). Consider the simplest case of two plates where the reception wall is connected to a second plate at one edge as illustrated in Figure 7.30.

The power balance equation for plate 1 is now a function of internal and coupling loss factors [16], [12]:

$$P_{in} = \omega E_1'(\eta_1 + \eta_{12}) - \omega E_2' \eta_{21} \tag{7.7}$$

The negative term represents the power gained by the excited structure from the adjacent plate. Consider the excited wall alone as the reception plate where measurements of the energy and total loss factor are restricted to it. This requires that the negative term in equation (7.7) is negligible for the stationary condition and that the measured total loss factor of the excited plate represents only power losses and no power gains.

The power balance equation for the connected plate 2 is given by:

$$\omega E_2'(\eta_2 + \eta_{21}) = \omega E_1' \eta_{12} \tag{7.8}$$

Substitution of equation (7.7) into equation (7.8) yields:

$$P_{in} = \omega E_1'(\eta_1 + \eta_{12}) - \frac{\omega E_1' \eta_{21} \eta_{12}}{\eta_2 + \eta_{21}} \tag{7.9}$$

With the assumption that the shaker power into the single free plate 1 is the same as into plate 1 when connected to plate 2, then from (7.1) the discrepancy of the plate 1 energy can be expressed as:

$$\frac{E_1}{E_1'} = 1 + \frac{\eta_{12}}{\eta_1} - \frac{\eta_{21}\eta_{12}}{\eta_1(\eta_2 + \eta_{21})} \tag{7.10}$$

Prior to measuring the spatial average square velocity, the loss factor of plate 1 will be obtained as a total loss factor

$$\eta_{tot} = (\eta_1 + \eta_{12}) \tag{7.11}$$

rather than the internal loss factor of equation (7.1). Assume the two plates are similar such that $\eta_1 = \eta_2; \eta_{21} = \eta_{12}$. Estimates for the coupling and internal loss factors in buildings can be found in [12], where

$$\eta_{tot} = \frac{1}{\sqrt{f}} + 0.015 \tag{7.12}$$

The first term represents the coupling losses and the second term the internal losses of building structures. Using these values, the ratio E_1 / E_1' is about 2 at low frequencies and about 1.5 at high frequencies and thus the

reception plate method would underestimate the true power by about 3 dB and 2 dB, respectively.

This simple consideration is not exhaustive as in buildings, walls and floors are usually connected to many more plates (side walls, etc.). It however indicates the reception plate method will in general underestimate the injected power if measurements are restricted to the excited plate.

However, this simple model does not address problems in estimating the total loss factor. This is because the loss factor is usually determined by decay measurements and the present model does not deal with time dependent vibration fields. A transient SEA (TSEA) model could address this issue, but an accepted model is not available. Kling proposes a model, based on a quasi-stationary approach [16] and reference is now made to it.

7.3.4 Transient SEA model

In the first step of the analysis the energy distribution over the subsystems is calculated in the stationary condition. The power balance for the excited structure i in the stationary condition is:

$$\begin{aligned} P_{in,i} &= \omega E_i \eta_{ii} + \sum_j \omega E_i \eta_{ij} - \sum_j \omega E_j \eta_{ji} \\ &= \omega E_i \eta_i - \sum_j \omega E_j \eta_{ji} \end{aligned} \tag{7.13}$$

Again, the negative terms represent the power gain of the excited structure i by flanking elements j. The energy distribution in a system is calculated with coupling loss factors from Craik [12] with material- and geometric properties

of the plates forming the junction. The transmission loss between the plates is calculated for random incidence:

$$\eta_{ij} = \frac{c_0}{\pi^2 \sqrt{f \cdot f_{c,i}}} \cdot \frac{L_{ij}}{S_i} \cdot \tau_{ij} \tag{7.14}$$

Similarly rooms can be added as subsystems. The coupling losses between the room and structure depend on the radiation, the room to room transmission in the non – resonant case and the room absorption, calculated as:

$$\eta_{room \to structure} = \frac{\rho_0 \cdot c_0^2 \cdot S_{structure} \cdot f_c \cdot \sigma}{8\pi \cdot V_{room} \cdot m' \cdot f^3} \tag{7.15}$$

$$\eta_{structure \to room} = \frac{\rho_0 \cdot c_0 \cdot \sigma}{2\pi \cdot m' \cdot f} \tag{7.16}$$

$$\eta_{room1 \to room2} = \frac{13,7 \cdot S_{room2} \cdot \tau_{room1 \to room2}}{f \cdot V_{room1}} \tag{7.17}$$

$$\eta_{room} = \frac{13,7 \cdot \sum S_{room} \cdot \alpha}{f \cdot V_{room}} \tag{7.18}$$

With known power input $P_{in,i}$ and internal and coupling loss factors the energy distribution over the subsystems can be calculated in the stationary condition. This is the starting point for the Transient SEA.

On terminating the power input into the system, such as $P_{in,i}(t \geq 0) = 0$, the energy levels of all subsystems begin to decrease. The rate of change of energy is set equal to the power losses of the subsystem. Therefore the input power is replaced by the power losses.

$$\begin{aligned} P_{loss,i}(t) &= -\frac{d}{dt}E_i(t) \\ &= \omega \cdot \eta_i \cdot E_i(t) - \sum_j \omega \cdot \eta_{ji} \cdot E_j(t) \\ &= \omega \cdot \eta_{loss,i}(t) \cdot E_i(t) \end{aligned} \tag{7.19}$$

The power losses for each time increment give a new quasi-stationary energy distribution, obtained by subtracting the energy lost in that increment (e.g. Δt = 0,1 ms) from the energy of the element in the previous increment. This results in an energy decay curve for each subsystem.

An example level decay is shown in Figure 7.31. The incoming power flow from an adjacent subsystem j depends on the energy ratio $E_j(t)/E_i(t)$, the level difference between the subsystems and this level difference reduces over the decay because of energy exchange.

The TSEA approach by [16] was implemented into MatLab with the option of steady state and transient excitation. The left section of the staircase test facility was modelled and the decay characteristic of the stair wall investigated.

In Figure 7.32 the left section of the staircase test facility (red frame) is shown. It represents a well defined system since the section is decoupled from the remaining test facility and the environment. All walls are of 24 cm CaSi with density 2000 kg/m^3, all ceilings are of 18 cm concrete with density 2300 kg/m^3. The remaining properties of the plates as used for the simulations are given in Table 7.1.

In Figure 7.33 the modelled section is shown with subsystem numbers indicated. The upper stair wall is the excited element. The walls and floors

are coupled by corner – or T – joints. To simulate real conditions, the following was assumed:

Openings like for doors or the stairs were included as reductions in the subsystem areas. This meant that less energy could be stored in the subsystems. Acoustic linings on the inner side of the walls, which may reduce sound radiation, were not considered. The concrete frame of the real test wall was not included and direct connection of the walls and ceilings was assumed. It was thus expected that the coupling loss factors and from this the power flows would be overestimated.

The obtained decay curves for all subsystems are shown in Figure 7.34 for f = 1000 Hz along with the backward integrated energy curve of the stair wall.

At t = 0 s, power is introduced to the stair wall (dashed line) due to a single impact to give a maximum energy level on the stair wall. The energy is then distributed within the system. After the impact, the energy levels of the adjacent elements and rooms arise to maxima, followed by a continuous decay. The room energy levels (pointed lines) decay slowly compared to the structures because of smaller values of coupling loss factor and room absorption. However, the room response does not influence the decay of the stair wall. After t ≈ 0,03 s, all structures decay with the same gradient; the power flow is balanced in the system. As a result of energy sharing with the adjacent elements, the energy level of the excited stair wall shows a non-linear decay.

In Figure 7.35 and Figure 7.36 the backward integrated decay curves of the stair wall are shown for 100 Hz and 1000 Hz, respectively along with numerical results for T_{start} and T_{system} resulting from evaluation of the initial decay / the part of the decay where all structures within the system decay with the same gradient. In addition, T_{20} was calculated from -5 dB to -25 dB as this is the typical evaluation range for measurements.

T_{20} and T_{system} are similar and significantly higher than T_{start}.

Accordingly, the first few milliseconds must be evaluated as T_{start} is the desired quantity for the reception plate method when measurements are restricted to the excited plate. From the simulation it is indicated that even an evaluation of a T_5 would result in an underestimation of the loss factor representing the stair wall.

The SEA simulation indicates that even in the stationary condition there are reversed power flows such that $\eta_i > \eta_{stationary}$. Even if a measured loss factor represents the energy losses of the excited structure there remains a power gain in the stationary condition which is not included in the power balance and the real imparted power is always greater than the measured reception plate power. The error is represented by the negative term in equation (7.13). The minimum error in the power balance is equally given by the ratio:

$$\Delta L_P = 10 \log \frac{\eta_i}{\eta_{stationary}} \tag{7.20}$$

Thus the power balance when only considering the excited stair wall will yield an underestimate of the real imparted power. The discrepancy is

however relatively small because the energy losses of the excited stair wall are significantly greater than the energy gains in the stationary condition.

The discrepancy of the loss factors obtained from T_{20} and from T_{start} is shown in Figure 7.37 as a function of frequency. The discrepancy is 8 dB at 50 Hz reducing to 2 dB at 3150 Hz.

To summarise, the total loss factor is usually determined by the decay rate method and evaluation of T_{20}. The evaluation starts 5 dB below the stationary energy level. According to the TSEA simulation, the power flows in the system are then already balanced, to give, not the structure's loss factor but rather the system's loss factor. Consequently the reception plate power will always yield an underestimate of the real imparted power. Loss factor measurement is discussed in the next section.

7.3.5 Loss factor measurement

Decay curves were obtained in 3rd octave bands as described in section 7.2.3. In Figure 7.38 the backward integrated impulse response is shown for excitation at the stair/wall contact and at a fixed response position for 50, 100, 250 and 1 kHz.

In contrast to the isolated plate (Figure 7.2) the decay curves exhibit a steep initial decay followed by multiple slopes indicating reversed energy flow from adjacent walls and floors during the decay. This supports the findings of the TSEA simulation in the preceding section which indicated that only the first milliseconds of the initial decay should be used for the evaluation of the loss

factor. Again, evaluation of T_{20} leads to significant underestimates. An evaluation of the initial decay e.g. the first milliseconds was however not possible because of the inherent sampling time of 4 ms and the distortion from the digital filters [7]-[9].

Visual inspection (yellow lines in Figure 7.38) yielded more or less a T_5 which was used for the evaluation of a "T_5 loss factor". The red lines in Figure 7.38 correspond to the T_{20} as calculated by the analyser. In Figure 7.39 are shown the loss factors obtained from T_{20} and T_5, with regression curves. Also shown in is the loss factor from evaluation of the half-power bandwidth, obtained from a modal analysis of the wall (Chapter 8.3.3). It is observed that evaluation of T_5 yields a significantly higher loss factor than from T_{20}. The loss factor obtained from half-power bandwidth generally lies between. The difference resulting from T_5 and T_{20} evaluation is about 4 dB at 50 Hz reducing to 0 dB at 5 kHz.

In Figure 7.40 the corresponding level difference is shown. In Figure 7.41 and Figure 7.42 is shown the directly measured cross-spectral power of the shaker attached to the stair/wall contact and the estimate from the reception plate method using the loss factor obtained from T_5. The agreement is significantly better than for T_{20} (Figure 7.27, Figure 7.28) but Figure 7.43 shows that the real power is still underestimated by 2 dB

The evaluation of the reception plate power for the concrete floor, investigated by Späh [2], [4], was revisited. The floor is situated in a transmission suite as illustrated in Figure 7.44. The position and construction of the inner walls in this study were different to those of the

initial investigations by Späh. However the relevant aspects remained the same as the flanking walls were lightweight and decoupled from the reference floor. Only the area of the floor sections changed with the position of the walls. For the investigations by Späh the area of the reference floor was restricted to the cross-junction with the inner walls. For the present investigations the floor was subdivided into two sections that were defined by the inner walls. In Figure 7.45 section 1 of the reference floor is shown.

Velocity levels and loss factors were measured for the two sections for shaker excitation at a central position of floor section 1. The reception plate power was first evaluated for floor section 1, from T_{20}. This procedure was similar to the investigations by Späh. The comparison with the power measured directly is shown in Figure 7.46. The discrepancy is about 10 dB confirming the results in [2], [4].

Next, the whole floor was considered as reception plate i.e. the average velocity and the loss factor were obtained from measurements on both floor sections. The result for a loss factor from T_{20} is shown in Figure 7.47.

The discrepancy is now reduced to about 5 dB. This shows that a significant part of vibration energy is stored in section 2 of the floor which was not considered in the initial investigation. The inner walls don't provide a high junction reduction due to the low mass and the decoupling from the floor.

Finally, the loss factor was obtained from visual inspection of the first gradient which approximates T_5. From the corresponding loss factor the discrepancy reduced to 2-3 dB as shown in Figure 7.48, with both an overestimate indicated below 200 Hz and an underestimate above 200 Hz.

7.3.6 Power substitution

The reception plate method yields a systematic underestimate of the real source power when coupled plates are used, largely due to difficulties in loss factor measurement. Other difficulties can occur in the field, such as in estimating the plate mass e.g. defining the subsystem boundaries, and in accurately sampling of the velocity field.

Assuming linear systems, a power substitution method [18] can be used to circumvent the above difficulties. A source with known power, such as a shaker with in-line force transducer, is attached to the receiving plate and the average plate velocity measured. The ratio of imparted power to the spatial average velocity is constant and the power of the source under test is obtained from:

$$\frac{P_{calibration}}{\overline{\tilde{v}}^2_{calibration}} = \frac{P_{source}}{\overline{\tilde{v}}^2_{source}} \Rightarrow P_{source} = \frac{P_{calibration}}{\overline{\tilde{v}}^2_{calibration}} \cdot \overline{\tilde{v}}^2_{source} \tag{7.21}$$

For the case considered, the power from shaker at the stair/wall contact and the spatial average response velocity was recorded. The spatial average velocity then was obtained for the attached stair excited by either a shaker or tapping machine as described in Chapter 5.

In Figure 7.49 and Figure 7.50 is shown the power of the stair excited by the shaker and tapping machine, respectively. The power obtained from the reciprocal method was used for comparison. The agreement is within +/- 2 dB over most of the frequency range 100 – 2 kHz.

In the case considered, the stair could be removed for the power substitution. However direct access to the source contacts is often not possible and so the measurements were repeated with the stair installed throughout. . The spatial average velocity was sampled for 12 wall positions for each excitation position (Figure 7.51).

In Figure 7.52 are shown the individual power-velocity functions for 5 shaker positions. In Figure 7.53 is shown the mean value of the power-velocity functions and for excitation at the stair contact. The agreement is within ± 2 dB. The same deviation is observed in the estimates of source power from equation (7.21).

7.4 SUMMARY

For isolated reception plates, the power imparted by the source under test can be estimated with little difficulty. The plate mass can be estimated with good accuracy, likewise the mean squared velocity. The total loss factor also can be measured without difficulty by decay measurements as the gradient is constant throughout the decay.

For plates, i.e. floors and wall, bonded into the surrounding building elements, measurement of the total loss factor is problematical, with the result that the source power is underestimated.

In particular, decay gradients change with time and the required early gradient, corresponding to T_5, at least requires visual inspection by an experienced observer. Only then will the underestimate be within 2 dB.

A power substitution method has been investigated, to circumvent the above problems. The agreement with the true source power is within 2 dB, with no consistent over- or underestimate.

It is further shown that the power substitution can be undertaken with the source installed throughout. This is because of the high source-receiver (stair-wall) mobility ratio, which corresponds to little or no dynamic loading of the wall.

It remains to consider how the source data, obtained in the laboratory, can be used for prediction of the resultant sound pressure in rooms adjacent to the room, with party wall, containing the stair system of interest.

7.5 REFERENCES

[1] Cremer, L., Heckl, M., Petersson B.A.T.: Structure-borne sound, Springer Verlag, Berlin, 2005

[2] Späh, M. M.: Characterisation of structure-borne sound sources in buildings, PhD Thesis of The University of Liverpool, 2006

[3] Späh, M. M.; Gibbs, B.M.: Reception plate method for characterisation of structure-borne sound sources in buildings: Installed power and sound pressure from laboratory data, Applied Acoustics, Vol. 70 (11-12), 1431-1439, 2009

[4] Späh, M. M.; Gibbs, B.M.: Reception plate method for characterisation of structure-borne sound sources in buildings: Assumptions and application, Applied Acoustics, 70 (11-12), 361-368, 2009

[5] EN 15657-1: Acoustic properties of building elements and of buildings - Laboratory measurement of airborne and structure borne sound from building equipment - Part 1: Simplified cases where the equipment mobilities are much higher than the receiver mobilities, taking whirlpool baths as an example, 2009

[6] Getzner (Manufacturer): Data-sheet for Sylodamp HD 30, identification DB-HD-30-D-V03, 2003

[7] Meier A.: Die Bedeutung des Verlustfaktors bei der Bestimmung der Schalldämmung im Prüfstand (The importance of the loss factor for the determination of the sound reduction in the laboratory), PhD Thesis of the RWTH Aachen, 2000

[8] F. Jacobsen, J. H. Rindel, Letters to the Editor: Time reversed decay measurements, Journal of sound and vibration, 117 (1), 187-190, 1987

[9] Hopkins, C.: Sound Insulation, Butterworth-Heinemann, 2007

[10] EN ISO 10848-1: Laboratory measurement of the flanking transmission of airborne and impact sound between adjoining rooms – Part 1: Frame document, August 2006

[11] Späh M. M., Blessing S., Fischer H.-M.: Verifizierung des Rechenverfahrens für die Luftschalldämmung nach EN 12354-1 für den Massivbau; Teil 1: Einfluss von Eingangsgrößen (Verification of the calculation model for airborne sound insulation according to EN 12354-1 for homogeneous heavyweight buildings; Part 1: influence of the input data), Proc. DAGA, Hamburg, Germany, 2001

[12] Craik R. J. M.: Sound Transmission Through Buildings using Statistical Energy Analysis, Gower Publishing Limited, 1996

[13] EN 12354-1: Building acoustics – Estimation of acoustic performance of buildings from the performance of elements – Part 1: Airborne sound insulation between rooms, September 2000

[14] Taşkan, E.; Scheck, J.; Fischer, H.-M. Vibration Behaviour and Structure-Borne Sound Transmission of a Resiliently Supported Landing. The Sixteenth International Conference on Sound and Vibration, Kraków, Poland, 2009

[15] Fahy, F. and Walker, J.: Advanced Applications in Acoustics, Noise and Vibration. E&FN Spon, London, 2004. Chapter 9: Mobility and impedance methods in structural dynamics

[16] Lyon, R. H., DeJong, R. G.: Theory and application of statistical energy analysis. Butterworth-Heinemann Boston – Second Edition, 1995

[17] Kling, C.: Investigations into damping in building acoustics by use of downscaled models, Dissertation RWTH Aachen, Logos Verlag Berlin, 2008

[18] Ohlrich, M. et al.: Round Robin test of technique for characterizing the structure-borne sound-source-strength of vibrating machines, Euronoise 2006, Tampere, 2006

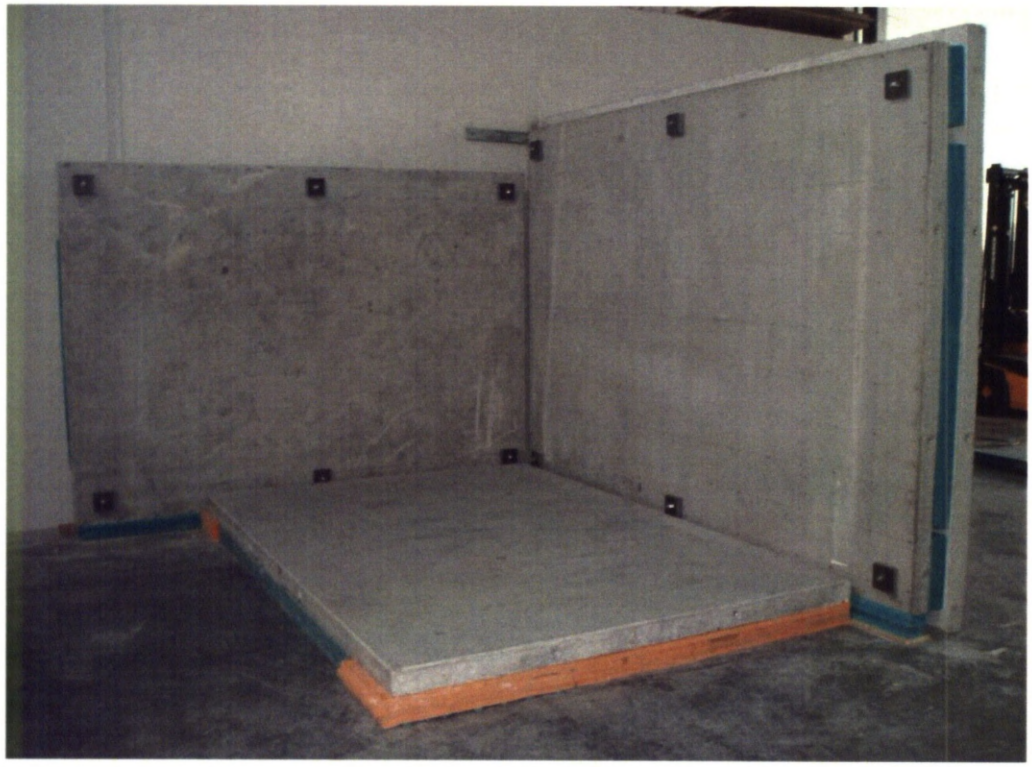

Figure 7.1: Reception plate test rig at the University of Applied Sciences Stuttgart

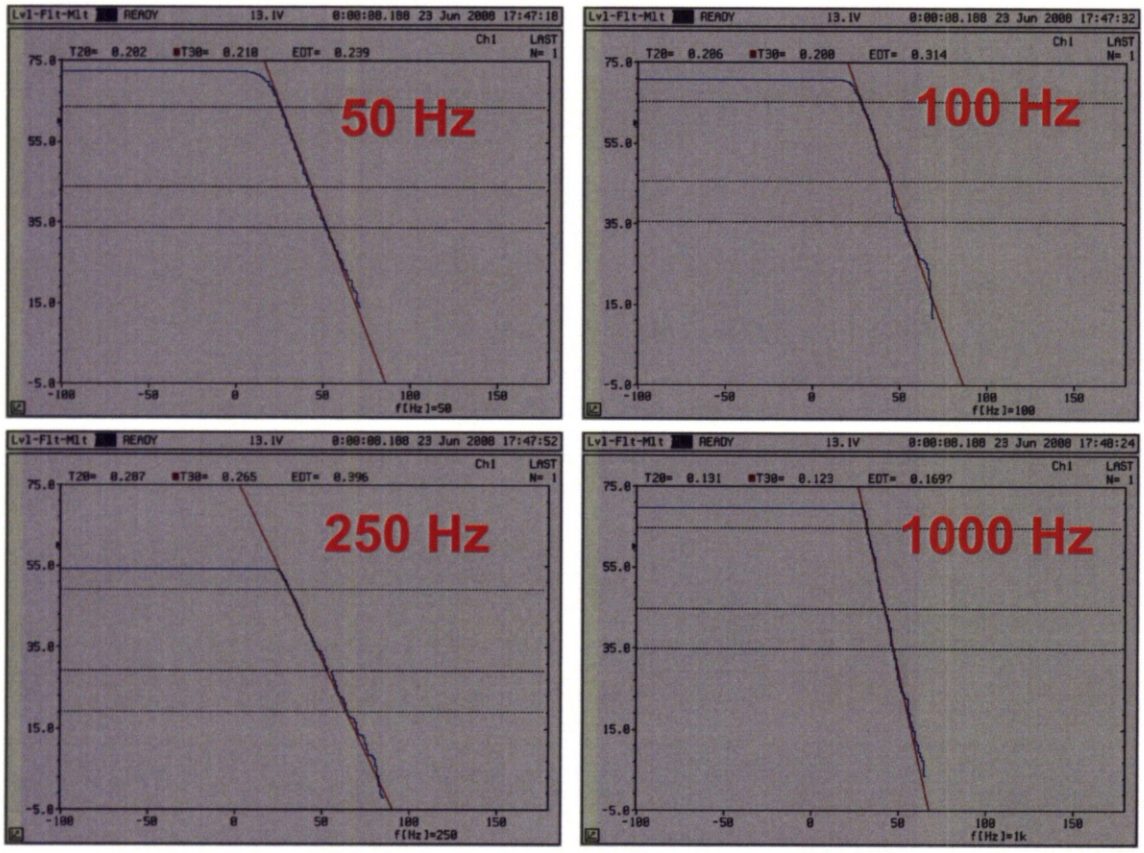

Figure 7.2: Decay curves for the isolated reception plate for 50, 100, 250 and 1 kHz

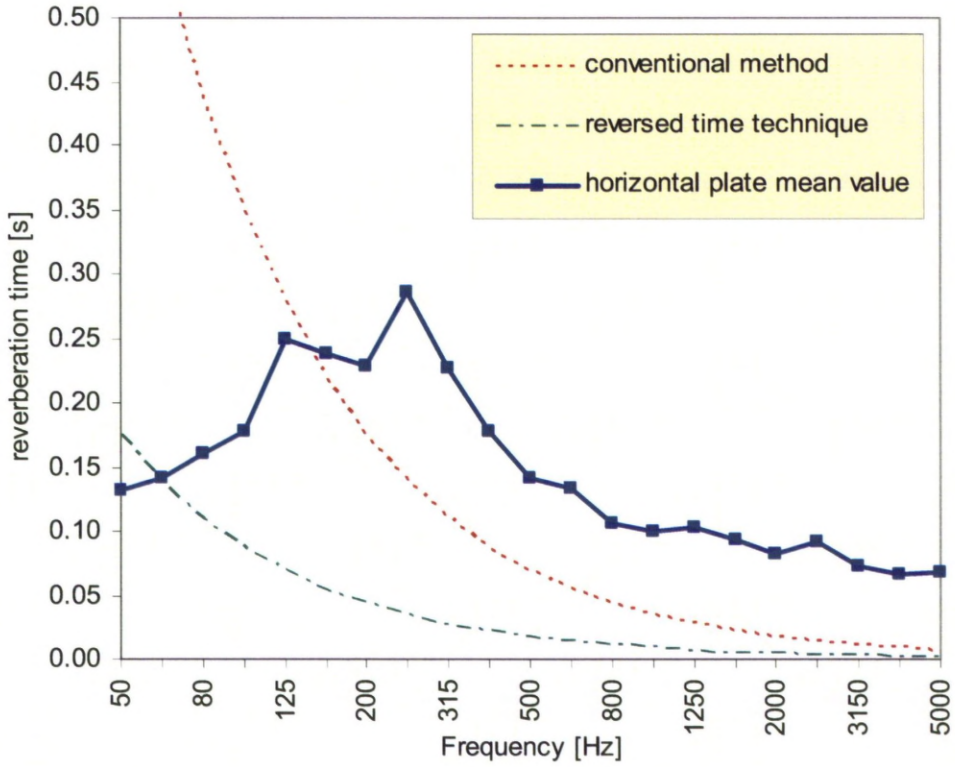

Figure 7.3: Structural reverberation time: mean value of horizontal plate and lowest measurable values due to filtering, after [10]

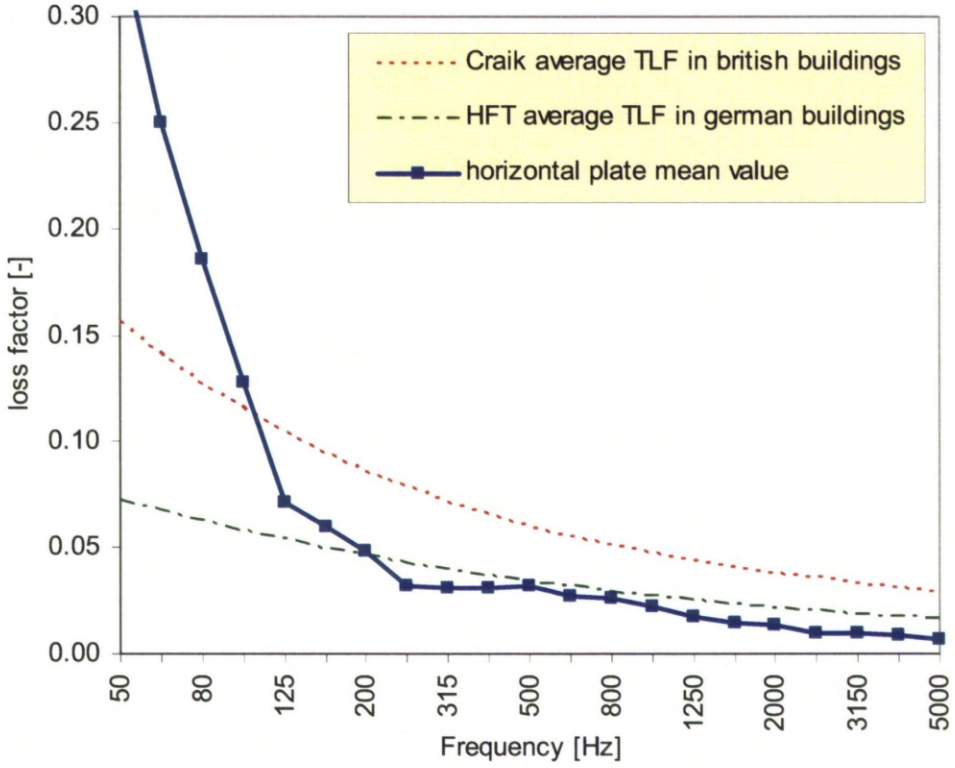

Figure 7.4: Total loss factor: mean value of horizontal plate

Figure 7.5: Horizontal plate and large vertical plate coupled by steel angles

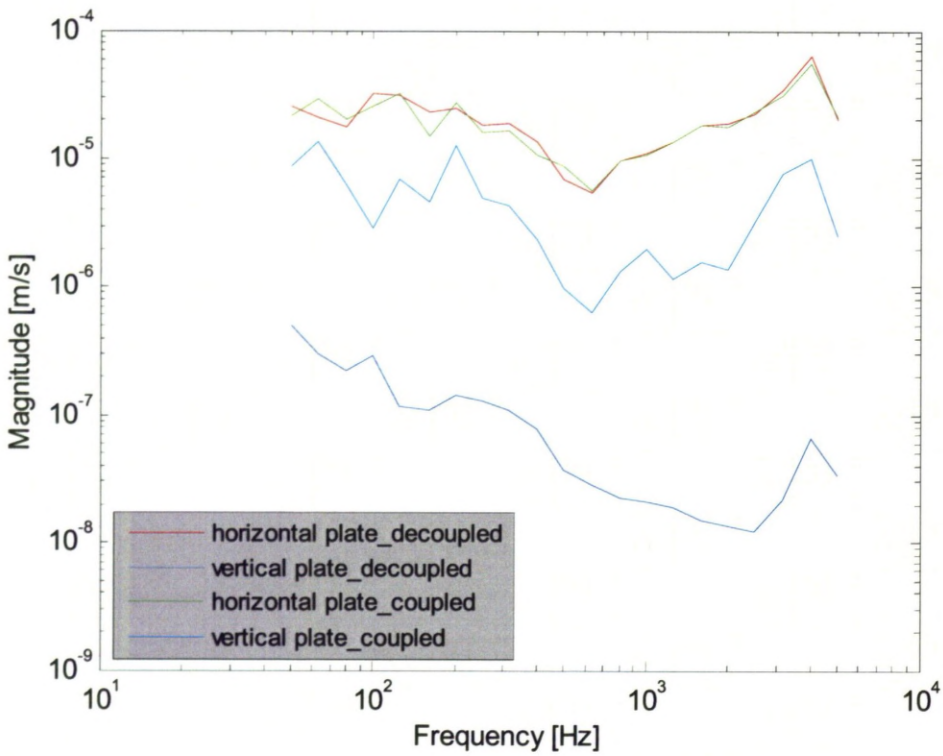

Figure 7.6: Velocity levels – horizontal plate to large vertical plate

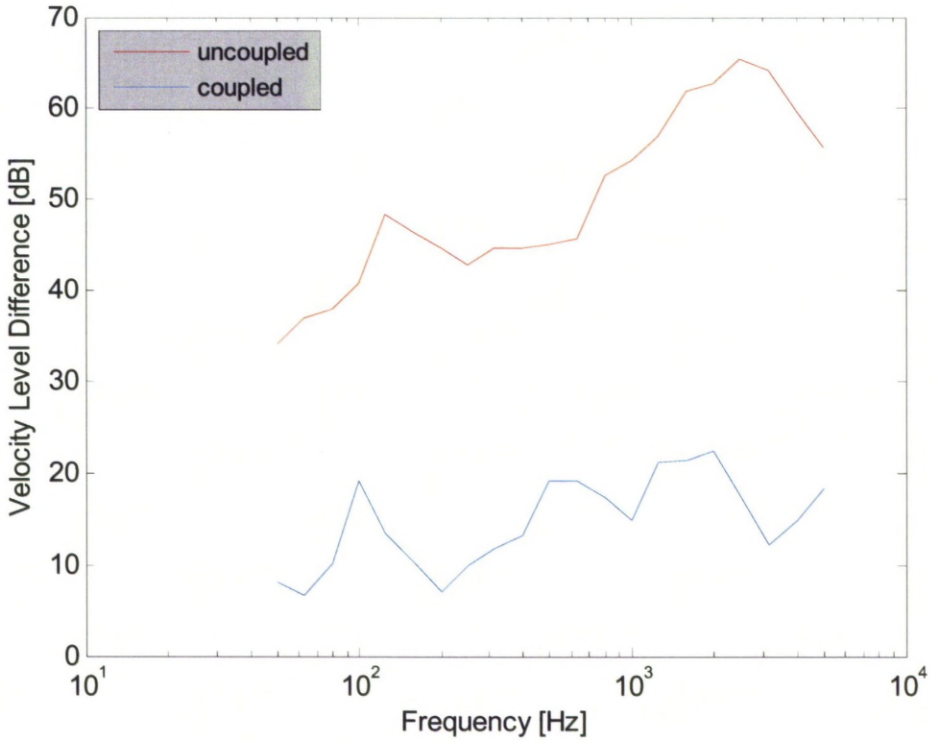

Figure 7.7: Velocity level difference – horizontal plate to large vertical plate

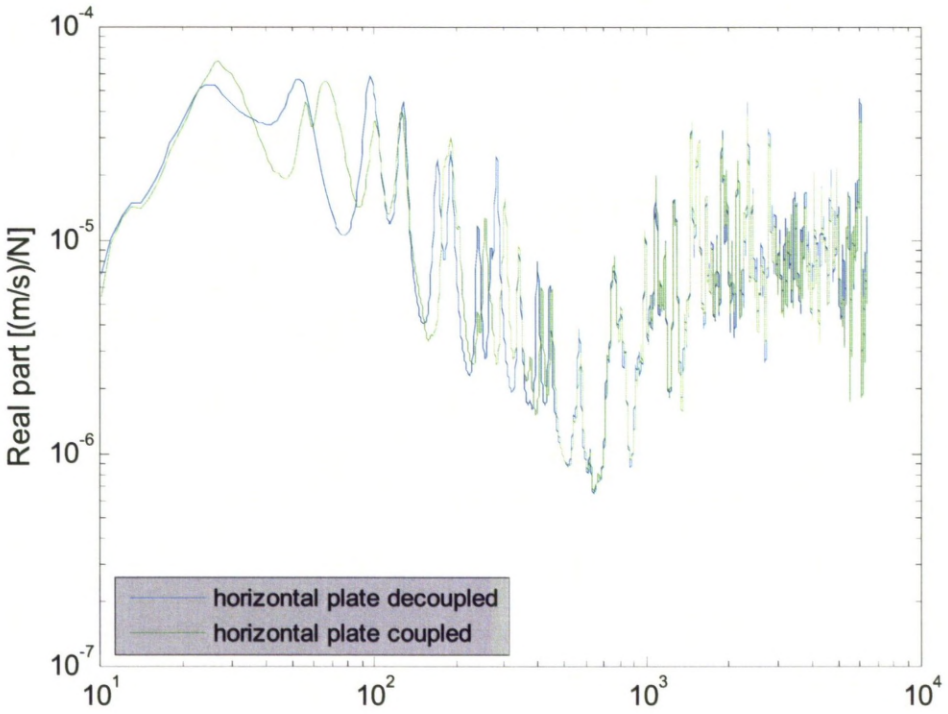

Figure 7.8: Point mobility of horizontal plate, when decoupled and coupled

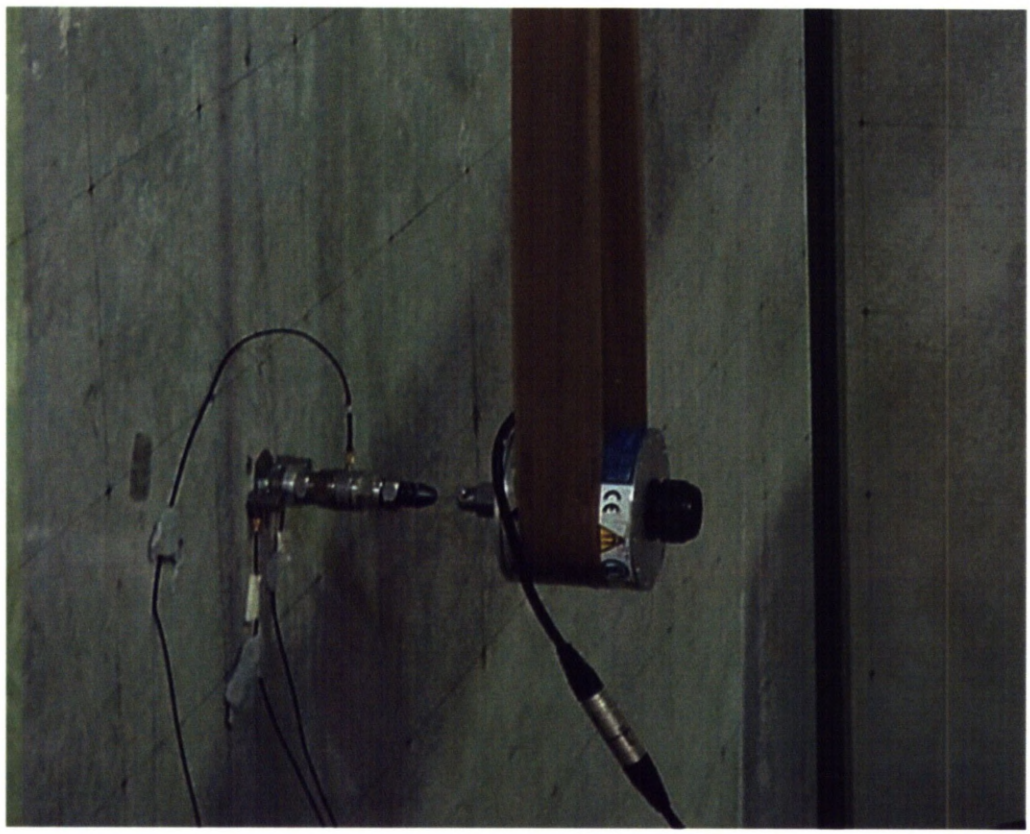

Figure 7.9: Direct power generation and registration by a shaker attached to a vertical reception plate.

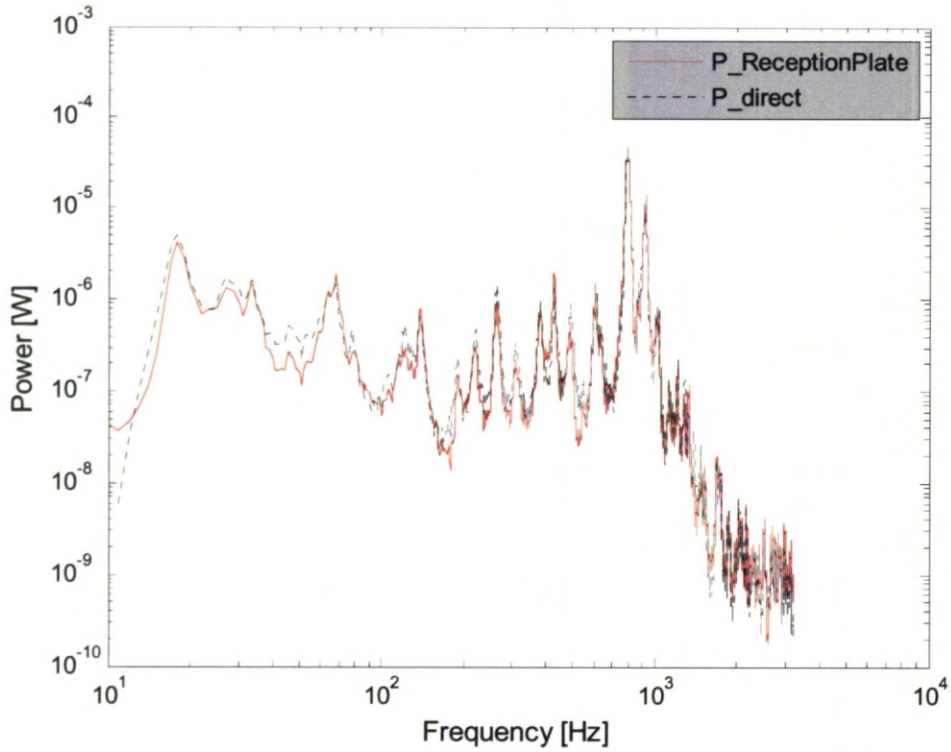

Figure 7.10: Direct power and from reception plate method – vertical plate

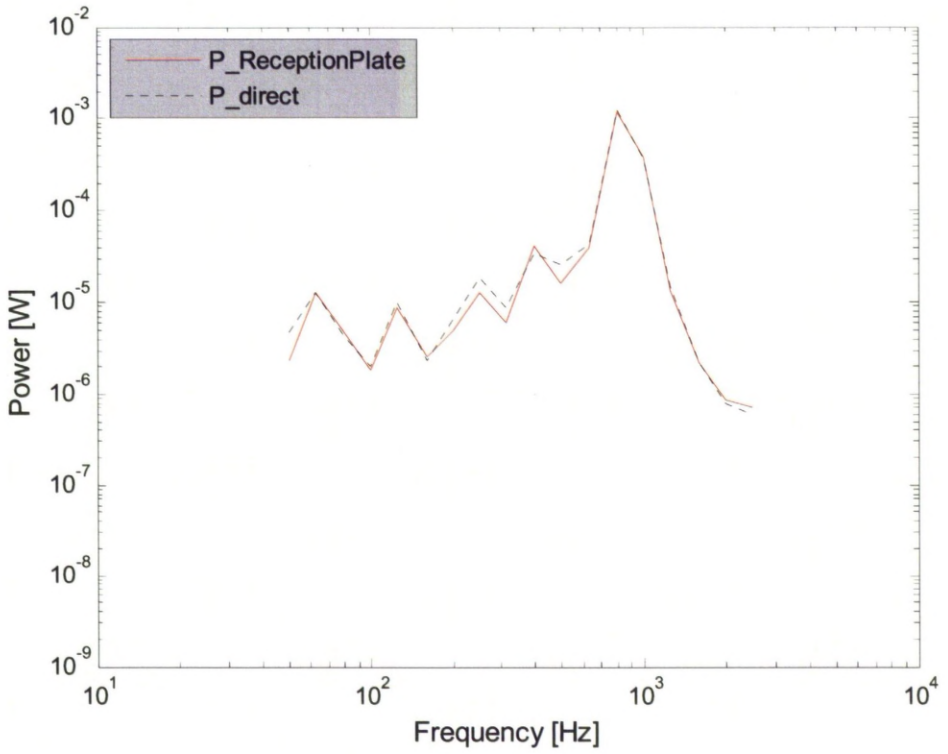

Figure 7.11: Direct power and from reception plate method in 3rd octave bands – vertical plate

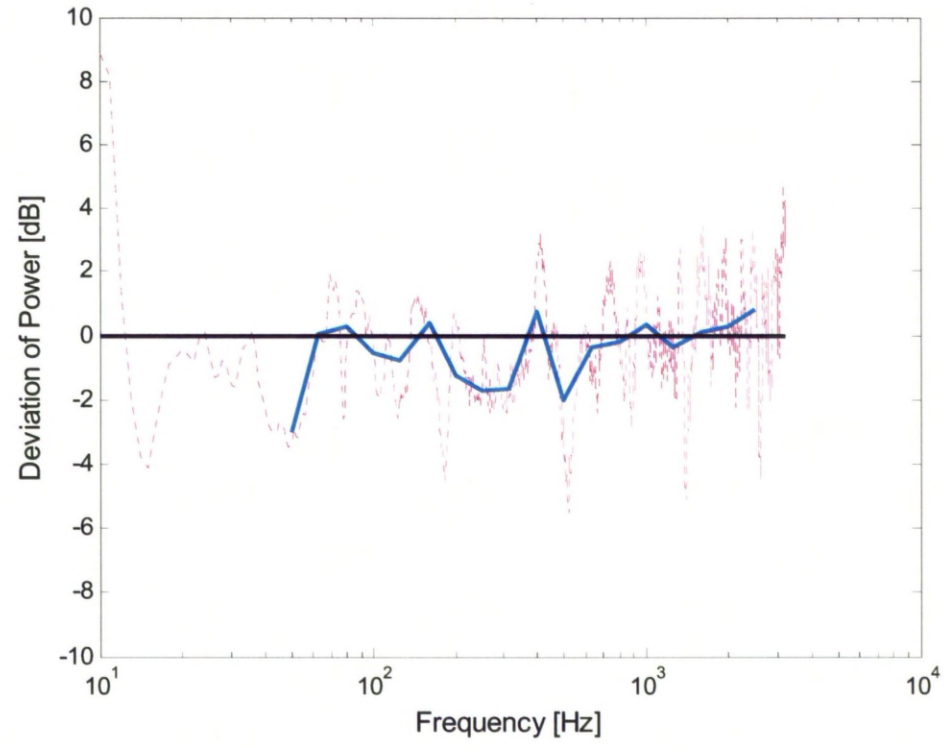

Figure 7.12: Level difference between direct power and from reception plate method – vertical plate

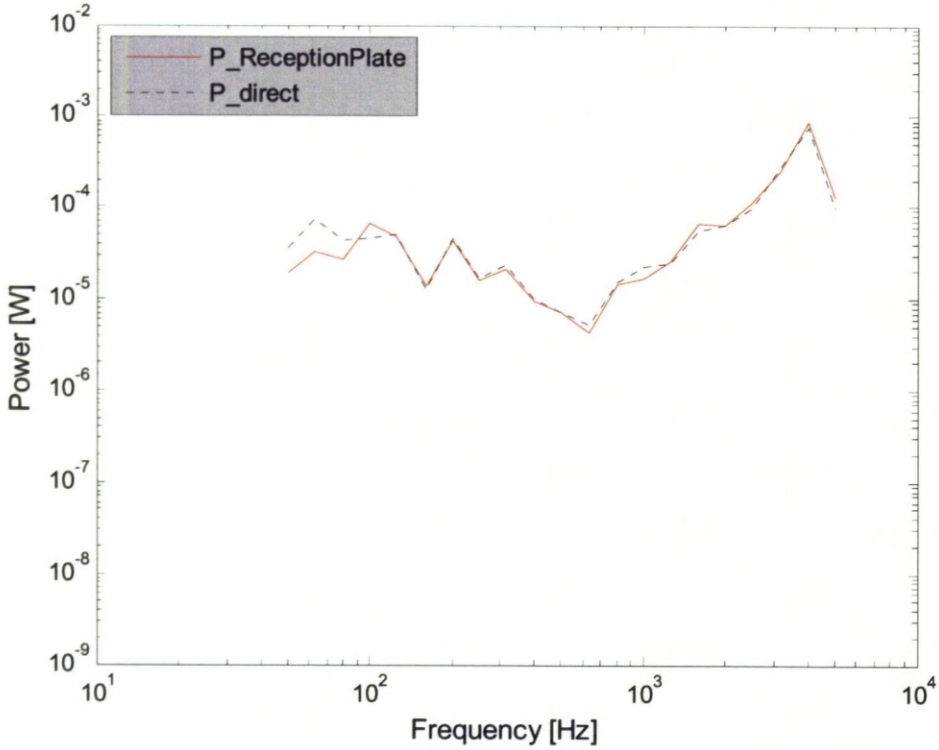

Figure 7.13: Direct power and from reception plate method in 3rd octave bands – horizontal plate coupled to a vertical plate

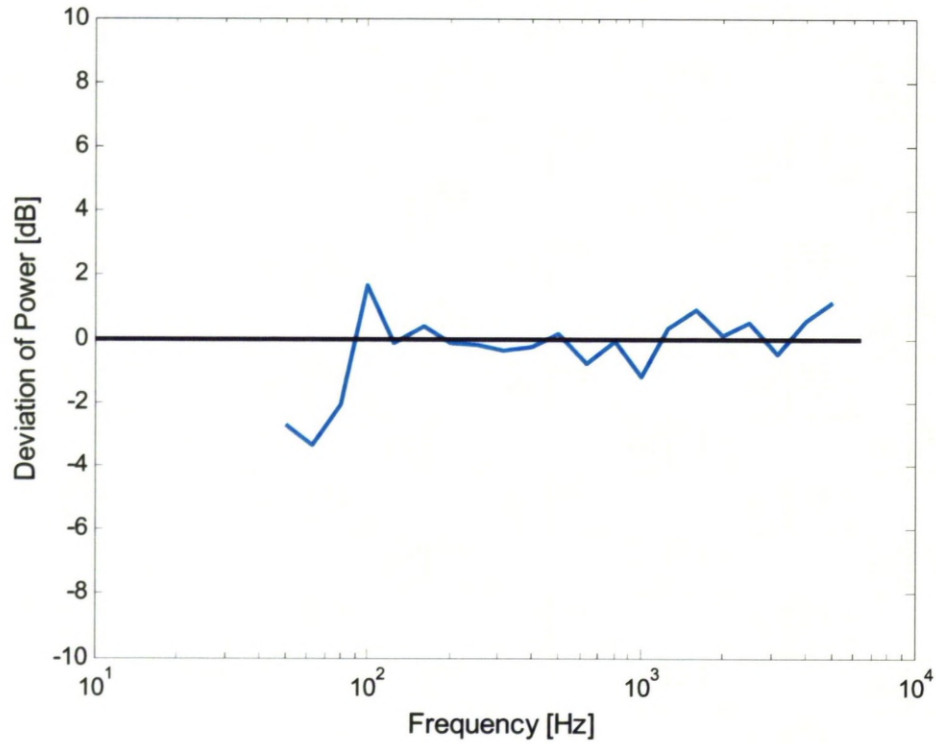

Figure 7.14: Level difference between direct power and measured from reception plate method – coupled horizontal plate

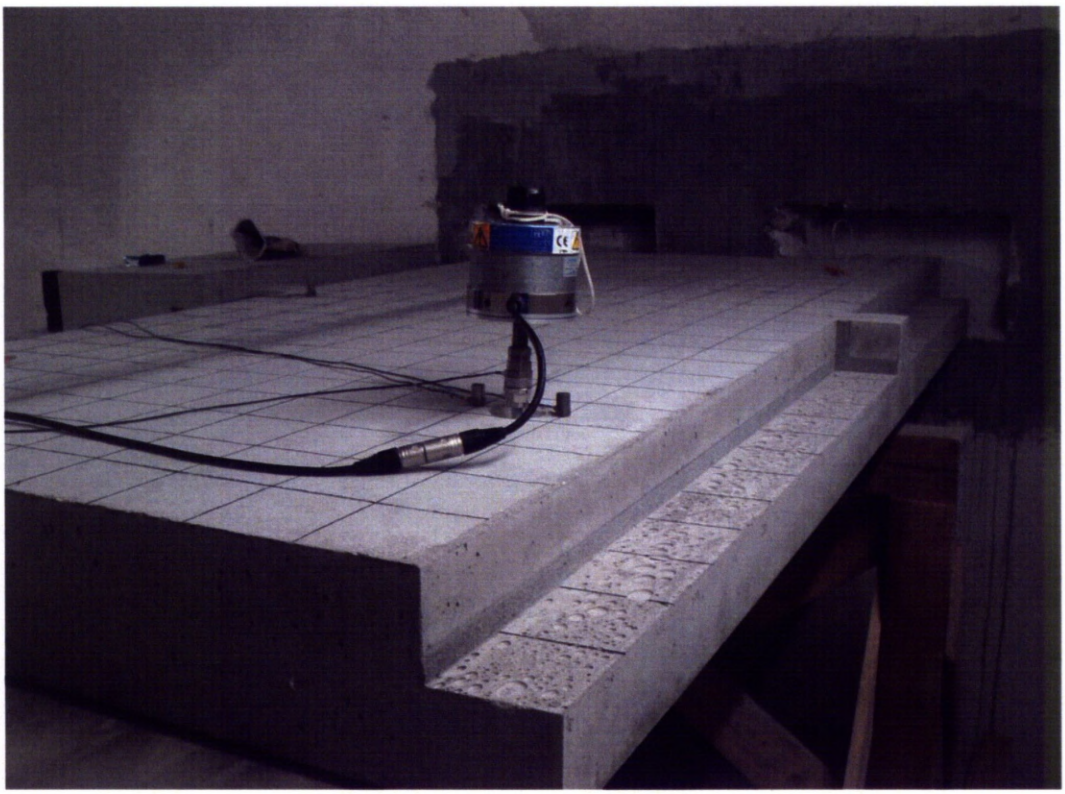

Figure 7.15: Validation of the reception plate method using a staircase landing

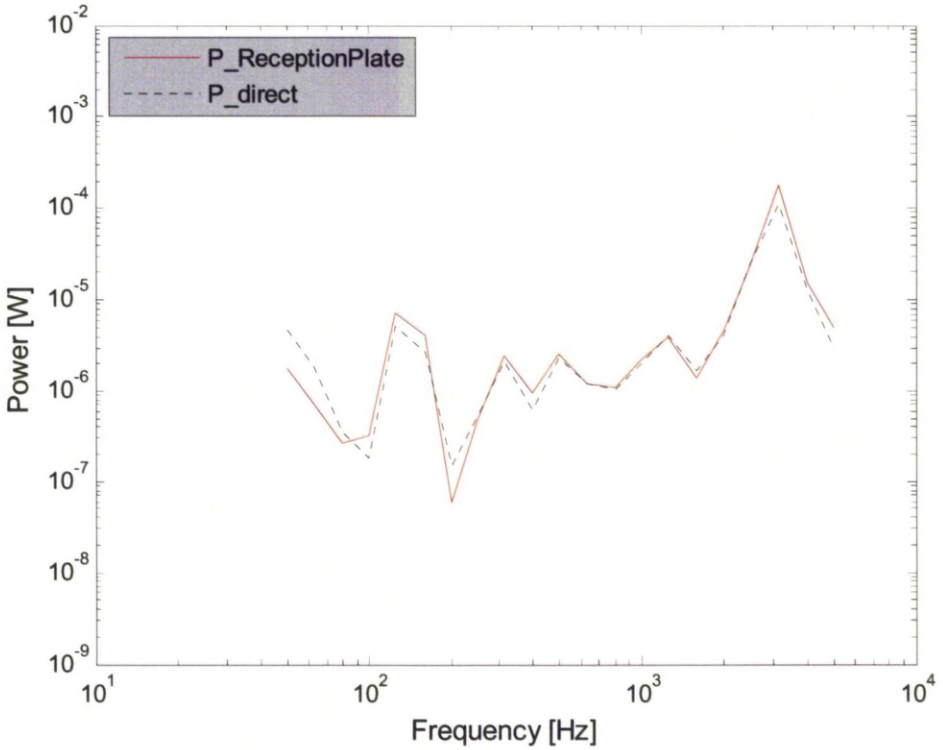

Figure 7.16: Direct power and from reception plate method in 3rd octave bands – staircase landing

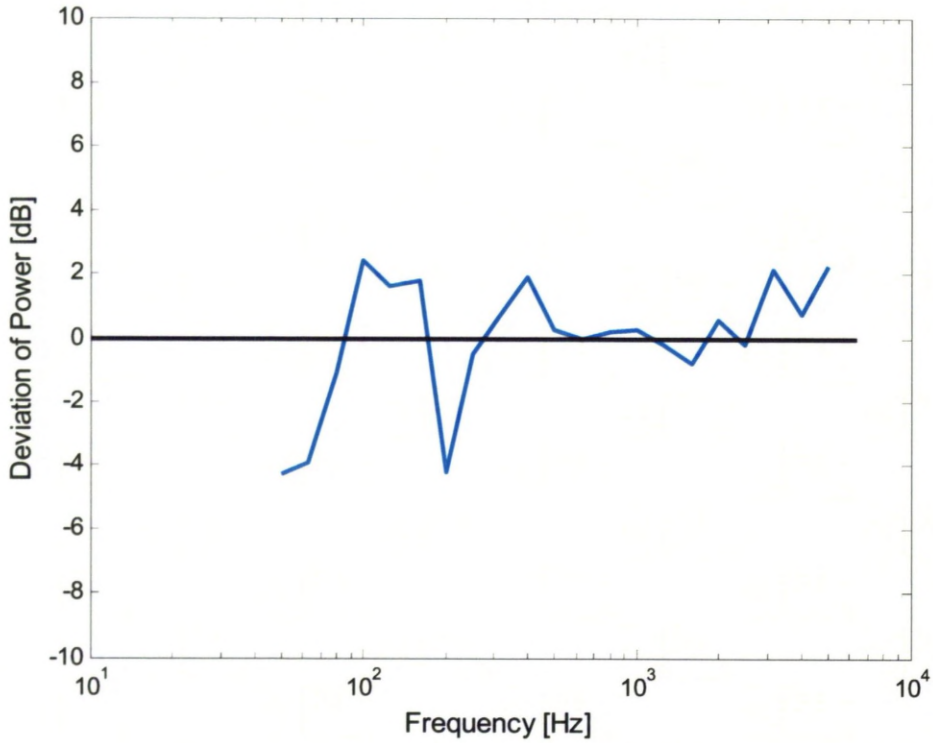

Figure 7.17: Level difference between direct power and from reception plate method – staircase landing

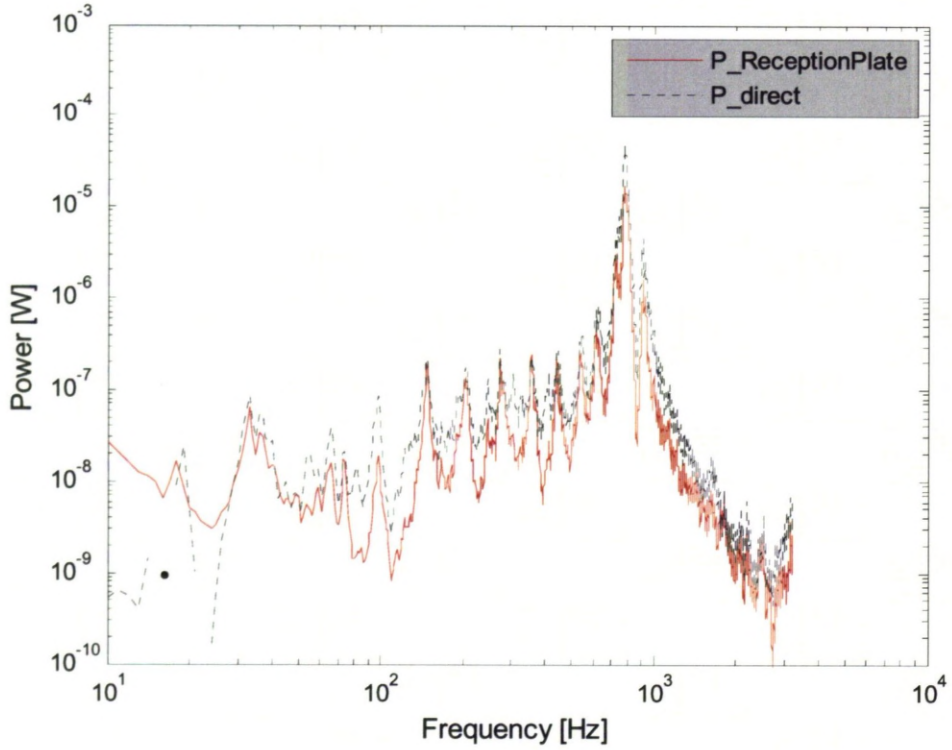

Figure 7.18: Direct power and from reception plate method – stair wall

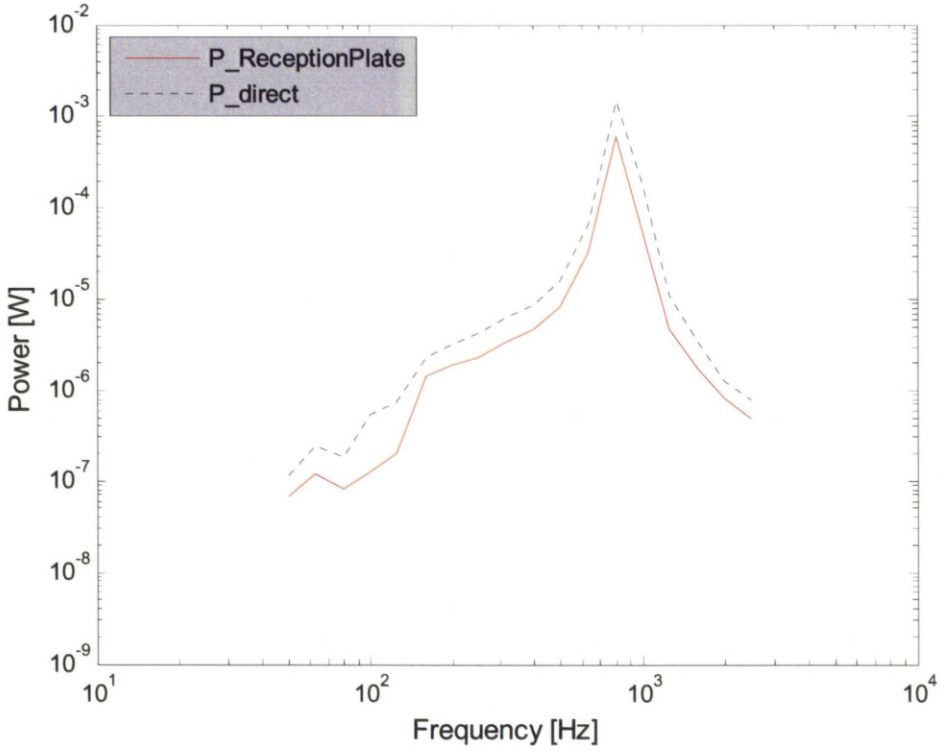

Figure 7.19: Direct power and from reception plate method in 3rd octave bands – stair wall

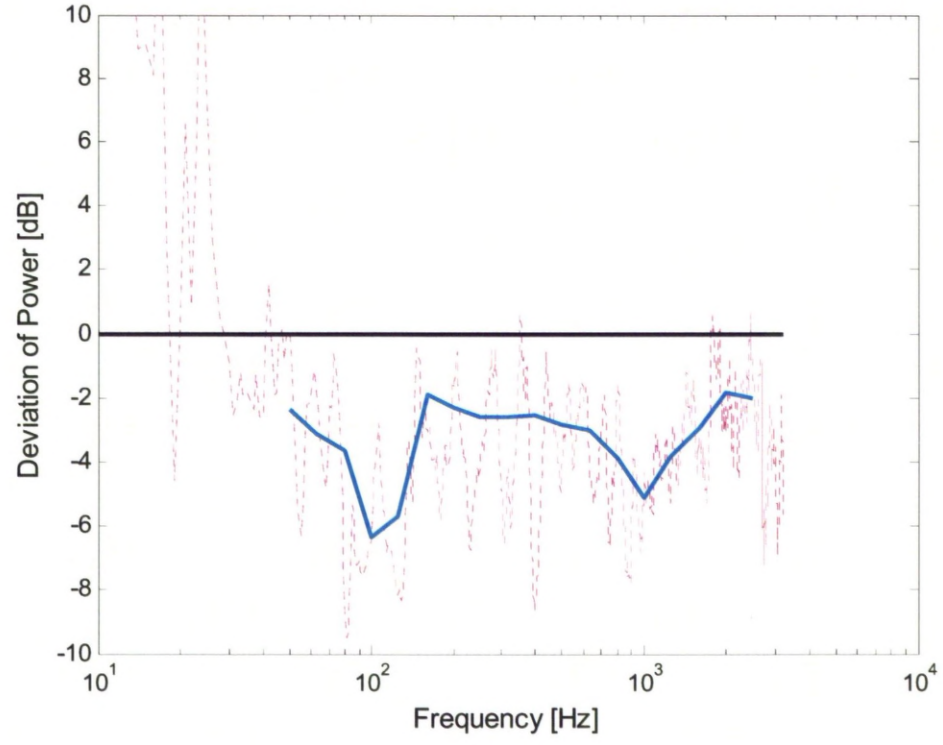

Figure 7.20: Level difference between direct power and from reception plate method – stair wall

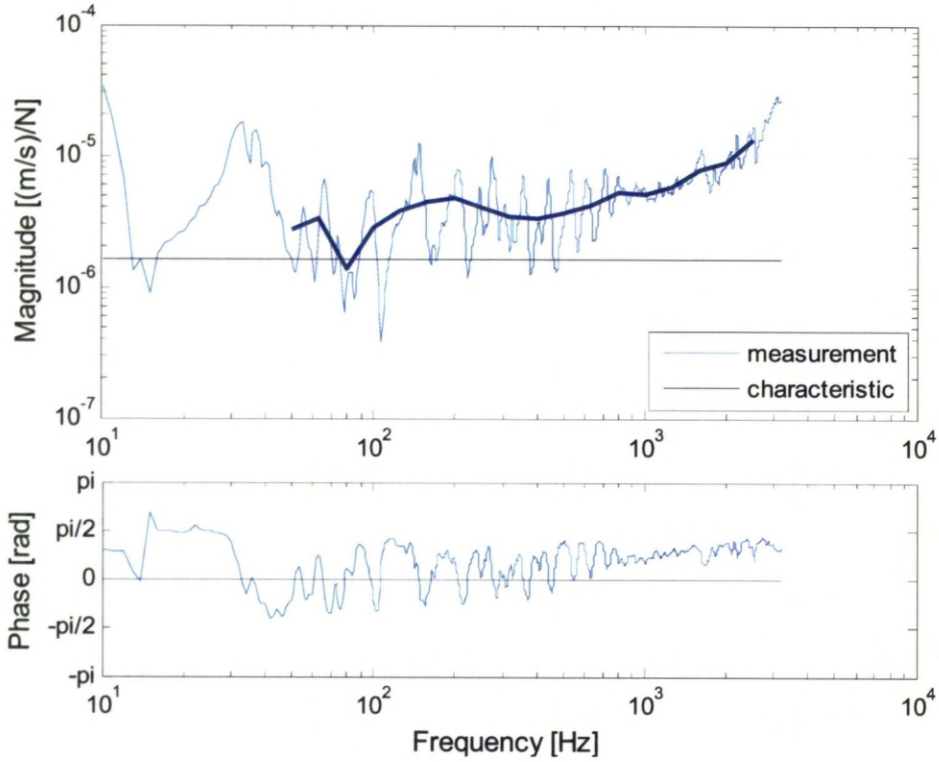

Figure 7.21: Mobility of stair wall – measured and characteristic mobility

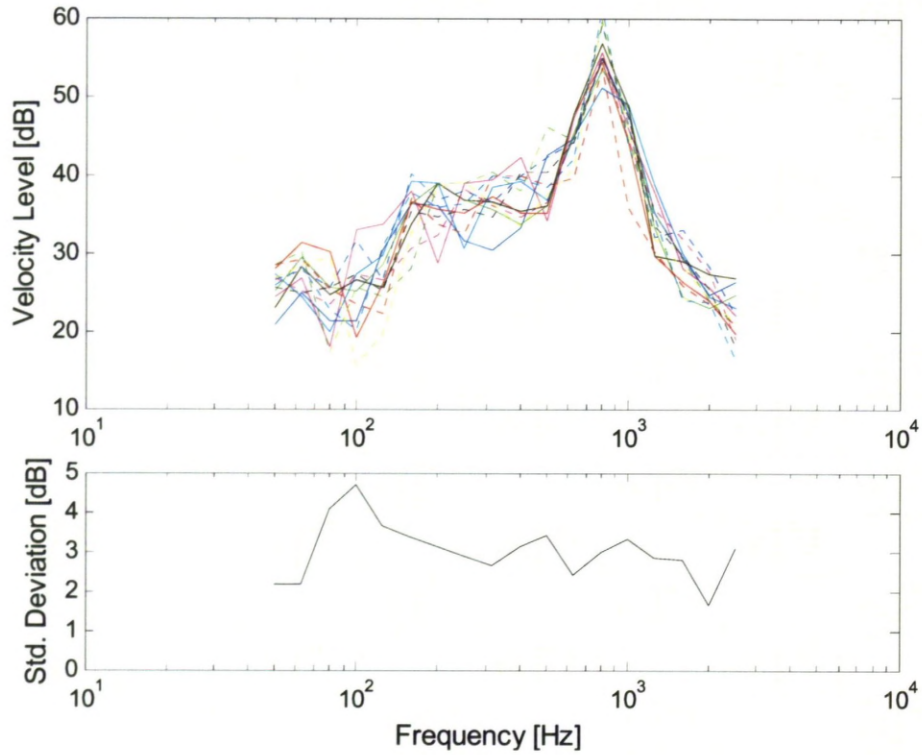

Figure 7.22: Velocity levels on stair wall at 14 sampling points

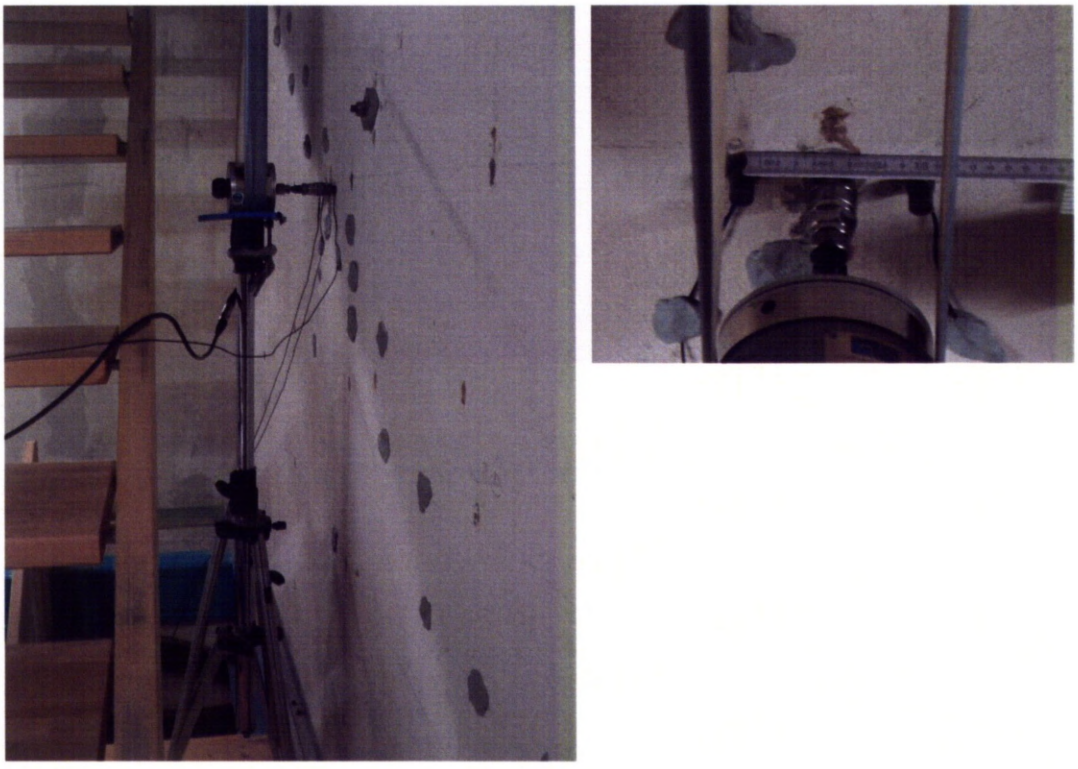

Figure 7.23: Set-up for comparison of direct power and reception plate power: excitation at the contact point of stair and wall

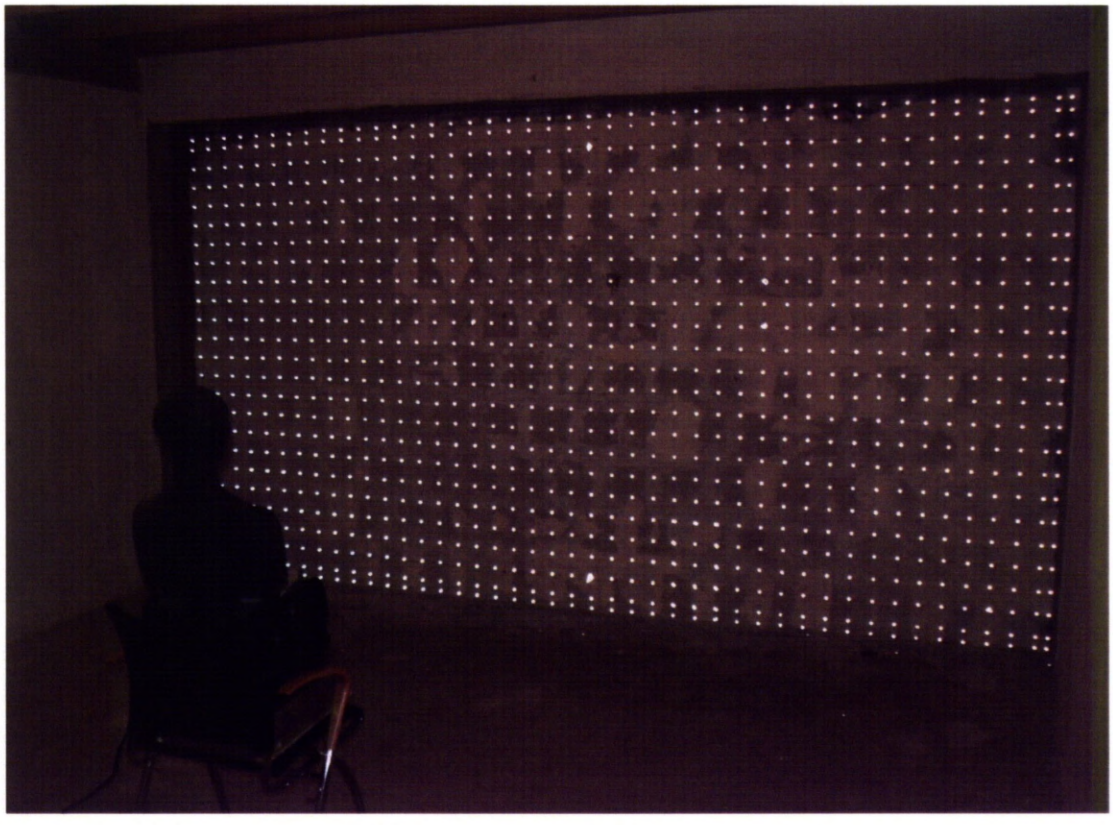

Figure 7.24: Laser vibrometer scanning grid for wall velocity

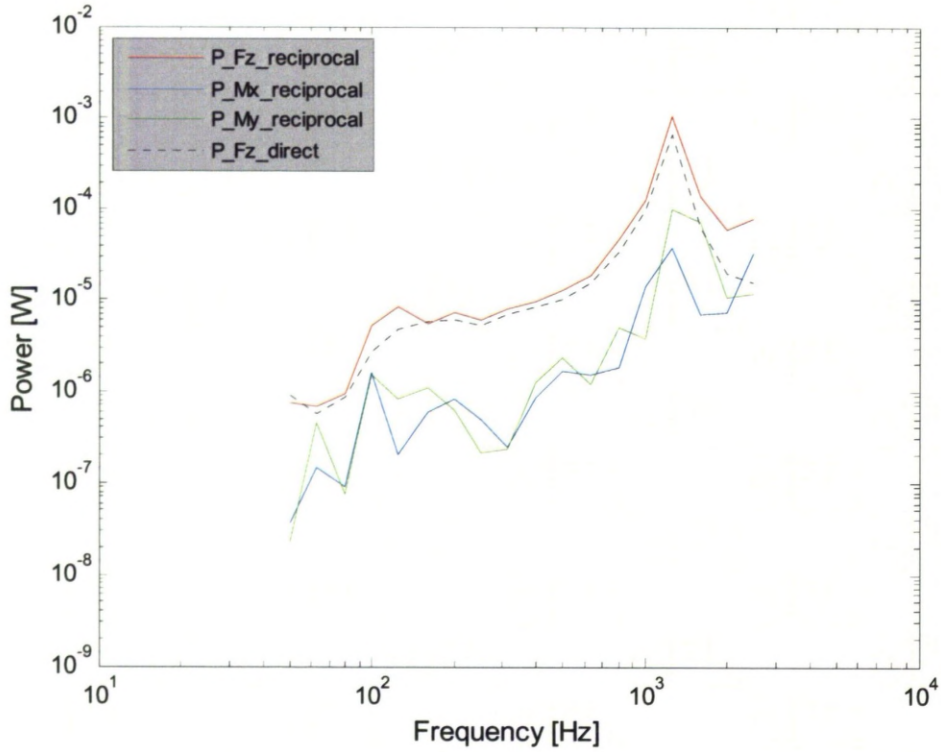

Figure 7.25: Direct and reciprocal powers for shaker excitation at the contact between stair and wall

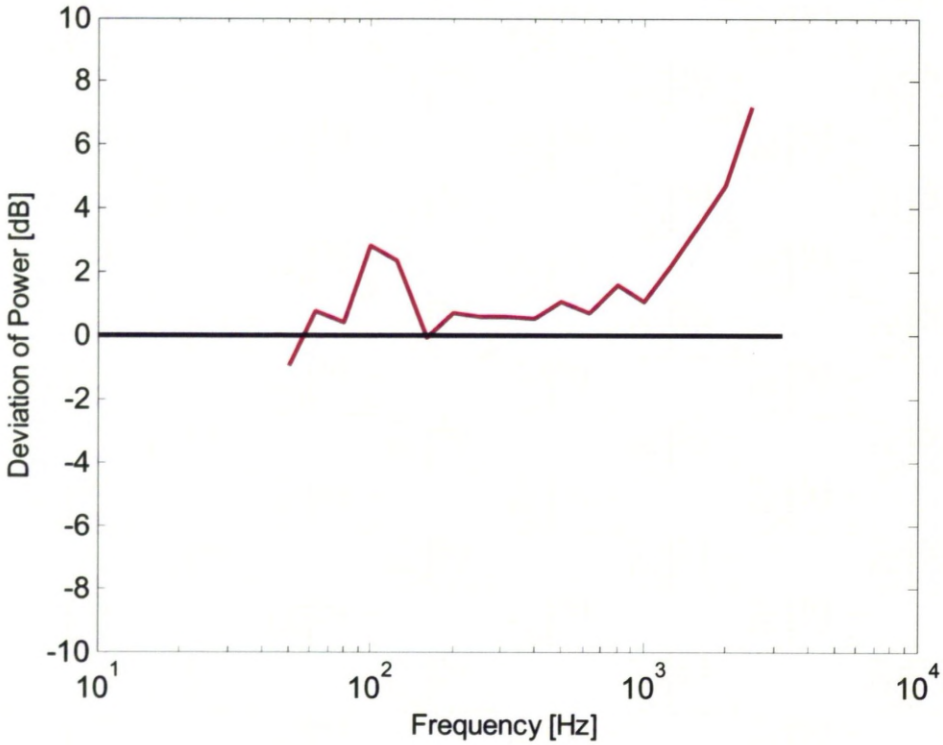

Figure 7.26: Level difference between direct and reciprocal power.

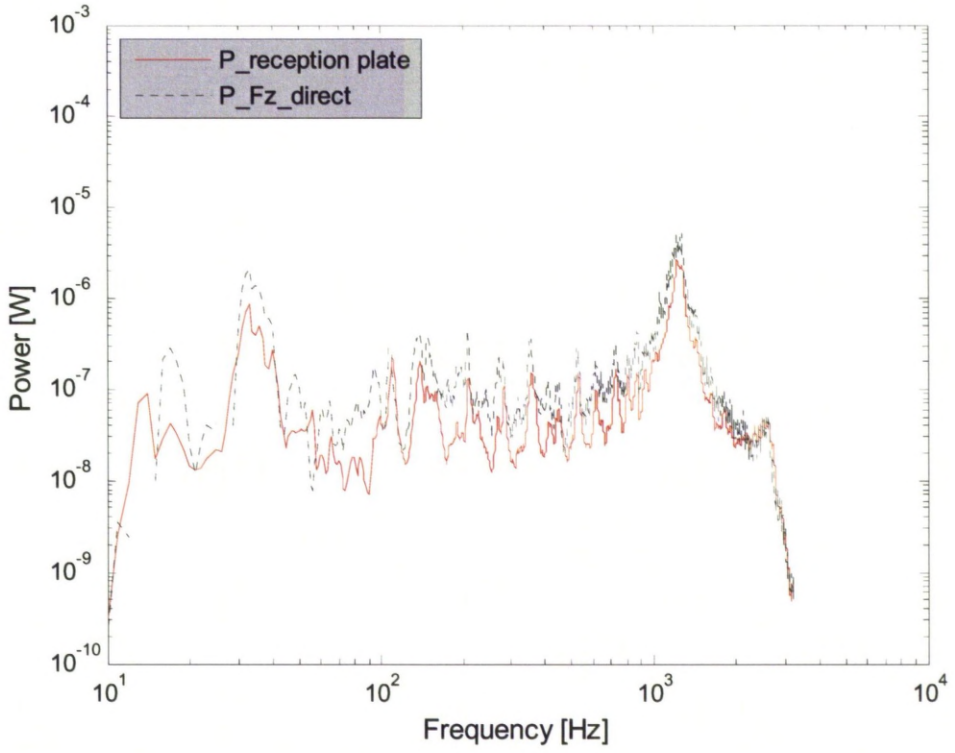

Figure 7.27: Direct power and from reception plate method – stair wall

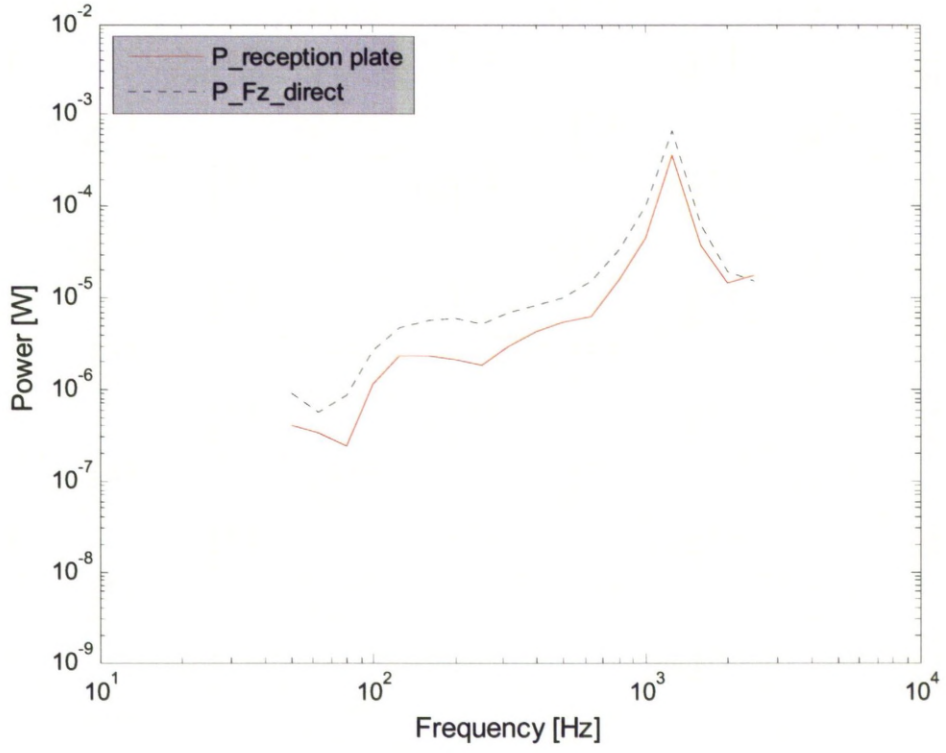

Figure 7.28: Direct power and from reception plate method in 3rd octave bands – stair wall

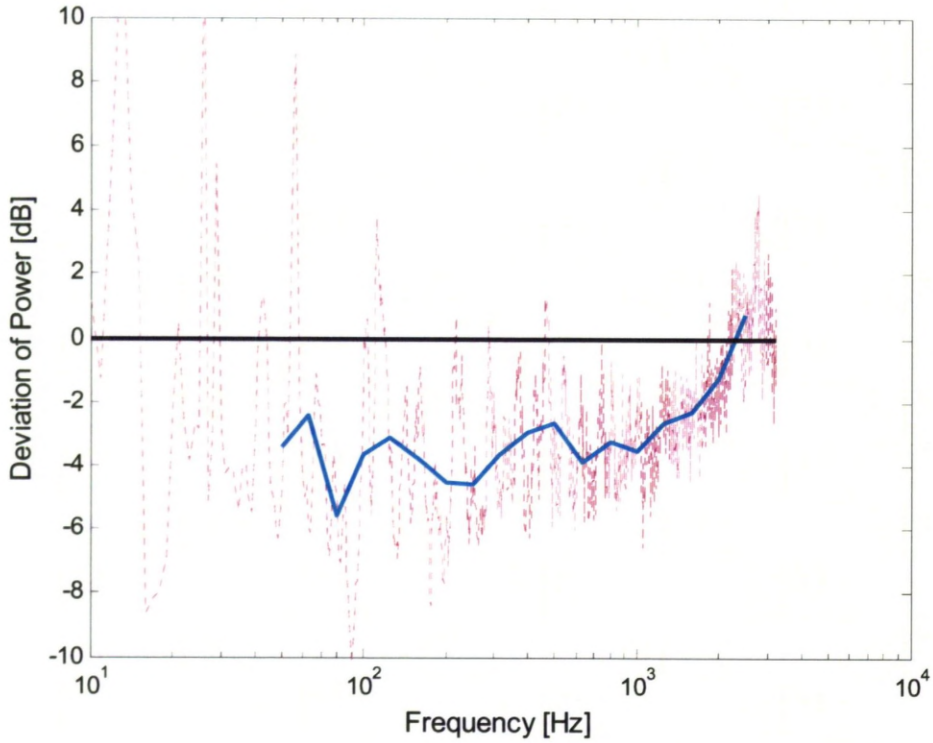

Figure 7.29: Level difference between direct power and from reception plate method – stair wall

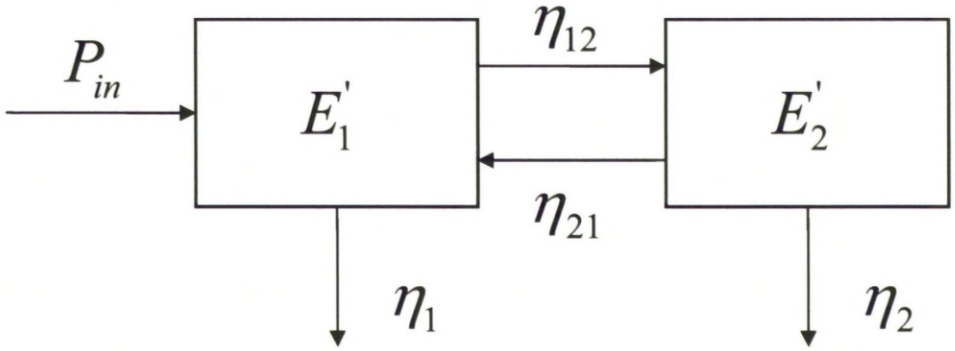

Figure 7.30: SEA model of two connected plates

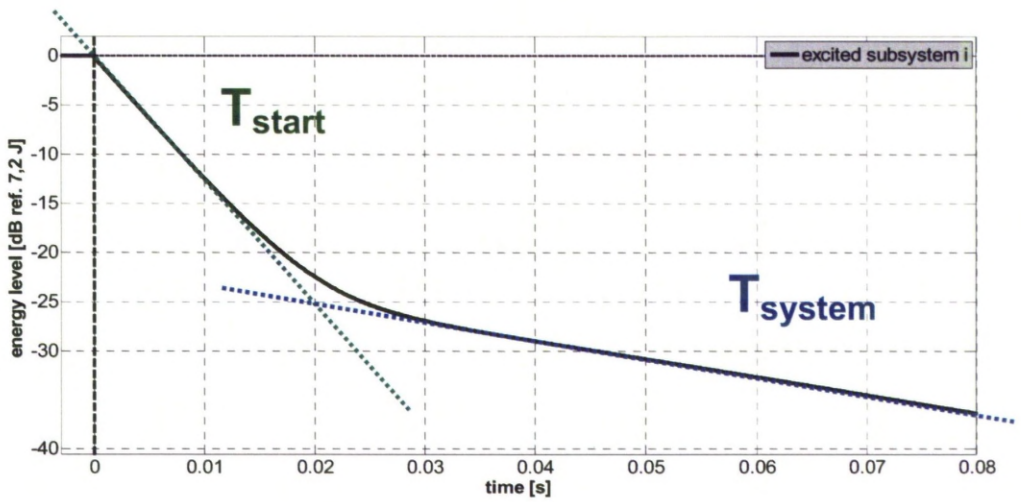

Figure 7.31: Example decay curve simulated with TSEA

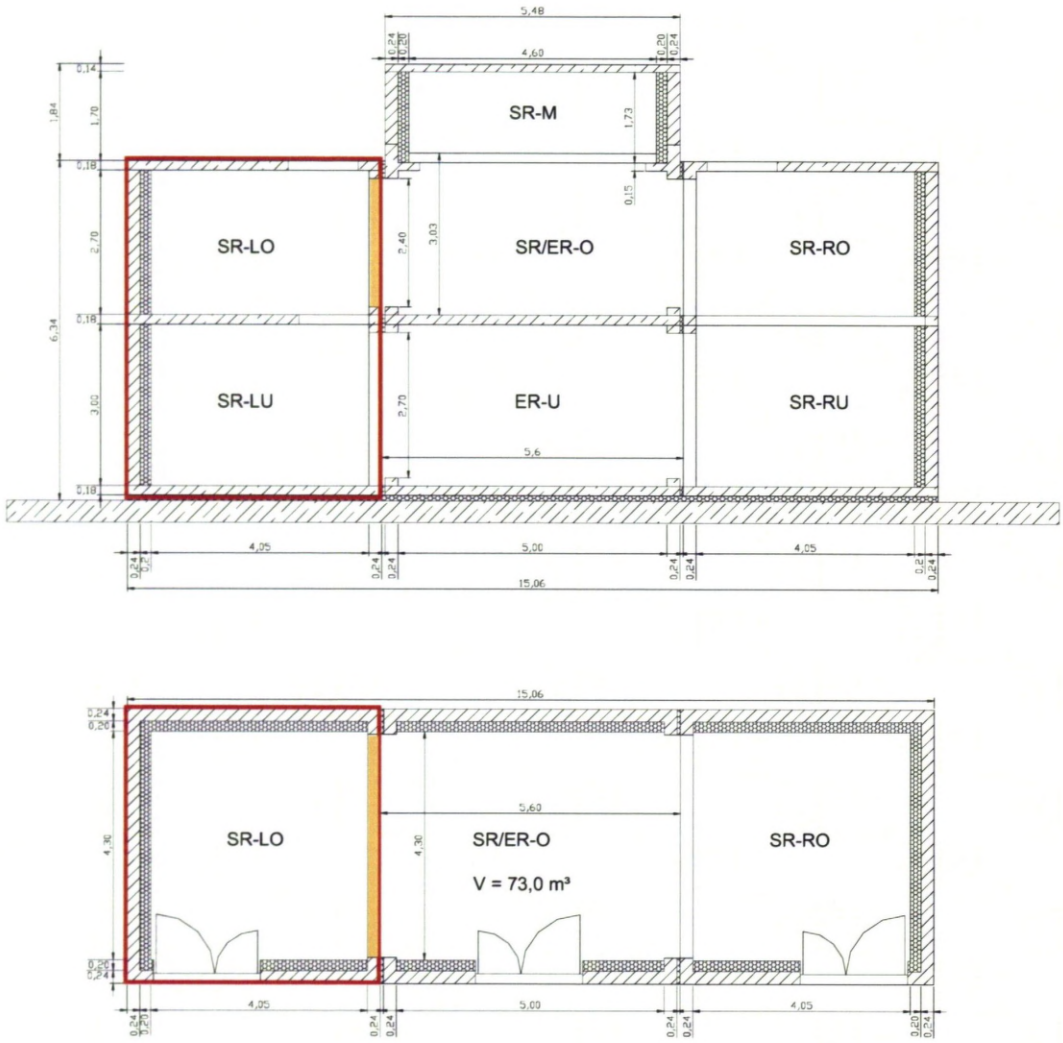

Figure 7.32: Staircase test facility with indication of isolation

	Concrete (d=0,18m)	**Calcium silicate (d=0,24m)**
Youngs modulus E [N/m²]	$3*10^{10}$	$1,27*10^{10}$
Density ρ [kg/m³]	2300	2000
Internal loss factor η_{int} [-]	0,006	0,015
m' [kg/m²]	414	432
Subsystems number	3, 4, 5	1, 2, 6, 7, 8, 9, 10, 11

Table 7.1: Properties of the plates as used in the simulation

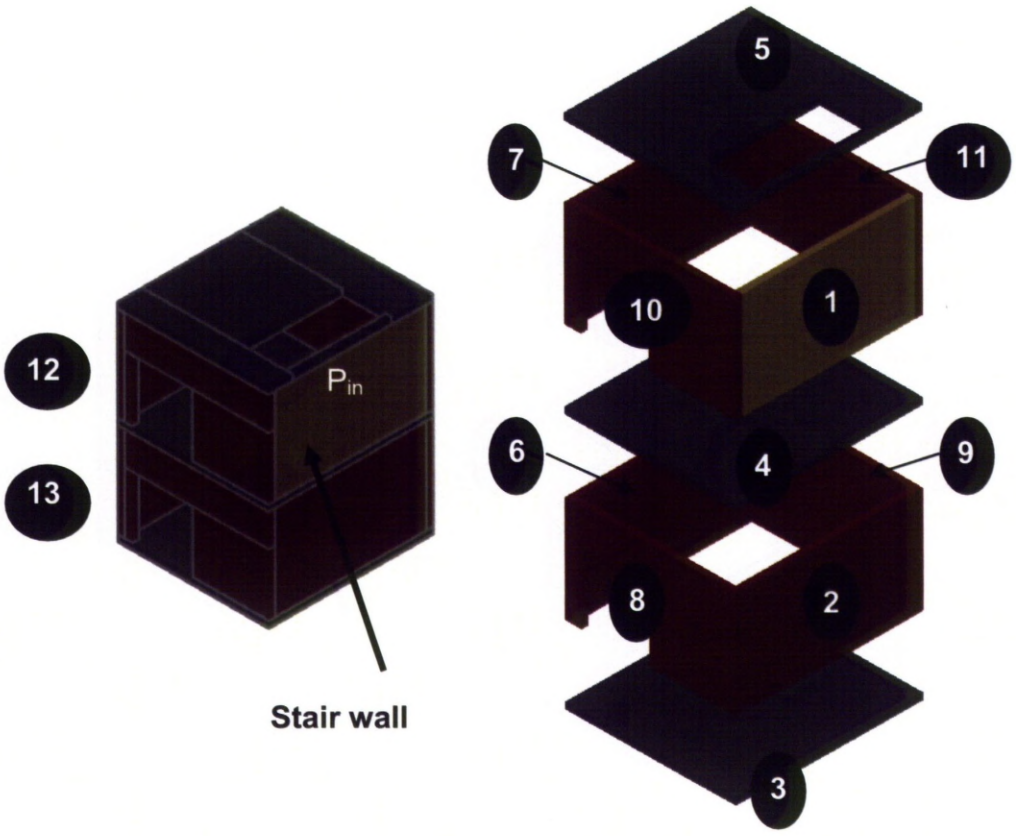

Figure 7.33: TSEA model of the staircase test facility with denotation of the subsystems (1 is the stair wall, 12 and 13 are rooms)

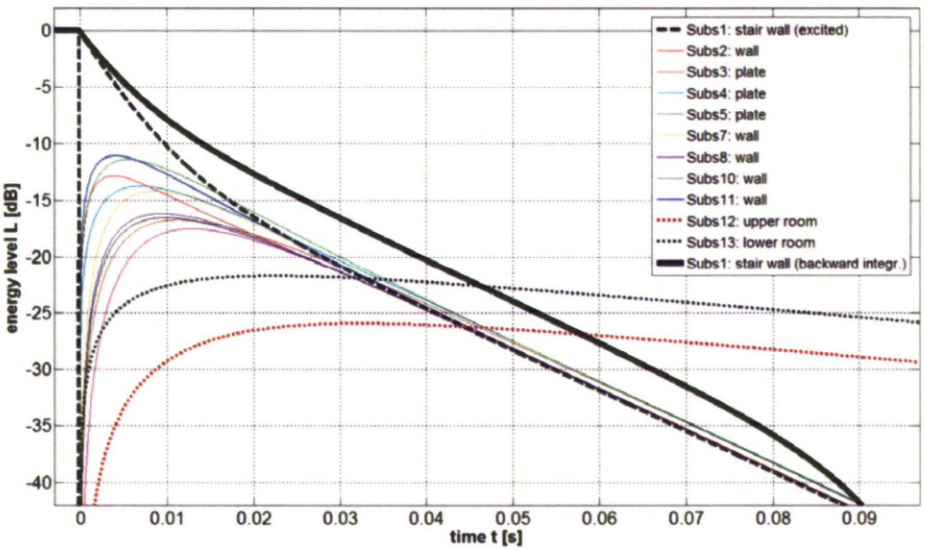

Figure 7.34: Decay of the subsystems resulting from transient excitation at 1000 Hz

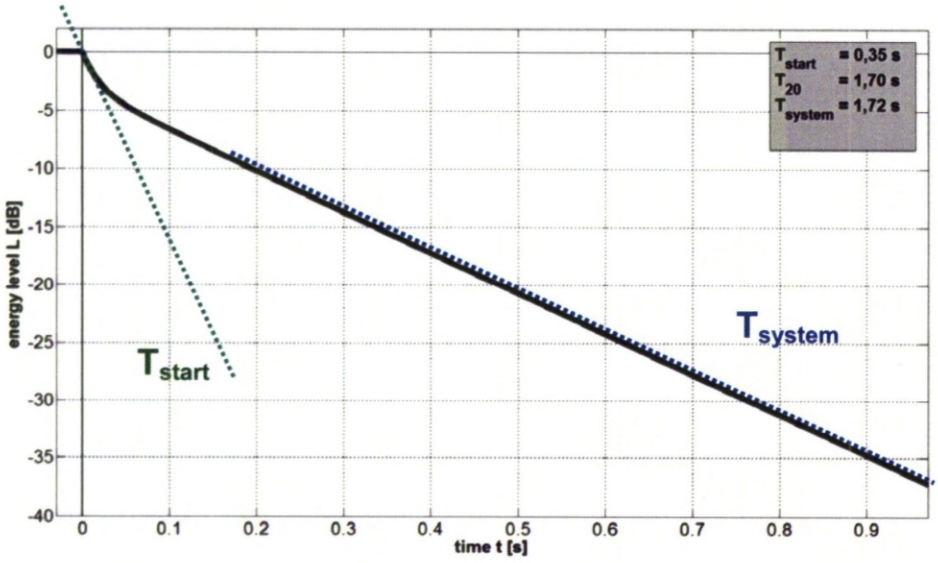

Figure 7.35: Decay for the stair wall resulting from transient excitation at 100 Hz

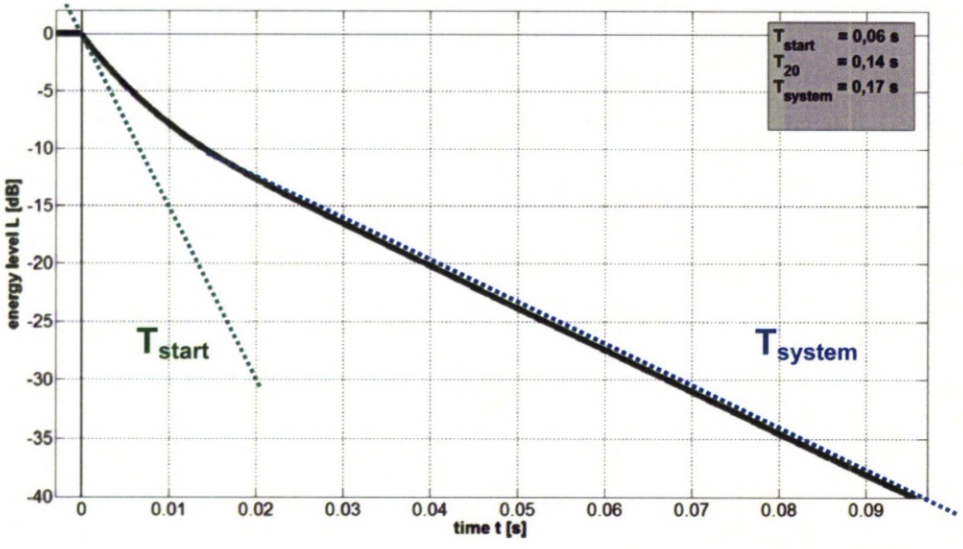

Figure 7.36: Decay for the stair wall resulting from transient excitation at 1000 Hz

f [Hz]	η_{start} [-]	η_{20} [-]	η_{system} [-]
50	0,072	0,010	0,010
63	0,069	0,011	0,011
80	0,066	0,012	0,010
100	0,063	0,013	0,013
125	0,059	0,013	0,012
160	0,056	0,013	0,012
200	0,053	0,013	0,011
250	0,051	0,014	0,012
315	0,048	0,014	0,013
400	0,046	0,014	0,013
500	0,043	0,014	0,012
630	0,041	0,015	0,013
800	0,039	0,015	0,013
1000	0,037	0,015	0,013
1250	0,035	0,016	0,013
1600	0,033	0,016	0,013
2000	0,032	0,016	0,013
2500	0,031	0,017	0,013
3150	0,029	0,017	0,012
4000	0,028	0,017	0,013
5000	0,027	0,017	0,013

Table 7.2: Loss factors of the stair wall in 3rd octave bands

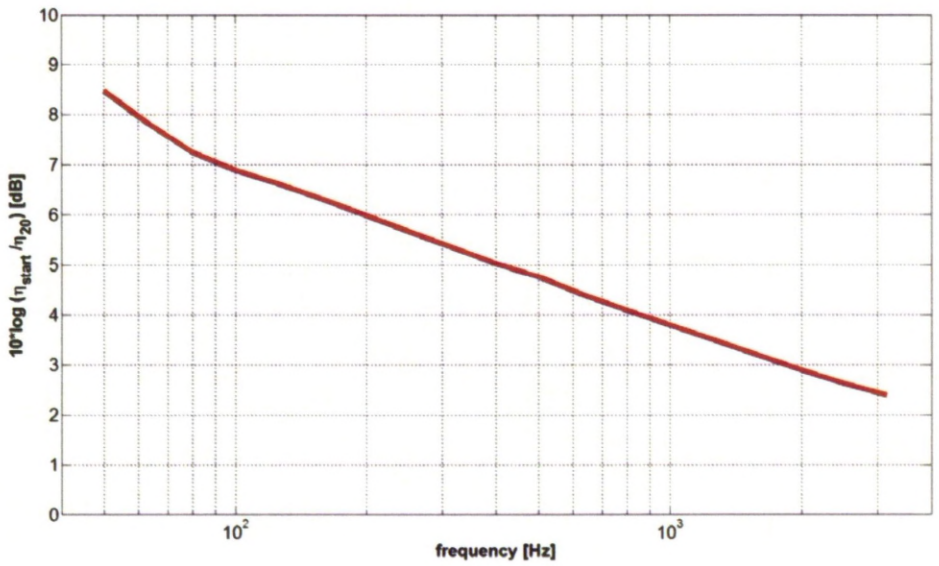

Figure 7.37: Decay level difference between $\eta_{stationary}$ and η_{20}

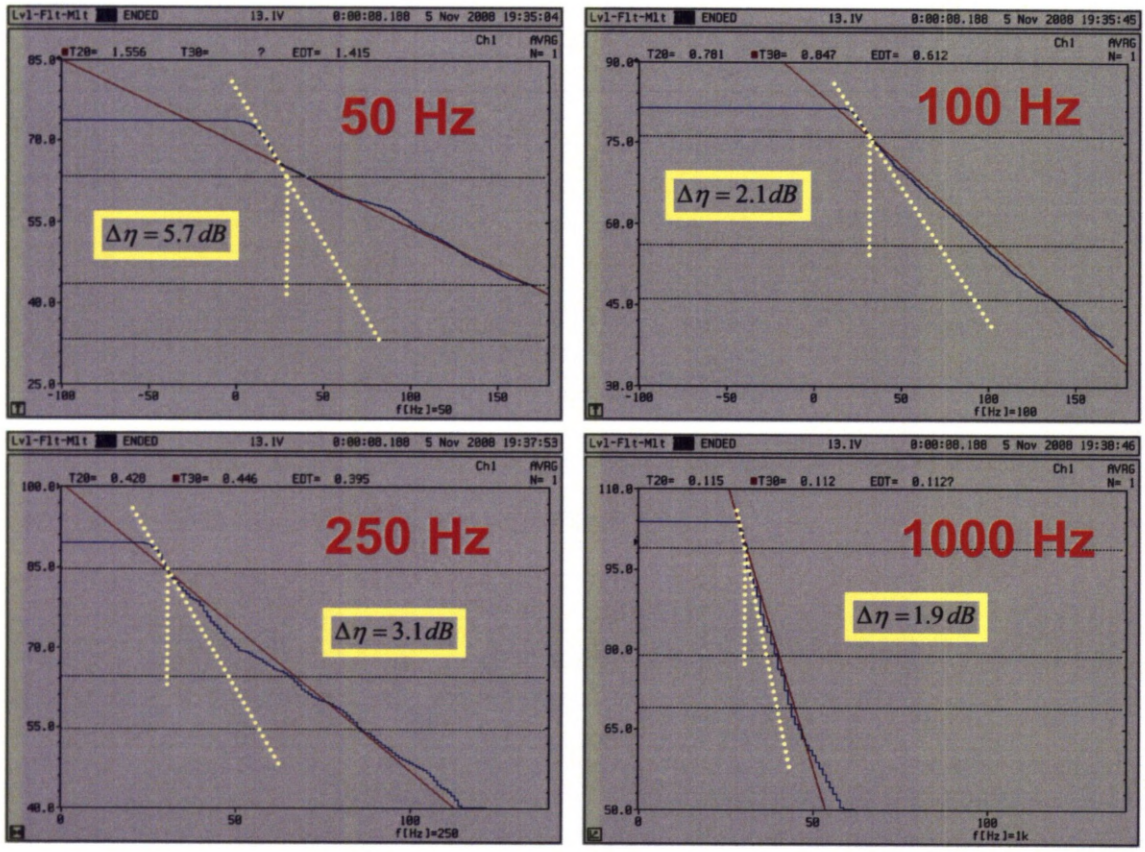

Figure 7.38: Measured decays for the stair wall at 50, 100, 250 and 1k Hz

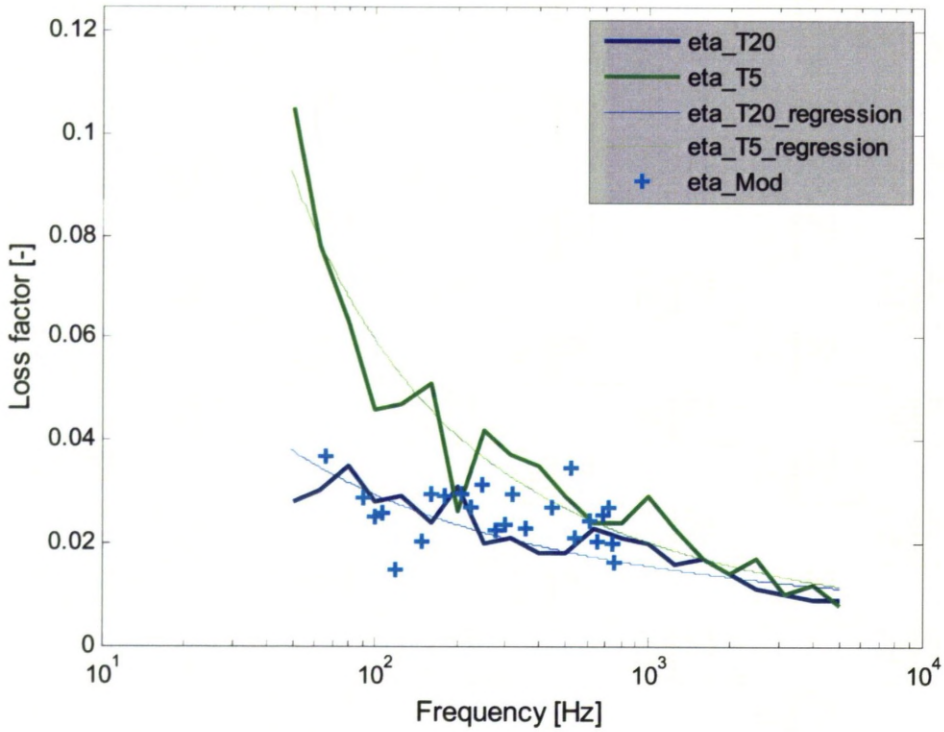

Figure 7.39: Total loss factor from T_{20}, T_5 and half power-bandwidths

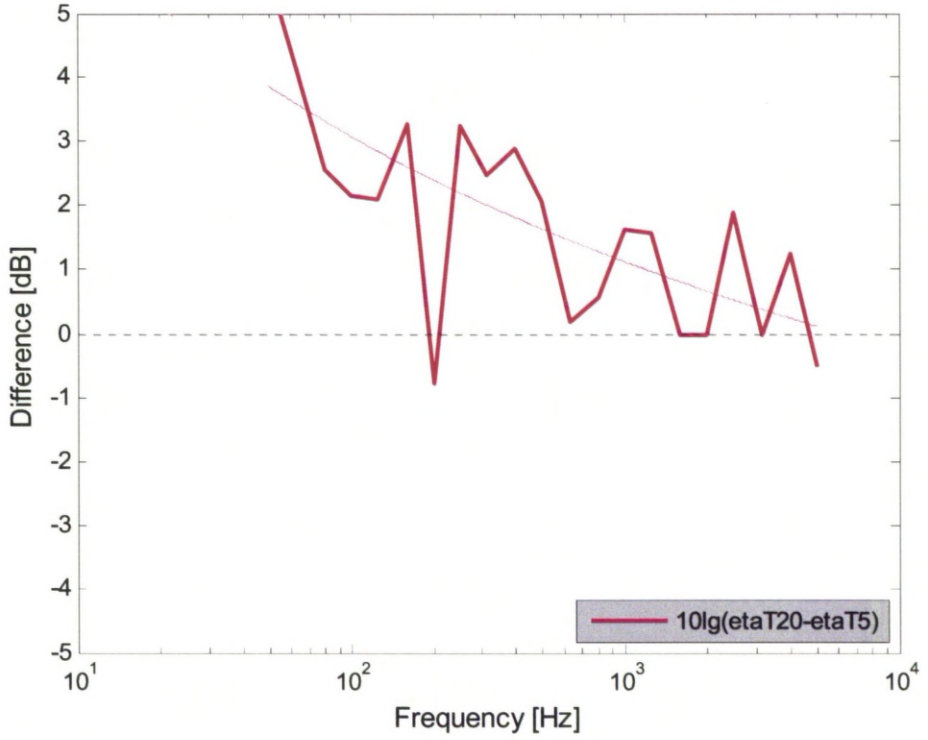

Figure 7.40: Level difference between loss factors from T_{20} and T_5

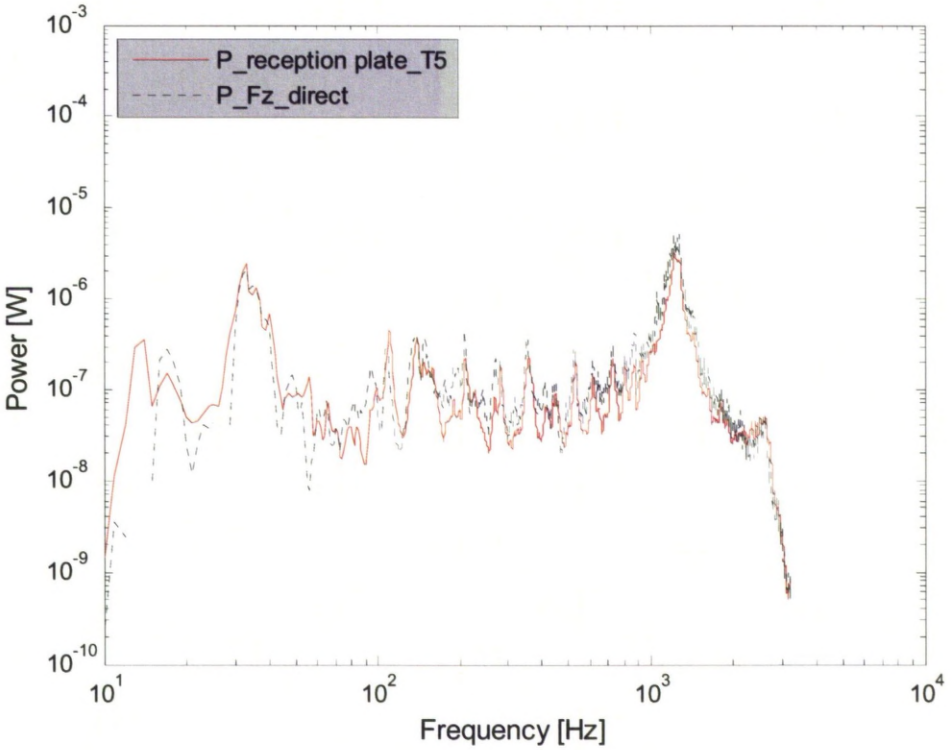

Figure 7.41: Direct power and from reception plate method using T_5 – stair wall

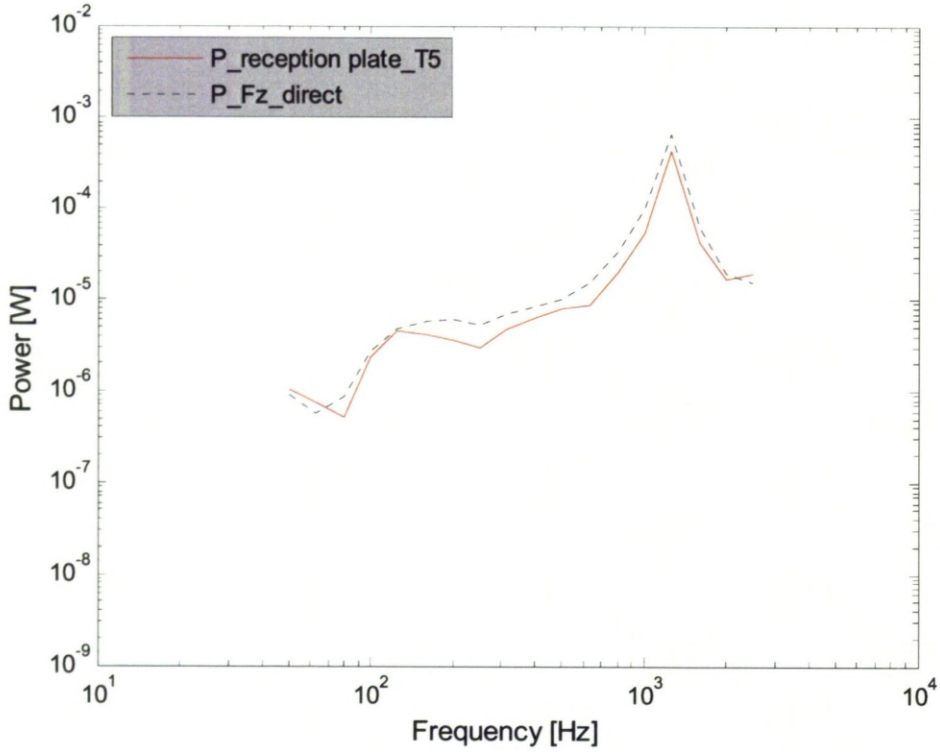

Figure 7.42: Direct power direct and from reception plate method T_5 in 3rd octave bands – stair wall

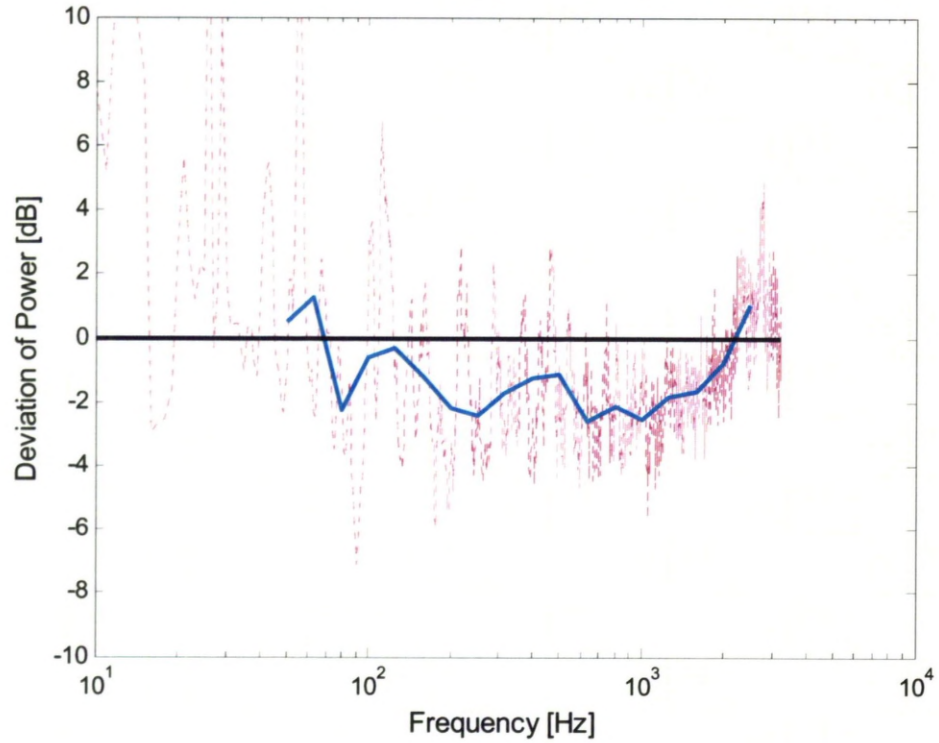

Figure 7.43: Level difference between direct power and from reception plate method – stair wall

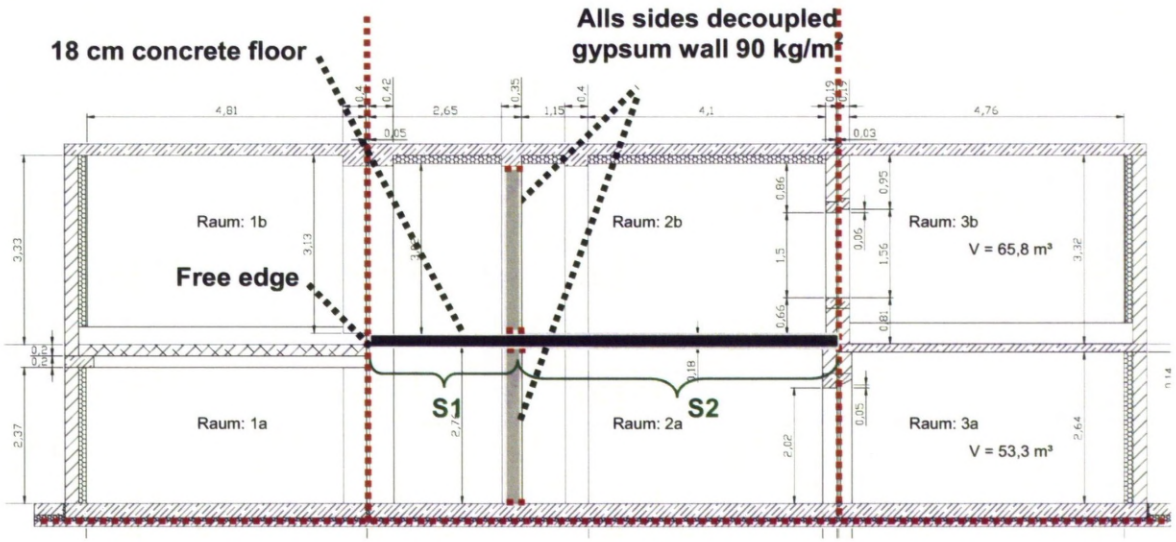

Figure 7.44: Transmission suite with floor used as a reception plate (red: indication of isolation); measurements at 2 floor sections S1, S2

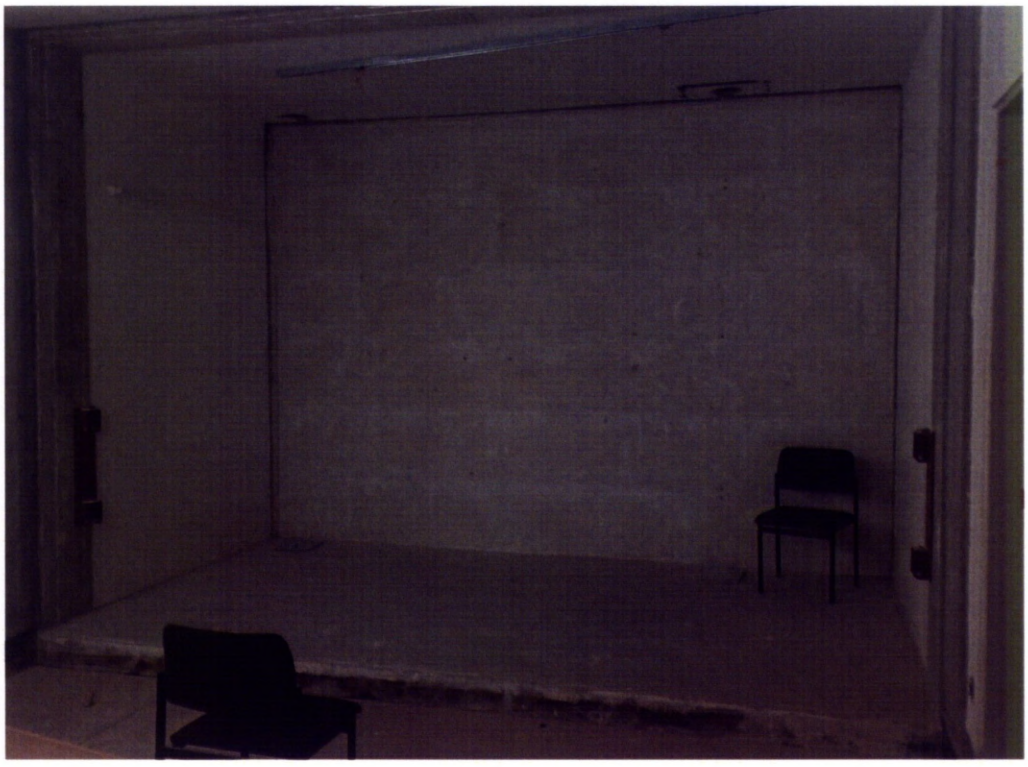

Figure 7.45: Section 1 (S1) of the reference floor with one free edge

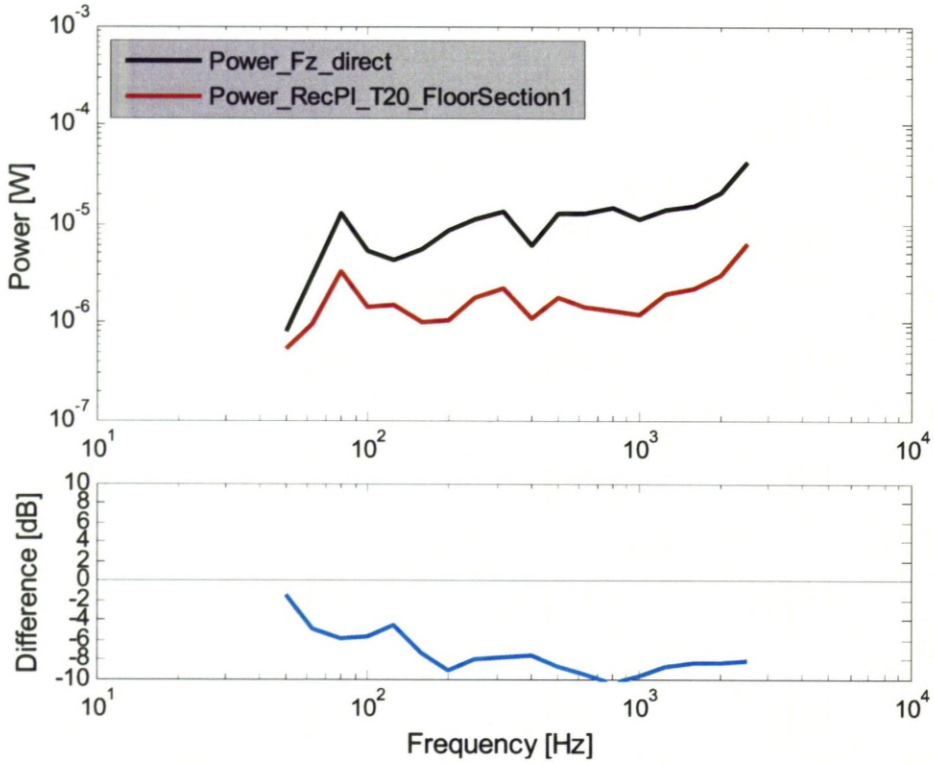

Figure 7.46: Direct power and from reception plate method using T_{20} – reference floor – floor section 1

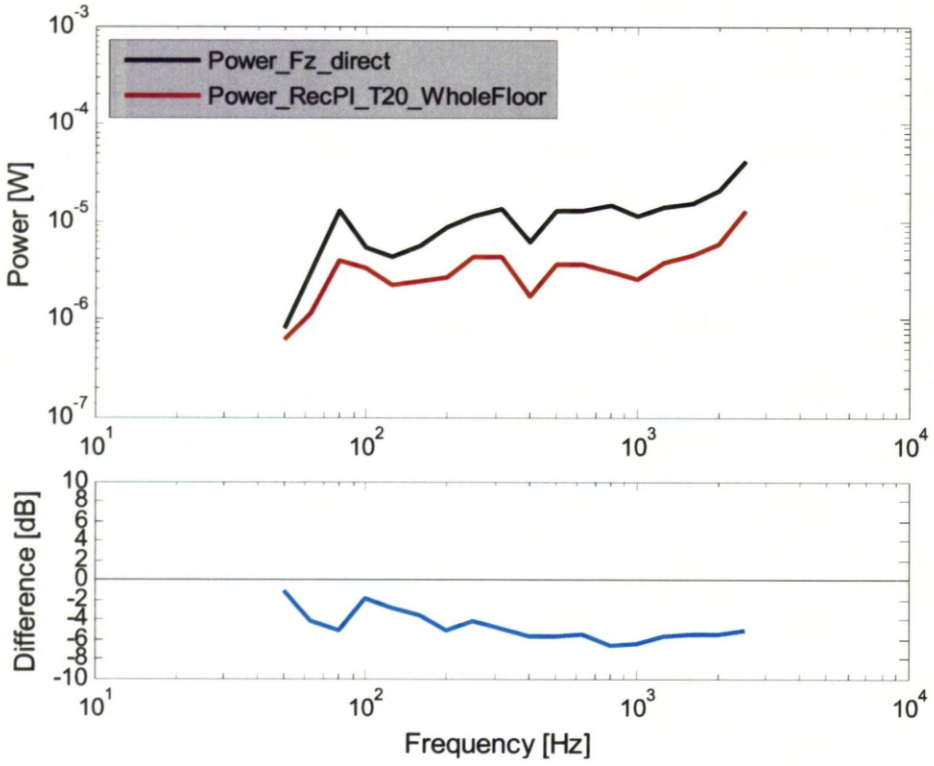

Figure 7.47: Direct power and from reception plate method using T_{20} – reference floor – whole floor

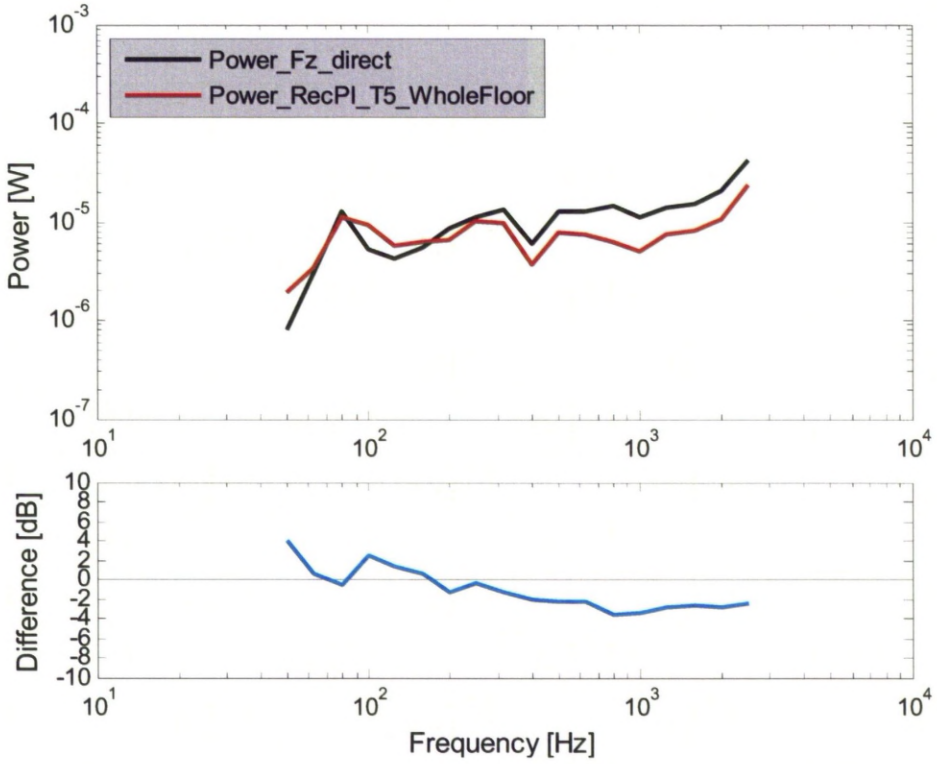

Figure 7.48: Direct power and from reception plate method using T_5 – reference floor – whole floor

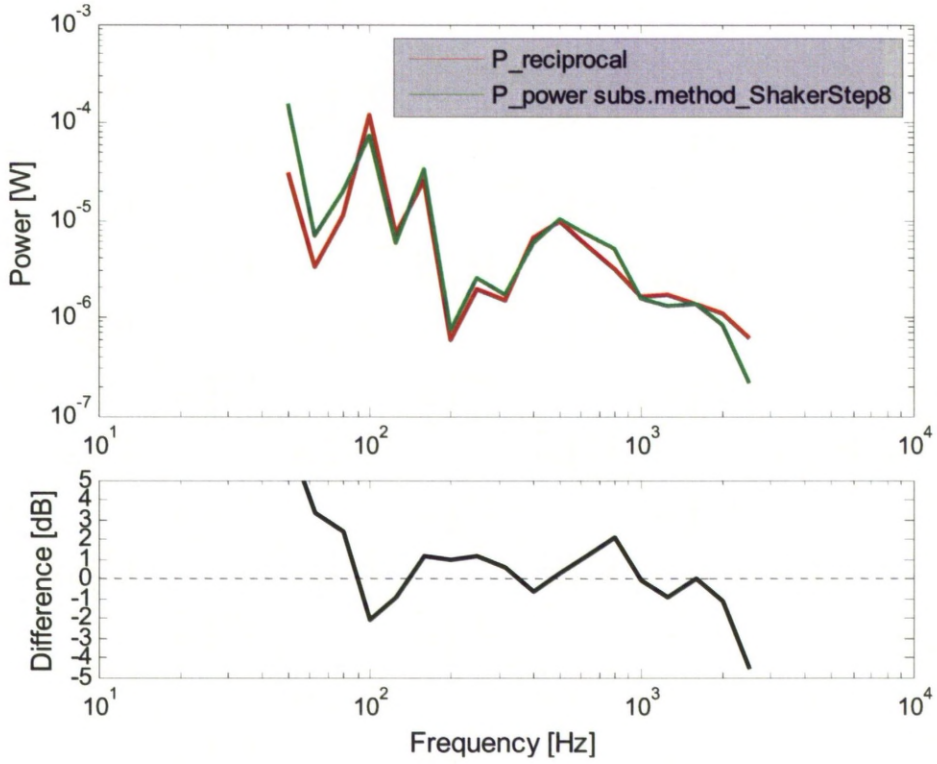

Figure 7.49: Reciprocal power and from substitution method - stair wall – stair excited with shaker on step 8

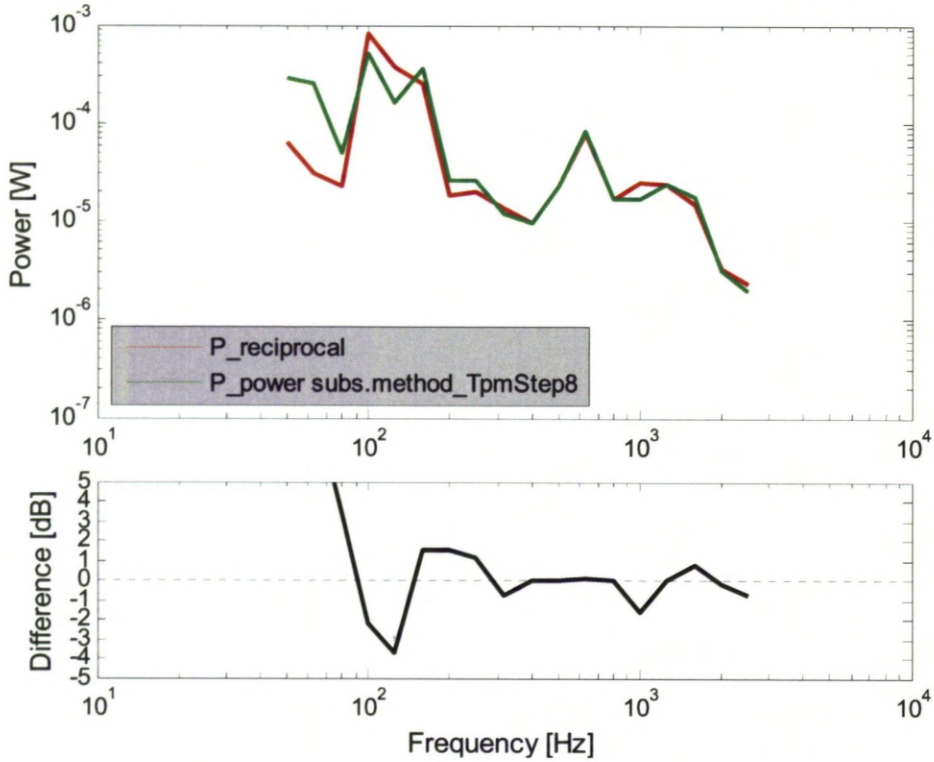

Figure 7.50: Reciprocal power and from substitution method - stair wall – stair excited with tapping machine on step 8

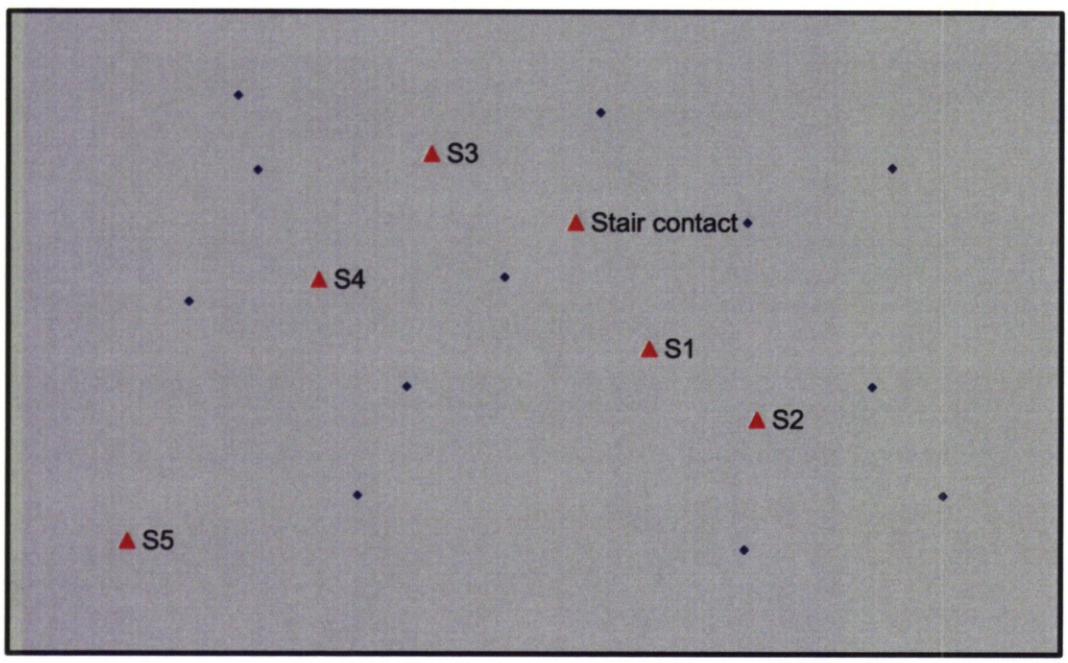

Figure 7.51: Shaker excitation and accelerometer positions

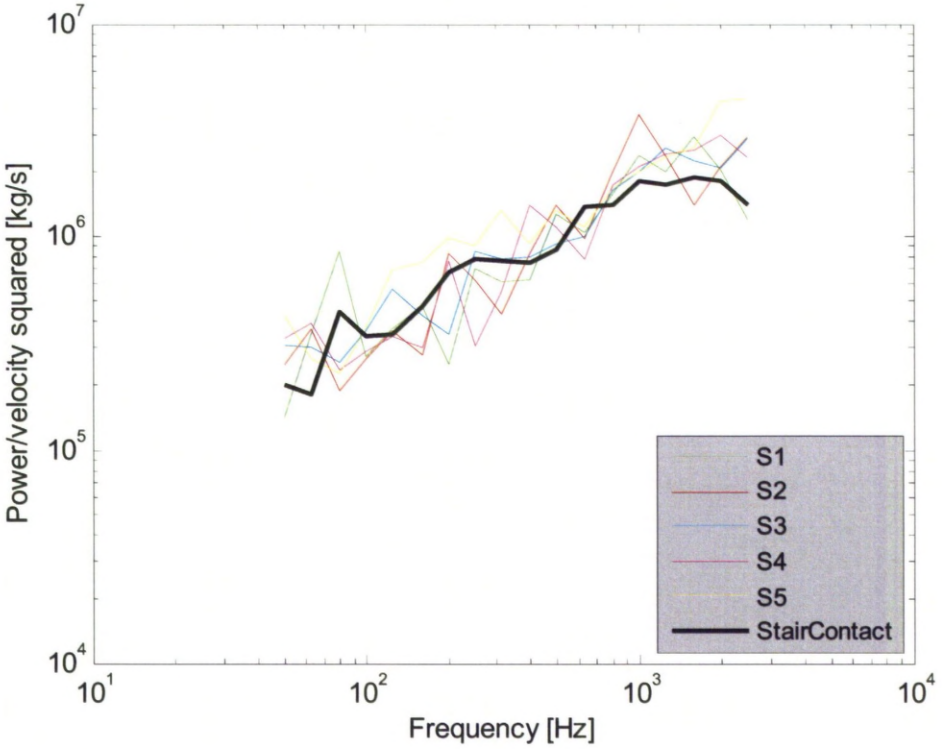

Figure 7.52: Power-velocity ratios for excitation at different wall locations

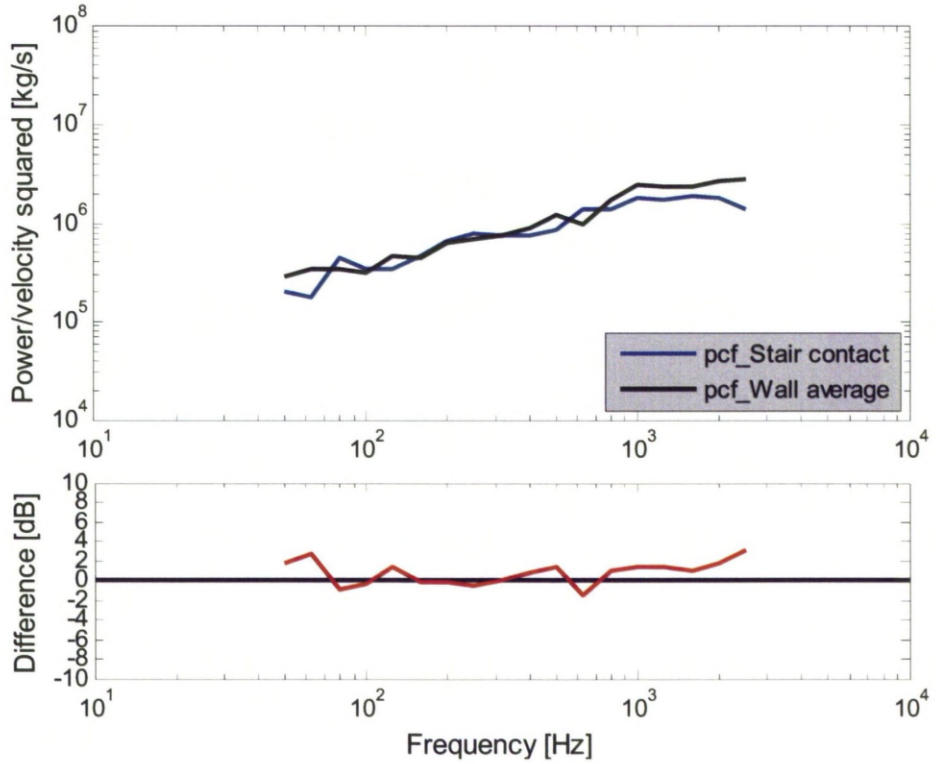

Figure 7.53: Power-velocity ratio for excitation at the stair contact

8 PREDICTION OF SOUND PRESSURE LEVELS IN BUILDINGS

8.1 INTRODUCTION

Methods for the prediction of sound pressure levels from impacted stairs in buildings are investigated. Existing building propagation models such as EN 12354 [1], [2] and a modal approach [3] are used that require different source quantities as input. It is shown how laboratory data as obtained from the previous investigations can be transformed for such predictions. By comparison of predicted and measured impact sound pressure levels, the achievable accuracy is assessed and sources of uncertainty are highlighted.

8.2 TRANSFORMATION OF LABORATORY DATA

In the previous sections, it has been shown how characteristic source quantities can be obtained from measurements. In order to serve as input data for prediction, the data has to be transformed. Only the force component, perpendicular to the receiving surface, is considered, as this has been identified as the dominant component. The aim of the following sections is to show how the characteristic source quantities can be used to predict sound pressure levels in buildings. The building propagation model EN 12354 is described in sufficient detail for this discussion. For full details, refer to [1], [2], [4].

8.2.1 Blocked force - EN 12354-2

EN 12354-2 [1] was developed to predict impact sound transmission through floors by a standard source. It can equally be used for prediction of the horizontal transmission through walls, although the conventional falling-hammer impact source cannot be applied to vertical surfaces. Here, it is applied to the resultant sound pressure level due to horizontal transmission due to the blocked force generated by a stair system, which is excited by a standard impact source. The predicted normalised level is given by:

$$L_n = L_F + 10\lg\frac{\mathrm{Re}\{Y\}}{m'} + 10\lg T_s + 10\lg\sigma + 10,6dB \qquad (8.1)$$

L_F is the force level at the contact between the stair and the supporting wall. It is treated in the same way as for a tapping machine used for evaluation of the normalized impact sound pressure level.

The contact force can be determined in-situ from reciprocal measurements (Chapter 4 and 5). Alternatively, the contact force can be evaluated from the (reception) plate power and mobility [5]:

$$\tilde{F}^2 = \frac{P}{\mathrm{Re}\{Y_R\}} \qquad (8.2)$$

It has been shown that the contact force approximates the blocked force, as the stair constitutes a high-mobility source. It has also been demonstrated that the blocked force also can be obtained from source free velocity and mobility (Chapter 6).

Prior to measurement of the sound pressure due to the installed stair, the airborne sound reduction index was measured (Chapter 3.2). In Figure 8.1 is shown the predicted [4] and measured sound reduction index. For the total loss factor, the first 5 dB of the reverberant decay (T_5) was used. The agreement is within 2 dB between 250 Hz and 2.5 kHz. The discrepancy below 250 Hz is expected due to room and wall modal behaviour and also the difficulty in predicting the radiation efficiency below the critical frequency, which is at 108 Hz. The measured value is consistently higher than predicted.

In order to apply the prediction method for the impact sound pressure level, the blocked forces obtained from source free velocity and mobility and from the reception plate power (8.2) were used. In Figure 8.2 is shown the predicted normalized sound pressure level for excitation of step 8, in comparison with measurement. There is agreement in the mid frequency range from 125 Hz – 800 Hz. At higher frequencies, the prediction underestimates the sound pressure level. This is associated with an underestimation in the predicted mobility of the wall (Chapter 7.3.1).

At low frequencies, the prediction overestimates the sound transmission, due to an overestimation of the radiation efficiency, also observed for the airborne sound transmission. With the in-situ measured stair force from (8.2) as input (predicted 2 in legend of Figure 8.2) a better agreement is observed. Also shown are the single rated values, which are relevant to impact sound insulation.

A maximum and minimum mobility according to Moorhouse [6] was incorporated to account for spatial and spectral variation of the point

mobility. In Figure 8.3 are shown the characteristic mobility of the stair wall along with maximum- and minimum mobility, compared to measured point mobility. The measured value lies between these limits for the frequency range up to 1 kHz. At higher frequencies the measurement is higher due to the local stiffness effect.

For the prediction of the normalized impact sound pressure level, the narrow band maximum and minimum mobilities were converted in 3rd octave bands (Figure 8.4).

In Figure 8.5 are shown the maximum and minimum values for the normalised impact sound pressure level using the stair force from (8.2) along with the prediction by use of the characteristic mobility and maximum and minimum mobility. The range of the normalised impact sound pressure level is of the order of 15 dB at low frequencies and 5 dB at high frequencies, with respect to the location of the stair/wall contact.

8.2.2 Characteristic reception plate power - EN 12354-5

The installed power is the input quantity for the prediction of the sound propagation in buildings according to EN 12354-5 [2]. The installed power is obtainable from the characteristic reception plate power of the source and the actual receiver mobility. For a high mobility point source, with a dominant force component perpendicular to the plate, the transmitted power is directly related to the input mobility of the reception plate at the contact:

$$P_{\text{rec.}} = \frac{1}{2}|F|^2 \,\text{Re}\{Y_{\text{rec.}}\} \tag{8.3}$$

In order to correct the reception plate power for multi-point sources and for the properties of the finite reception plate, in particular its modal behaviour, the infinite or characteristic reception plate power is proposed [7], given by,

$$P_{\text{infinite}} = P_{\text{rec.}} \cdot \frac{Y_{\text{infinite}}}{\text{Re}\{\overline{Y}_{\text{rec.}}\}} \tag{8.4}$$

Here $\overline{Y}_{\text{rec.}}$ is the spatial average of the point mobility for forces perpendicular to the reception plate. This correction is a simplification, as for multi-point sources the interaction between the contacts is not considered.

The term $P_{\text{rec.}}$ is the installed power in the laboratory. It has been shown in Chapter 7.3 how $P_{\text{rec.}}$ can be determined when non isolated receiver plates are used.

The characteristic reception plate power is transformed into the installed power when the source is in a building:

$$P_{\text{inst.}} = P_{\text{infinite}} \cdot \frac{\text{Re}\{\overline{Y}_{\text{build.}}\}}{\text{Re}\{\overline{Y}_{\text{infinite}}\}} \tag{8.5}$$

$\overline{Y}_{\text{build.}}$ is the spatial average of the point mobility of the building element in contact with the source. Again, the simplest estimate for the receiver mobility is the infinite plate mobility.

The reception plate power of the stair excited by the tapping machine is shown in Figure 8.6 along with the infinite plate power. The difference corresponds to that between measured and characteristic mobility (Figure 7.21).

The normalized sound pressure level in a building situation is calculated from:

$$L_{n,s,ij} = L_{Ws,inst,i} - D_{s,a,i} - R_{ij,ref} - 10\lg\frac{S_i}{S_{ref}} - 10\lg\frac{A_{ref}}{4} \qquad (8.6)$$

For the case considered the installed power can be obtained from:

$$L_{Ws,inst,i} = L_{F,stair} + 10\lg \mathrm{Re}\{Y_{infinite}\} \qquad (8.7)$$

As Part 5 and Part 2 of EN 12354 are based on the same underlying theory, this yields the same result as the prediction according to Part 2 (8.1). As discussed earlier, the advantage of using Part 5 is that airborne radiation of sources in the sending room and transmission into a receiver room also can be considered.

Part 5 recently has been used to predict the sound pressure levels in a building from wall mounted heating devices, previously measured in the laboratory by use of the reception plate method [8]. Measured and calculated sound pressure levels showed good agreement, but the predicted values tended to overestimate the measurement.

8.3 PREDICTION USING A DETERMINISTIC MODEL

Reference to Figure 8.2 indicates that, at low frequencies, the modal behaviour of structures and rooms must be considered. The assumption of diffuse sound fields in SEA based prediction, such as EN12354, does not apply to the behaviour of floors/walls and rooms at low frequencies.

An analytical approach has been implemented, based on a model for impact sound transmission of floors [3]. The model includes the effects of location of the impact, type of floor, edge conditions, floor and room dimensions, position of the receiver and room absorption. The approach is based on a natural mode analysis of the vibration field of a floor, the pressure field of a rectangular room beneath the floor and the coupling between the two fields.

The sound field model enables prediction of room transfer functions for arbitrary source and receiver locations in the same room. The vibration field model is used to predict transfer mobility (floor velocity at one location to the vibration response at another location on the floor). The coupling model enables prediction of the sound pressure level at an arbitrary room position caused by a point force excitation at an arbitrary floor position. Flanking transmission e.g. through inner walls in the receiving room is not considered.

In the first stage of the analysis, the natural frequencies of the systems plate and room are calculated by solving the eigenvalue problem using the homogeneous wave equation. The sound radiation into a room is then calculated from normal mode analysis as proposed by Kihlman [9].

Here, the model is used to predict the sound pressure in an adjacent room, caused by vibrating lightweight stairs. Therefore, the horizontal sound transmission through the separating brick wall into the receiver room was investigated.

8.3.1 Transmission in the staircase test facility

The situation in the staircase test facility, as illustrated in Figure 8.8, is more complicated than that for laboratory validation of the prediction model in [3]. The room geometry is not well defined as there is a wooden ceiling and there were linings at the side walls. In addition, the surfaces of the door and the wall were not in alignment with the rest of the room enclosing surface. The wall and room height are not identical. This is because the wall is built inside a concrete frame. The radiating surface is obviously the part of the wall inside the frame. However the coupling model cannot account for this. In the model the wall and room height are assumed identical. Moreover, the boundaries were expected to exhibit varying surface impedance and thus absorption. Such variations could not be incorporated into the prediction of the sound field in the receiver room.

The dimensions of the receiver room (SR/ER-0 in Figure 8.8) were set to x / y / z = 5,60 / 4,30 / 2,88. The x-coordinate, the room length, was set equal to the distance between the separating walls e.g. the stair wall and the opposite wall. The y-coordinate, the room width, was set equal to the distance between the surfaces of the side walls given by the structural linings. The z-coordinate, the room height, was set equal to the distance

between the concrete floor and the bottom side of the wooden ceiling, neglecting the wooden beams.

For the experimental validation of the model, the room modes were first obtained from visual inspection of the measured transfer function, using a loudspeaker positioned in a lower corner and a microphone in the diagonally opposite upper corner, at 10 cm distance from room surfaces. The transfer function was determined as the ratio of sound pressure to the voltage to the amplifier (generator output). The result is shown in Figure 8.9. The magnitude of the transfer function increases with frequency due to non-linear behaviour of the loudspeaker below 100 Hz. The peaks correspond to the room modes. The first four observed eigenfrequencies correspond to the calculated values. The calculated and measured eigenfrequencies for the first axial room modes are shown in Table 8.1.

Room mode	1/0/0	0/1/0	0/0/1
Calculated [Hz]	31	40	60
Measured [Hz]	32,5	40	60

Table 8.1: First three axial room modes

Results indicate that the setting of the room dimensions is correct and therefore can be applied to the coupling model.

8.3.2 Coupled wall/room system

It was shown that the sound field in the room can be accurately modelled with the room dimensions x / y / z = 5,60 / 4,30 / 2,88. However, the room height does not correspond to the radiating wall surface inside the concrete

frame; the real wall height is z = 2.35 m. It was decided to set the z-dimension equal to the room height because, as reported in [3], [10], [12], the sound field in the room is mainly controlled by the room modal characteristics.

Regarding the modal behaviour of the wall, it has been concluded by others, e.g. [10], that the pinned (or simply supported) boundary condition is generally the best approximation at low frequencies

The room absorption was obtained from standard measurement of reverberation time [11]. In Figure 8.10 is shown the measured reverberation time and a regression curve as used for the narrow band calculations. The pressure to force p/F transfer function was measured in the same arrangement as described in (Chapter 7.3.2). Microphone positions in a corner, and at the room centre, are shown in Figure 8.11.

In Figure 8.12 is shown the calculated and measured transfer function for excitation of the stair/wall contact and microphone position in the corner opposite to the wall. Figure 8.13 shows the comparison in 3rd octave bands.

There is agreement in the frequency range 70 Hz – 200 Hz, within 8 dB reference to a 20 log value. Below 70 Hz, there are large discrepancies, although the first three axial modes are indicated in both curves.

In Figure 8.14 and Figure 8.15 are shown the calculated and measured transfer function for the microphone position in the room centre. The first axial room mode 1/0/0 exhibits a node in the centre of the room and thus does not show a peak in the calculation. The first and second peak in the calculation at 47 Hz both result from coupling of the 1/1 structure mode to

the 2/0/0 room mode. The discrepancies between prediction and measurement are even higher than for the corner position.

8.3.3 Wall vibration field

The wall vibration field was considered in more detail by use of the vibration field model and comparison with measurements. The wall dimensions were restricted to the wall area inside the concrete frame as it is assumed that the frame and ceiling constitute the (non-moving) subsystem boundaries. Again, pinned boundaries were initially assumed. For the total loss factor, the regression for T_5 derived from measurement in 3rd octave bands (Chapter 7.3.5) was used.

In Figure 8.16 is shown the measured and calculated driving point mobility at the stair/wall contact in the frequency range 20 Hz to 200 Hz with the calculated eigenmodes indicated. The calculated modes (1/1, 2/1, 3/1) occur below 200 Hz. In contrast, the measurement exhibits many more peaks representing global modes [7]. The calculated fundamental wall mode (1/1) is at 63 Hz whereas the first significant peak in the measured curve occurs at about 33 Hz. There is no agreement in the frequencies of the resonance peaks, giving discrepancies of about 10-15 dB.

The assumption of pinned edges required further investigation. An experimental modal analysis, using the roving hammer method (Chapter 3.5), was performed. The wall grid consisted of 286 points with spacing of 20 cm. A reference accelerometer was positioned at the stair wall contact at coordinates x = 2.325 / y = 1.57.

In Figure 8.17 are shown the mode shapes at some distinct resonances representing local wall modes. By inspection, it is verified that the wall vibrates like a homogeneous plate despite being of a brick-mortar construction. However, the nodal lines are generally not straight or symmetrical. This implies that the four edge conditions may differ and are frequency dependent. Some edges are moving at particular frequencies, although the corners appear always to be at rest. This behaviour was not expected since the wall was assumed rigidly connected to the concrete frame via a butt joint.

This kind of joint is also encountered in buildings and was so far considered as a rigid connection similarly to a bonded joint. It could not be identified if the apparently not rigid connection is the result of the butt connection alone or if vibrations of the concrete frame at eigenfrequencies also have an effect.

Therefore, a free edge condition was incorporated into the calculation. The mode shapes of a free plate are well known [13] and are not shown. In Figure 8.18 is shown the measured and calculated point mobility at the stair/wall contact. With free edges, eight calculated modes occur below 200 Hz. The first three dominant modes (2/0, 3/0, 0/2) eigenfrequencies agree with measured values. Above 120 Hz, there is little or no correspondence.

In Figure 8.19 and Figure 8.20 are shown the measured and calculated point mobility in narrow bands and 3rd octave bands in the frequency range up to 3200 Hz along with the characteristic e.g. infinite plate mobility and the maximum and minimum mobility according to Moorhouse [6]. Below the fundamental wall mode the measured phase is $+\pi/2$, indicating spring

behaviour as expected for a structure with pinned edges. Nevertheless, from 20 Hz to 100 Hz, there is agreement with calculated values for the assumption of free edges. Comparison of the 3rd octave band values underlines the above statement. However, with this assumption, the predicted mobility is generally lower than the measured value. Likewise, the characteristic mobility is below the measured mobility. Above 500 Hz, the magnitude of the measured mobility increases with frequency and the phase converges to a value $\pi/2$, indicating spring-like behaviour. This is due to the local stiffness effect, discussed earlier.

8.3.4 Prediction of the stair impact sound transmission

For the coupled wall/room system, maximum sound transmission results where wall modes occur in the vicinity of room modes with a non-zero x-component. This is indicated by distinct peaks in the p/F transfer functions in Figure 8.12 and Figure 8.14.

As a result of setting the wall height equal to the room height in the coupling model, the wall eigenmodes occur at lower frequencies and thus partly compensate for the wrong setting of the wall's boundary condition. However the actual wall modes are still well below the predicted ones for the assumption of pinned boundaries as in the coupling model.

In the calculation the fundamental wall mode occurs at 47 Hz (with the wall height 2,88 m) which results in a stronger coupling with the 1/0/0 room mode than for the real wall height of 2,35 m with the fundamental wall mode occurring at 63 Hz. Nevertheless the measured transfer function is

underestimated by the calculation because the fundamental wall mode occurs at 33 Hz and is perfectly coupled to the 1/0/0 room mode occurring at the same frequency.

In contrast the calculation overestimates in the vicinity of the simulated wall eigenfrequency at 47 Hz, resulting in a strong coupling to the 1/1/0 room mode in the calculation.

The high deviations in narrow bands are significantly reduced when the values are presented in 3rd octave bands (Figure 8.13, Figure 8.15).

In order to compare the sound transmission from the stair with the prediction according to EN 12354 and measurement, an average sound pressure level in the room was predicted with the deterministic model and the stair force from (8.2) as input. Six arbitrary room positions were selected with respect to the measurement guidelines in ISO 140 [14].In Figure 8.21 are shown the sound pressures at six room positions and the average value. Also shown is the measured average sound pressure (Chapter 3.4).

Below 125 Hz there are variations of the (linear) sound pressures of one decade for the six room positions, which corresponds to a variation in level of 20 dB. Above 125 Hz, the sound field in the room is fairly diffuse and the effect of room location reduces significantly. In contrast, the wall vibration field is still strongly modal and errors in the prediction have a dominant effect on the resultant sound pressure level.

In Figure 8.22 is compared the predicted sound pressure level with the deterministic model and according to EN 12354. The deterministic model overestimates the sound pressure level by 10-15 dB at 50 Hz, 63 Hz and

163 Hz but is in good agreement from 80 Hz – 125 Hz, whereas the EN 12354 prediction constantly overestimates the measurement by 10 dB at 50 Hz reducing to 2 dB at 200 Hz.

8.4 SUMMARY

The sound pressure level from vibrating stairs can be predicted using EN 12354-2 with the in-situ force. If the high mobility source condition is retained in the building installation then the blocked force only is required. The blocked force can be obtained in the laboratory from the (reception) plate power and receiver mobility with good accuracy.

The sound pressure level from vibrating stairs can be predicted using EN 12354-5 with the in-situ plate power. Again, if the high mobility source condition is retained in the building installation then the characteristic plate power only is required.

Spatial and spectral variations of the receiver mobility can be incorporated using minimum and maximum mobility estimates. It is indicated that the range of the normalised impact sound pressure level can be up to 15 dB at low frequencies and 5 dB at high frequencies.

In EN 12354-5 airborne sound transmission can be considered, which is not relevant in the case considered, but could be relevant for stairs that are decoupled from the building elements.

Alternatively, a deterministic model can be used for the prediction at low frequencies that requires proper assumptions for modelling the sound field

in the room and the wall vibration field. For the case considered, a major difficulty was found in the modelling of the wall vibration field, mainly due to the boundary conditions that do not correspond to idealised conditions, such as pinned or free edges.

8.5 REFERENCES

[1] EN 12354-2: Building acoustics – Estimation of acoustic performance of buildings from the performance of elements – Part 2: Impact sound insulation between rooms, September 2000

[2] EN 12354-5: Building acoustics – Estimation of acoustic performance of buildings from the performance of elements – Part 5: Sounds levels due to the service equipment, October 2009

[3] Neves e Sousa, A.; Gibbs, B. M.: Low frequency impact sound transmission in dwellings through homogeneous concrete floors and floating floors, Applied Acoustics, Vol. 72, 177-189, 2011

[4] EN 12354-1: Building acoustics – Estimation of acoustic performance of buildings from the performance of elements – Part 1: Airborne sound insulation between rooms, September 2000

[5] Drechsler, A., Scheck, J., Fischer, H.-M.: Wie kann die Trittschallübertragung leichter Treppen prognostiziert werden? (How can the impact sound transmission from lightweight stairs be predicted?), Fortschritte der Akustik, DAGA 2007, Stuttgart, 2007

[6] Moorhouse, A. T., Gibbs, B. M.: Calculation of the Mean and Maximum Mobility for Concrete Floors. Journal of Applied Acoustics, Vol. 45, 227-245, 1995

[7] Späh, M. M.; Gibbs, B.M.: Reception plate method for characterisation of structure-borne sound sources in buildings:

Installed power and sound pressure from laboratory data, Applied Acoustics, Volume 70 (11-12), 1431-1439, 2009

[8] Ruff, A.; Mayr, A. R.; Fischer H.-M.: Predicition of the sound transmission of heating devices in buildings according EN 12354-5, Internoise 2010, Lisbon, Portugal, 2010

[9] Kihlman, T.: Sound radiation into a rectangular room. Applications to airborne sound transmission in buildings, Acustica, Vol. 18, 11–20, 1967

[10] Maluski, S.P.S., Gibbs, B.M.: Application of a finite-element model to low-frequency sound insulation in dwellings, Journal of the Acoustical Society of America, Vol. 108, 1741-1751, 2000

[11] EN ISO 3382-2: Acoustics - Measurement of room acoustic parameters - Part 2: Reverberation time in ordinary rooms, August 2008

[12] Goydke, H.: Guidance for the measurement of sound insulation of building elements in low frequency bands, Proceedings of the Internoise 1990, 175-178, Gothenburg, Sweden

[13] Leissa, A.W.: Vibration of plates, NASA SP-160, Ohio State University Columbus, 1969

[14] EN ISO 140-6: Measurement of sound insulation in buildings and of building elements – part 6: laboratory measurements of impact sound insulation of floors, December 1998

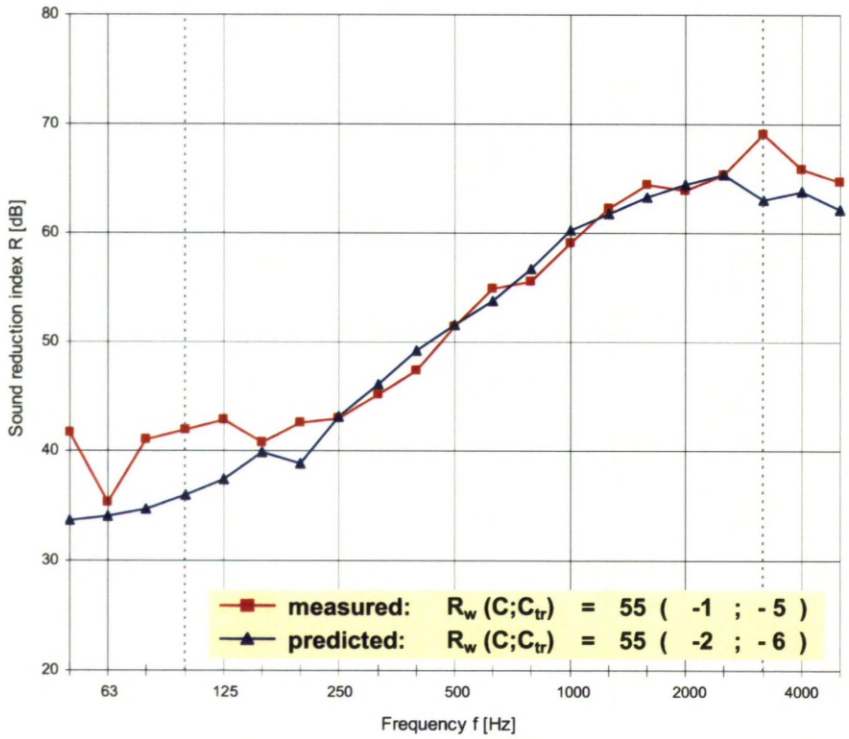

Figure 8.1: Sound reduction index of the stair wall, measured and predicted using EN 12354-1

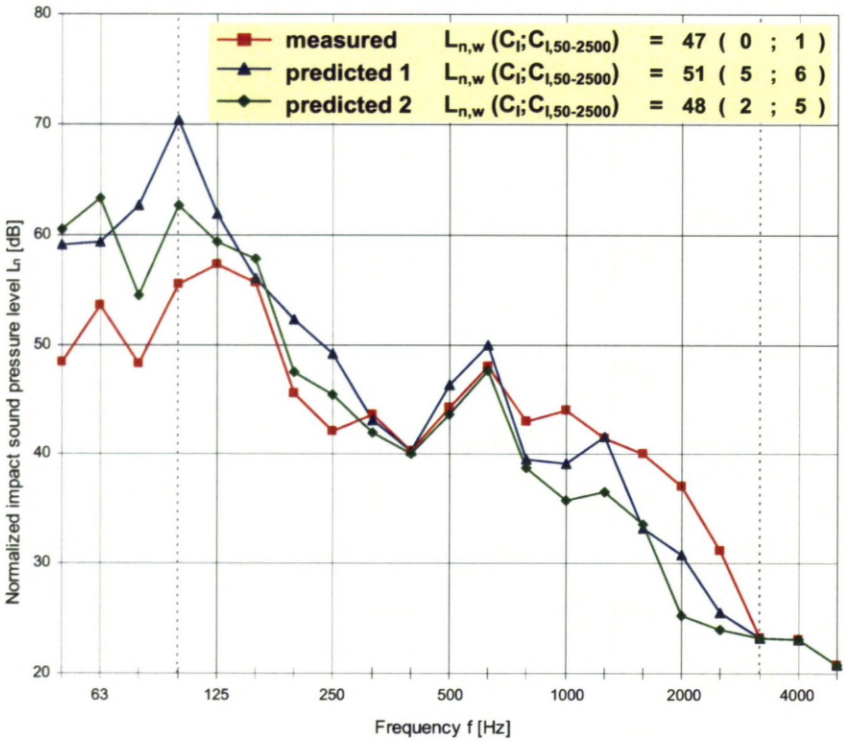

Figure 8.2: Normalised sound pressure level, measured and predicted with force from free velocity and mobility (1) and from reception plate method (2)

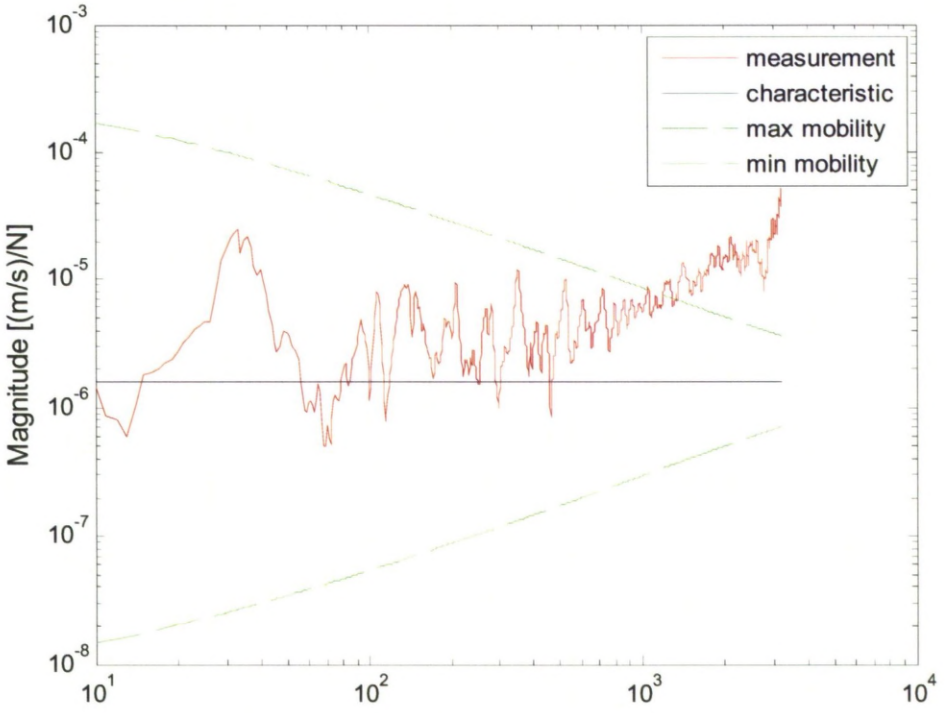

Figure 8.3: Characteristic mobility of stair wall along with maximum- and minimum mobility, compared with measured point mobility

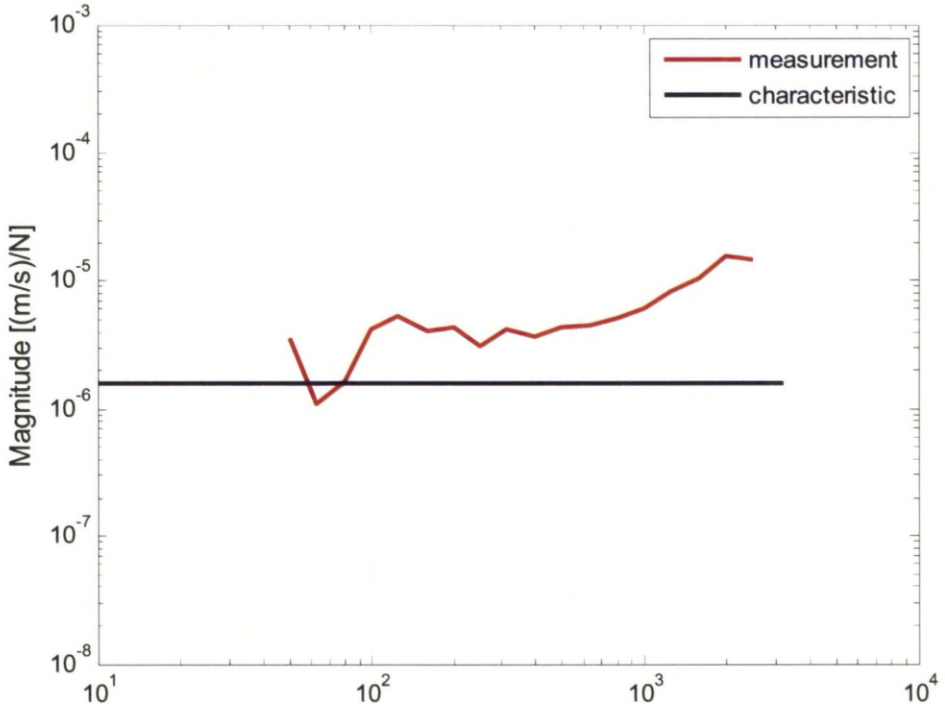

Figure 8.4: Characteristic mobility of stair wall along with max and min mobility, compared with measured point mobility – 3rd octave bands

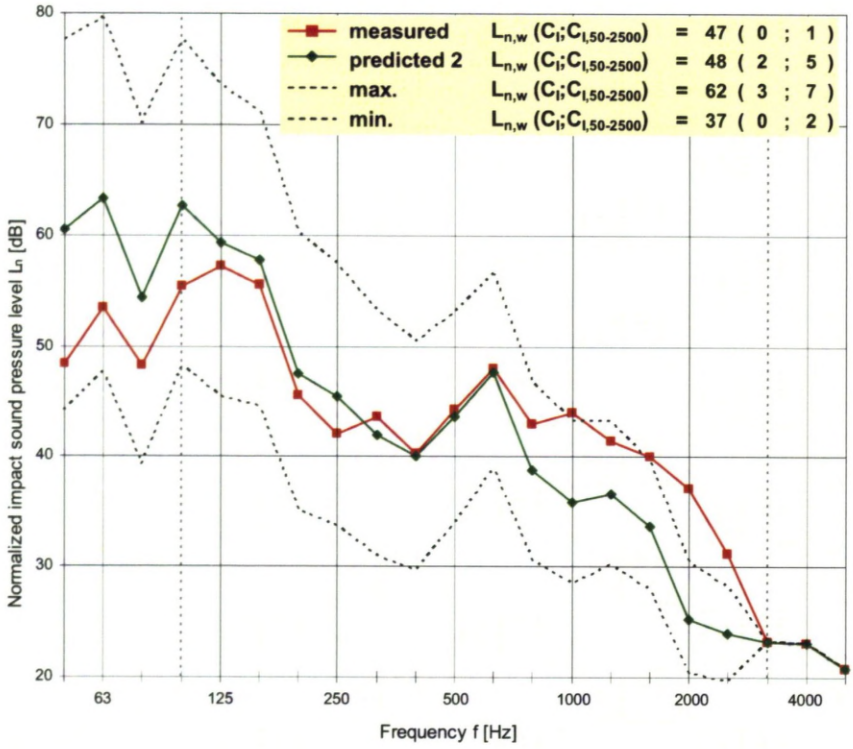

Figure 8.5: Normalised sound pressure level, measured and predicted with force from reception plate method and characteristic / maximum / minimum mobility

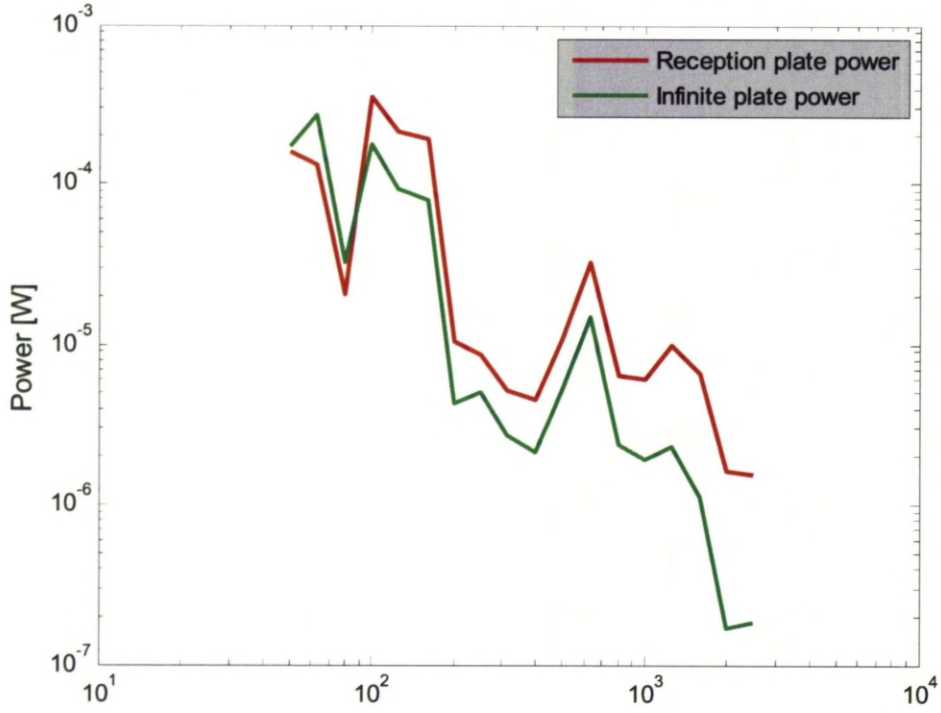

Figure 8.6: Reception plate power and infinite plate power of the stair (tapping machine on step 8)

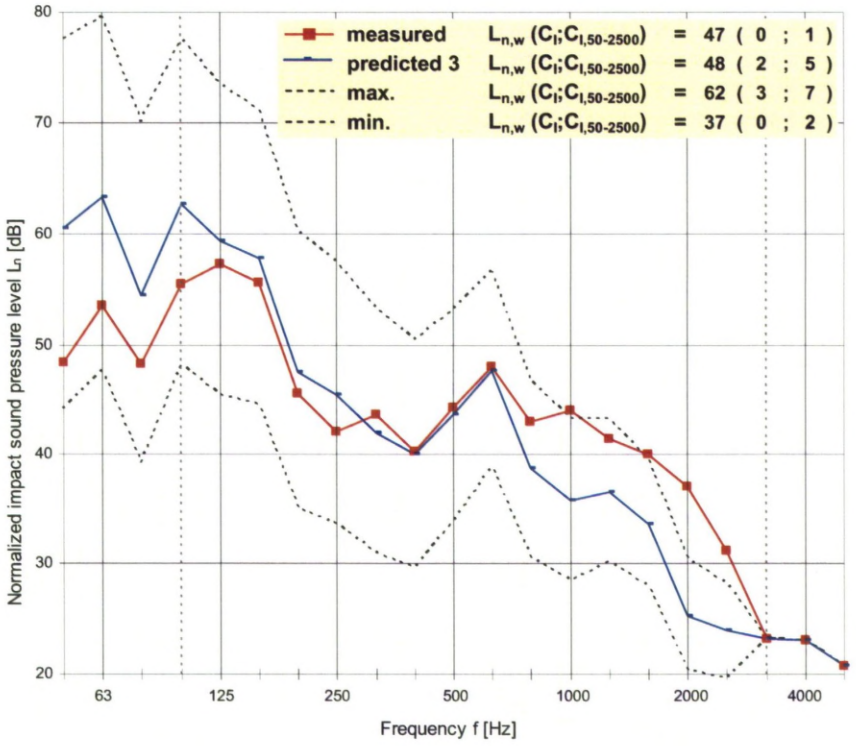

Figure 8.7: Normalised impact sound pressure level measured and predicted using EN 12354-5 and characteristic / maximum / minimum mobility

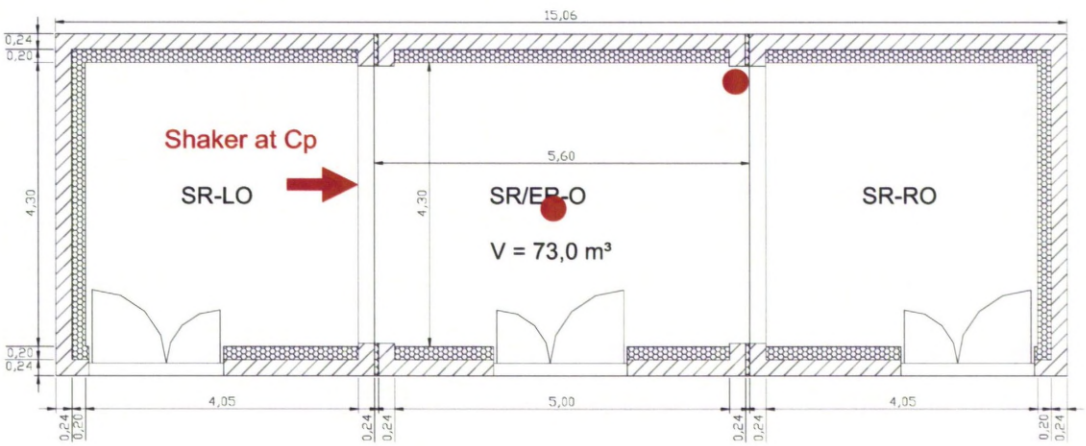

Figure 8.8: Staircase test facility with microphone positions in the room centre and in a corner

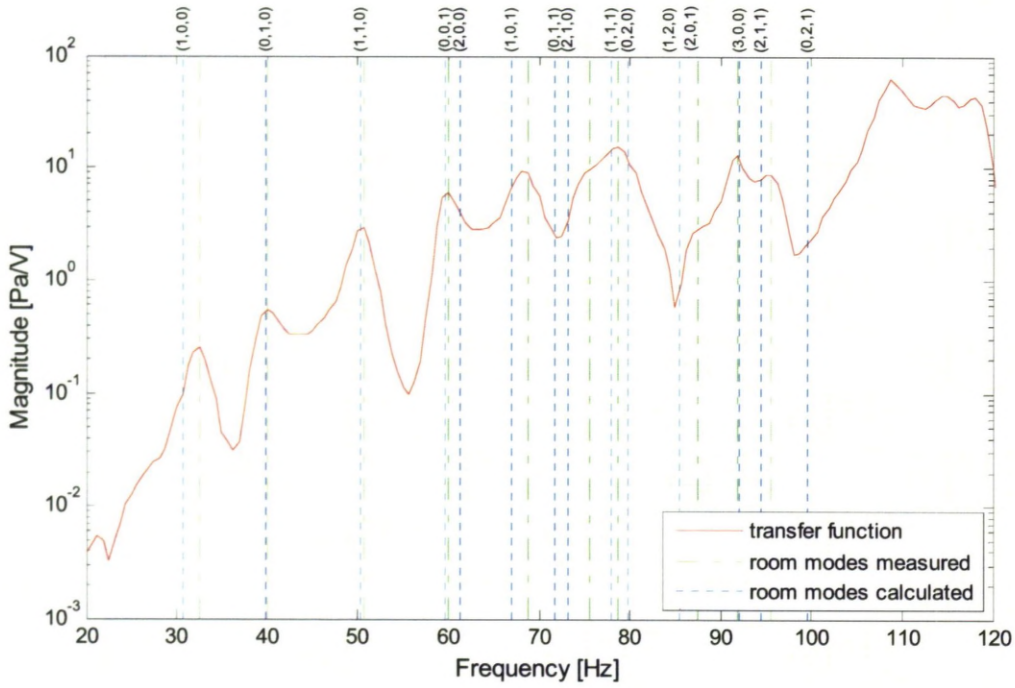

Figure 8.9: Measured room transfer function with calculated eigenfrequencies indicated.

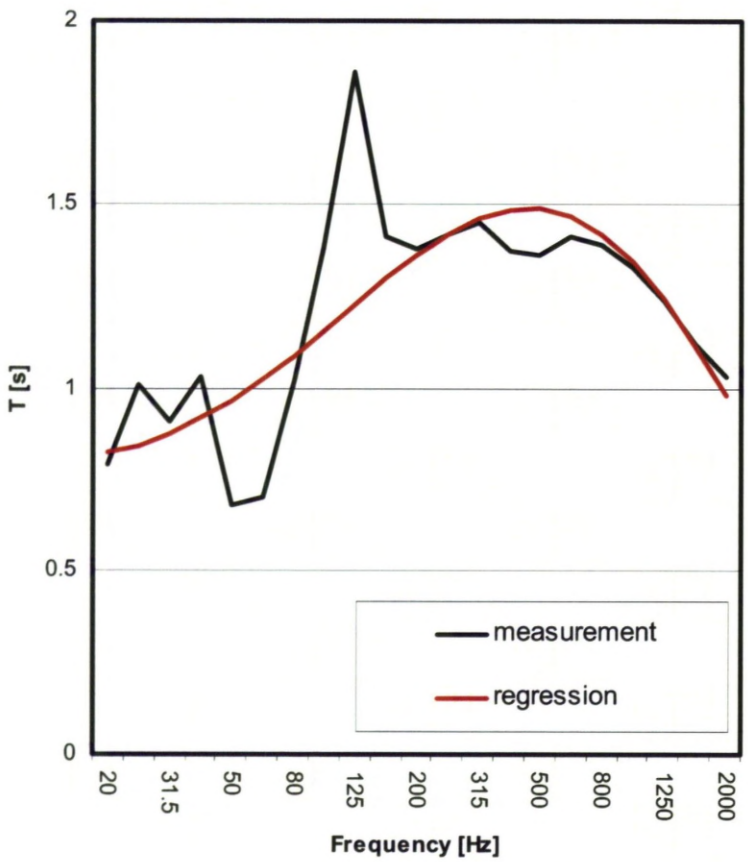

Figure 8.10: Measured reverberation time in receiver room and regression

Figure 8.11: Measurement of wall-room transfer function in the staircase test facility

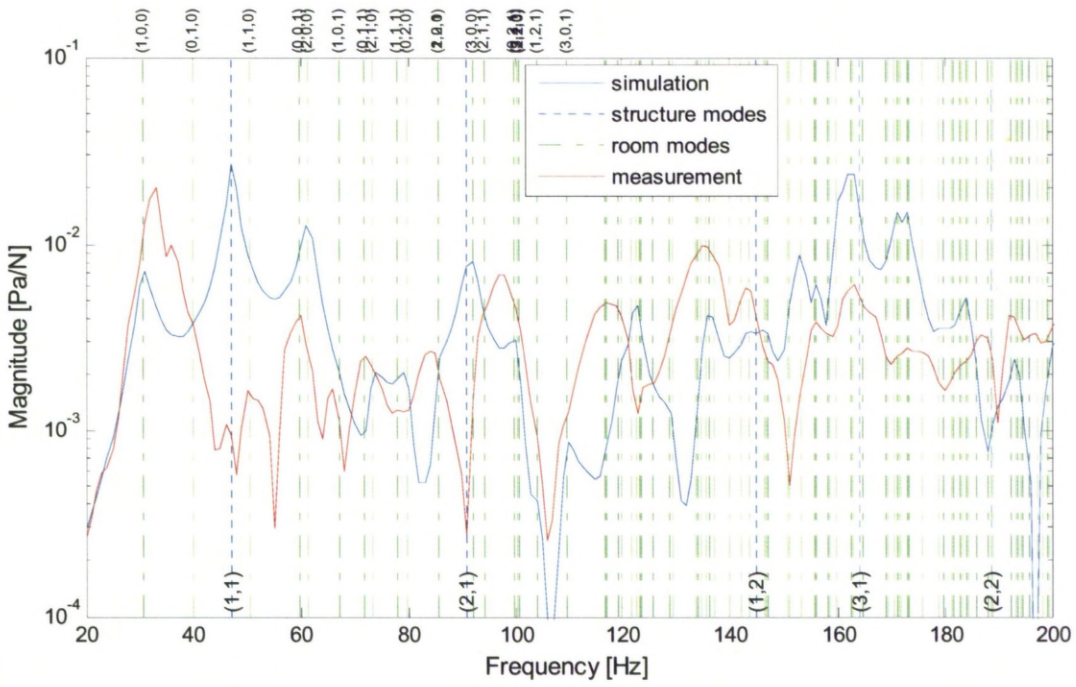

Figure 8.12: Calculated and measured p/F transfer function – corner

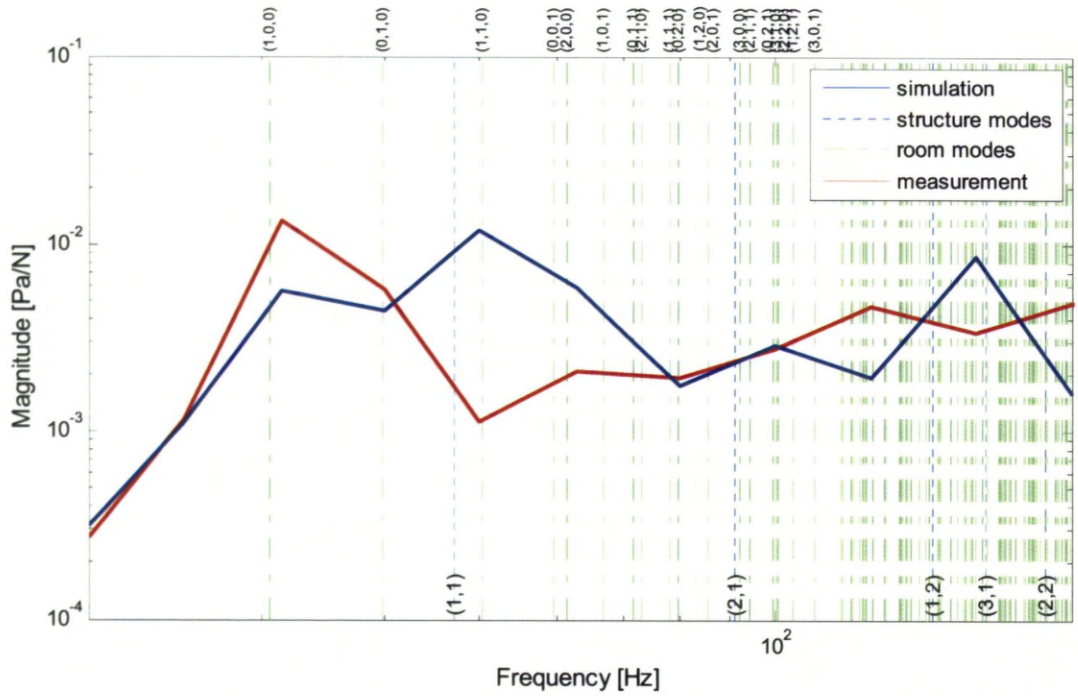

Figure 8.13: Calculated and measured p/F transfer function – corner - 3rd octaves

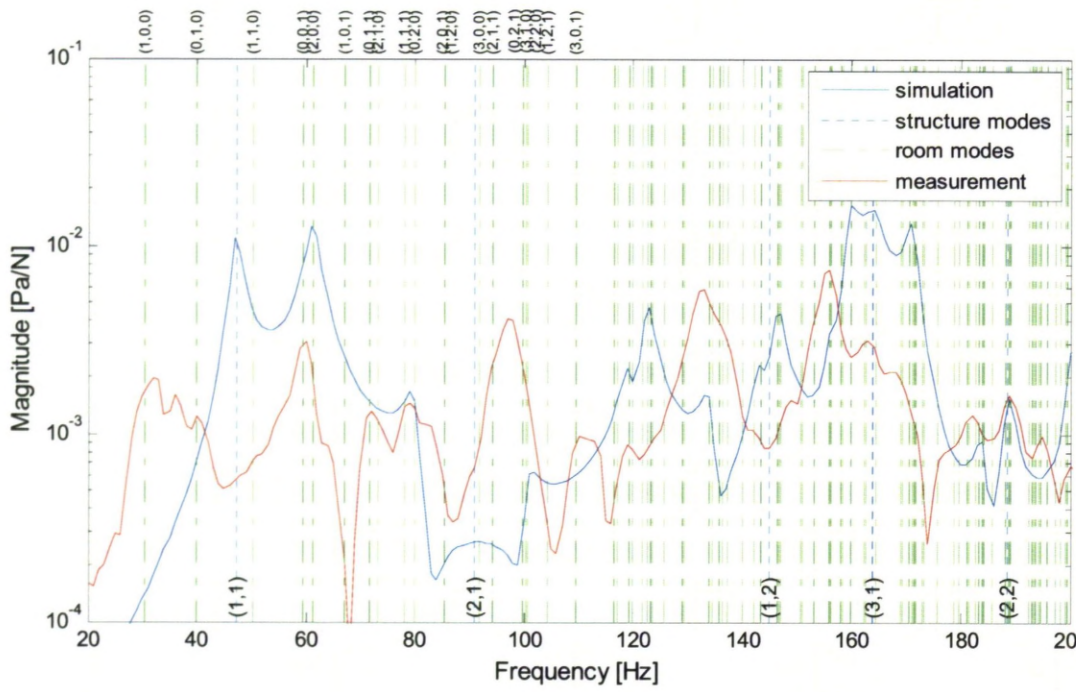

Figure 8.14: Calculated and measured p/F transfer function – centre

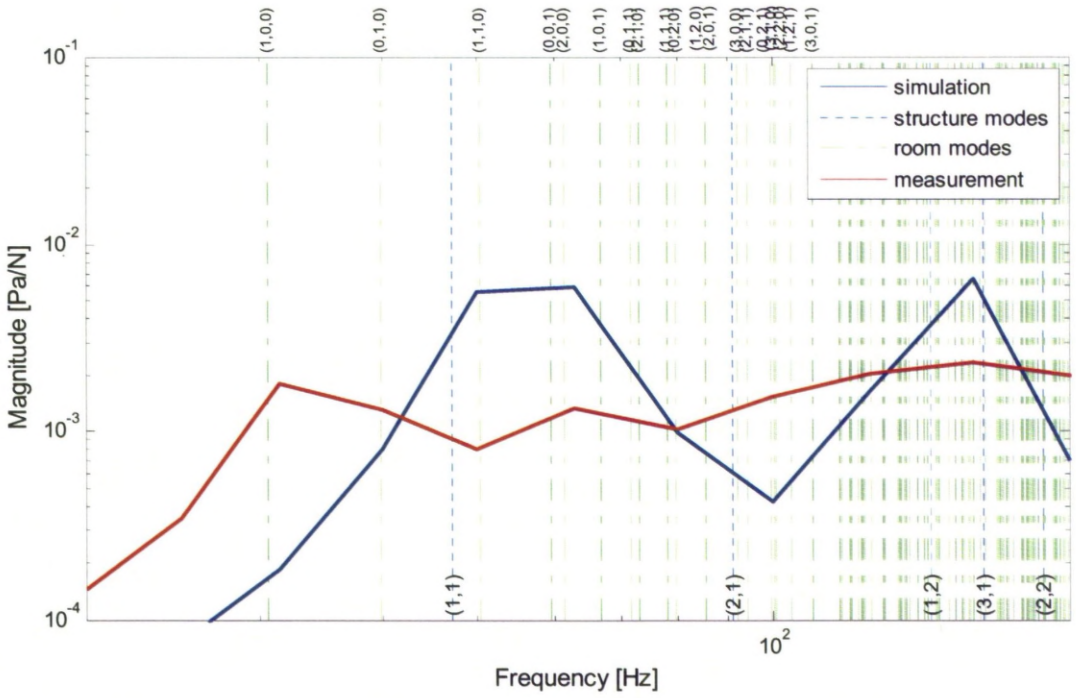

Figure 8.15: Calculated and measured p/F transfer function – centre - 3rd octaves.

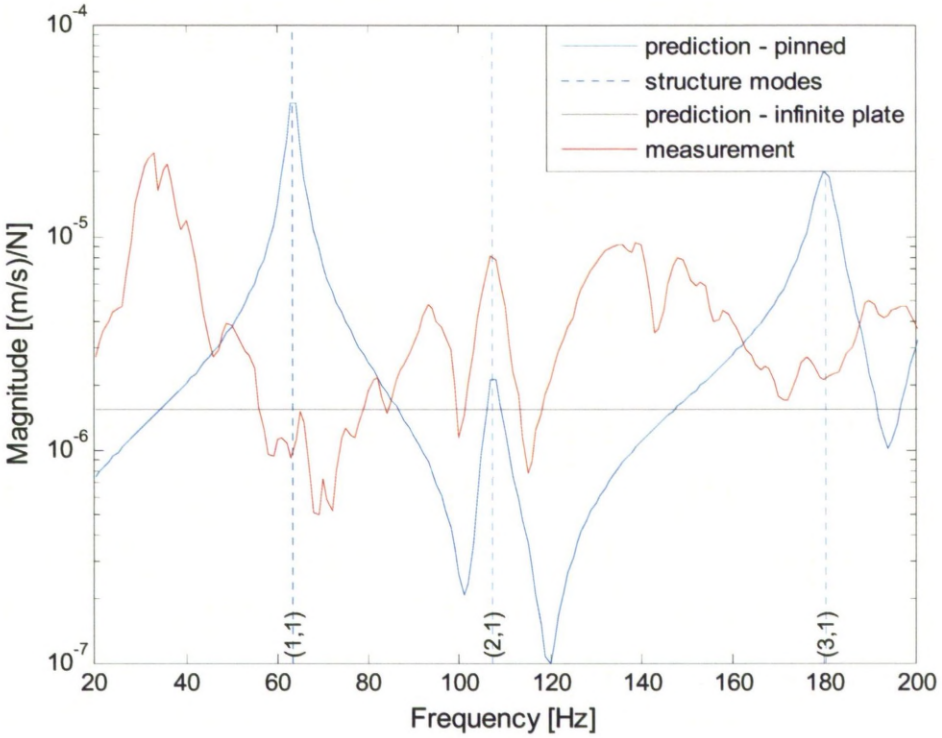

Figure 8.16: Measured and predicted point mobility at the stair/wall contact with structural modes indicated – edge condition: pinned

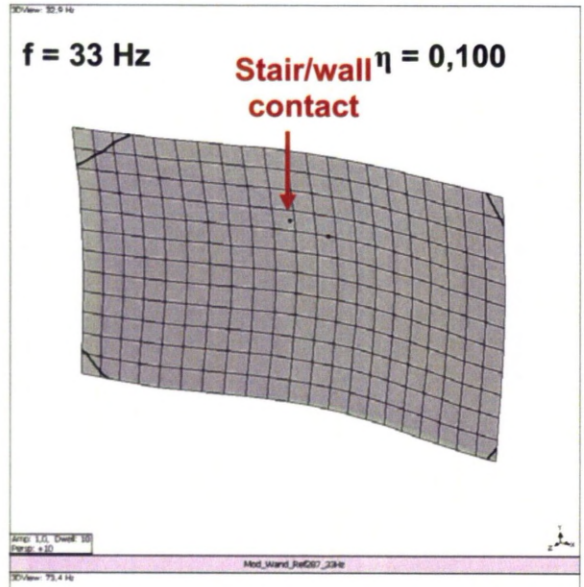
f = 33 Hz
Stair/wall contact
η = 0,100

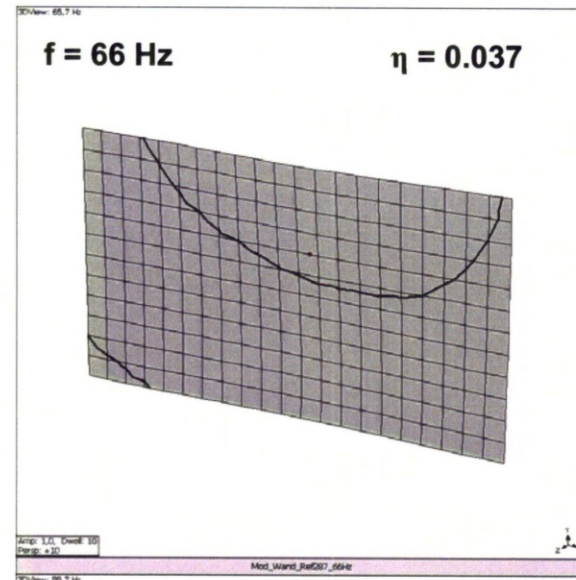
f = 66 Hz
η = 0.037

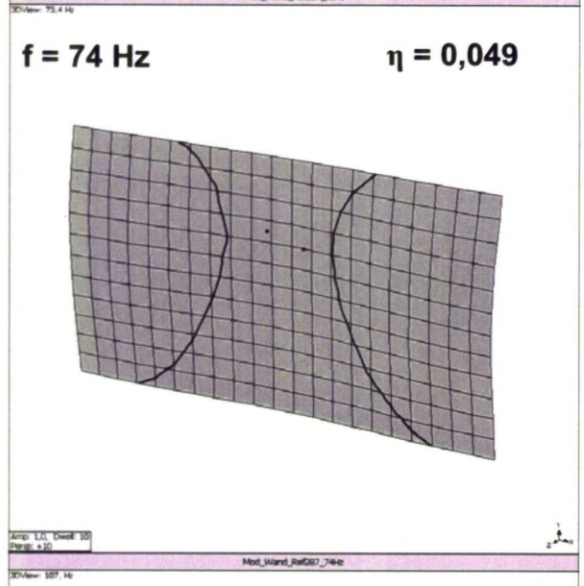
f = 74 Hz
η = 0,049

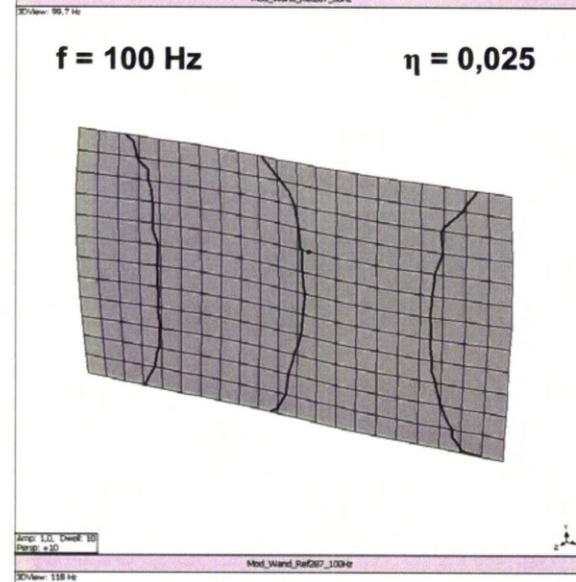
f = 100 Hz
η = 0,025

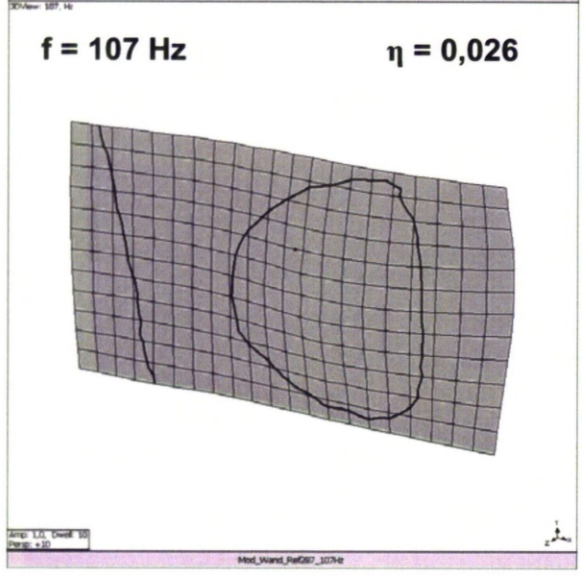
f = 107 Hz
η = 0,026

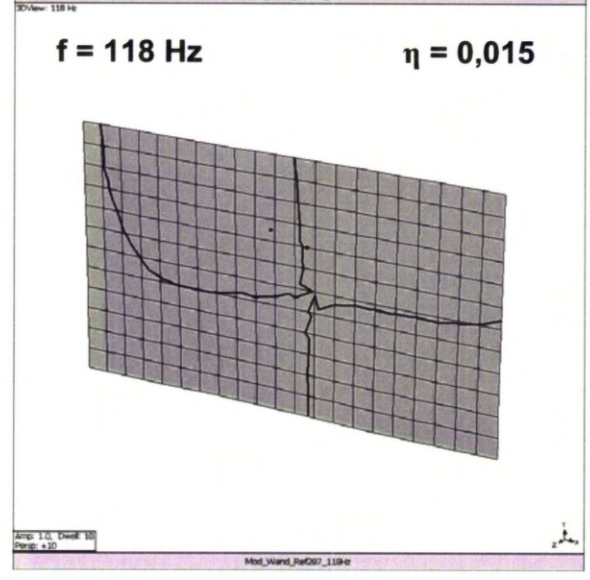
f = 118 Hz
η = 0,015

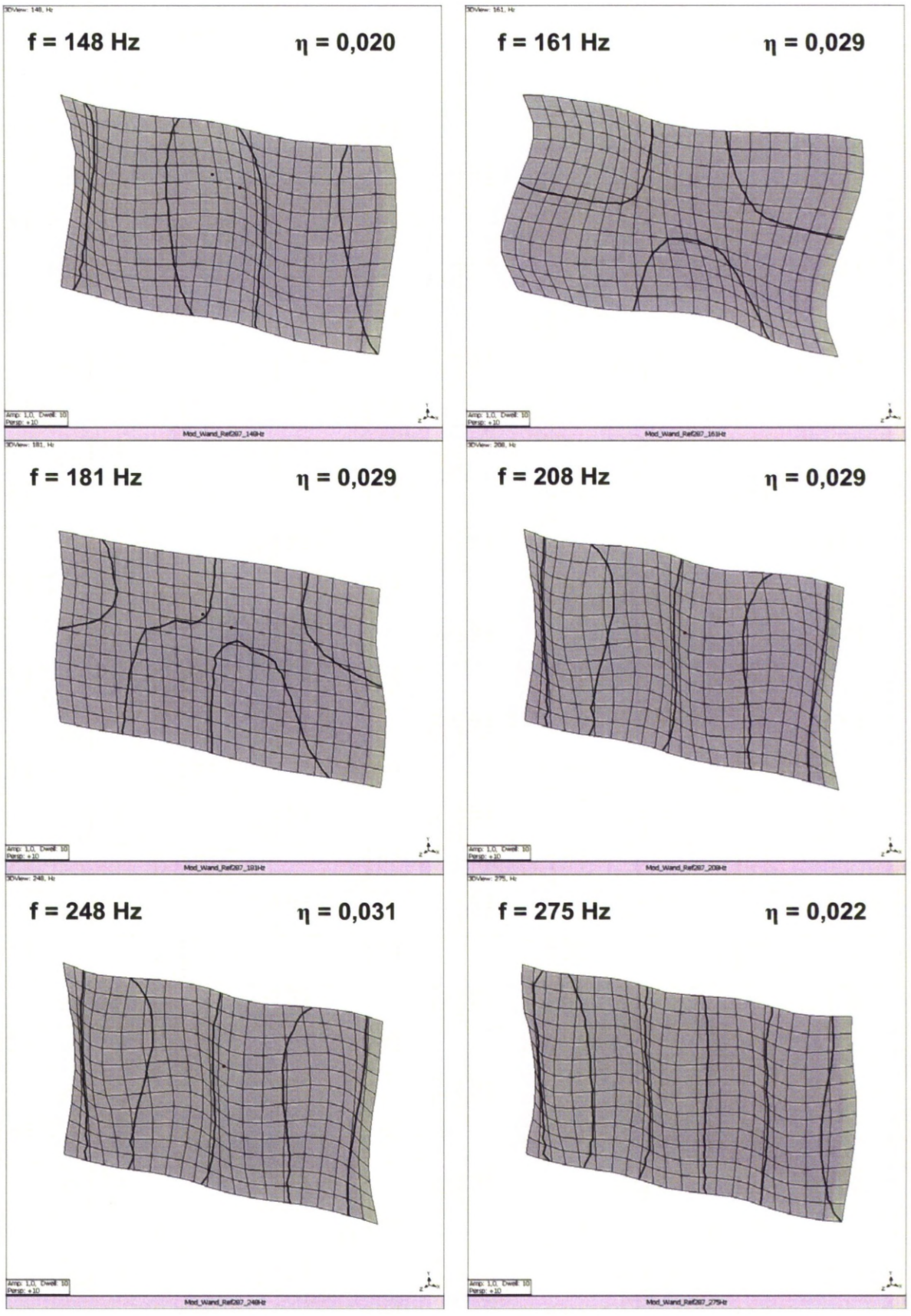

Figure 8.17: Mode shapes of stair wall from experimental modal analysis

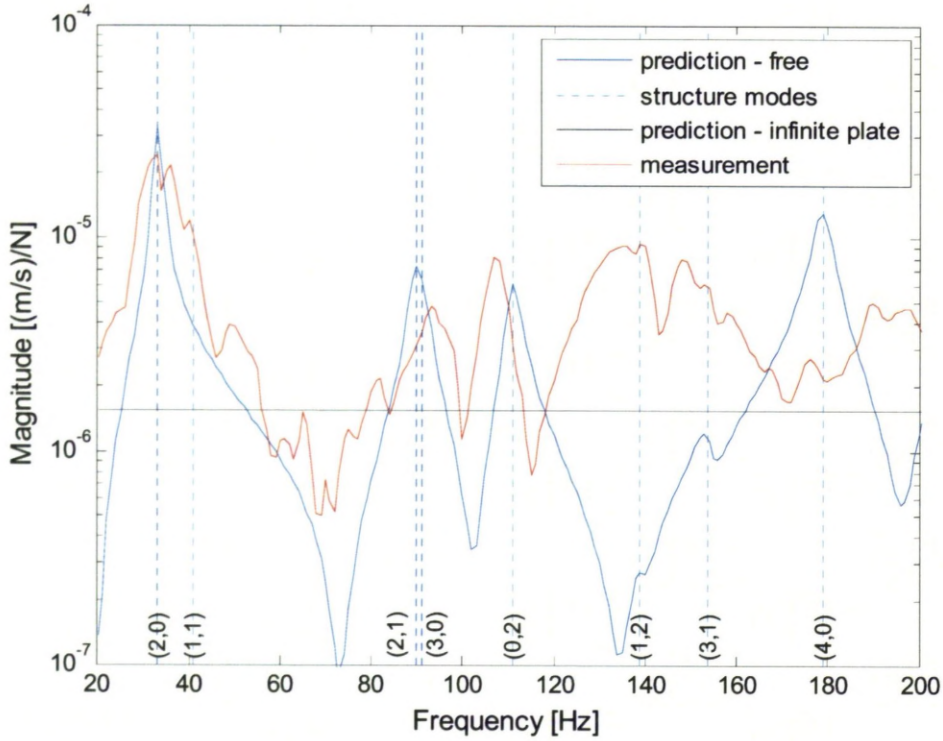

Figure 8.18: Measured and predicted point mobility at the stair/wall contact with structural modes indicated – edge condition: free

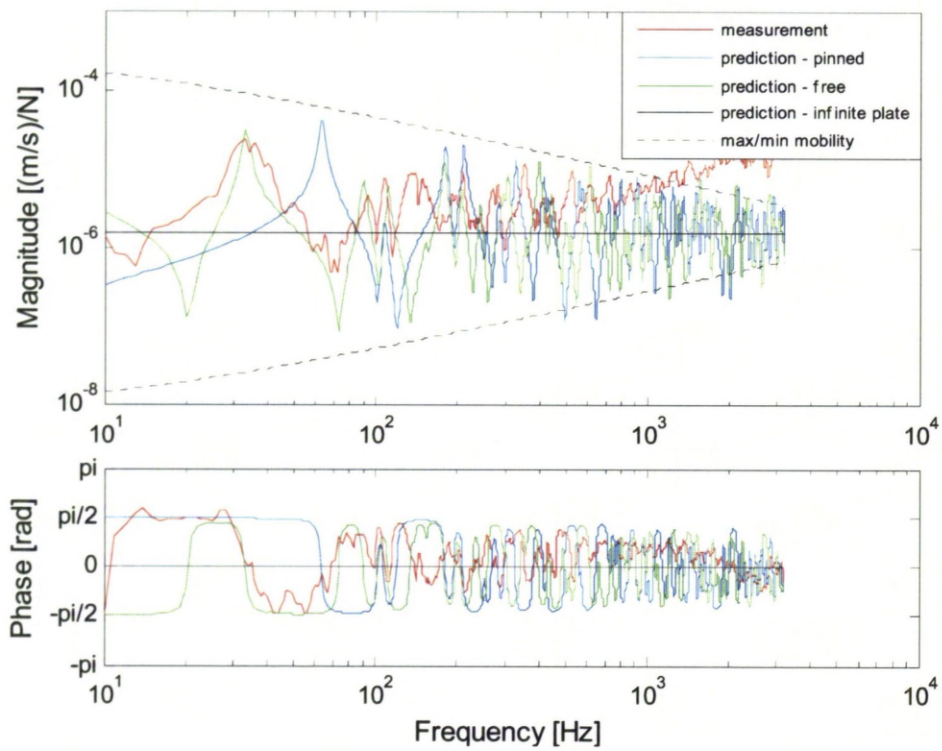

Figure 8.19: Measured and predicted point mobility at the stair/wall contact

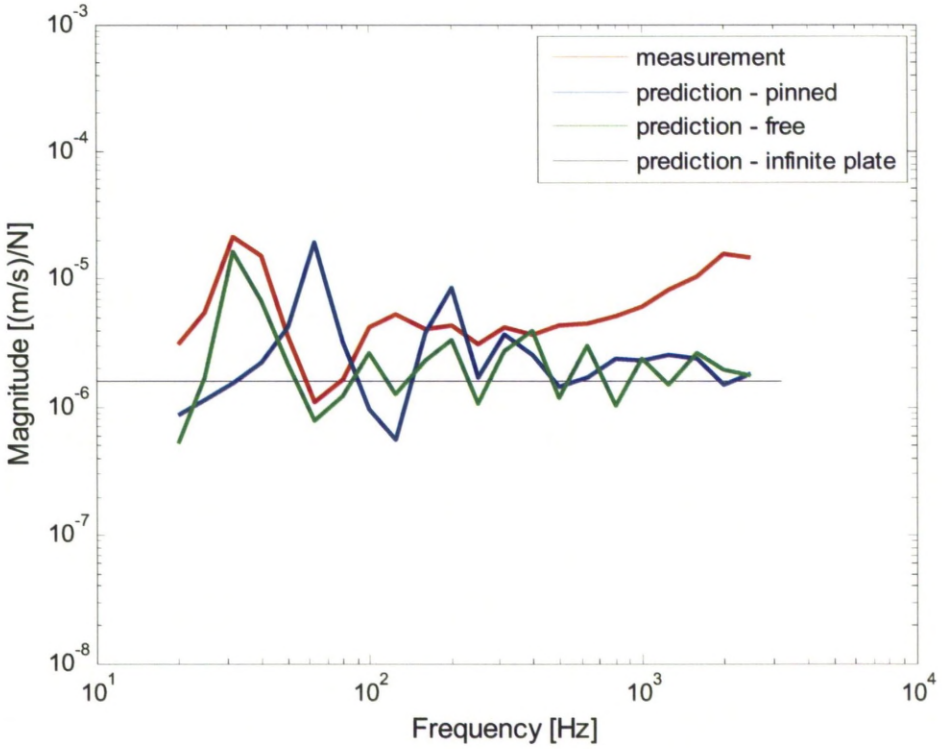

Figure 8.20: Measured and predicted point mobility at the stair/wall contact in 3rd octave bands

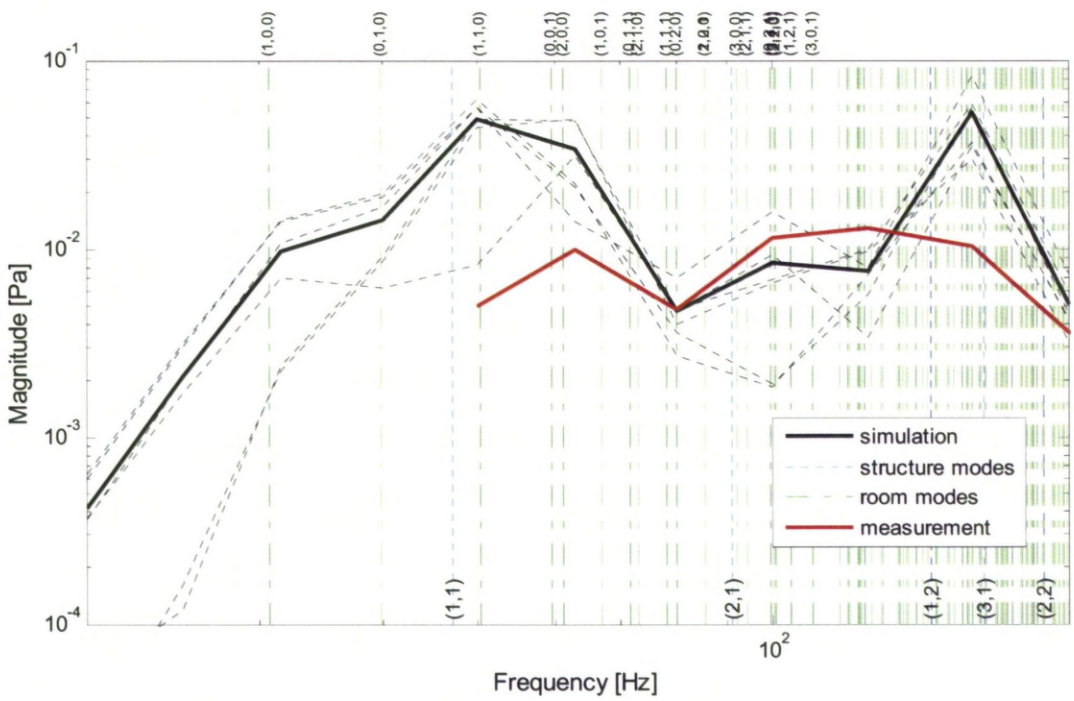

Figure 8.21: Calculated sound pressure at six room positions and average sound pressure level (bold) and measured sound pressure level - 3rd octaves

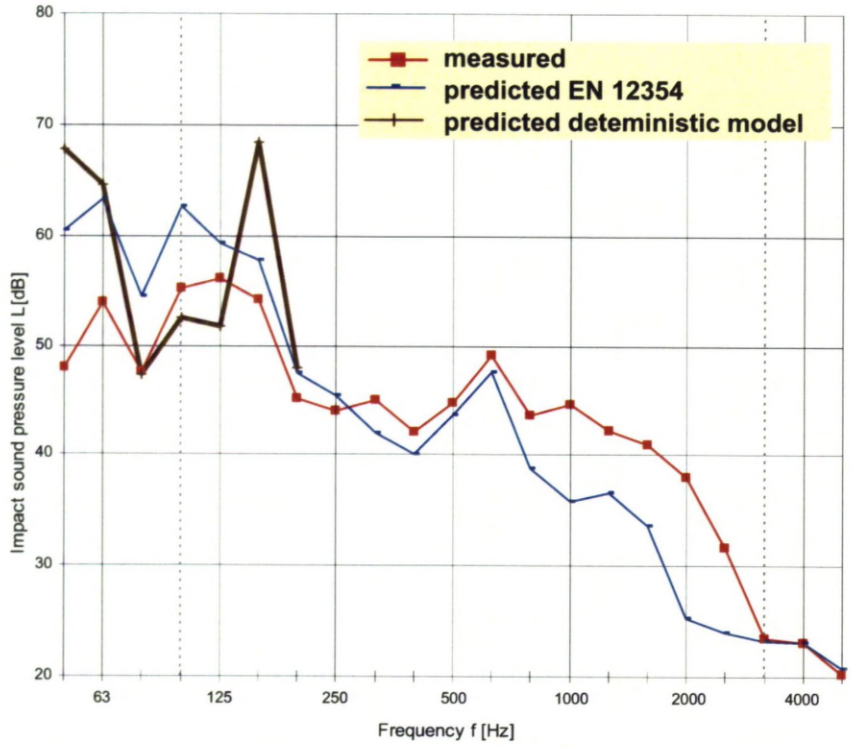

Figure 8.22: Measured and predicted impact sound pressure level using EN 12354 and deterministic model

9 CONCLUDING REMARKS

9.1 INTRODUCTION

The primary aim of this thesis study was to develop and validate a laboratory method for characterisation of lightweight stairs as structure-borne sound sources to predict the sound transmission in heavyweight building situations. Previously developed methods, to characterise structure-borne sound sources in buildings, apply to mechanical or water installations that generate vibrations due to internal excitation mechanisms. Lightweight stairs are actually passive building components that become active due to excitation by people walking on the steps. By treating the stair system, combined with impact source(s), as an active component, an adaptation of the available methods was investigated.

The impact sound transmission from vibrating stairs, through wall connections, involves multiple contacts and degrees of freedoms. Contacts can form a lever and moment excitation may be significant. This was investigated by a reciprocal method that enabled the determination of the component powers in-situ.

For a practical characterisation, special attention has been given to the reception plate method. So far, isolated reception plates have been used in laboratories. However, this is not practical for stairs connected to real walls and floors. Therefore, the reception plate method was adapted to real walls.

Existing building propagation models, such as EN 12354-5 and –2, also have been adapted to predict the sound transmission from stairs. Both assume diffuse sound fields and this assumption is tenuous at low frequencies, where structures and rooms display modal behaviour. As an alternative, a deterministic model has been investigated that considers the coupling of structural and room modes at low frequencies.

9.2 CONCLUSIONS

1. It has been shown, on example of impacted lightweight stair systems, that existing methods for the characterisation of active structure-borne sound sources can be applied to passive building elements in combination with a standard source in order to predict the sound transmission.

2. The structure-borne power can be used as input data for prediction models, such as EN 12354-5 to predict the sound transmission in heavyweight building situations.

3. The structure-borne sound transmission of an impacted timber stair in a staircase test facility through one rigid wall contact and radiation of the separating wall is significant in the frequency range up to 1 kHz.

4. The vibration behaviour of lightweight stairs is complex and not easily predictable. In addition the interaction of impact source and stair is complicated due to mobility matching. This applies for walking persons

and the standard tapping machine. By treating impact source and stair as one system the characterisation reduces to the measurement of the activity and mobility at the contact.

5. A reciprocal method for the in-situ measurement of forces and moments and their associated powers has been developed and experimentally investigated. The advantage of the method is that problems in installation of transducers between source and receiver are avoided.

6. The component powers, resulting from a shaker source point connected to an isolated reception plate and also to a real wall as the stair wall, were evaluated by reciprocal measurements. The components were the perpendicular force F_z and two moments M_x and M_y around axes in the plane of the receiving structure. By use of directly measured transfer mobilities it was demonstrated that the moment induced powers were significantly overestimated as a result of (small) experimental errors in the reciprocal transfer mobility measurements. Furthermore it was shown that the moment induced powers result from cross-coupling of force and angular velocity and not from the presence of real moments. The agreement of directly and reciprocally measured force induced power was within 2 dB.

7. The force perpendicular to the wall is the dominant component of the vibrating stair under investigation, moments can be neglected.

8. The force induced power by a vibrating stair can be predicted from contact free velocity and mobility or similarly by the blocked force.

9. Lightweight stair systems constitute high mobility sources in heavyweight buildings that can be characterised by the blocked force. The blocked force can be used as input data for prediction models, such as EN 12354-2 or a deterministic model to predict the sound transmission in heavyweight building situations.

10. It has been confirmed that for isolated reception plates, the power imparted by the source under test can be estimated with little difficulty by application of the reception plate method. The plate mass can be estimated with good accuracy, likewise the mean squared velocity. The total loss factor also can be measured without difficulty by decay measurements as the gradient is constant throughout the decay.

11. For plates, i.e. floors and wall, bonded into the surrounding building elements, measurement of the total loss factor is problematical, with the result that the source power is underestimated. In particularly, decay gradients change with time and the required early gradient, corresponding to T_5, at least requires visual inspection by an experienced observer. Only then will the underestimate be within 2 dB.

12. A real wall can be used as reception plate along with a power calibration. For the case considered the agreement with the true source power is within 2 dB, with no consistent over- or underestimate. This result could provide the basis for the development of a standard method.

13. The sound pressure level from vibrating stairs can be predicted using EN 12354-2 with the in-situ force. If the high mobility source condition is retained in the building installation then the blocked force only is required. The blocked force can be obtained in the laboratory from the (reception) plate power and receiver mobility.

14. The sound pressure level from vibrating stairs can be predicted using EN 12354-5 with the in-situ plate power. If the high mobility source condition is retained in the building installation then the characteristic plate power only is required.

15. Spatial and spectral variations of the receiver mobility can be incorporated using minimum and maximum mobility estimates. It is indicated that the range of the normalised impact sound pressure level can be up to 15 dB at low frequencies and 5 dB at high frequencies.

16. A deterministic model can be used for the prediction at low frequencies that requires proper assumptions for modelling the sound field in the room and the wall vibration field. For the case considered, a major difficulty was found in the modelling of the wall vibration field, mainly due to the boundary conditions that do not correspond to idealised conditions, such as pinned or free edges.

9.3 SUGGESTIONS FOR FURTHER WORK

1. The suggested methods for the laboratory characterisation should be applied to other types of lightweight stairs, including such with multi-point connections and line and area connections and also support contacts at the top and the bottom. In particular the suggested power substitution method should be investigated further in order to provide a method that would also enable a field characterisation of structure-borne sound sources.

2. The use of the methods developed should be investigated for the design of intrinsically quiet stairs, i.e. stair material and geometries that result in low free velocities at contacts. In particular the quantification of the isolation efficiency of resilient sleeved wall connections should be tested.

3. With the source data obtained in the laboratory the uncertainty of the prediction of sound pressure levels from impacted lightweight stairs in buildings according to EN 12354 should be investigated. This would provide valuable information for users of the prediction model, in the form of confidence limits for the prediction of the normalized sound pressure level.

4. So far, the stair wall has been assumed to be solid. If cavity walls are to be considered, then it will be necessary to estimate the power into the second leaf at the same time as for the first leaf in order to predict the

sound transmission in buildings. An implementation of double-leaf walls in the EN 12354 models is required.

5. The sound transmission at low frequencies should be investigated further by more in-situ tests and a parametric survey using the deterministic model to understand and solve the existing problems. In this context a characterisation of stairs for footfall excitation either by free velocity or the reception plate method should be investigated. Moreover a modified rating procedure is required to avoid annoyance by low frequency noise from impacted stairs.

6. A practical method for the characterization of lightweight stairs that are attached to lightweight building structures should be developed along with a prediction model to predict the sound transmission in lightweight building structures.

APPENDIX – CONFERENCE PAPERS

Congress Paper presented at Internoise 2010, Lisbon, Portugal, 2010

Congress Paper presented at 16th International Congress on Sound and Vibration, Krakow, Poland, 2009

Congress Paper presented at Acoustics 2008, Paris, France

Congress Paper presented at 19th International Congress on Acoustics, Madrid, Spain, 2007

Congress Paper presented at DAGA 2007 of the German Acoustical Society, Stuttgart, Germany, 2007

Congress Paper presented at 13th International Congress on Sound and Vibration, Vienna, Austria, 2006

Congress Paper presented at Forum Acusticum, Budapest, Hungary, 2005

Congress Paper presented at DAGA 2005 of the German Acoustical Society, Munich, Germany, 2005

inter.noise 2010
noise and sustainability
13-16 June 2010 . Lisbon . Portugal
www.internoise2010.org

Preparation of a Round Robin on the Reception Plate Method to Characterise Structure-Borne Sound Sources in Buildings

Jochen Scheck[1,2], Maximilian Chamaoun[1], Heinz-Martin Fischer[1], Barry Gibbs[2]

[1] Stuttgart University of Applied Sciences, Schellingstrasse 24, 70174 Stuttgart, Germany
(jochen.scheck@hft-stuttgart.de)
[2] Acoustics Research Unit, School of Architecture, University of Liverpool, Liverpool L69 3BX, UK
(bmg@liverpool.ac.uk)

Abstract
The reception plate method provides a simple means for the characterisation of structure-borne sound sources in buildings. A standard recently was formulated and now several acoustics research groups and test institutes in Europe have reception plates at their disposal. Recently a European Standards working group initiated a round robin test in order to investigate the reproducibility of results obtained in different laboratories and to validate the measurement guidelines of the current standard. For that purpose, a test source was designed and constructed by the University of Applied Sciences Stuttgart. Several aspects had to be considered in order to yield a representative, controllable and powerful source, which should in addition be easy to handle and transport. FE simulations were used in the design process to optimise the source characteristics and formed the basis for the construction of the device. Initial measurements have confirmed the adequacy of the source and potential sources of uncertainty have been highlighted. These have been taken into consideration in setting out the parameters of the round robin.

Keywords: structure-borne sound, source characterization, reception plate method

1 Introduction

Sound propagation in buildings is often dominated by structure-borne sound sources. Common sources are bath tubs, whirlpools, washing machines, etc. In order to avoid noise problems, resulting from such sources, a prediction model for heavyweight building situations has been developed [1]. As input data, a measure of the structure-borne source strength is required, which can be expressed as the power obtained in a laboratory by the reception plate method [2]. A standard for the reception plate method [3] was formulated in 2009 and now several acoustics research groups and test institutes in Europe have reception plates at

their disposal. Recently a European Standards working group initiated a round robin test in order to investigate the reproducibility of results obtained in different laboratories and to validate the measurement guidelines of the current standard. For that purpose, a test source was designed and constructed by the University of Applied Sciences, Stuttgart. Several aspects had to be considered in order to yield a representative, controllable and powerful source, which should in addition be easy to handle and transport. FE simulations were used in the design process to optimise the source characteristics and formed the basis for the construction of the device. Initial measurements have confirmed the adequacy of the source and potential sources of uncertainty have been highlighted. These have been taken into consideration in setting out the parameters of the round robin.

2 Reception plate method

The power input to a freely suspended reception plate is assumed equal to the total emission of a source connected to it through multiple contacts and components of excitation [2]. In turn, the power gained by the plate is the bending wave energy loss (due to internal losses, acoustic radiation and additional damping),

$$P_{\text{rec.}} = \omega m \overline{\tilde{v}}^2 \eta \tag{1}$$

For a high mobility point source, with a predominant force component perpendicular to the plate, the power is directly related to the input mobility Y_{rec} of the reception plate at the contact,

$$P_{\text{rec.}} = \frac{1}{2}|F|^2 \,\text{Re}\{Y_{\text{rec.}}\} \tag{2}$$

In order to correct the reception plate power for multi-point sources and for the properties of the finite reception plate, in particular its modal behaviour, the infinite or characteristic reception plate power is proposed, given by,

$$P_{\text{infinite}} = P_{\text{rec.}} \cdot \frac{Y_{\text{infinite}}}{\text{Re}\{\overline{Y}_{\text{rec.}}\}} \tag{3}$$

Here $\overline{Y}_{\text{rec}}$ is the spatial average of the point mobility for forces perpendicular to the reception plate. This correction is a simplification as for multi-point sources the interaction between the contacts is not considered in detail.

The characteristic reception plate power can be transformed into the installed power when the source is in a building and the high source mobility condition is retained,

$$P_{\text{inst.}} = P_{\text{infinite}} \cdot \frac{\text{Re}\{\overline{Y}_{\text{build.}}\}}{\text{Re}\{\overline{Y}_{\text{infinite}}\}} \tag{4}$$

$\overline{Y}_{\text{build.}}$ is the spatial average of the point mobility of the building element in contact with the source. Again the simplest estimate for the receiver mobility is the infinite plate mobility.

3 Requirements of the reference source

The main requirement of the reference source is that it is representative of typical sources in buildings. This means in the first instance that the source has multiple contacts and is of a representative size. Moreover the source mobility must be at least 10 dB more than the mobility of the reception plate, to assure a force source condition. In order to enable measurements within the frequency range 50Hz – 5000Hz, the excitation by the source must be powerful enough such that the reception plate response velocity is well above the background noise level. The dominant excitation path must be structure-borne; airborne excitation due to sound radiation of the source elements should be at least 10 dB lower. For the purposes of the round robin, the reference source must be easy to transport, and thus the dimensions and the weight must not be too great. An important requirement is that the source's characteristics remain constant throughout the round robin. The source will be sent around to different laboratories and thus the potential for damage, during transportation or operation, has to be taken into consideration.

4 Source Design

The source configuration, agreed after discussions by the working group, was a plate standing on three rounded feet, which is excited by an inertial shaker screwed to the plate. The source plate modes act as a frequency filter of the force injected by the shaker. The three feet ensure that each is in contact with the reception plate even when the reception plate surface is uneven. A force transducer is inserted between shaker and source plate, for monitoring and control. The shaker is driven with white or pink noise which should result in a broadband excitation of the reception plates.

In designing the source, FE models were developed to investigate variations in plate and feet geometry, material and shaker excitation position. The velocity of the reception plate was predicted to ensure that the excitation is strong enough, over the frequency range of interest. In addition, that the high source mobility condition is maintained over the whole frequency range. The source was constructed, based on these simulations and on other practical aspects, with the following components:

- Aluminium plate (0.5m x 0.35m x 0.1m)
- Steel feet (0.07 m, diameter: 0.015m)
- Data Physics Inertial Shaker IV 40 (Force Vector 30 N)
- Data Physics 30 W Power Amplifier
- Kistler Force Transducer Type 9311B

Screw connections of the feet and shaker, enable rapid assembly and simplifies transportation. In Figure 1 is shown the reference source in position.

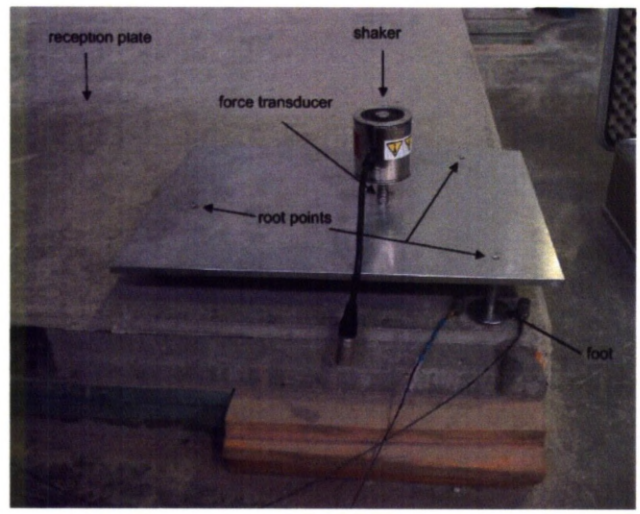

Figure 1 – Reference source on the horizontal reception plate of HFT Stuttgart (100 mm concrete plate, resiliently supported at the edges according to [3])

5 Source characteristics

5.1 Source mobility

The source mobility was measured with the source (plate with feet and shaker with force transducer) freely suspended, according to [5]. In Figure 2 is shown the source mobility at one foot and receiver mobility at a central and edge location. At low and mid frequencies the reception plate mobility is about 10 dB higher for the edge position than for the centre. This is because the vibration behaviour is that of a freely suspended plate with maximum amplitudes at the edges, particularly the corners. At all plate positions, the source mobility is at least 10 dB higher and a high mobility source condition can be assumed. The characteristic reception plate mobility approximates the frequency average mobility in the centre; the fluctuations of the measured mobility are within ± 3dB.

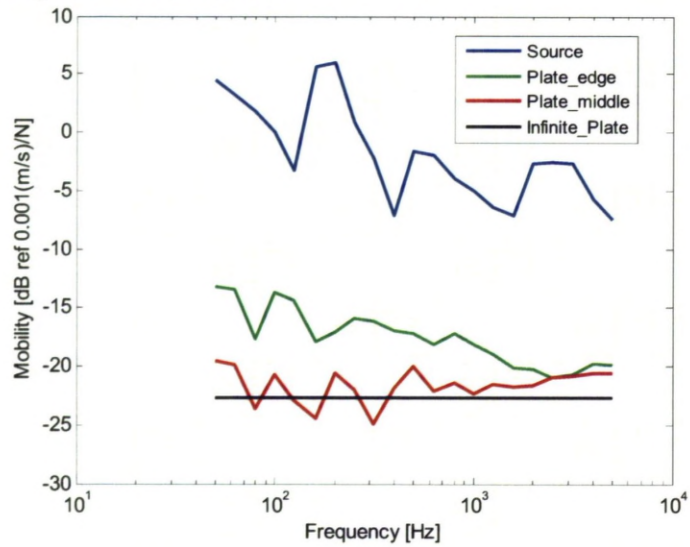

Figure 2 - Source mobility and reception plate mobility in 3rd octave bands

5.2 Excitation signal

The excitation by the shaker is adjustable by control of the excitation signal. Optimum reproducibility is obtained for the power amplifier set to maximum (it was confirmed that the amplification is linear). The excitation strength is controlled by adjustment of the generator settings in the measurement analyser. White and pink noise was used, to obtain the optimum excitation strength. The upper limit is when acceleration at the feet exceeds the acceleration due to gravity g. This was indicated by a rattling sound and any migration will reduce reproducibility. In Figure 3 is shown the spatial average reception plate velocity (12 sampling positions) for white and pink noise signals, for the reference source positioned near a corner. The signal/noise ratio is sufficient for excitation with pink noise and 100 mVrms in the frequency range 50-5000 Hz. At the same time, the acceleration of the feet is well below g. Therefore this setting is proposed for the round robin.

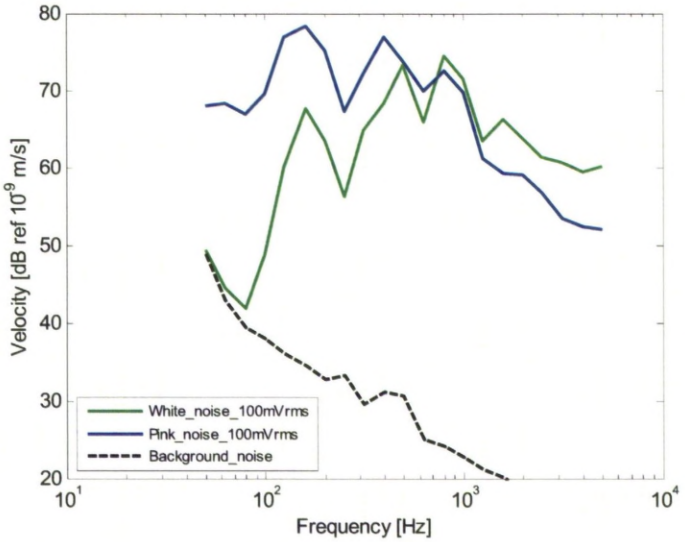

Figure 3 – spatial average velocity on the reception plate for shaker excitation with white noise and pink noise and 100mVrms amplification; source near a corner

5.3 Structure-borne and airborne excitation

The structure-borne and airborne excitation was investigated by measurement of the reception plate velocity with the source standing on the plate and when decoupled from the reception plate. The decoupled condition was realised by inserting soft foam elements between feet and reception plate. Although the sound radiation is not exactly the same for both conditions, an estimate of the radiated sound in the "coupled" condition is obtained. In Figure 4 the respective reception plate velocities are shown. In the "coupled" condition the reception plate velocity is generated by structure-borne and airborne excitation. The velocity level is at least 20 dB more than for the decoupled condition. From this it can be concluded that airborne excitation is negligible under normal operation of the source.

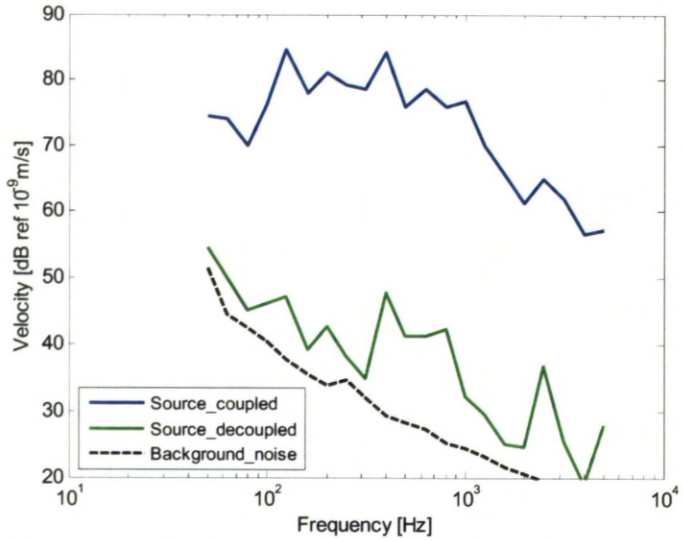

Figure 4 – reception plate velocity at a fixed reference position (near a corner) with the source standing regularly on the plate (near a corner) and with the feet decoupled

5.4 Repeatability

For transportation the reference source will be disassembled. It was therefore investigated if the source characteristics remain constant when the source is disassembled and reassembled. The screwed connections of feet and plate were repeated using a torque wrench to ensure constancy. It was possible to repeat a rigid screwed connection, between shaker and plate, without mechanical devices. In Figure 5 is shown the reception plate velocity at a fixed reference position before and after disassembly. The deviation is within ± 0.5 dB. It can therefore be stated that the source characteristics remain constant when the previously described steps are taken. In addition the sampling time, which was 20 s for each velocity measurement, was found to be sufficient.

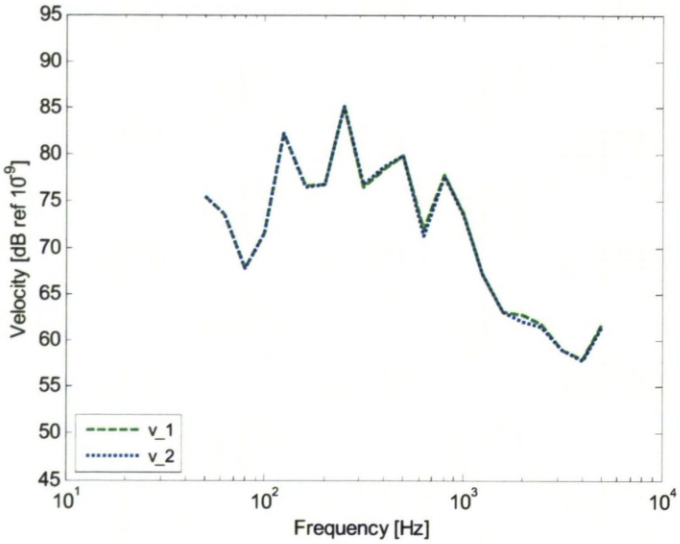

Figure 5 - Reception plate velocity a fixed reference position (near a corner) – repeatability for the source disassembled and reassembled again

5.5 Linearity of the source / Normalization to the shaker force

Different laboratories have different measurement analyzers and therefore an unambiguous specification of the shaker operating conditions is not feasible. For example the generator frequency span was set to 0-6400 Hz for the current investigations. Other analyzers do not allow the same specification but e.g. only an upper frequency limit of 5000 Hz. Consequently the shaker force will not be identical even when the generator gain is equal. In addition it is expected that different laboratories are exposed to different background noise and a higher amplification might be required. For these reasons a normalization of the reception plate power to the simultaneously measured shaker force is proposed. This assumes linearity of the transfer mobility as the ratio of reception plate velocity and shaker force. The reception plate velocities, normalised to the shaker force, was obtained as,

$$P_{\text{infinite,normalized}} = P_{\text{infinite}} \cdot \frac{F_0^2}{\tilde{F}_{\text{Shaker}}^2} \tag{5}$$

As an extreme case the normalization of the reception plate velocities resulting from shaker excitation with pink and white noise (Figure 3) to the respective shaker force was applied according to (5). Results are shown in Figure 6.
The high deviations below 80 Hz are due to insufficient signal/noise when using white noise. In the frequency range above 80 Hz the agreement of the normalized velocities is within ± 2 dB. These deviations are not caused by changes in the sampling of plate velocity since the accelerometer positions were identical in both cases. To check for linearity, the transfer mobility (the ratio of reception plate velocity to shaker force) was obtained as narrow band values and third octave values simultaneously. In Figure 7 are shown the average transfer mobility for 12 remote positions. The agreement is much better for the narrow band measurement which indicates that the 3rd octave band filtering causes some deviation.

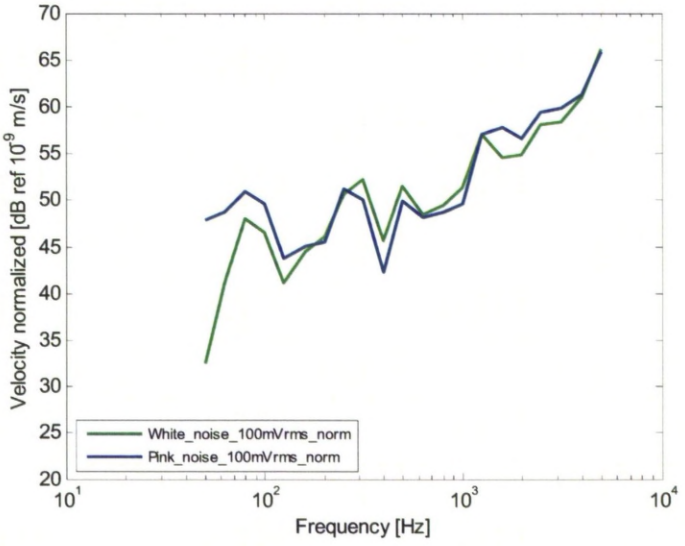

Figure 6 – Spatial average reception plate velocities from Figure 3 normalized to shaker force

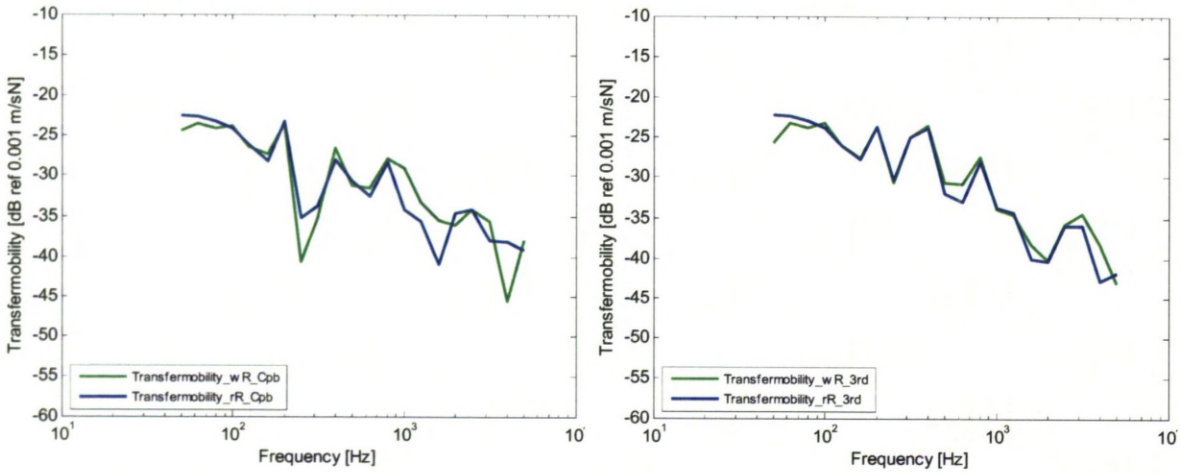

Figure 7 – Reception plate velocity normalised to shaker force, for white and pink noise excitation; left: measurement 3rd octave, right: 3rd octave calculated from narrow band data

6 Application of the reception plate method

The method was applied, in order to detect potential sources of uncertainty of the procedure outlined in [3] before finalizing the parameters of the round robin. From previous investigations [2], it is known that the sampling of the spatial average velocity has to be performed over the whole plate, including edge positions. Otherwise, the imparted power is underestimated, as significant energy is stored near the free edges. This is contrary to other recommendations [3], which require that the measurement points should be as far as possible from the plate edges. For this investigation, the sampling was performed over the entire plate using 12 sampling points. The measurement of total loss factor is another potential source of uncertainty, also reported in [2]. Apart from the spatial uncertainty in the determination of the total loss factor a problem can arise in the measurement of the structural reverberation time due to filtering. For highly damped reception plates, as for this case, the reversed time technique should be used, particularly below 100 Hz.

In the following the effect of varying source positions is investigated. According to [3], a specific location of the source is not specified. It was thus investigated how (extreme) positions at the plate's centre and near a corner affect the estimate of reception plate power. The results are illustrated in Figure 8. Below 400 Hz, the measured power in-situ is consistently higher for the corner position. This is expected as the power is a function of the input mobility, which is a maximum at the corners of a freely vibrating plate. In Figure 10 are shown the real parts of the input mobility at the locations of the feet. For the corner position the mobilities are considerably higher in the frequency range below 400 Hz than for the centre position. Moreover the variation of the input mobility for the three feet positions is significantly greater for the corner than for the centre position. The reception plate mobility is highest for one foot position (blue curve) very close to a corner. Assuming similar (blocked) forces for each of the feet it is expected that the foot at the corner dominates the power transmission. In that case the correction for the average input mobility would not be adequate. Actually the characteristic reception plate power is in good agreement for both source positions. The deviations are generally within $\pm$ 3 dB.

By use of a numerical model [6] it was confirmed that the reception plate mobility increases significantly when approaching the corners. A significant increase was observed at approximately 50 cm distance from the corner (Figure 10). It is thus suggested that this area be excluded in standard measurements. This recommendation will be confirmed or otherwise after completion of the round robin.

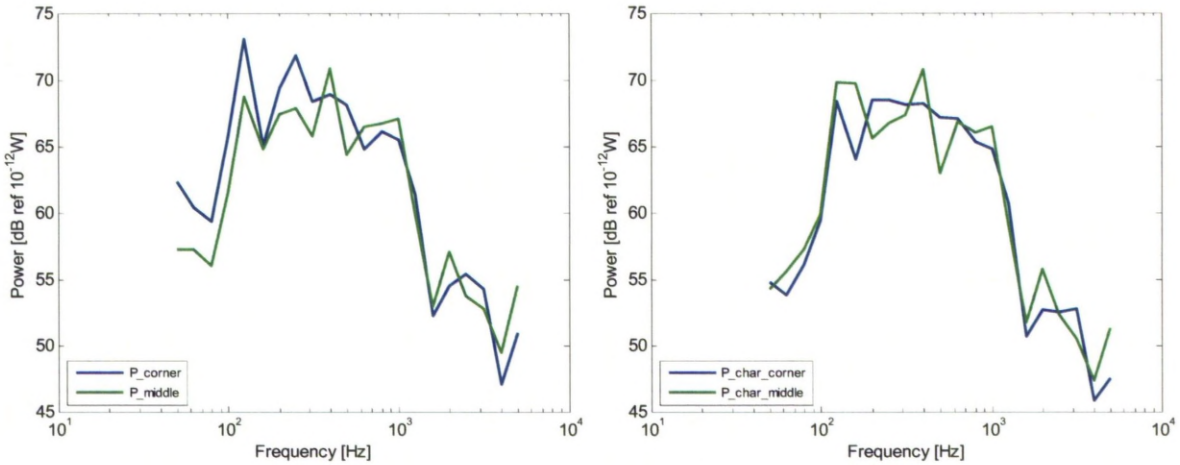

Figure 8 – Reference source in the centre and at a corner;
left: In-situ reception plate power; right: Characteristic reception plate power

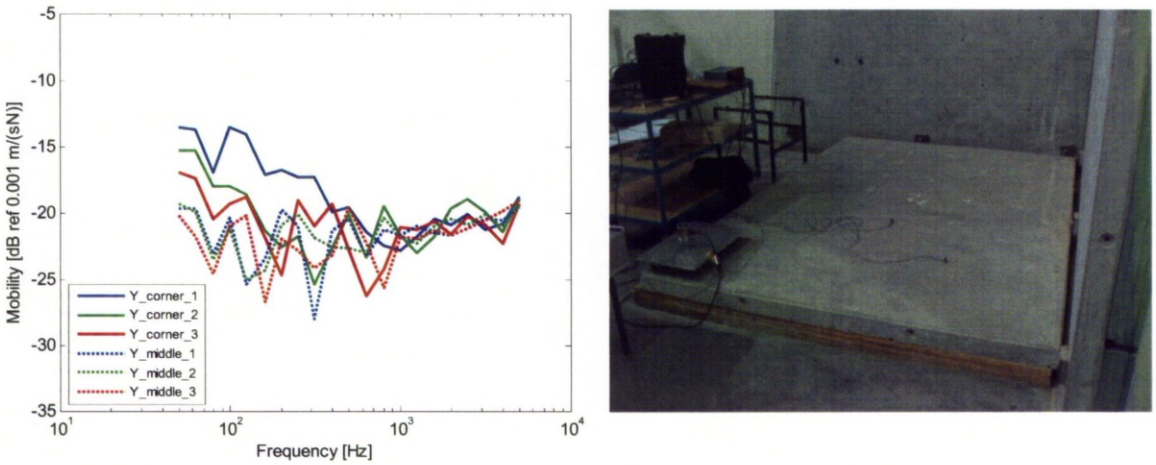

Figure 9 – Mobility at the connection points of the reference source for centre and corner

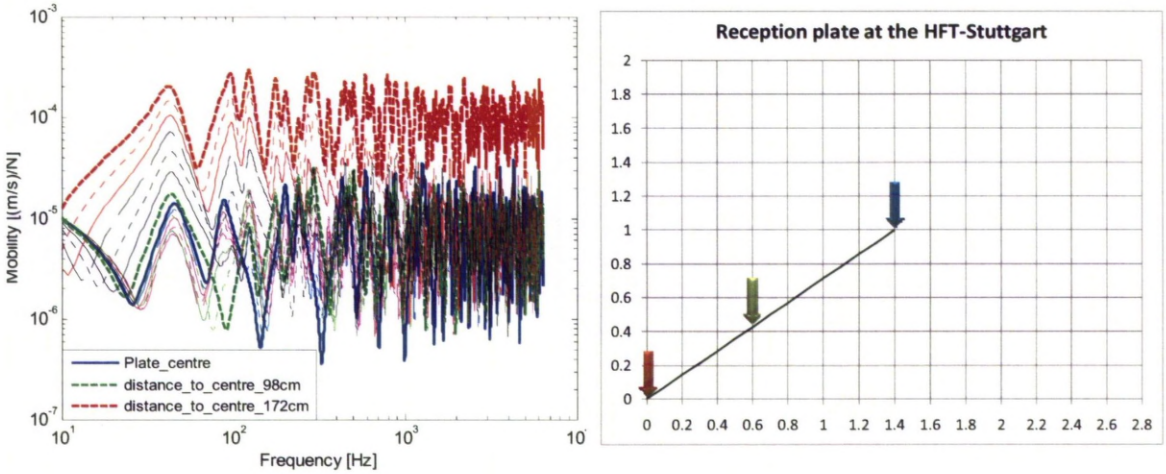

Figure 10 – Predicted reception plate mobility along the line from the plate's centre to a corner in increments of 12.5 cm

7 Conclusions

For a round robin on the reception plate method a reference structure-borne sound source was designed, constructed and its appropriateness confirmed by experimental investigations. Due to the simplicity of the construction and the implementation of shaker with force transducer the source characteristics are sufficiently constant and controllable. Initial investigations on the reception plate method with the reference source indicated that source positions near the plate's corners/edges should be avoided if possible.

Acknowledgments

The authors acknowledge the contribution of the members of CEN/TC 126/WG 7 AHG1.

References

[1] DIN EN 12354-5: Building acoustics. Estimation of acoustic performance of building from the performance of elements. Sounds levels due to the service equipment, 2009

[2] Späh, M.; Gibbs, B. Reception plate method for characterisation of structure-borne sound sources in buildings: Assumptions and application, Applied Acoustics, 2009. 70: pp. 361-368

[3] EN 15657-1: Acoustic properties of building elements and of buildings - Laboratory measurement of airborne and structure borne sound from building equipment - Part 1: Simplified cases where the equipment mobilities are much higher than the receiver mobilities, taking whirlpool baths as an example, 2009

[4] Späh, M.; Gibbs, B. Reception plate method for characterisation of structure-borne sound sources in buildings: Installed power and sound pressure from laboratory data, Applied Acoustics, 2009. 70: pp. 1431-1439

[5] ISO 9611: Acoustics – Characterization of sources of structure-borne sound with respect to sound radiation from connected structures – Measurement of velocity at the contact points of machinery when resiliently mounted, 1996

[6] Gardonio, P. B.; Brennan, M. J. Mobility and impedance methods in structural dynamics. Advanced Applications in Acoustics, Noise and Vibration, Ed. F. Fahy, J. Walker, Spon Press, 2004, 389-447

The Sixteenth International Congress on Sound and Vibration
Kraków, 5-9 July 2009

CHARACTERISATION OF STRUCTURE-BORNE SOUND SOURCES USING WALLS AND FLOORS AS RECEPTION PLATES

Jochen Scheck

Florian Mack

Heinz-Martin Fischer

Stuttgart University of Applied Sciences, Schellingstrasse 24, 70174 Stuttgart, Germany

Barry Gibbs

Acoustics Research Unit, School of Architecture, University of Liverpool, L69 3BX, UK

The full characterisation of structure-borne sources is complicated or even intractable when several contacts and degrees of freedom are considered. For high-mobility sources the so-called reception plate method provides a simple means for the characterisation. So far, reception plates with free edges have been successfully used in laboratories. A field characterisation of sources using real walls and floors with the edges bonded into surrounding structures as reception plates would be of great benefit especially when the source of interest cannot be easily moved to a laboratory. The relationship between the (real) source power and the power estimate from measurements on the receiving structure has been investigated. It was found that the reception plate method as applied so far tends to underestimate the real source power and this underestimate was largely due to errors in the estimate of the loss factor of the wall or floor. This has been confirmed using a Transient Statistical Energy Analysis (TSEA) model. It is shown that this problem can be avoided by employing an alternative method, using an instrumented shaker as a substitute structure-borne sound source.

1. Introduction

The structure-borne sound sources to be considered in massive buildings are usually high mobility sources with the perpendicular force being predominant in comparison with other components like moments. For this kind of source the so-called reception plate method[1] also termed reverberant plate method[2] provides a simple means for the characterisation to provide input data for prediction models such as EN 12354. So far, reception plates with free edges have been used in laboratories. A field characterisation of sources, using real walls and floors as reception plates, but with the edges bonded into surrounding structures, would be of great benefit especially when the source of interest cannot be easily moved to a laboratory. In previous investigations it was found that application of the reception plate method for a real wall, situated in a staircase test facility, yields a significant underestimate of the installed power[3]. By use of a simplified SEA model it was furthermore indicated that the underestimate is a result of power-sharing between the walls and floors connected to the reception wall. This was investigated in more detail by use of an SEA simulation including all

connected structural elements and rooms of the staircase test facility. A Transient SEA simulation was performed to obtain an insight into the power flows during the decay, which is relevant in the loss factor measurement using the reverberation decay rate method. It is found that measurement of the total loss factor, as required for the power balance for non-isolated plates, is difficult. The problems observed can be circumvented by using a power substitution method, which enables a proper characterisation of structure-borne sound sources using coupled plates as encountered in the field.

2. Reception Plate Method – Isolated Reception Plate

The power input to a freely suspended reception plate is assumed equal to the total emission of a source connected to it through multiple contacts and components of excitation. In turn, the power gained by the plate is the bending wave energy loss according to (1).

$$P_{\mathrm{in,i}} = \omega E_{\mathrm{i}} \eta_{\mathrm{i}} . \tag{1}$$

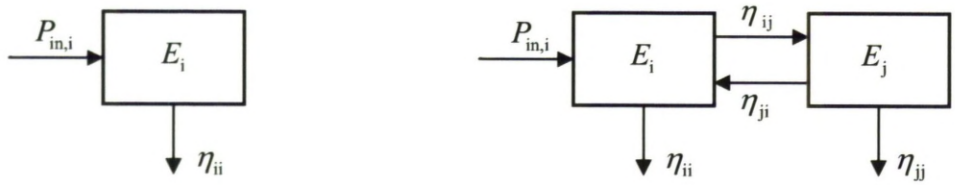

Figure 1. SEA model of an isolated plate (left) and SEA model of two connected plates (right).

The bending wave energy conserved in the plate equals the product of plate mass and spatial average velocity in the far field (2) (Figure 1).

$$E_i = m_i \overline{\tilde{v}}_i^2 . \tag{2}$$

The bending wave energy loss is controlled by the total loss factor. In[1,3] it is demonstrated that the reception plate power equals the cross-spectral power from a connected shaker for an isolated reception plate of 10 cm concrete and with the plate edges supported with resilient pads with high internal damping. The power imparted by the source is wholly contained in the reception plate, due to the isolation, and can be measured without difficulties as the plate's mass is clearly defined. The total loss factor of the plate equals the internal loss factor (plate and resilient support are seen as one subsystem) which can equally be measured without difficulties. The total loss factor is usually obtained from vibration decay measurements in 3rd octave bands and by evaluation of the integrated impulse response. To avoid filtering problems (ringing of the band pass filter and smoothing caused by the averaging device) the reversed time technique generally is used[4]. Distortion only occurs at the initial part of the decay curve which therefore should be discarded.

In Figure 2 the backward integrated impulse response of the isolated reception plate is shown at 100 Hz and 1 kHz. The measurement was performed in 3rd octave bands with a Norsonic 840 analyser and a Maximum Length Sequence (MLS) as signal. The decay curves are almost straight lines. Evaluation of a T_{20} (excluding the first 5 dB of the decay) yields the total loss factor as required.

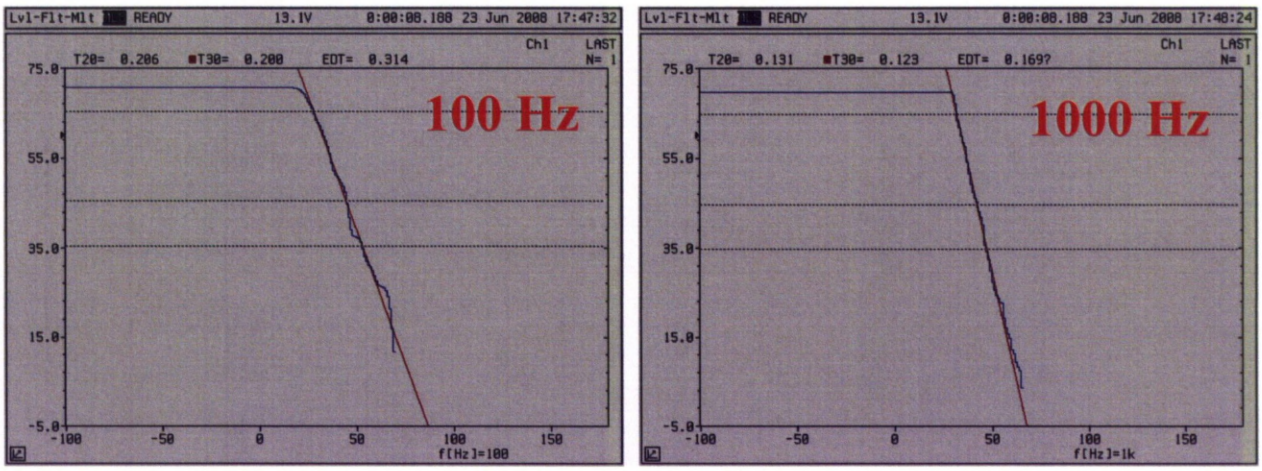

Figure 2. Decay curves for the isolated reception plate for 100 Hz and 1 kHz

3. Reception Plate Method – Coupled Reception Plate

3.1 Power balance

If a source is attached to a wall or floor in a building, then the excited plate is connected to other plates (i.e. walls and floors). The power balance equation for the excited plate i is now a function of internal and coupling loss factors (3) (Figure 1).

$$P_{\mathrm{in,i}} = \omega E_{\mathrm{i}} \eta_{\mathrm{ii}} + \sum_{\mathrm{j}} \omega E_{\mathrm{i}} \eta_{\mathrm{ij}} - \sum_{\mathrm{j}} \omega E_{\mathrm{j}} \eta_{\mathrm{ji}} = \omega E_{\mathrm{i}} \eta_{\mathrm{i}} - \sum_{\mathrm{j}} \omega E_{\mathrm{j}} \eta_{\mathrm{ji}} \tag{3}$$

The negative terms represent the power gain of the excited structure from adjacent plates. In order to keep the simplicity of the reception plate method, measurements of the energy and total loss factor is restricted to the excited plate. This requires that the negative term in equation (3) is negligible for the stationary condition and that the measured total loss factor of the excited plate represents only power losses and no power gains.

3.2 Investigated Situation

The background of the present study is the characterisation of lightweight stairs as structure-borne sound sources; see staircase test facility in Figure 3. The reception plate under investigation is a wall of 24 cm CaSi with density 2000 kg/m^3. The flanking walls are of similar construction, the floors and ceilings are of 180 mm reinforced concrete with density 2300 kg/m^3. The stair wall is built inside a concrete frame of the same thickness. The building is subdivided into three isolated sections and decoupled from the environment.

The reception plate method was applied with restricting measurements on the stair wall and considering only the wall mass[3]. A direct measurement of power was obtained using a shaker with a force transducer, attached to the wall and driven with random noise. The spatial average velocity was recorded using a Polytec laser scanning vibrometer on a scanning grid with in total 1100 points distributed over the whole wall surface. For the evaluation of the reception plate power, accelerometer positions within 0.25 m around the excitation point and from the wall's edges were excluded, to minimise the influence of direct and near fields. The total loss factor was measured as described before. Example decay curves are shown in Figure 4.

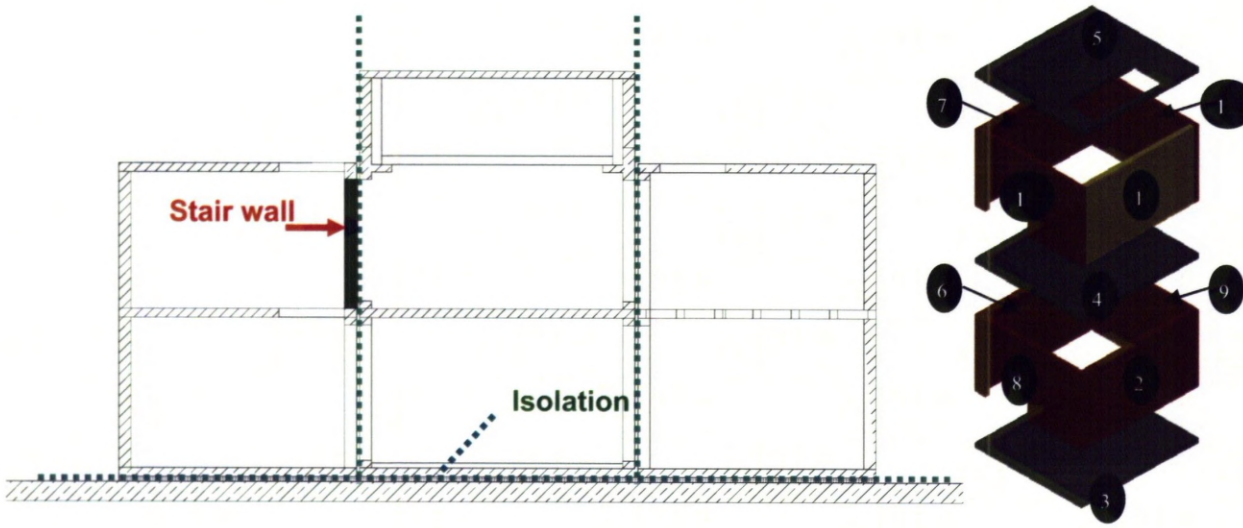

Figure 3. Staircase test facility (left) and TSEA model of the left section (right)

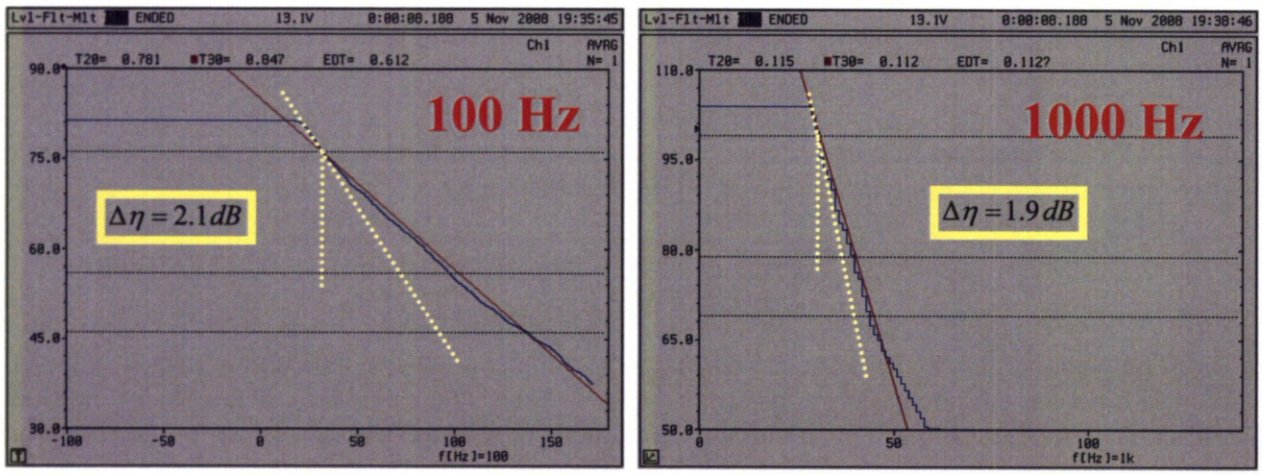

Figure 4. Decay curves for the stair wall for 100 Hz and 1 kHz

In contrast to the isolated plate (Figure 2) the decay curves for the stair wall exhibit a steep initial decay followed by multiple slopes indicating energy coming back from adjacent walls and floors during the decay. By evaluation of the T_{20} these power back flows are included and the loss factor is significantly underestimated. An evaluation by visual inspection (yellow lines), considering only the first gradient, yielded more or less a T_5 and a better approximation of the total loss factor required for the power balance of the excited wall.

In Figure 5 the total loss factor obtained from T_{20}, T_5 (including regression lines used for narrow band calculations) is shown along with the total loss factor from evaluation of the half-power bandwidth. The latter was obtained from a modal analysis of the wall. It is observed that evaluation of T_5 yields a significantly higher loss factor than from T_{20}; the loss factor obtained from half-power bandwidth generally lies between. The difference resulting from T_5 and T_{20} evaluation is about 4 dB at 50 Hz reducing to 0 dB at 5 kHz. This "improvement" also is found in the evaluation of the source power by the reception plate method. In Figure 6 is shown the directly measured cross-spectral power of a shaker connected to a central wall position and the estimate from the reception plate method using the loss factor obtained from T_5. The real power is still underestimated by the order of magnitude of 2 dB. The assumption that energy is coming back during the decay and thus the initial decay should be considered in evaluation of the loss factor is further strengthened by the results from a TSEA simulation which is described in the following.

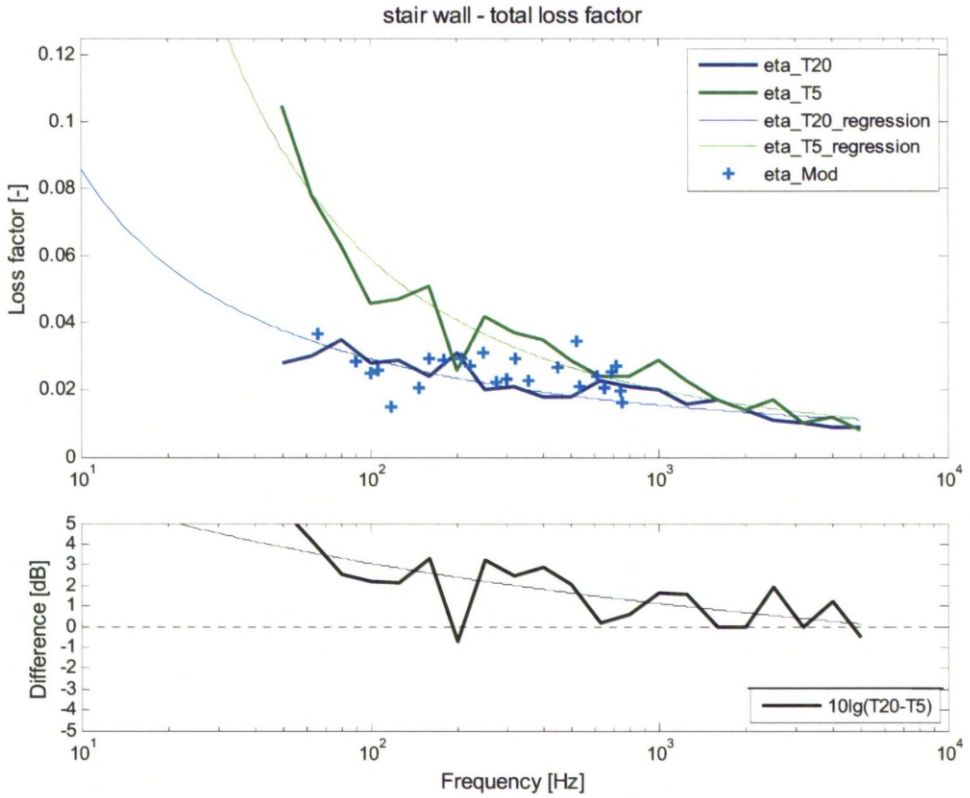

Figure 5. Total loss factor from evaluation of T20, T5, half power-bandwidth (modal analysis)

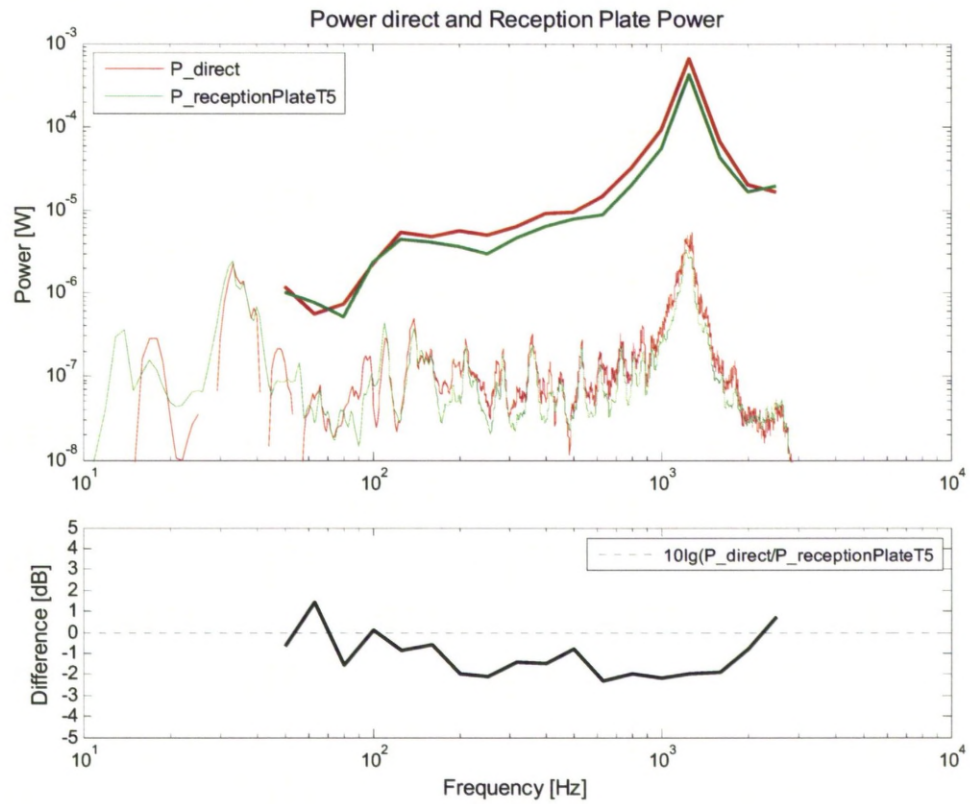

Figure 6. Power measured directly and from reception plate method with total loss factor from T5

4. Transient SEA simulation of the sound level decay

The TSEA approach recently was used by Kling[5] to investigate the damping effect of coupled subsystems. Using the same approach, the left section of the staircase test facility (Figure 3) was modelled and the decay characteristic of the stair wall investigated.

In the first step of the analysis the energy distribution over the subsystems is calculated in the stationary condition using internal and coupling loss factors from[6]. On terminating the power input into the system, such as $P_{in,i}(t \geq 0) = 0$, the energy levels of all subsystems begin to decrease. The rate of change of energy is set equal to the power losses of the subsystem. Therefore the input power is replaced by the power losses.

$$P_{loss,i}(t) = -\frac{d}{dt} E_i(t) = \omega \cdot \eta_i \cdot E_i(t) - \sum_j \omega \cdot \eta_{ji} \cdot E_j(t) = \omega \cdot \eta_{loss,i}(t) \cdot E_i(t) \tag{4}$$

After calculating the power losses for each time increment, a new energy distribution is obtained by subtracting the energy lost in that increment (e.g. Δt = 0,1 ms) from the energy of the element in the previous increment. The basic assumption in the TSEA is that the energy exchange between the plates happens in each time interval. With this new energy distribution the power losses of each subsystem are calculated for the next increment and so on. This results in an energy decay curve for each subsystem and gives the TSEA transient loss factor also termed the "observable" or "apparent" loss factor $\eta_{loss,i}$ (5).

$$\eta_{loss,i}(t) = \eta_i - \sum_{j(j \neq i)} \eta_{ji} \frac{E_j(t)}{E_i(t)} \tag{5}$$

Examples of the simulated decay curves of all subsystems are shown in Figure 7 for f = 1000 Hz, along with the backward integrated energy curve of the stair wall.

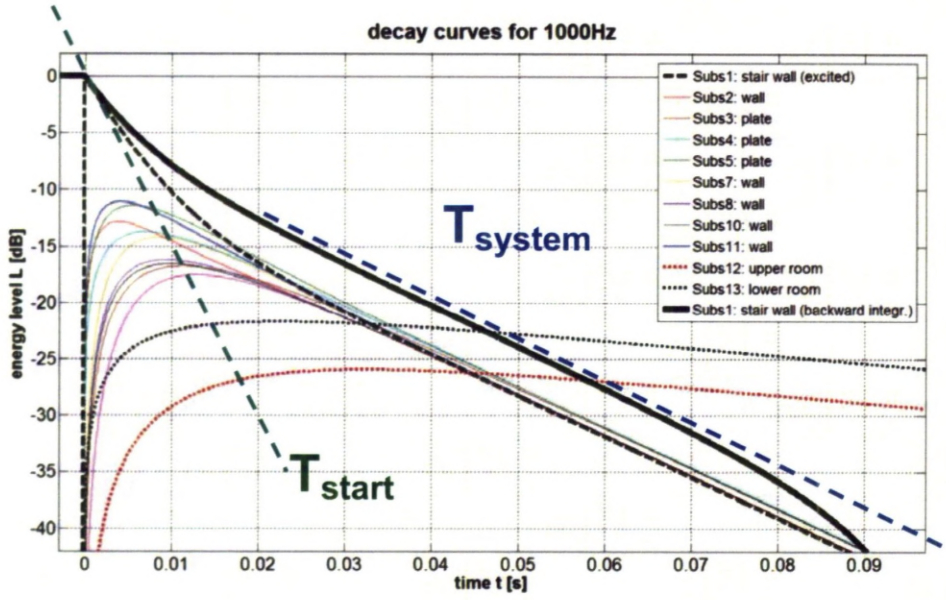

Figure 7. Simulated decay curves of the subsystems resulting from transient excitation for 1000 Hz

At t = 0 s, power is introduced to the stair wall (dashed black line) by a single impact and a maximum level is generated. This initial energy is then distributed within the system. Immediately

after the impact, the energy level on the adjacent elements and in the rooms rises to a maximum followed by a continuous decay. Due to the small coupling losses and absorption the room energy levels (pointed lines) decay slowly compared to the structures. However the room response does not influence the decay of the stair wall. After t ≈ 0,03 s all structures decay with the same gradient, the power flow is balanced in the system. As a result of energy sharing with the adjacent elements the energy level of the excited wall shows a non-linear decay curve. The backward integrated decay curve of the stair wall is further analysed. In the first milliseconds of the decay, power losses dominate on the stair wall. This is represented by an initial decay time T_{start} yielding a stationary loss factor $\eta_{stationary}$. After t ≈ 0,03 s the power flow is balanced in the system which is represented by a system decay time T_{system} yielding the system's loss factor η_{system}. In the measurement of a T_{20} the evaluation range will be from -5dB to -25 dB. Generally it is expected that $\eta_{stationary} > \eta_{T20} > \eta_{system}$. In the case considered, T_{20} and T_{system} are similar and significantly longer than T_{start}. The same trend is expected in decay rate measurements and thus "justifies" the evaluation of T_5. The discrepancy of the simulated loss factors obtained from T_{20} and from T_{start} is shown in Figure 8. The same trend is observed in Figure 5 in the difference of T_{20} and T_5 which is expected to be smaller as $T_5 > T_{start}$.

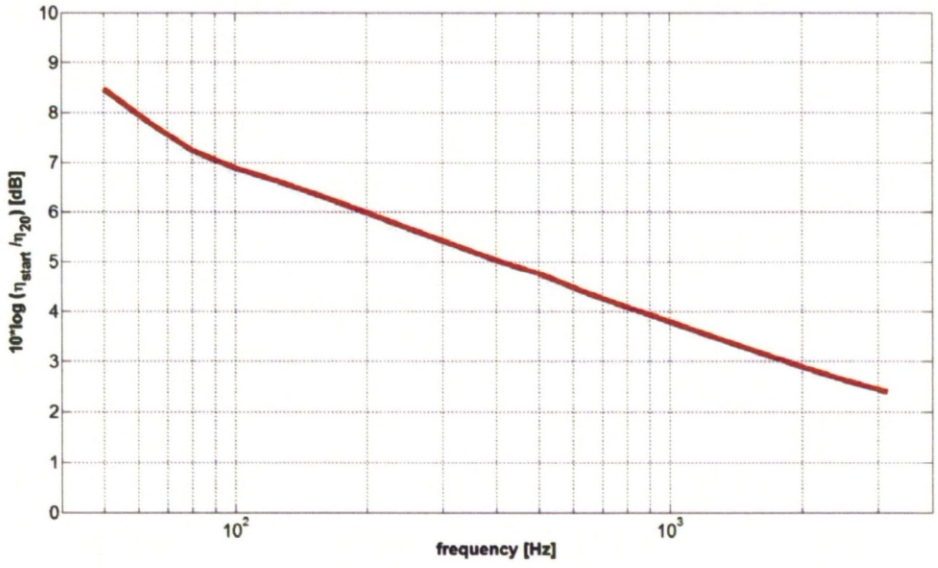

Figure 8. Simulated decay level difference between $\eta_{stationary}$ and η_{20}

5. Power Substitution Method

The reception plate method, as applied so far, yields a systematic underestimate of the real source power when coupled plates are used. This is due to difficulties in the loss factor measurement. Other difficulties can occur in the field, such as in estimating the plate mass e.g. defining the subsystem boundaries, and in accurately sampling of the velocity field.

Assuming linear systems a power calibration can be used to circumvent the above difficulties. A source with known power input, like the shaker with in-line force transducer, is attached to the receiving plate and the average plate velocity measured. The ratio of imparted power to the average velocity is constant and the power of the test source is obtained from (5).

$$\frac{P_{calibration}}{\overline{\tilde{v}}^2_{calibration}} = \frac{P_{source}}{\overline{\tilde{v}}^2_{source}} \tag{5}$$

In Figure 9 is shown the power from a vibrating lightweight stair excited by the ISO tapping machine by use of the power calibration function and by a reciprocal method[3]. The power obtained from the reciprocal method is used as benchmark here since direct power measurement was not possible. Using the power calibration function an acceptable agreement is obtained. In the case considered the stair was point connected to the stair wall and could be removed for the actual power calibration. The accuracy of the method should be investigated further for sources with multiple contacts and for cases where direct access to the source contacts is not possible.

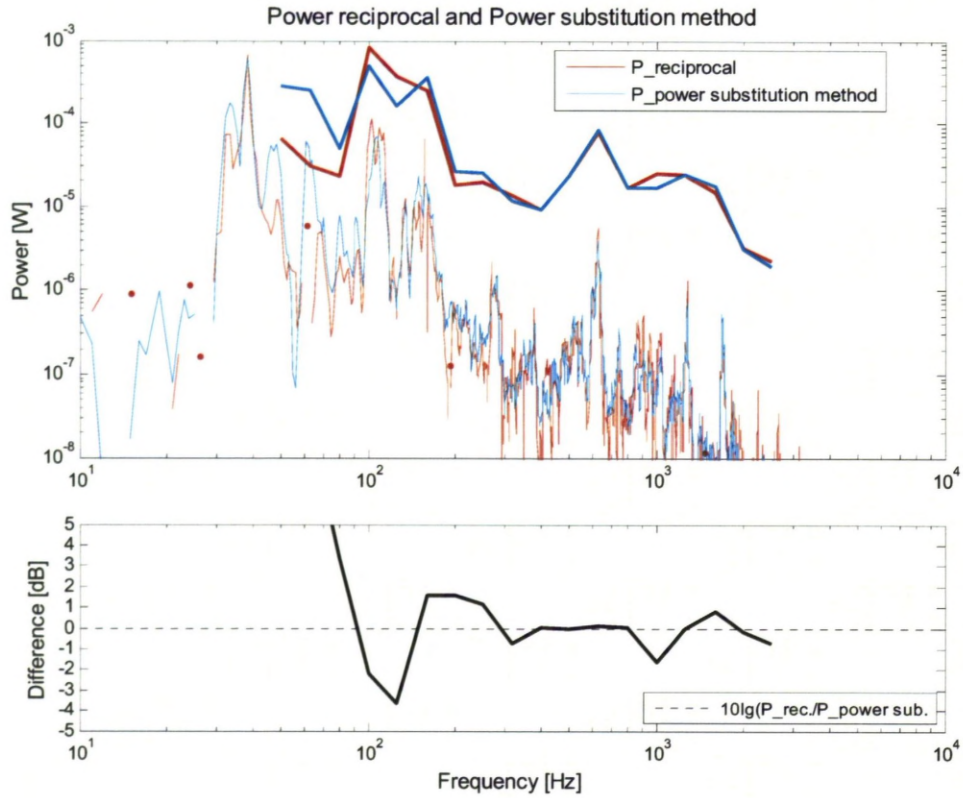

Figure 9. Power measured directly and from reception plate method with total loss factor from T5

REFERENCES

1. M.M. Spaeh, B.M. Gibbs, Reception plate method for characterization of structure-borne sources in buildings: Assumptions and application, Applied Acoustics 70, 361-368, 2009.
2. E.B. Evans, Characterization of structure-borne noise sources using a reverberant or anechoic plate, Proc. Internoise 06, Hawaii, 2006.
3. J. Scheck et al., Towards a prediction of the sound transmission from lightweight stairs, Acoustics '08, Paris.
4. F. Jacobsen, J. H. Rindel, Letters to the Editor: Time reversed decay measurements, Journal of sound and vibration, 117(1), 187-190, 1987.
5. C. Kling, Investigations into damping in building acoustics by use of downscaled models, Dissertation RWTH Aachen, Logos Verlag Berlin, 2008.
6. R.J.M. Craik, Sound Transmission through Buildings using Statistical Energy Analysis; Gower Publishing Ltd., 1996

euronoise

Towards a prediction of the sound transmission from lightweight stairs

J. Scheck[a], B. M Gibbs[b], A. Drechsler[c] and H.-M. Fischer[c]

[a]Stuttgart University of Applied Sciences, Schellingstrasse 24, 70174 Stuttgart, Germany
[b]University of Liverpool, School of Architecture, Abercromby Square, L693BX Liverpool, UK
[c]University of Applied Sciences, Schellingstr. 24, 70174 Stuttgart, Germany
jochen.scheck@hft-stuttgart.de

The sound transmission from lightweight stairs which are connected to separating walls often gives rise for complaints. One reason for this is that at present there is no prediction method available. Treating the stair as an active component in a similar manner like vibrating machines stairs can be characterised as structure-borne sound sources. The source data then can be used to predict the sound transmission in buildings using parts of EN 12354. Following this approach investigations on a timber stair have been carried out in a staircase test facility. Based on a full characterisation by contact free velocity and mobility and in-situ measurement using an indirect method, more practical methods like the reception plate method and a characterisation based on a reference power calibration are investigated. The source data obtained was used to predict the sound transmission in buildings.

1 Introduction

This paper reports on investigations aimed to provide a laboratory characterisation of lightweight stairs as structure-borne sound sources, in order to then predict the sound transmission in buildings using parts of EN 12354. The characterisation sought was to be on a power basis. Three methods were considered and compared. The first method is based on source activity and mobility and requires complex valued data [1]. However, significant data reduction is possible if unimportant components of excitation can be neglected. This was established by a reciprocal measurement method. The second method seeks to exploit the simplicity of the reception plate method, which has been successfully used previously for isolated plates in laboratories [2]. For practical reasons, a real wall is proposed as a reception plate. However, the obtained power is an underestimate of the source power. This is demonstrated experimentally using a shaker source of known input power. It also is confirmed by reference to Statistical Energy Analysis (SEA) that the underestimate is a result of power-sharing between the walls and floors connected to the reception wall. The third method circumvents this problem by calibrating the selected reception wall with a source of known power, again a shaker. The source considered for test was a lightweight timber stair with the string board rigidly point connected to a single-leaf wall (24 cm CaSi with density 2000 kg/m^3). The wall is connected to 2 similar side walls and 2 concrete floors and is contained in a test facility for stairs (Fig. 1).

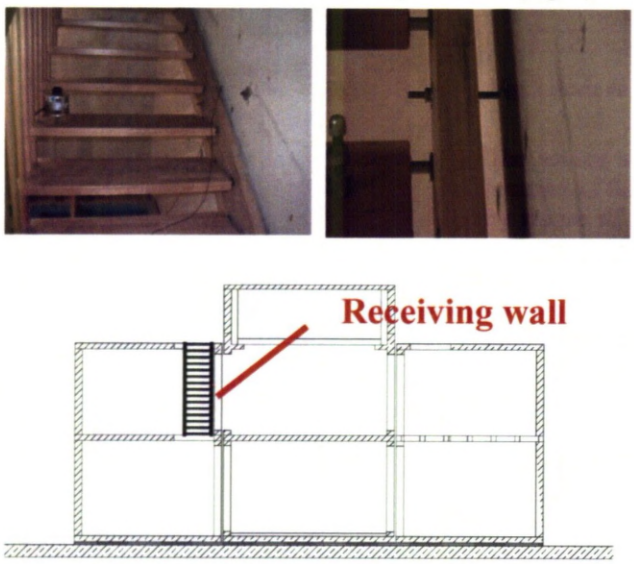

Fig.1 Investigated stair system (top) and test facility for stairs (bottom)

2 Source activity and mobility

Stairs firstly constitute passive structures that become active due to excitation by a walking person or a tapping machine. If the stair system and the excitation are treated as one system, then source characterisations developed for vibrating machines can be used. This is straightforward since the vibration behaviour of stairs is complicated and hardly predictable [3]. The source activity can be expressed as the free velocity or blocked force. The transmitted structure-borne sound power to a receiving structure then is a function of source activity and mobility and of receiver mobility [4]. For a full description of the transmission, three quantities are required for each contact and for up to six components of excitation at each contact [5-7]. An independent source characterisation is possible (the source descriptor), using the free velocity and source mobility [8]. Then when combined with the receiver mobility, in the form of the coupling function, the installed power is obtained (Fig. 2).

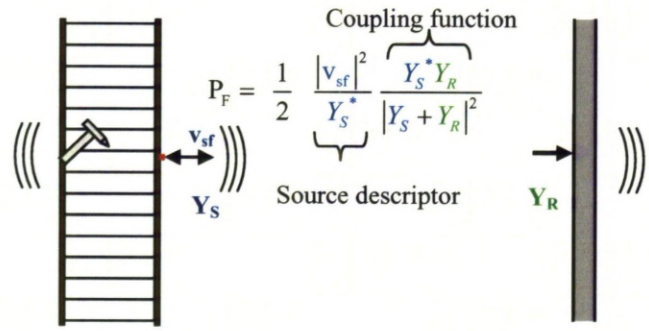

Fig.2 Stair as active component – source descriptor concept

The source activity of the stair strongly depends on the location of the excitation. This effect can be considered e.g. by means of averaging the free velocities to be measured over all steps.

2.1 Data reduction

The characterisation by free velocity and mobility becomes complicated or even intractable when several contacts and degrees of freedom have to be considered. There is a need to establish a hierarchy of the component power transmission (forces and moments) and thence, by elimination of the least influential components, simplify calculation. The power through several components of excitation was investigated in the installed condition using a reciprocal measurement method as described in [3, 9, 10]. The force perpendicular to the wall and the two moments

around the axes in plane of the wall were considered (Fig. 3).

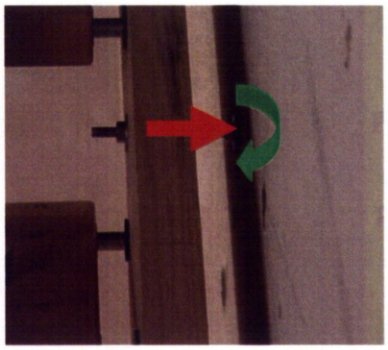

$$P_F = \frac{1}{2}\mathrm{Re}\{F \cdot v^*\}$$

$$P_M = \frac{1}{2}\mathrm{Re}\{M \cdot w^*\}$$

Fig. 3 Excitation of the wall by forces and moments

The stair was excited by a shaker attached to a central step and driven with random noise (Fig. 1). The reciprocally measured component powers are shown in Fig. 4.

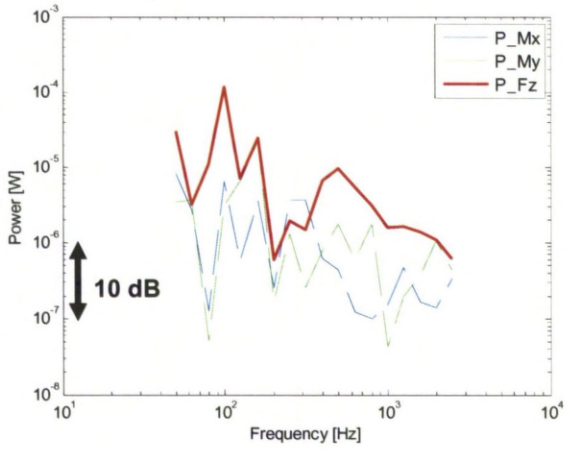

Fig. 4 Component power from stair excited by a shaker on central step

The force perpendicular to the wall is the predominant component in the case considered. This finding allows a significant simplification regarding the prediction of the sound transmission since only the translational component perpendicular to the wall has to be taken into account. A general statement about the role of forces and moments for all types of stairs cannot be deduced from this case study.

According to this result the free velocity (again with the shaker as external source) and mobility were measured with the stair disconnected from the wall as shown in Fig. 5.

Fig.5 Set-up for free velocity and mobility measurement

Fig. 6 shows the contact mobility of the stair to be significantly higher than the contact mobility of the wall. Mobility matching only occurs in the very low frequency range near the fundamental wall mode at 33 Hz. In general the stair constitutes a high-mobility source and thus the blocked force alternatively can be used to characterise the stair system. It can be assumed that this finding holds true for other lightweight stair systems (e.g. steel-wood constructions) since the variations in mass are not significant and also the variation of wall mobilities tends to be small due to requirements on the sound insulation of separating walls. The blocked force can be used as input for the prediction of the sound transmission in buildings according to 12354-2.

In Fig. 7 the power, predicted from free velocity and source and receiver mobility, and by reciprocal measurement, are compared. The agreement is within +/- 3 dB in the relevant frequency range up to 1 kHz. Thus, the free velocity and mobility method is generally applicable for stair systems as building elements.

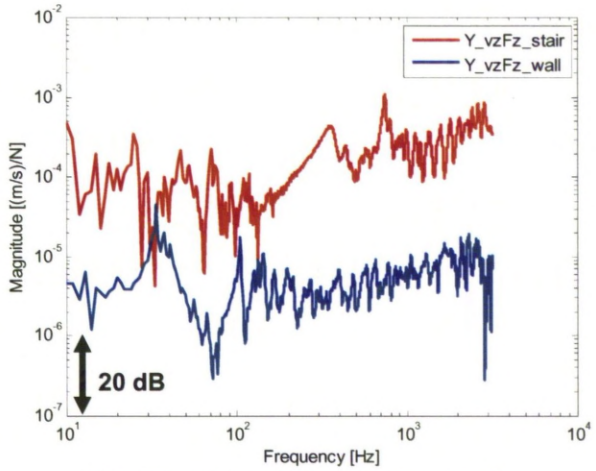

Fig.6 Contact mobility of stair and wall

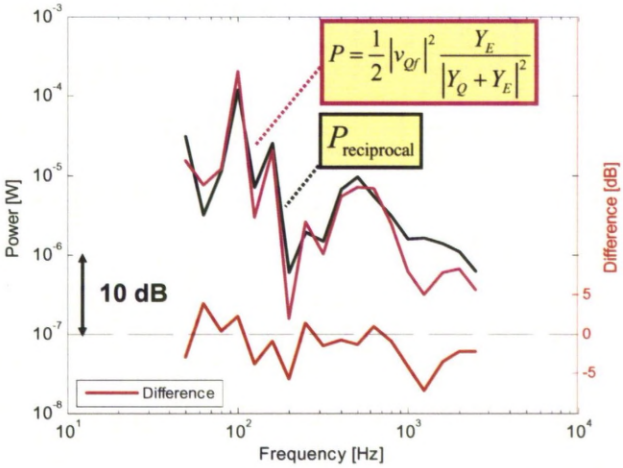

Fig.7 Power predicted from free velocity and mobility and from reciprocal measurement.

3 Reception plate method

The apparent advantage of the reception plate method, when compared to the free velocity and mobility method is the easy application and handling of the data. In [2, 10] it is demonstrated experimentally that the reception plate power equals the cross-spectral power from a connected shaker for free plates but not for walls or floors with the edges bonded into surrounding walls and floors like in real buildings. For

the latter case, a consistent underestimate of the installed power was observed in previous investigations. This problem is addressed using a simplified SEA model.

3.1 Simplified SEA model

A Statistical Energy Analysis (SEA) representation of the reception plate method is given in Fig. 8.

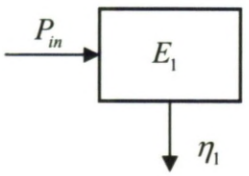

Fig.8 SEA model of a single freely suspended plate

The source power into the isolated plate equals the bending wave energy loss on the plate,

$$P_{in} = \omega E_1 \eta_1 \tag{1}$$

For an isolated plate, the total loss factor is equal to the internal loss factor η_1. The bending wave energy conserved in the plate equals the product of plate mass and spatial average velocity squared over the plate,

$$E_1 = m\overline{\tilde{v}}^2 \tag{2}$$

However, if we attach the source to a wall or floor in a building, then the excited plate is connected to other plates (i.e. walls and floors). Consider the simplest case where the reception wall is connected to a second plate at one edge (Fig. 9).

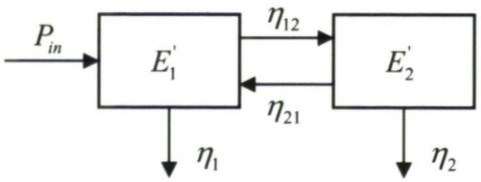

Fig.9 SEA model of two connected plates

The power balance equation for plate 1 is now a function of internal and coupling loss factors,

$$P_{in} = \omega E_1'(\eta_1 + \eta_{12}) - \omega E_2' \eta_{21} \tag{3}$$

The power balance equation for plate 2 is given by,

$$\omega E_2'(\eta_2 + \eta_{21}) = \omega E_1' \eta_{12} \tag{4}$$

Substitution of equation 4 into equation 3 yields,

$$P_{in} = \omega E_1'(\eta_1 + \eta_{12}) - \frac{\omega E_1' \eta_{21}\eta_{12}}{\eta_2 + \eta_{21}} \tag{5}$$

With the assumption that the shaker power into the single free plate 1 is the same as into plate 1 when connected to plate 2, then from (1) and (5) the discrepancy of the plate 1 energy can be expressed as (6).

$$\frac{E_1}{E_1'} = 1 + \frac{\eta_{12}}{\eta_1} - \frac{\eta_{21}\eta_{12}}{\eta_1(\eta_2 + \eta_{21})} \tag{6}$$

Prior to measuring the spatial average square velocity, the loss factor of plate 1 will be obtained as a total loss factor $\eta_{tot} = (\eta_1 + \eta_{12})$ rather than the internal loss factor η_1 of equation (1). Assume the two plates are similar such that $\eta_1 = \eta_2; \eta_{21} = \eta_{12}$. Estimates for the coupling and internal loss factors in buildings can be found in [11], where

$$\eta_{tot} = \frac{1}{\sqrt{f}} + 0.015 \tag{7}$$

Using these values of loss factor, the ratio E_1 / E_1' is about 2 at low frequencies and about 1.5 at high frequencies and thus for two connected plates, the reception plate method would underestimate the exact power by about 3 dB and 2 dB, respectively.

In buildings, walls and floors are usually connected to many more plates (side walls, etc). With the gross assumption of N similar plates with the connected plates only interacting with the directly excited plate 1, all connected plates have the same energy and the energy discrepancy is obtained as,

$$\frac{E_1}{E_1'} = 1 + N\frac{\eta_{12}}{\eta_1} - N\frac{\eta_{21}\eta_{12}}{\eta_1(\eta_2 + \eta_{21})} \tag{8}$$

For 4 connected plates the reception plate method underestimates the exact power by about 6 dB at low frequencies and by 4 dB at high frequencies.

3.2 Experimental investigation

A shaker with a force transducer, for direct power measurement, was attached to the wall and driven with random noise. The spatial average velocity was recorded using a Polytec laser scanning vibrometer on a scanning grid with in total 1100 points distributed over the whole wall surface (Fig. 10).

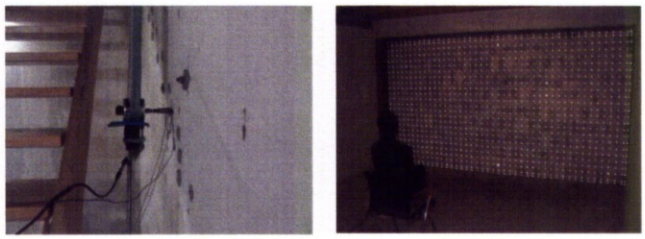

Fig.10 Shaker attached to the wall (left) and laser scanning grid with 1100 points (right)

In Fig. 11 the directly measured power is compared to the value obtained by the reception plate method. Also shown is the value obtained by reciprocal measurements.

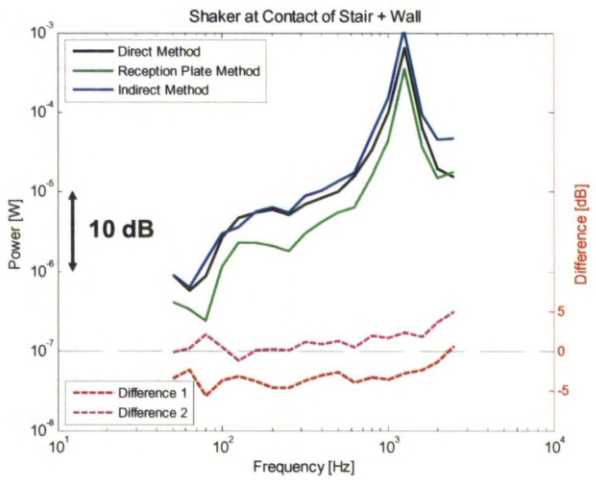

Fig.11 In-situ power from a shaker source attached to wall

The reciprocally measured power overestimates the exact power but is within 2 dB at frequencies up to 1600 Hz. The reception plate power underestimates the exact power. The discrepancy is about 5 dB at low frequencies and reduces with frequency, as predicted from the simplified SEA model. So far, loss factors according to [11] were used for the prediction of the discrepancies. It is well known that the coupling loss factor in (7) tends to overestimate the edge losses in modern buildings [12]. Therefore a more detailed investigation involving measured coupling loss factors is in progress.

4 Power substitution method

The reception plate method as applied so far yields a systematic underestimate of the real source power for coupled plates. The discrepancy depends on the boundary conditions – but in a linear system, it is independent from the source. Therefore a power calibration [13] can be used to circumvent this problem.

Fig. 12 and Fig. 13 show the power from the vibrating stair excited by a shaker and the tapping machine obtained by the reception plate method, using the power calibration function and by the reciprocal method. Again a significant underestimation of the stair power by the reception plate method is observed. Using the power calibration function an acceptable agreement is obtained. The method is thus found very useful for the purpose of characterising sources where the use of coupled reception plates only is possible or practical.

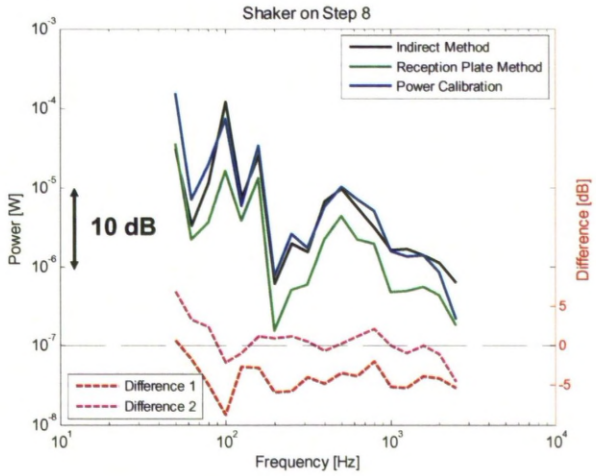

Fig.12 In-situ power from the stair excited by a shaker driven with random noise

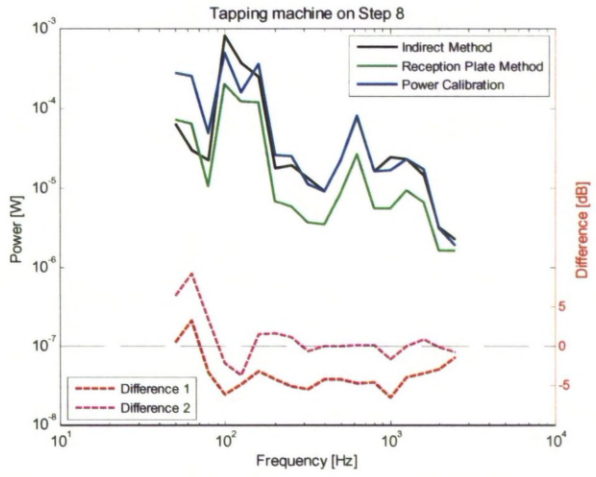

Fig.13 In-situ power from the stair excited by the tapping machine

5 Conclusion

A mobility method, a reception plate method and a power substitution method have been considered to characterise structure-borne sound sources, with a timber stair system as a case study. Stairs are treated as active elements with respect to an arbitrary external excitation e.g. by the tapping machine or a walking person. A precise characterisation is obtained from the free velocity and mobility. For the investigated timber stair, the characterisation can be reduced to one component which is the force perpendicular to the receiving structure. Furthermore the stair constitutes a high-mobility source when attached to typical separating walls in solid buildings. Data acquisition for the (future) prediction of the sound transmission from lightweight stairs according to EN 12354 is thus significantly simplified. The blocked force can be used to characterise the stair system at least when solid building situations are considered.

The reception plate method gives a systematic underestimate for reception plates coupled to other plates, such as is found in buildings. This was confirmed experimentally and by a simplified SEA model.

A power substitution method was successfully applied as a simple characterisation of structure-borne sound sources where the use of coupled reception plates, such as walls and floors, only is possible or practical.

References

[1] B.M.Gibbs, N.Qi, A.T.Moorhouse: 'A practical characterisation for vibro-acoustic sources in buildings', Acta Acustica united with Acustica 93, 84-93, 2007.

[2] M.M. Späh: 'Characterisation of structure-borne sound sources in buildings', PhD thesis, University of Liverpool, (2006).

[3] Scheck, J. et al.: Approach for the Characterisation of Wooden Staircases as Structure-borne Sound Sources, Forum Acusticum 2005, Budapest.

[4] L. Cremer., M. Heckl, B. A. T. Petersson, Structureborne Sound", Springer Verlag (2005)

[5] B. A. T. Petersson, B. M Gibbs, "Towards a structureborne sound source characterization", Applied Acoustics 61, 325-343 (2000)

[6] A. T. Moorhouse, "On the characteristic power of structure-borne sound sources", J. Sound and Vibration 248(3), 441-459 (2001)

[7] T. ten Wolde, T. G. R. Gadefelt, "Development of standard methods for structure-borne sound emission", Noise Control Engineering Journal 28, 5-14 (1987

[8] Mondot, Petersson: 'Characterisation of structure-borne sound sources: the source descriptor and the coupling function', Journal of sound and vibration 114, pp. 507-518, 1987.

[9] Scheck, J. et al.: Structure–borne Power transmission from a lightweight Stair into a connected wall. The Thirteenth International Congress on Sound and Vibration, ICSV 13, Wien.

[10] Scheck, J. et al.: Direct and indirect methods to assess the structure-borne power transmission into receiving structures, ICA 19, Madrid.

[11] Craik, R.J.M.: Sound transmission through buildings using statistical energy analysis, Gower Publishing Limited, (1996).

[12] Fischer, H.-M. et al.: Einheitliches Konzept zur Berücksichtigung des Verlustfaktors bei Messungen und Berechnung der Schalldämmung massiver Wände, DAGA 2001, Hamburg.

[13] Ohlrich, M. et al.: Round Robin test of technique for characterizing the structure-borne sound-source-strength of vibrating machines, Euronoise 2006, Tampere.

Characterisation of a Wooden Stair as Structure-borne Sound Source

J. Scheck[1], Barry Gibbs[2], H.-M. Fischer[1]

[1]*Hochschule für Technik Stuttgart, Schellingstr. 24, D-70174 Stuttgart, Email: jochen.scheck@hft-stuttgart.de*

[2]*University of Liverpool - Acoustics Research Unit, Liverpool L69 3BX*

Introduction

A characterisation of lightweight stairs as structure-borne sound sources is needed to predict the sound transmission in building situations. An approach is followed where a stair is treated as an active component, in a similar manner to that used for vibrating machines (Figure 1) [1]. For a given external excitation e.g. by the tapping machine or a walking person the characterisation is obtained from the measured contact free velocity and mobility. A characterisation based on measurements is practical since the vibration behaviour is complicated which was already shown in [2]. The system under investigation is a straight wooden stair with stringboard rigidly point connected (Figure 2) to a single-leaf receiver wall (24 cm CaSi, density 2000 kg/m^3) which is a typical separating wall in dwellings. To make sure that excitation of the wall results only from transmission through this wall contact the stair is resiliently supported on the ceilings.

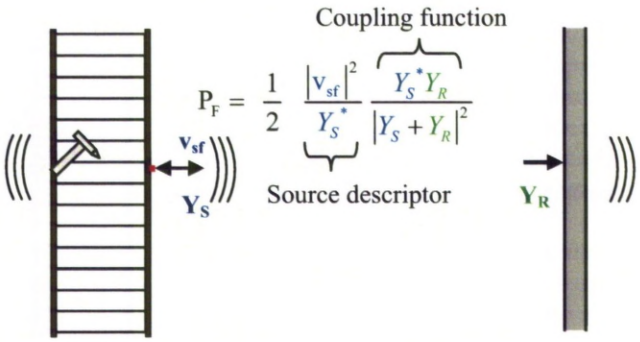

Figure 1: stair as active component – source descriptor concept

Predominant component of excitation

Before the characterisation as illustrated above was applied the predominant components of excitation were identified in the installed condition by means of a reciprocal method [3]. The force perpendicular to the wall and the two moments around the axes in plane of the wall were considered (Figure 2). A shaker attached to a central step (Figure 4) was used for the excitation of the stair. As a result the force perpendicular to the wall was clearly identified to be the predominant component in the case considered. This finding allows a significant simplification regarding the characterisation and prediction of the sound transmission into a receiving room using EN 12354 since only the translational z-component (perpendicular to the wall) has to be taken into account. A general statement about the role of forces and moments for all types of stairs cannot be deduced from this case study. It is however indicated that moment excitation is not as important as it could have been assumed regarding the screwed connection as a lever.

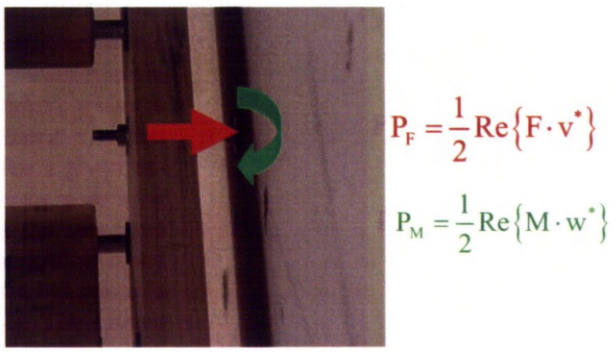

Figure 2: excitation of the wall by forces and moments

Characterisation by free velocity and mobility

The translational contact free velocity and mobility were measured for the z-component (perpendicular to the wall). Figure 3 shows the contact mobility of the stair to be significantly higher than the contact mobility of the wall. Mobility matching only occurs in the very low frequency range near the fundamental wall mode. In general the stair constitutes a force source and thus the blocked force can equally be used to fully characterise the stair system. It can be assumed that this finding still holds true for other lightweight stair systems (e.g. steel-wood constructions) since the variations in mass are not significant and also the variation of wall mobilities tends to be small due to requirements on the sound insulation of separating walls. The blocked force can be used as input quantity for the prediction of the sound transmission in buildings according to 12354-2 [4].

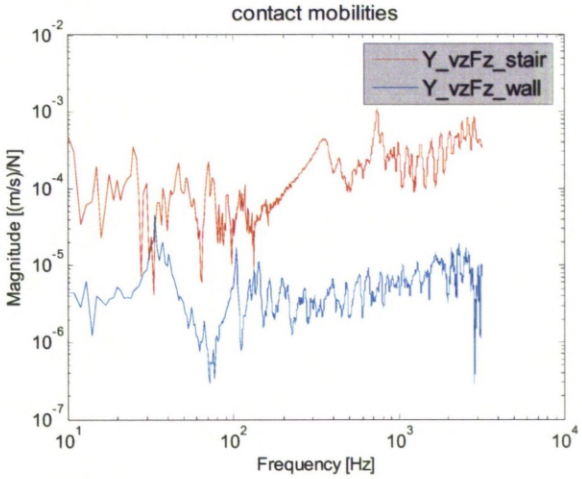

Figure 3: contact mobilities of stair and wall

The contact free velocity was measured for excitation of the stair at the same position as in the former experiment (Figure 4) and afterwards for the tapping machine situated on the central step near the wall contact.

Figure 4: setup for free velocity measurement

From this data the power imparted to the wall was predicted as narrow band values and finally converted into 3rd octave band values. Figure 5 shows the comparison of the predicted power to the "in-situ" power obtained by the reciprocal method. The agreement is very good in the relevant frequency range up to 1 kHz. Thus it can be stated that the free velocity and mobility method is applicable to characterise stair systems as building elements.

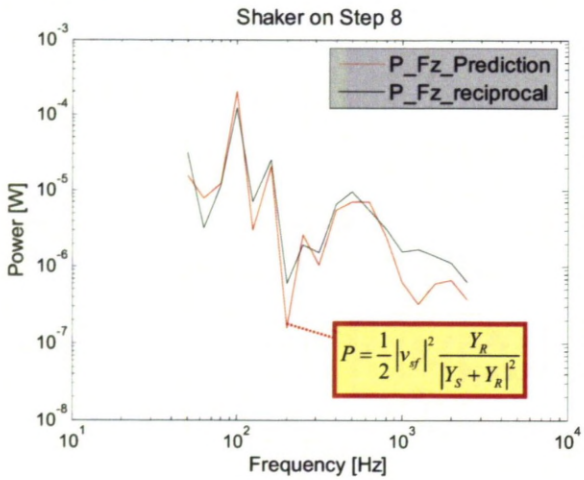

Figure 5: predicted and "in-situ" measured power transmission for excitation of the stair with a shaker

Reception plate method

The free velocity and mobility method is precise but on the other hand time consuming and complicated especially regarding multiple contacts where the interaction between contact points has to be considered. In addition handling of the data is complicated since complex narrow band values are required. For this reason the so-called reception plate method is investigated. The method was initially developed for the simplified characterisation of service equipment like for example sanitary installations. The power emitted by the source can be estimated from the spatial average velocity, loss factor and mass of the plate. In [5] it is shown that this method is appropriate when the reception plate is a free plate with known mass. In the case considered the stair wall is not a free plate but connected to the surrounding walls and ceilings. However the method was applied for the excitation of the stair by the tapping machine. In Figure 6 the "in-situ" power from the reception plate method is compared with the prediction from mobility and free velocity.

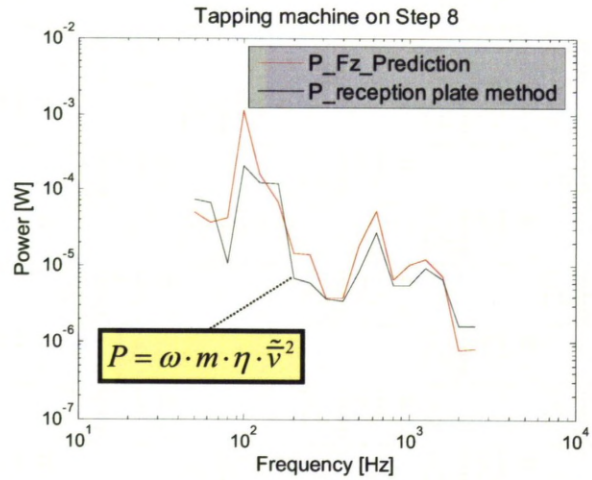

Figure 6: predicted and "in-situ" measured power transmission for excitation of the stair with the tapping machine

The agreement is promising but it is found that the reception plate method tends to underestimate the power going into the wall. This could be due to the sampling of the point velocities, measurement of the loss factor or estimation of the mass. A detailed investigation is currently in progress.

Summary

Different measurement methods were investigated in order to characterise stair systems as structure-borne sound sources. The stair is treated as an active element with respect to an arbitrary external excitation e.g. by the tapping machine or a walking person. A precise characterisation is obtained from the free velocity and mobility. The reception plate method can be used for a simplified characterisation. From these methods input data appropriated for the prediction of the sound transmission of stairs in buildings is obtained [4]. The proceeding is simplified by the fact that stairs constitute force sources when attached to separating walls.

References

[1] Mondot, Petersson: 'Characterisation of structure-borne sound sources: the source descriptor and the coupling function', Journal of sound and vibration 114, pp. 507-518, 1987.

[2] Scheck, J. et al.: Approach for the characterization of a Wooden Staircase as Structure–borne Sound Source. Fortschritte der Akustik, DAGA 2005, München.

[3] Scheck, J. et al.: Structure–borne Power transmission from a lightweight Stair into a connected wall. The Thirteenth International Congress on Sound and Vibration, ICSV 13, Wien.

[4] Drechsler, A. et al.: Wie kann die Trittschallübertragung leichter Treppen prognostiziert werden?, Fortschritte der Akustik, DAGA 2007, Stuttgart.

[5] M.M. Späh: 'Characterisation of structure-borne sound sources in buildings', PhD thesis, University of Liverpool, (2006).

ICSV13 - Vienna
The Thirteenth International Congress on Sound and Vibration
Vienna, Austria, July 2-6, 2006

STRUCTURE-BORNE POWER TRANSMISSION FROM A LIGHTWEIGHT STAIR INTO A CONNECTED WALL

Jochen Scheck*[1], Barry Gibbs[2], and Heinz-Martin Fischer[1]

[1]Stuttgart University of Applied Sciences, Schellingstraße 24, D-70174 Stuttgart, Germany
[2]School of Architecture and Building Engineering, University of Liverpool, L69 3BX, UK
Jochen.Scheck@hft-stuttgart.de

Abstract

Measurement and prediction of the structure-borne powers from vibro-acoustic sources in buildings is an important task. It is in particular useful to evaluate the predominant components of excitation (forces and moments) since this can lead to simplifications in the representation by, for example, neglecting the least significant components. In the installed condition, direct measurement of the component powers is difficult or even impossible since it requires the installation of force transducers between the source and receiver. The registration of moments is particularly problematical. Using reciprocity principles, an indirect method is investigated that circumvents these difficulties. The reciprocal method was applied to investigate the power flow from a vibrating lightweight stair into a receiving wall through a single contact. The aim was to establish the predominant components of excitation and thus simplify the characterisation of the stair as structure-borne sound source by means of the contact free velocity and mobility.

INTRODUCTION

Prediction of the structure-borne sound transmission from vibro-acoustic sources in buildings is complicated because several contacts and up to six degrees of freedom can contribute to the overall emission. There is a need to establish a hierarchy of transmission paths and thence, by elimination of the least influential components, simplify calculation. The full transmission process can only be investigated accurately in the installed condition but the direct measurement of forces and moments at the contact(s) however is difficult or even impossible. In this paper a reciprocal method is investigated that circumvents the problem of registering force and moment directly. The method was applied to investigate the power flow from a vibrating lightweight stair into a receiving wall through a single contact.

RECIPROCAL METHOD

For a single contact point, there are up to six degrees of freedom (3 translational; 3 rotational), which can contribute on the excitation of a receiving structure; in this case, a wall which supports a lightweight stair system.

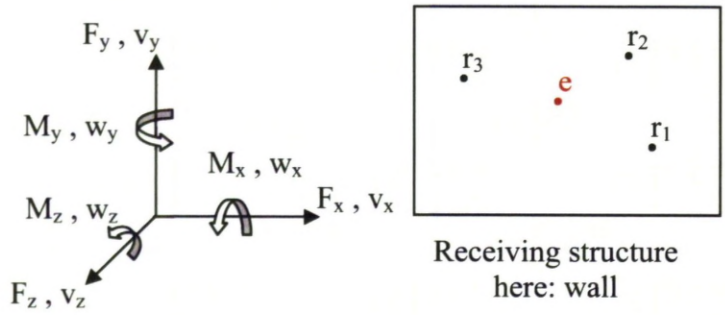

Figure 1 – coordinate system: e = excitation point; r = remote point

The structure-borne power, imparted to the wall by a force F_e and a moment M_e acting at the contact e is given by [1]:

$$P_{F_e} = \frac{1}{2}\mathrm{Re}\left\{F_e \cdot v_e^*\right\} \qquad P_{M_e} = \frac{1}{2}\mathrm{Re}\left\{M_e \cdot w_e^*\right\} \tag{1}$$

All quantities in equation (1) are complex, the asterisk denotes complex conjugate. The component powers are obtained directly if the cross-spectrum of force and translational velocity, and moment and angular velocity, are known. Direct measurement of the cross-spectra requires the installation of transducers to register force or moment directly which is difficult or even impossible. Using reciprocity principles, these practical measurement difficulties can be circumvented.

Single component case

In the simplest case, the receiving structure (the wall) is excited by a perpendicular force $F_{e,z}$ only. Under action of this force the translational response velocity at the contact point e is $v_{e,z}$. Considering an arbitrary remote point r excited simultaneously the translational response velocity at this point is $v_{r,z}$. The power transmitted through the contact is:

$$P_{F_{e,z}} = \frac{1}{2}\mathrm{Re}\left\{F_{e,z} \cdot v_{e,z}^*\right\} = \frac{1}{2}\mathrm{Re}\left\{F_{e,z} \cdot v_{e,z}^* \cdot \frac{v_{r,z}}{v_{r,z}}\right\} = \frac{1}{2}\mathrm{Re}\left\{Y^{-1}_{v_{r,z}F_{e,z}} \cdot v_{e,z}^* \cdot v_{r,z}\right\} \tag{2}$$

$Y_{v_{r,z}F_{e,z}}$ is the transfer mobility from the contact point e to the reference point r. It can be measured reciprocally by exciting the remote point and registering the velocity at the contact point, where $Y_{v_{r,z}F_{e,z}} = Y_{v_{e,z}F_{r,z}}$. Thus this arrangement converts the problem of direct force measurement to a simpler transfer mobility measurement and cross-spectra of velocities. Transfer mobilities can easily be measured using a calibrated hammer and a pair of matched accelerometers situated in equal distance around the contact point. The velocity at the contact point is given by the average of the accelerometer signals.

Multi component case

The reciprocal method as described above can be expanded to the problem of multiple degrees of freedom and points of excitation. Consider the case of a perpendicular force F_z and two moments M_x and M_y at a single contact. The net active power is:

$$P = \frac{1}{2}\mathrm{Re}\left\{F_{e,z} \cdot v^*_{e,z} + M_{e,x} \cdot w^*_{e,x} + M_{e,y} \cdot w^*_{e,y}\right\} \tag{3}$$

The contribution of the remaining components $F_{e,x}$, $F_{e,y}$ and $M_{e,z}$ is assumed to be insignificant, which is reasonable for typical walls and ceilings in buildings [2]. It also is assumed that cross-coupling between components (for example, the excitation of velocity $v_{e,z}$ by moment $M_{e,x}$) can be neglected at central locations of the receiving structure.

Three remote points r_1, r_2, r_3 are required for estimating the three excitation components. The translational velocities at the remote points with the source in operation result from a superposition of all components including cross-transfer terms:

$$\begin{Bmatrix} v_{r1,z} \\ v_{r2,z} \\ v_{r3,z} \end{Bmatrix} = \begin{bmatrix} Y_{v_{r1,z}F_{e,z}} & Y_{v_{r1,z}M_{e,x}} & Y_{v_{r1,z}M_{e,y}} \\ Y_{v_{r2,z}F_{e,z}} & Y_{v_{r2,z}M_{e,x}} & Y_{v_{r2,z}M_{e,y}} \\ Y_{v_{r3,z}F_{e,z}} & Y_{v_{r3,z}M_{e,x}} & Y_{v_{r3,z}M_{e,y}} \end{bmatrix} \cdot \begin{Bmatrix} F_{e,z} \\ M_{e,x} \\ M_{e,y} \end{Bmatrix} \tag{4}$$

By virtue of reciprocity the moment cross-transfer mobility can be replaced by its associated force cross-transfer mobility e.g. $Y_{v_{r,z}M_{e,x}} = Y_{w_{e,x}F_{r,z}}$ which requires no moment excitation. The angular velocity required in the reciprocal measurement is obtained using the finite difference approximation e.g. a pair of matched accelerometers. In order to obtain the phase relationship between the excitation components, a reference point r_1 is used with complex velocity transfer functions φ between it and remote points r_2, r_3. The components are then obtained by inversion of the mobility matrix as complex values phase linked to r_1:

$$\begin{Bmatrix} F_{e,z} \\ M_{e,x} \\ M_{e,y} \end{Bmatrix} = \begin{bmatrix} Y_{v_{e,z}F_{r1,z}} & Y_{w_{e,x}F_{r1,z}} & Y_{w_{e,y}F_{r1,z}} \\ Y_{v_{e,z}F_{r2,z}} & Y_{w_{e,x}F_{r2,z}} & Y_{w_{e,y}F_{r2,z}} \\ Y_{v_{e,z}F_{r3,z}} & Y_{w_{e,x}F_{r3,z}} & Y_{w_{e,y}F_{r3,z}} \end{bmatrix}^{-1} \cdot \begin{Bmatrix} 1 \\ \varphi(v_{r1,z}, v_{r2,z}) \\ \varphi(v_{r1,z}, v_{r3,z}) \end{Bmatrix} \cdot \left| v_{r1,z} \right| \tag{5}$$

The velocities at the contact point are equally obtained as complex values phase linked to r_1 from autospectra and velocity transfer functions:

$$\begin{Bmatrix} v_{e,z} \\ w_{e,x} \\ w_{e,y} \end{Bmatrix} = \begin{Bmatrix} \varphi(v_{r1,z}, v_{e,z}) \\ \varphi(v_{r1,z}, w_{e,x}) \\ \varphi(v_{r1,z}, w_{e,y}) \end{Bmatrix} \cdot \left| v_{r1,z} \right| \tag{6}$$

The component powers accordingly are:

$$\begin{aligned} P_{F_{e,z}} &= \frac{1}{2}\mathrm{Re}\left\{ F_{e,z} \cdot \left| v_{r1,z} \right| \cdot \varphi^*(v_{r1,z}, v_{e,z}) \right\} \\ P_{M_{e,x}} &= \frac{1}{2}\mathrm{Re}\left\{ M_{e,x} \cdot \left| v_{r1,z} \right| \cdot \varphi^*(v_{r1,z}, w_{e,x}) \right\} \\ P_{M_{e,y}} &= \frac{1}{2}\mathrm{Re}\left\{ M_{e,y} \cdot \left| v_{r1,z} \right| \cdot \varphi^*(v_{r1,z}, w_{e,y}) \right\} \end{aligned} \tag{7}$$

Note that the contact velocities are measured as "sum" of all excitation components and thus involve cross-coupling between components. For this reason it is in principle not possible to segregate and quantify the relative contribution of the components due to the pure and cross mobility terms.

EXPERIMENTAL RESULTS

Validation by a shaker experiment

The reciprocal method was applied to investigate the structure-borne sound transmission from a shaker source driven with random noise attached to a staircase wall through a force transducer, to obtain the force directly (Figure 2). To avoid moment excitation, a piano wire formed the contact with the wall.

Despite the fact that the shaker represents a pure force source three components $F_{c,z}$, $M_{c,x}$ and $M_{c,y}$ were assumed to contribute to the excitation of the wall.

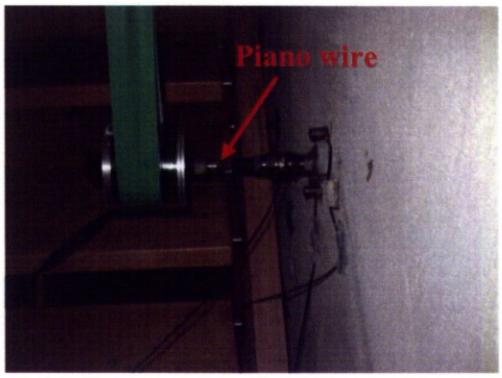

Figure 2 – shaker experiment: set-up

In Figure 3 the force spectra obtained directly and reciprocally are shown as narrow band and 3rd octave band values. The agreement is satisfactory up to about 1.5 kHz. The discrepancy at higher frequencies is due to a longitudinal resonance of the piano wire at approximately 800 Hz resulting in a force maximum and a strong decrease to higher frequencies along with insufficient signal/noise ratio in the reciprocal measurement. In the frequency range below 1.5 kHz discrepancies at certain frequencies result partly from the measurement of the transfer mobility which is inaccurate when the excitation or response coincides with nodal points.

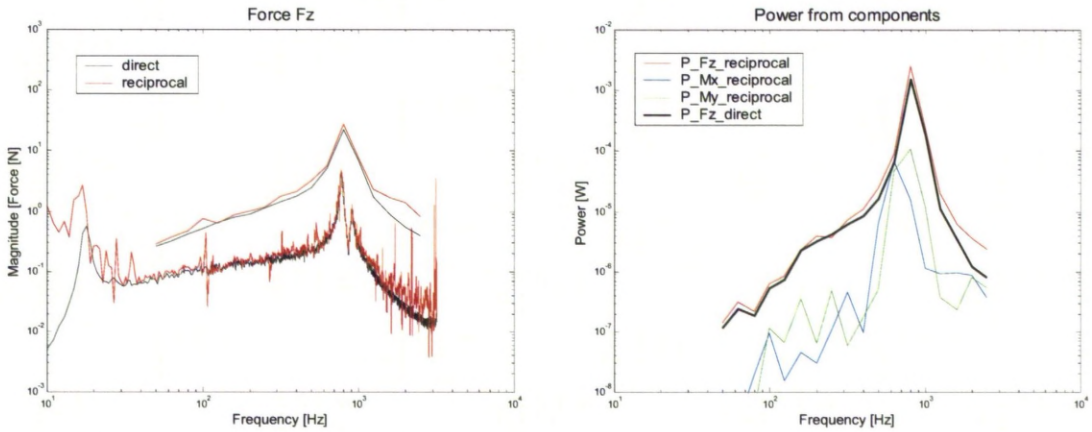

Figure 3 – shaker attached to wall: force (left) and component powers (right) measured directly and reciprocally

The evaluation inevitably gives results for the two moments considered. The respective powers are shown in Figure 3 (right) as 3rd octave band values. The directly and reciprocally measured force induced powers are almost identical. As expected, the moment induced powers are typically well below the force induced power. However, in the frequency range around 600 Hz the moments appear influential. This is likely the result of cross-coupling of the components e.g. the force

produces a high angular velocity. The total power imparted to the wall, including cross coupling, can be written as:

$$\begin{aligned} P_{total} = & \frac{1}{2}\left|F_{e,z}\right|^2 \cdot \mathrm{Re}\left\{Y_{v_{e,z}F_{e,z}}\right\} + \frac{1}{2}\left|M_{e,x}\right|^2 \cdot \mathrm{Re}\left\{Y_{w_{e,x}M_{e,x}}\right\} + \frac{1}{2}\left|M_{e,y}\right|^2 \cdot \mathrm{Re}\left\{Y_{w_{e,y}M_{e,y}}\right\} \\ & + \mathrm{Re}\left\{F^*_{e,z} \cdot M_{e,x}\right\} \cdot \mathrm{Re}\left\{Y_{w_{e,x}F_{e,z}}\right\} + \mathrm{Re}\left\{F^*_{e,z} \cdot M_{e,y}\right\} \cdot \mathrm{Re}\left\{Y_{w_{e,y}F_{e,z}}\right\} \\ & + \frac{1}{2}\mathrm{Re}\left\{M^*_{e,x} \cdot M_{e,y} \cdot Y_{w_{e,x}M_{e,y}}\right\} + \frac{1}{2}\mathrm{Re}\left\{M^*_{e,y} \cdot M_{e,x} \cdot Y_{w_{e,y}M_{e,x}}\right\} \end{aligned} \tag{8}$$

The first row terms give the pure force and moment induced power, the second row terms give the power due to cross-coupling between force and angular velocity. The third row is the power due to cross-coupling between moment and angular velocity at right angle to the moment, and is most likely negligible. The second row terms were calculated from the reciprocally obtained components and the directly measured point cross mobilities from excitation with the shaker. It was found that the second row terms are almost equal to the moment induced powers shown in Figure 2. From this it could be assumed that the apparently high moment induced powers are actually resulting from cross-coupling effects.

In general, the reciprocal measurement of the force induced power as the dominant excitation component is reliable. It is indicated that the reciprocal measurement of the moment induced powers is more sensitive to experimental error at least when moment excitation is not predominant.

Case study: power flow from a vibrating stair

The reciprocal method was applied to investigate the power flow from a vibrating lightweight stair with a single rigid wall contact at a central wall location. Background of this study is the characterization of stairs as structure-borne sound sources allowing a prediction of the sound transmission into a receiving room e.g. the normalized impact sound pressure level. The stair was excited by the shaker attached to a central step and driven with random noise. The experimental set-up is shown in Figure 4, the results in Figure 5.

Figure 4 – vibrating stair: set-up

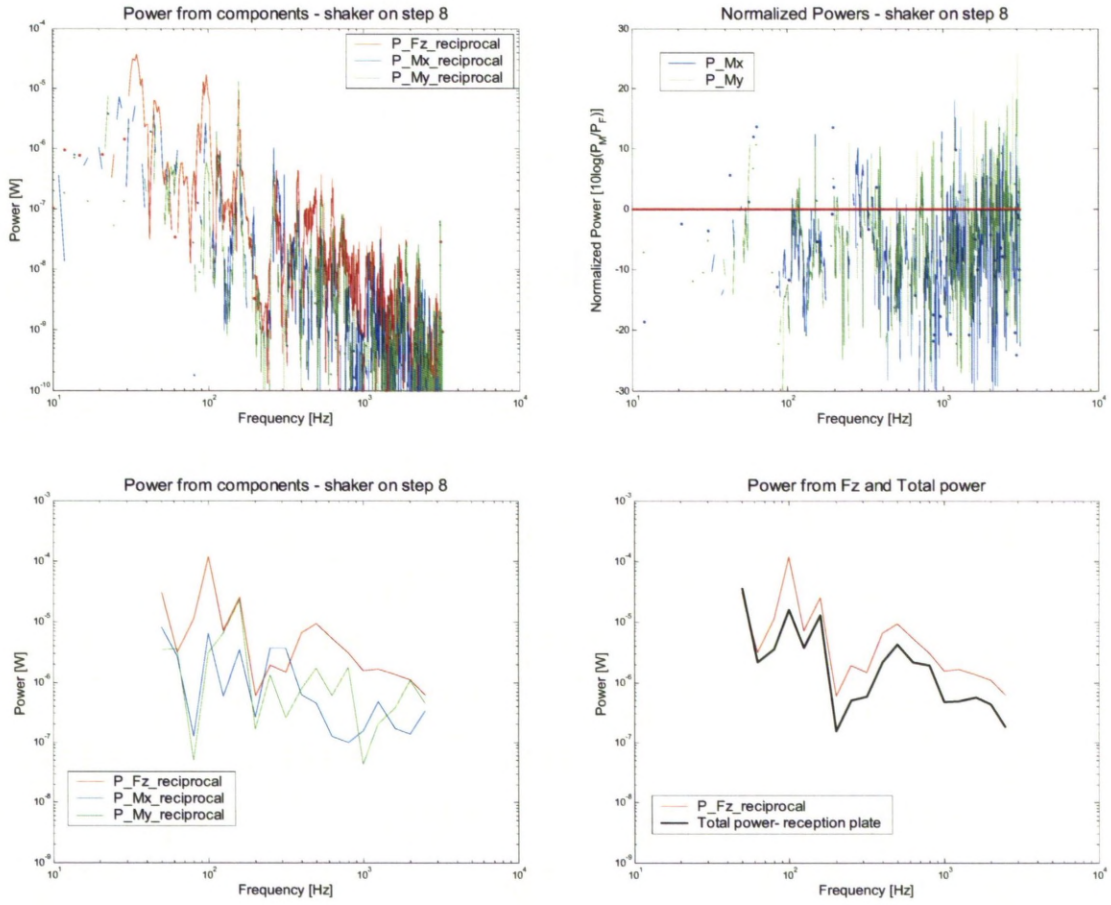

Figure 5 – vibrating stair: narrow band component powers (upper left); normalized component powers (upper right); 3rd octave band component powers (lower left); comparison of force induced power to reception plate power (lower right)

The force induced power is generally dominant within the considered frequency range. This can be seen clearly from the normalized narrow band powers and the component powers in 3rd octave bands. The force curve is generally continuous which indicates that the wall is primarily energised by the perpendicular force. In contrast, the moment induced power curves show discontinuities indicating negative power flow e.g. experimental error. The moment induced power increases with frequency as expected from theory but also contributes to the excitation in the frequency range below 1 kHz which is of prime concern for the impact sound transmission from stairs.

As validation for the results the total power was additionally evaluated from the reception plate approach e.g. measurement of the spatial average velocity and the total loss factor:

$$P = \omega \cdot m \cdot \eta \cdot \tilde{\bar{v}}^2 \tag{9}$$

As shown in the lower right corner of Figure 5 the force induced power is similar to the total power from (9) but generally higher about 3 dB. The same discrepancy occurred for the shaker attached directly to the staircase wall. It is thus assumed that the underestimation of the total power by the reception plate method is related to the "properties" of the wall which differs from an ideal reception plate as investigated in [4] e.g. in the boundary condition.

However the total power is reasonably approximated by force induced power alone and thus neglect of the moment contributions seems to be acceptable within engineering accuracy.

SUMMARY

Reciprocal measurement methods can be used in assessing the relative contribution of several components of excitation from vibrating sources when operating in the installed condition. Problems of directly registering forces and moments are therefore avoided and dimensionally incompatible components can be compared on a power basis.

In the case considered, it has been demonstrated that lightweight timber stair systems, which are attached and supported by a wall separating dwellings, excite the wall predominantly by perpendicular forces. Obviously the normal excitation of the stair causes strong bending vibration of the stringer normal to the wall. Moments can assume importance if the cross mobility of the wall at the contact point is significant, but, in general moments can be neglected. This result points to simplifications in characterising such stair systems as structure-borne sound sources. Only one component of the free velocity [3] needs to be considered, which corresponds to the perpendicular force. This, with the component source mobility, provides sufficient source data for prediction of the installed power by mobility methods.

It also has been demonstrated that a reception plate method can be employed to characterise the stair system on a power basis.

REFERENCES

[1] L. Cremer, M. Heckl: 'Structure-borne Sound', Springer Verlag Berlin, 1996.

[2] S.H.Yap and B.M.Gibbs, *Structure-borne sound transmission from machines in buildings, part 1,* Journal of Sound and Vibration, 222 (1), 85-98, 1999, *part 2,* J 222 (1), 99-113, 1999

[3] Mondot, Petersson: 'Characterisation of structure-borne sound sources: the source descriptor and the coupling function', Journal of sound and vibration 114, pp. 507-518, 1987.

[4] M.M. Späh: 'Characterisation of structure-borne sound sources in buildings', PhD thesis, University of Liverpool, (2006).

19th INTERNATIONAL CONGRESS ON ACOUSTICS
MADRID, 2-7 SEPTEMBER 2007

DIRECT AND INDIRECT METHODS TO ASSESS THE STRUCTURE-BORNE POWER TRANSMISSION INTO RECEIVING STRUCTURES

Scheck, Jochen[1]; Heinz-Martin Fischer[1]; Gibbs, Barry[2]
[1]Stuttgart University of Applied Sciences, D-70174, Germany; jochen.scheck@hft-stuttgart.de
[2]Acoustics Research Unit, The University of Liverpool, UK-L693BX, UK; bmg@liverpool.ac.uk

ABSTRACT
This paper focuses on measurement and prediction methods to assess the structure-borne power transmission from vibro-acoustic sources in buildings. Direct measurement of the "in-situ" power in many cases is difficult or even impossible since it requires the installation of transducers between source and receiver. Using reciprocity principles this difficulty can be circumvented and an indirect method can be used to assess the role of forces and moments in the installed condition. Another indirect method that gives the installed power is the reception plate method. The apparent advantage of this method is that it is easy to apply since the power can be estimated from the mean square velocity, loss factor and mass of the plate. So far it has been demonstrated that the method can be used for a free plate but in real installations the receiving structure is attached to surrounding structures and applicability for this situation is currently under investigation. Finally the installed power can be predicted from the contact free velocity of the source and the contact mobilities of source and receiver. The above methods were applied and compared for a shaker and for a lightweight stair as structure-borne sound sources attached to a receiving wall. The latest results will be presented.

INTRODUCTION
A characterisation of structure-borne sound sources is required to predict the sound transmission in buildings. The characterisation for 'real' sources is mainly based on measurements since the internal mechanisms of structure-borne sources are often complicated and the dynamic behaviour is not predictable from construction data. In order to predict the sound transmission it is sufficient to describe the dynamic behaviour at the contact points with the receiving structure. The required quantities for the characterisation are the free velocity and the mobility at the contacts [1]. The proceeding becomes complicated when several contacts and degrees of freedom have to be considered. Regarding the latter there is a need to establish a hierarchy of the component power transmission (forces and moments) and thence, by elimination of the least influential components, simplify calculation. The full transmission process can only be investigated accurately in the installed condition but the direct measurement of forces and moments at the contact(s) is difficult or even impossible. Using a reciprocal method the problem of registering forces and moments directly can be circumvented and the components' contribution can be assessed in the installed condition without any modifications of the transmission system. Another indirect method to assess the power transmission in the installed condition is the so-called reception plate method. Based on a power balance principle the total power imparted to a structure is easily obtained from the mean square velocity, loss factor and mass of the plate. Taking into consideration the mobility relationship of the source and the reception plate the method can be used for the characterisation of sources. As a result of recent investigations a two reception plate laboratory method is proposed [2]. So far the considered reception plates are free plates. As certain types of sources - like stairs that are considered here - cannot be attached to free plates there is a need to investigate the applicability of the reception plate method for clamped plates. This paper reports on experimental investigations of the above methods using a shaker source and a vibrating timber stair each single point connected to a low mobility receiving wall in a building-like situation. Background of the study is the characterisation of lightweight stairs as structure-borne sound sources as basis for the prediction of their sound transmission in buildings using EN 12354. In the followed approach stairs are treated as active elements in a similar manner to that used to characterise vibrating machines.

MEASUREMENT METHODS

For a single contact point e, there are up to six degrees of freedom (3 translational; 3 rotational), which can contribute on the excitation of a receiving structure as illustrated in Figure 1. Theoretical and experimental case studies that were carried out by e.g. [3, 4] point out that only three degrees of freedom - the force $F_{e,z}$ perpendicular to the structure and the two moments $M_{e,x}$ and $M_{e,y}$ around axes in plane of the wall - are likely to contribute in the general case. Based on this finding the experimental studies in the scope of this work are restricted to these components.

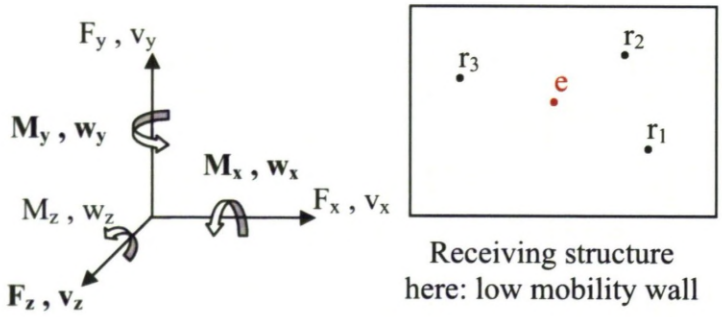

Figure 1.- coordinate system: e = excitation point; r = remote point

Direct method

Considering a pure force $F_{e,z}$ acting perpendicular to the receiving structure the structure-borne power imparted is [5]:

$$P_{F_{e,z}} = \frac{1}{2}\mathrm{Re}\left\{F_{e,z}^{*} \cdot v_{e,z}\right\} = \frac{1}{2}\mathrm{Re}\left\{F_{e,z} \cdot v_{e,z}^{*}\right\} \qquad \text{(Eq. 1)}$$

For pure moment excitation the power transmitted is given by Equation 2 where M is the moment and w the angular velocity in the respective x or y direction:

$$P_{M_e} = \frac{1}{2}\mathrm{Re}\left\{M_e^{*} \cdot w_e\right\} = \frac{1}{2}\mathrm{Re}\left\{M_e \cdot w_e^{*}\right\} \qquad \text{(Eq. 2)}$$

The component powers are obtained directly from the cross-spectrum of force and translational velocity e.g. moment and angular velocity. Measurement of the contact translational or angular velocity at the contact is possible using two accelerometers situated in equal distance around the contact (Figure 2). In order to obtain the translational contact velocity v the signals are averaged whereas the angular velocity w is obtained from the finite difference method. On the other hand direct measurement of the force / moment requires the installation of transducers between source and receiver. For real sources this is difficult or even impossible when the source cannot be detached from the receiver. Even in cases where the installation is possible the presence of a transducer might accidentally change the source characteristics. Using reciprocity principles the installation of transducers can be circumvented.

Reciprocal method

In the simplest case, the receiving structure (the wall) is excited only by a pure force $F_{e,z}$. Under action of this force the translational response velocity at the contact point e is $v_{e,z}$. Considering an arbitrary remote point r excited simultaneously the translational response velocity at this point is $v_{r,z}$. Introducing the transfer mobility between the contact and the remote point Equation 1 can be rewritten as:

$$P_{F_{e,z}} = \frac{1}{2}\mathrm{Re}\left\{F_{e,z} \cdot v_{e,z}^{*}\right\} = \frac{1}{2}\mathrm{Re}\left\{Y^{-1}_{v_{r,z}F_{e,z}} \cdot v_{e,z}^{*} \cdot v_{r,z}\right\} = \frac{1}{2}\mathrm{Re}\left\{Y^{-1}_{v_{e,z}F_{r,z}} \cdot v_{e,z}^{*} \cdot v_{r,z}\right\} \qquad \text{(Eq. 3)}$$

By virtue of reciprocity the transfer mobility from the contact point e to the reference point r can be measured reciprocally by exciting the remote point and registering the velocity at the contact point. Thus this arrangement converts the problem of direct force measurement to simpler transfer mobility and velocity cross-spectra measurements. For the latter a calibrated hammer can be used whereas the velocity transfer function is measured with the source in operation. In

case of moment excitation the same principle is used whereas the transfer mobility in Equation 3 is replaced by a cross-transfer mobility:

$$P_{F_{e,z}} = \frac{1}{2}\mathrm{Re}\left\{M_e \cdot w_e^*\right\} = \frac{1}{2}\mathrm{Re}\left\{Y^{-1}_{v_{r,z}M_e} \cdot w_e^* \cdot v_{r,z}\right\} = \frac{1}{2}\mathrm{Re}\left\{Y^{-1}_{w_e F_{r,z}} \cdot w_e^* \cdot v_{r,z}\right\} \qquad \text{(Eq. 4)}$$

In the more practical case of simultaneous excitation by a force and two moments the net active power is given by Equation 5 preconditioned that cross-coupling between components (for example, the excitation of velocity $v_{e,z}$ by moment $M_{e,x}$) can be neglected.

$$P = \frac{1}{2}\mathrm{Re}\left\{F_{e,z} \cdot v^*_{e,z} + M_{e,x} \cdot w^*_{e,x} + M_{e,y} \cdot w^*_{e,y}\right\} \qquad \text{(Eq. 5)}$$

Three remote points r_1, r_2, r_3 are required for estimating the three excitation components. The translational velocities at the remote points with the source in operation result from a superposition of all components including cross-transfer terms. From inversion of the mobility matrix in Equation 6 the excitation components are obtained as complex values phase-linked to a reference point r_1 through complex velocity transfer functions φ:

$$\begin{Bmatrix} F_{e,z} \\ M_{e,x} \\ M_{e,y} \end{Bmatrix} = \begin{bmatrix} Y_{v_{e,z}F_{r1,z}} & Y_{w_{e,x}F_{r1,z}} & Y_{w_{e,y}F_{r1,z}} \\ Y_{v_{e,z}F_{r2,z}} & Y_{w_{e,x}F_{r2,z}} & Y_{w_{e,y}F_{r2,z}} \\ Y_{v_{e,z}F_{r3,z}} & Y_{w_{e,x}F_{r3,z}} & Y_{w_{e,y}F_{r3,z}} \end{bmatrix}^{-1} \cdot \begin{Bmatrix} 1 \\ \varphi(v_{r1,z}, v_{r2,z}) \\ \varphi(v_{r1,z}, v_{r3,z}) \end{Bmatrix} \cdot \left|v_{r1,z}\right| \qquad \text{(Eq. 6)}$$

The translational and angular contact velocities with the source in operation are equally measured as complex values phase-linked to r_1.

Reception Plate method

The reception plate or reverberant plate method was initially developed and investigated for the practical characterisation of service equipment like for example sanitary installations [3]. The apparent advantage of the reception plate method is that it is comparatively simple to apply. Based on a power balance principle the total power emitted by a source connected to a reception plate can be estimated from the spatial average velocity, loss factor and mass of the plate:

$$P = \omega \cdot m \cdot \eta \cdot \tilde{\bar{v}}^2 \qquad \text{(Eq. 7)}$$

Taking into account the source / receiver mobility relationship a full source characterisation can be derived [2]. Free plates are currently used in laboratories since their plate-mass is exactly defined. In the case considered here a practical characterisation of stairs as structure-borne sound sources shall be obtained from measurements in a special staircase test facility with the receiver walls and ceilings connected to flanking building elements (Figure 2) like in real buildings. Thus applicability of the method for a non-free reception plate was investigated.

PREDICTION

In order to predict the sound transmission into receiving structures a method by [1] is commonly used. The component installed power can be predicted from the contact free velocity v_{sf} of the source and the contact mobilities of source Y_S and receiver Y_R:

$$P = \frac{1}{2}\left|v_{sf}\right|^2 \frac{Y_R}{\left|Y_S + Y_R\right|^2} \qquad \text{(Eq. 8)}$$

The contact free velocity and mobility of the source are measured with the source detached from the receiver and thus constitute inherent source quantities. The method is exact but complex and time consuming especially when multiple contacts and several components are considered. The concept of effective mobility can be used to simplify the proceeding when several contacts are given [6, 7]. The reciprocal method allows to determine the predominant component(s) in the installed condition and thus to reduce the effort for the characterisation significantly.

EXPERIMENTAL INVESTIGATIONS

The above methods were applied for a shaker as sound source and a real source represented by a vibrating stair attached to a single-leaf receiving wall made of 24 cm CaSi with density 2000 kg/m^3 (Figure 2).

Direct method vs. Reciprocal method

In the first step a shaker driven with random noise was used for comparison of the direct and indirect methods since in this case the installation of a force transducer to obtain the power directly was possible. The shaker was attached to a staircase wall at a central point through a force transducer, to obtain the force directly (Figure 2). To avoid moment excitation, a piano wire formed the contact with the wall. Despite the fact that the shaker represents a pure force source three components $F_{e,z}$, $M_{e,x}$ and $M_{e,y}$ were assumed to contribute to the excitation of the wall.

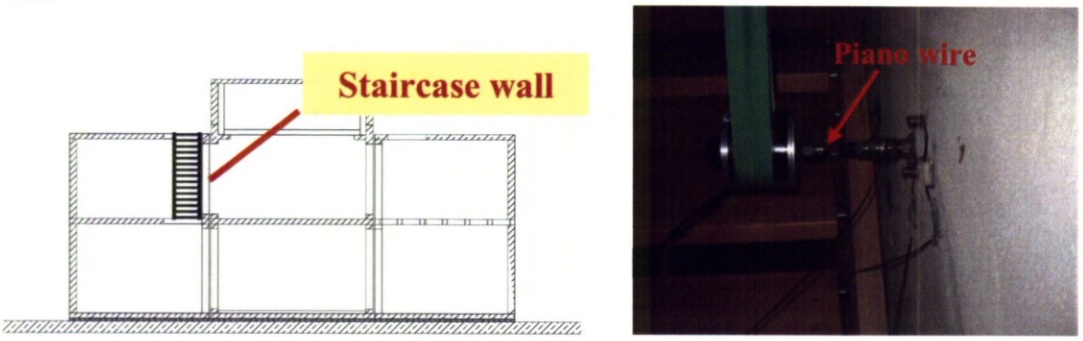

Figure 2.- left: staircase test facility; right: measurement set-up for the shaker experiment

In Figure 3 the force spectra obtained directly and reciprocally are shown as narrow band and 3rd octave band values. The agreement is satisfactory up to about 1.5 kHz. As a result of the type of shaker and the way of attachment to the wall that was used there is a force maximum and a strong decrease to higher frequencies along with insufficient signal/noise ratio in the reciprocal measurement. In the frequency range below 1.5 kHz discrepancies at certain frequencies result mainly from the measurement of the transfer mobility which is inaccurate when the excitation or response coincides with nodal points.

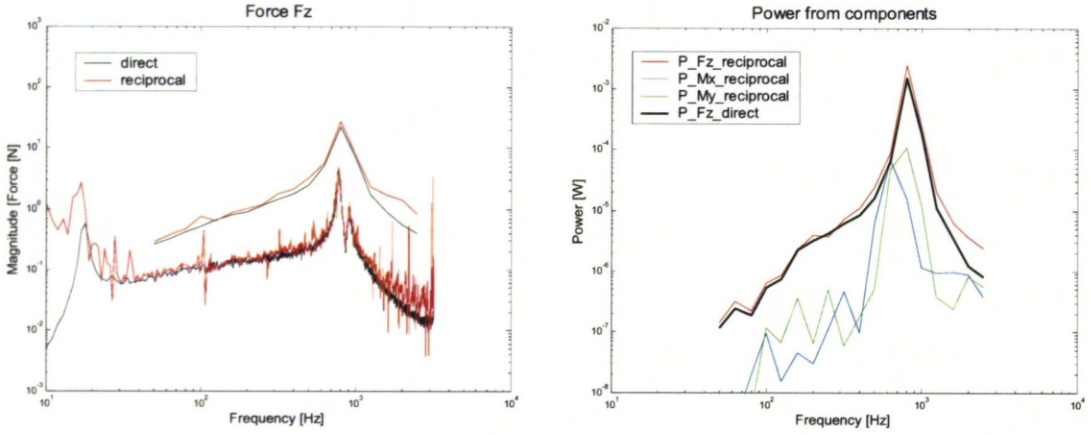

Figure 3.- shaker attached to wall: force (left) and component powers (right) measured directly and reciprocally

The evaluation inevitably gives results for the two moments considered. The respective powers are shown in Figure 3 (right) as 3rd octave band values. The directly and reciprocally measured force induced powers are almost identical and thus the reciprocal method is validated. As expected, the moment induced powers are typically well below the force induced power. However, in the frequency range around 600 Hz the moments appear influential which is likely the result of cross-coupling of the components e.g. the force produces a high angular velocity [8].

Direct method vs. Reception Plate method

In the same arrangement the transmitted power was calculated according to the reception plate method. The spatial average velocity was obtained from 14 arbitrary distributed sampling points. The loss factor was measured using the decay rate method. Figure 4 (left) shows the comparison of the powers as narrow band and 3rd octave band values.

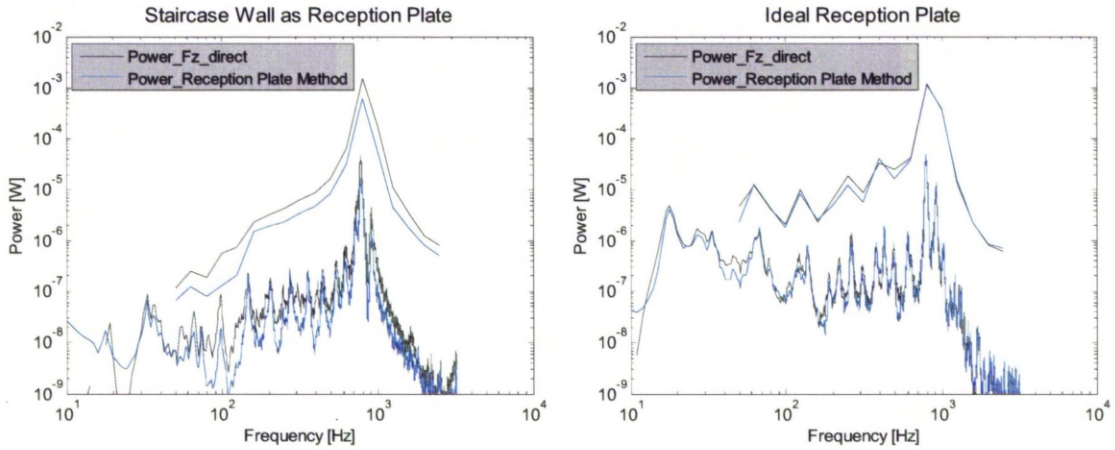

Figure 4.- shaker attached to wall: direct power vs. reception plate power – left: staircase wall; right: reception plate with free edges

The force induced power is similar to the total power from the reception plate approach but generally higher about 3 dB. The graph on the right of Figure 4 shows the comparison of both methods for a similar experiment but using an ideal reception plate made of 10 cm thick concrete with free edges as investigated in [3]. In this case the agreement is excellent. It is thus assumed that the underestimation of the power by the reception plate method is related to the 'properties' of the staircase wall which obviously differs from an 'ideal' reception plate. A similar but more detailed experiment was carried out recently in order to understand the reason for the discrepancies. With the shaker attached to the contact point of stair and wall the whole wall surface was scanned using a Polytec laser scanning vibrometer to obtain the average velocity with maximum accuracy. The evaluation of this experiment could not be completed yet but the first results indicate that the deviation of both methods in the left of Figure 4 is not due to inaccurate sampling.

Prediction vs. Reciprocal method

The reciprocal method was finally applied to investigate the power flow from a vibrating lightweight stair with a single rigid wall contact at a central wall location. The stair was excited by the shaker attached to a central step near the wall contact. As a result the force perpendicular to the wall could be clearly identified to be the predominant component [8]. Consequently the translational contact free velocity and mobility were measured for the z-component (perpendicular to the wall) with the stair moved away from the wall in order to predict the sound transmission into the staircase wall.

From the comparison of the contact mobility of stair and wall it is found that the stair clearly constitutes a force source [9] in the case considered. Accordingly the blocked force could equally be used to fully characterise the stair system at least for the prediction of the sound transmission in massive buildings. From the free velocity and mobilities the power imparted to the wall was predicted as narrow band values and finally converted into 3rd octave band values. Figure 5 shows the comparison of the predicted power to the 'in-situ' measured power obtained by the indirect methods. The agreement with the reciprocal measurement is very good in the relevant frequency range up to 1 kHz confirming that the force component is predominant. The free velocity and mobility method is generally applicable to characterise stair systems as sound sources with respect to an external excitation which could also be the tapping machine or a walking person instead of the shaker considered here. The power obtained from the reception plate method yields an underestimate of the power as expected from the previous experiment.

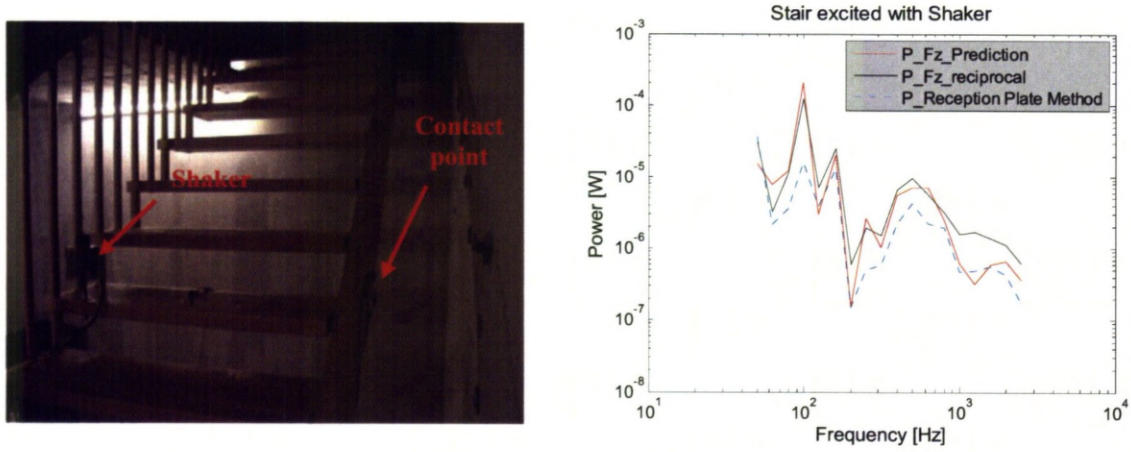

Figure 5.- characterisation of a timber stair excited with a shaker by free velocity and mobility- left: measurement set-up; right: predicted and 'in-situ' measured power

CONCLUSION

Direct and indirect measurement methods to assess the power transmission are investigated in order to characterise sources in general and stair systems in particular as structure-borne sound sources. Using a reciprocal method the component power transmission can be assessed in the installed condition. Problems of directly registering forces and moments are avoided and dimensionally incompatible components can be compared on a power basis. The reception plate method is in excellent agreement with the directly measured power for a plate with free edges but gives a systematic underestimate for a massive receiving wall with clamped edges as found in building situations. Further investigations in order to understand the reason for the discrepancies are in progress.

The indirect measurement methods can be used as benchmarks for comparison with the predicted power from the free velocity and contact mobilities. In the case considered it is demonstrated that lightweight stairs can be characterised as sound sources in a similar manner to that used for vibrating machines. For the investigated timber stair the characterisation can be reduced to one component which is the force perpendicular to the receiving structure. Furthermore the stair constitutes a high mobility force source when attached to typical separating walls in solid building situations. Data acquisition for the (future) prediction of the sound transmission from lightweight stairs according to EN 12354 is thus significantly simplified. The blocked force can be used to characterise the stair system at least when solid building situations are considered.

References:

[1] Mondot, Petersson: 'Characterisation of structure-borne sound sources: the source descriptor and the coupling function', Journal of sound and vibration 114, pp. 507-518, 1987.
[2] B.M.Gibbs, N.Qi, A.T.Moorhouse: 'A practical characterisation for vibro-acoustic sources in buildings', Acta Acustica united with Acustica 93, 84-93, 2007.
[3] M.M. Späh: 'Characterisation of structure-borne sound sources in buildings', PhD thesis, University of Liverpool, (2006).
[4] S.H.Yap and B.M.Gibbs, Structure-borne sound transmission from machines in buildings, part 1, Journal of Sound and Vibration, 222 (1), 85-98, 1999, part 2, J 222 (1), 99-113, 1999
[5] L. Cremer, M. Heckl: 'Structure-borne Sound', Springer Verlag Berlin, 1996.
[6] B.A.T. Petersson, J. Plunt: On effective mobilities in the prediction of structure-borne sound transmission between a source and a receiving structure, Journal of Sound and Vibration 82 (4), 1982
[7] R.A. Fulford, B.M. Gibbs: Structure-borne sound power and source characterisation in multi-point connected systems, Journal of Sound and Vibration 204 (4), 1997
[8] Scheck, J. et al.: Structure–borne Power transmission from a lightweight Stair into a connected wall. The Thirteenth International Congress on Sound and Vibration, ICSV 13, Wien.
[9] Scheck, J. et al.: Characterisation of a Wooden Stair as Structure-borne Sound Source, Fortschritte der Akustik, DAGA 2007, Stuttgart.
[10] H-Y. Lai: Alternative test methods for measuring structure-borne sound power, Inter-Noise 2006, Hawaii (2006)

ForumAcusticum
2 0 0 5

Approach for the Characterisation of Wooden Staircases as Structure-borne Sound Sources

Jochen Scheck [1,2], Heinz-Martin Fischer [1], Barry Gibbs [3], Andreas Drechsler [1]
[1] Fachhochschule Stuttgart – Hochschule für Technik, D-70174 Stuttgart, Email: jochen.scheck@hft-stuttgart.de
[2] Schalltechnisches Treppen-, Entwicklungs- und Prüfinstitut (STEP) GmbH, **www.steponline.de**
[3] University of Liverpool - Acoustics Research Unit, Liverpool L69 3BX

At present it is not possible to predict the sound transmission into adjacent rooms from footfalls on lightweight stairs, which are connected to the separating wall. This is because the dominant transmission process is structure-borne and involves direct excitation of the separating wall, with flanking paths also contributing. A characterization of lightweight stairs as structure-borne sound sources is needed. In particular, a test method is required which will provide data, which will indicate the noisiness of the stair system when installed in a building. An approach is followed where the stair is treated as an active element, in a similar manner to that used to predict the structure-borne power from vibrating machines in buildings and other structures. Investigations on a wooden stair with one rigid contact to the wall have been carried out in the staircase test facility. To get insight into the vibration behaviour of the stair an experimental modal analysis was carried out. It is shown that the vibration behaviour of the stair is determined by beam modes of handrail and string board and plate modes of the single steps. Therefore the vibrations of the stair are strongly dependant on the point of excitation. From this it is obvious that the position of the external source (e.g. the tapping machine) is a major influence regarding the structure borne sound transmission into the wall. Hence a characterization of the stair as structure-borne sound source has to be with respect to the location of the external source. Regarding the excitation of the wall the components of excitation (forces and moments) at the connections between stair and separating wall are considered. An approach is described which allows the power through each component to be obtained in the installed condition by means of a reciprocal method. Using this method the most important components can be identified which allows a simplification of the further proceeding.

1 Introduction

At present it is not possible to predict the sound transmission into adjacent rooms, from footfalls on lightweight stairs, which are connected to the separating wall. Especially at low frequencies excitation by human footfall and transmission is significant and often causes annoyance to the inhabitants. To reduce problems in the future a characterization of lightweight stairs as structure-borne sound sources is required. In particular, a test method is required which will provide data, which will indicate the noisiness of the stair system when installed in a building. Concerning this matter investigations have been carried out on a wooden staircase with string board which is a common type of stair in Germany. In this paper the investigation of the vibration behaviour of the stair and an approach for the characterisation as structure-borne sound source is outlined. Furthermore a reciprocal method is described which allows the power through each component to be obtained in the installed condition.

2 Wooden Staircases

In the case of wooden stairs, attached to walls separating dwellings, structure-borne energy enters the wall through the contact points as shown in figure 1.

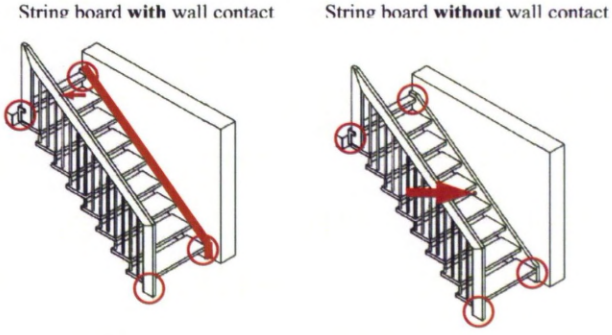

Figure 1: contact points and dominant transmission paths

The stair is supported by the ceilings e.g. the floating floors. Up to now it is common practice to mount the string board directly at the wall using screws. In this case the transmission from the string board into the wall is significant. Experience shows that with the

string board in contact with a common separating wall noise annoyance cannot be avoided. Even the normative requirements on the normalised impact sound pressure level L'_n can hardly be met. The string board must be moved away from the wall as indicated in the right sketch of figure 1. However, the string board still has to be fixed at the wall, for safety reasons (stability when walking on the stair). This can be achieved through one connection [1]. Investigations show that in general transmission through this wall contact is the dominant transmission path. A detailed investigation of the structure-borne energy trans-mission through a single wall contact therefore is the topic of this study.

3 Investigated System

Experimental investigations on a wooden staircase with string board were carried out in a staircase test facility. The string board was moved away from the wall and resiliently supported at both ends. The contact with the wall was through one rigid screwed connection, shown in figure 2. It was confirmed experimentally that, in this set-up, the dominant structure-borne sound transmission was through the screwed contact.

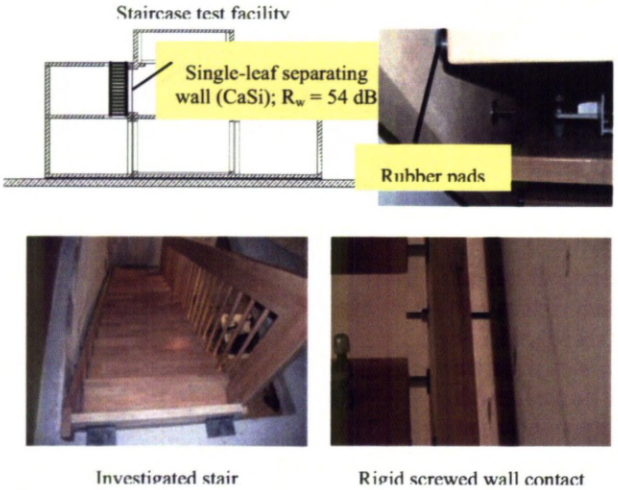

Figure 2: Investigated stair system

4 Experimental modal analysis

The vibration behaviour of the stair is a major influence regarding the excitation of the wall. To get an insight into the dynamic behaviour of the stair, an experimental modal analysis was conducted, using an instrumented hammer. Accelerometers were placed on a central step (the 8th step from the floor), near the contact point and also on the edge of the 5th step. Due to reciprocity, the measured operating deflection shapes, shown in figure 3, result from excitation at the accelerometer positions.

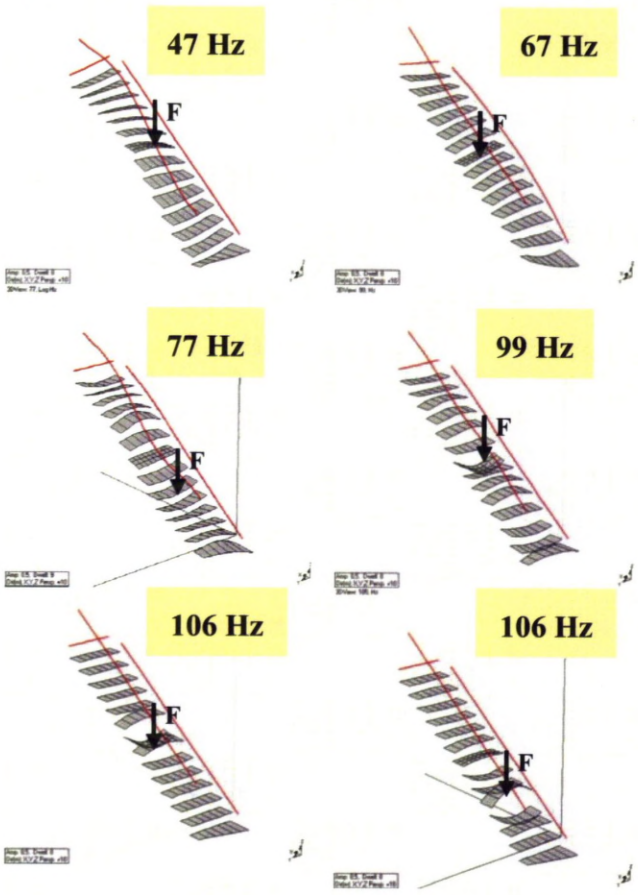

Figure 3: Vibration deflection shapes

In the frequency range below 100 Hz the vibration of the stair is determined by beam modes of the handrail (47 Hz, 77 Hz) and string board (67 Hz). The vibration strength at a particular frequency is therefore strongly dependant on the position of the excited step. The excitation of steps, situated at antinodes of the handrail / string board, causes significant vibration of the whole stair assembly. In contrast, excitation of steps at nodal positions, results in reduced vibration. For example the strong vibration of the stair at 77 Hz only occurs for excitation at step 5 since step 8 is situated at a nodal point of the corresponding handrail beam mode. In the frequency range above 100 Hz the vibration of the single steps is determined by plate modes (the first plate mode occurs at 106 Hz). The handrail acts as "deliverer" of vibration energy within the stair-system. At frequencies where step plate modes and handrail beam modes coincide, the vibration of the whole stair is strong (99 Hz). At frequencies where no handrail beam modes occur, the excitation energy is mainly contained in the directly excited step (e.g. 106 Hz). This is also the case if the hand-rail has a beam mode but the excited step is situated at a node. The beam

modes of the string board determine the motion at the contact, perpendicular to the wall, and thus influence the excitation of the wall. Strong vertical motion at the wall contact follows if the wall contact and the excited step are situated at an anti-node of the string board (67 Hz). On the other hand, in the case of the excited step at a node of the string board, there can still be motion at the wall contact by energy transmission within the stair system due to handrail modes.

5 Stair as sound source

The stair assembly is a passive structure until it is excited on one or several of its steps. It then can be treated as an active source, which vibrates and transmits structure-borne power into the separating wall. The stair now can be treated in a similar manner to that used to predict the structure-borne power from vibrating machines in buildings and other structures. Accordingly the source descriptor concept [3] can be applied. It allows a characterisation of the stair as structure-borne sound source on a power basis. The source descriptor by definition is an inherent quantity of the source. The required quantities are the free velocity and mobility at the contact point formed by the rigid screw connection (figure 2). As shown the vibration behaviour of the stair strongly depends on the location of the external source. This effect can be considered e.g. by means of averaging the free velocities to be measured over all steps. From the receiver (wall) mobility the coupling function can be calculated and thus the power transmission of the stair in the installed condition can be predicted for a defined receiving wall.

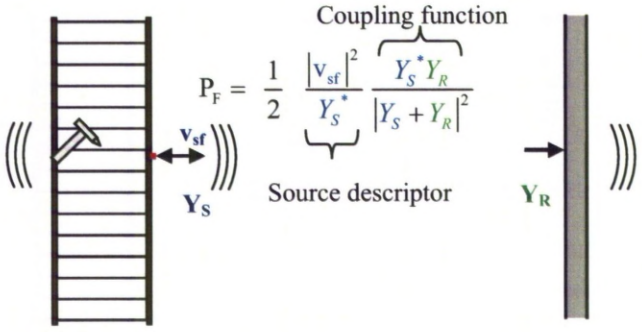

Figure 4: stair as active component – source descriptor concept

Before this method is applied it is reasonable to investigate the most important excitation components in order to determine which components can be neglected. This can be done in the installed condition using a reciprocal method.

6 Reciprocal method

For a single contact point, there are up to six degrees of freedom (3 translational; 3 rotational), which can contribute on the excitation of the wall (Figure 5). The structure-borne power imparted to the wall due to forces and moments is given by [2].

$$P_F = \frac{1}{2} \mathrm{Re}\{F\, v^*\} \quad ; \quad P_M = \frac{1}{2} \{M\, w^*\} \tag{1}$$

In order to obtain the structure-borne power from each component in the installed condition a reciprocal method as described in [4] will be used.

In the 1st stage a simple single component case is considered and experimentally validated. In the 2nd stage this method is extended to the multi component case which applies to the situation as found here.

6.1 Single component case

In the simplest case the receiving structure (here: the wall) is excited by a perpendicular force $F_{e,z}$ only. Under action of this force the translational response velocity at the contact point e is $v_{e,z}$. The power transmitted through the contact is (2):

$$P_{F,z} = \frac{1}{2} \mathrm{Re}\{F_{e,z}\, v_{e,z}^*\} \tag{2}$$

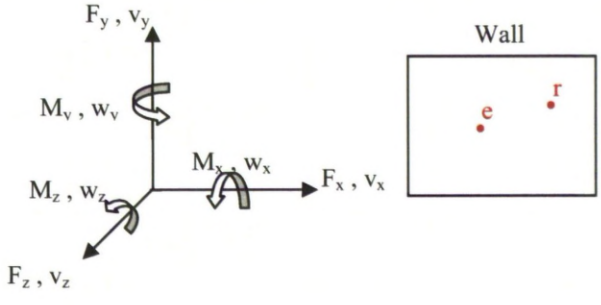

Figure 5: coordinate system

Following this the power can be calculated directly if the cross-spectrum of force and velocity at the excitation point is known. Direct measurement of the force at the mounting point(s) is difficult and often impossible since it requires the installation of a force transducer. Introducing an arbitrary remote point r, equation (2) can be rearranged:

$$\begin{aligned} P_{F,z} &= \frac{1}{2} \mathrm{Re}\left\{ F_{e,z} \cdot v_{e,z}^* \cdot \frac{v_{r,z}}{v_{r,z}} \right\} \\ &= \frac{1}{2} \mathrm{Re}\left\{ \breve{Y}^{-1}_{v_{r,z} F_{e,z}} \cdot v_{e,z}^* \cdot v_{r,z} \right\} \end{aligned} \tag{3}$$

In this arrangement $v_{r,z}$ is the velocity at the remote point due to excitation force $F_{e,z}$ at the contact point. The ratio $\breve{Y}_{v_{r,z}F_{e,z}}$ is termed the (loaded) transfer mobility from the contact point e to the reference point r. By principle of reciprocity it can be measured in the opposite direction e.g. excitation at the remote point and measure of the velocity at the contact point $\breve{Y}_{v_{r,z}F_{e,z}} = \breve{Y}_{v_{e,z}F_{r,z}}$.

Thus this arrangement converts the problem of direct force measurement to a simpler transfer mobility measurement and cross-spectra of velocities.

The reciprocal measurement of the force and respective power was experimentally validated using a shaker attached to the receiving wall (Figure 6). A force transducer was inserted to obtain the force directly. To avoid moment excitation a piano wire was inserted.

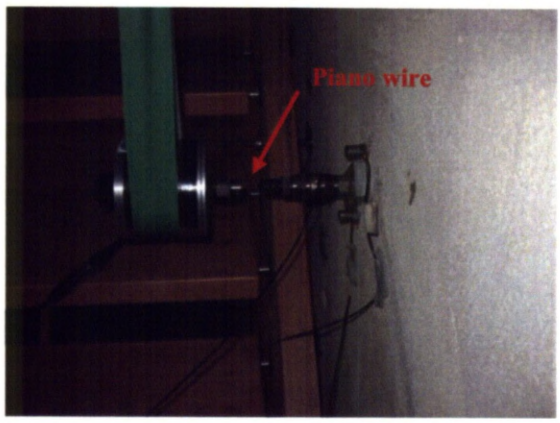

Figure 6: shaker attached to the test wall

The contact velocity $v_{e,z}$ was obtained by averaging the signals of the two accelerometers below and above the contact. The shaker was driven with random noise.

Figure 5 shows the force obtained directly and by the reciprocal method.

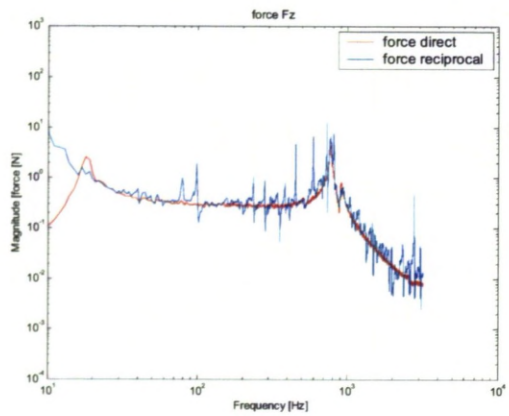

Figure 5: Force measured directly and reciprocally

The agreement in general is good. At certain frequencies discrepancies occur which result partly from the measurement of the transfer mobility which is inaccurate when the excitation or response coincides with nodal points. At approximately 800 Hz a peak of the force spectra occurs which corresponds to the first longitudinal resonance of the piano wire. Consequently the force decreases at higher frequencies as well as the signal / noise ratio and therefore the agreement between the two methods.

In Figure 6 the power obtained directly and by the reciprocal method is presented as narrow band and third octave band values. The agreement in general is promising. The power obtained reciprocally has negative values at some of the very low frequencies. This is the result of measurement uncertainty which is indicated as gaps in the curve. Although high deviations at certain frequencies occur the agreement of the third octave band values is in within ± 1 dB.

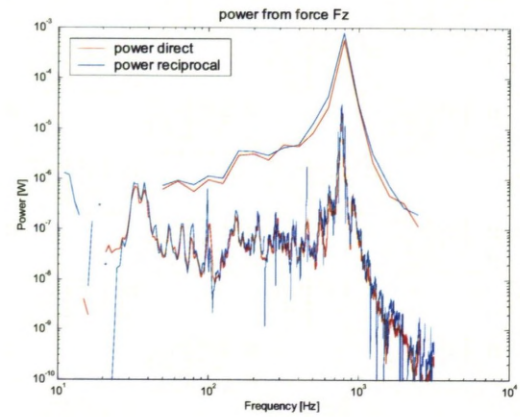

Figure 6: Power by direct and reciprocal measurement

So far it has been shown that the reciprocal method gives a reasonably good estimate of the power imparted to the wall by a perpendicular force. The total power imparted to the wall can be obtained by means of measuring the average velocity on the wall and the total loss factor [2] when the wall is treated as a reception plate:

$$P = \omega \cdot m \cdot \eta \cdot \tilde{\bar{v}}^2 \qquad (4)$$

The estimate of the input power, using this method, is shown in Figure 7. The agreement again is promising despite uncertainties in measurement of the loss factor and the average velocity.

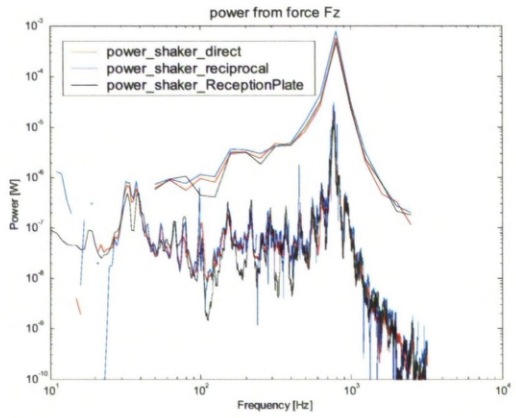

Figure 7: power from reception plate approach

6.2 Multi component case

The reciprocal method as described above can be expanded to the problem of multiple degrees of freedom at a single contact as given by the excitation of the wall through the screwed wall contact of the stair. It is likely that three components of excitation need to be considered: the force vertical to the wall F_z and the two moments about axes in the plane of the wall M_x and M_y. The component powers are given by (5):

$$P = \frac{1}{2}\mathrm{Re}\left\{F_{e,z}\cdot v^*_{e,z} + M_{e,x}\cdot w^*_{e,x} + M_{e,y}\cdot w^*_{e,y}\right\} \quad (5)$$

It has been assumed that the cross-mobility terms (for example, the excitation of velocity in the z-direction by a moment about the x-axis) can be neglected at a central wall location.

Three remote points r_1, r_2, r_3 are required for estimating three excitation components. The translational velocities result from a superposition of all components including cross-transfer terms:

$$\begin{Bmatrix} v_{r1,z} \\ v_{r2,z} \\ v_{r3,z} \end{Bmatrix} = \begin{pmatrix} \breve{Y}_{v_{r1,z}F_{e,z}} & \breve{Y}_{v_{r1,z}M_{e,x}} & \breve{Y}_{v_{r1,z}M_{e,y}} \\ \breve{Y}_{v_{r2,z}F_{e,z}} & \breve{Y}_{v_{r2,z}M_{e,x}} & \breve{Y}_{v_{r2,z}M_{e,y}} \\ \breve{Y}_{v_{r3,z}F_{e,z}} & \breve{Y}_{v_{r3,z}M_{e,x}} & \breve{Y}_{v_{r3,z}M_{e,y}} \end{pmatrix} \cdot \begin{Bmatrix} F_{e,z} \\ M_{e,x} \\ M_{e,y} \end{Bmatrix} \quad (6)$$

Using reciprocity relationships which in terms of the cross mobilities is e.g. $\breve{Y}_{v_{r,z}M_{e,x}} = \breve{Y}_{w_{e,x}F_{r,z}}$ the mobilities can be replaced by the corresponding "reciprocal" mobilities. The components are then obtained by inversion of the mobility matrix (7):

$$\begin{Bmatrix} F_{e,z} \\ M_{e,x} \\ M_{e,y} \end{Bmatrix} = \begin{pmatrix} \breve{Y}_{v_{e,z}F_{r1,z}} & \breve{Y}_{w_{e,x}F_{r1,z}} & \breve{Y}_{w_{e,y}F_{r1,z}} \\ \breve{Y}_{v_{e,z}F_{r2,z}} & \breve{Y}_{w_{e,x}F_{r2,z}} & \breve{Y}_{w_{e,y}F_{r2,z}} \\ \breve{Y}_{v_{e,z}F_{r3,z}} & \breve{Y}_{w_{e,x}F_{r3,z}} & \breve{Y}_{w_{e,y}F_{r3,z}} \end{pmatrix}^{-1} \begin{Bmatrix} v_{r1,z} \\ v_{r2,z} \\ v_{r3,z} \end{Bmatrix} \quad (7)$$

In order to obtain the required phase between the velocities, one remote point r_1 is selected as a reference value along with the velocity transfer functions between the reference point and the contact point as well as between the other remote points.

The component powers are then obtained by (8,9,10):

$$P_{F_{e,z}} = \frac{1}{2}\mathrm{Re}\left\{F_{e,z}\cdot\left|v_{r1,z}\right|\cdot\varphi^*(v_{r1,z}, v_{e,z})\right\} \quad (8)$$

$$P_{M_{e,x}} = \frac{1}{2}\mathrm{Re}\left\{M_{e,x}\cdot\left|v_{r1,z}\right|\cdot\varphi^*(v_{r1,z}, w_{e,x})\right\} \quad (9)$$

$$P_{M_{e,y}} = \frac{1}{2}\mathrm{Re}\left\{M_{e,y}\cdot\left|v_{r1,z}\right|\cdot\varphi^*(v_{r1,z}, w_{e,y})\right\} \quad (10)$$

In Figure 8 are shown the results of preliminary reciprocal measurements of the powers from the three components of excitation at the contact point between stair and wall. Also shown is the total power obtained from the spatial average velocity. As external source the tapping machine was situated at step 8 (in the middle of the stair near the wall contact).

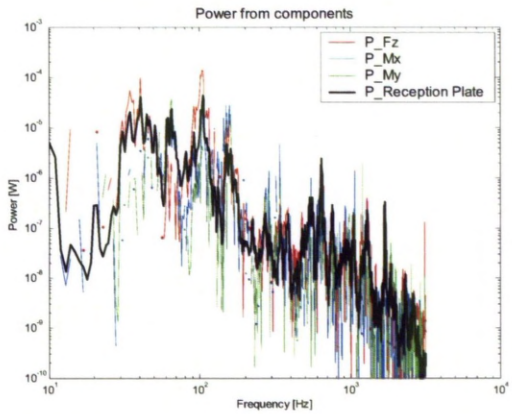

Figure 8: component powers

Figure 8 gives an early indication that the contribution from moments M_x and M_y is significant within the whole investigated frequency range. This early indication needs to be confirmed by further measurements.

7 Concluding remarks

A characterization of a wooden staircase with string board and a single rigid wall contact as structure-borne sound source is considered. An approach is proposed where the stair is treated in a similar manner to that used for vibrating machines. Therefore as first step the vibration behaviour of the stair was analysed by means of an experimental modal analysis. The vibration behaviour of the stair is determined by beam modes of handrail and string board and plate modes of the steps.

From this it follows that the vibration behaviour and thus the excitation of the wall is strongly dependant from the location of the external source exciting the stair. For a given external source and location on the stair the power imparted to the wall can be evaluated by means of a reciprocal method. With this method the relative contribution of the components (forces and moments) can be assessed in the installed condition and a hierarchy of the transmission paths can be established.

The capability of the reciprocal method was investigated for a single component source, a shaker, which generates a force perpendicular to the wall surface. A comparison of the directly and reciprocally obtained forces and associated powers show a reasonably good agreement. Preliminary reciprocal measurements of the power generated at the wall by the installed stair excited by the tapping machine, indicate that moments as well as forces contribute to the bending vibration field on the wall and thus to the radiated sound into the adjacent room. The relative contributions of each excitation component have yet to be correctly quantified but early indications are that no component can be neglected a priori.

References

[1] Andreas Drechsler, 'Untersuchungen zur Verbesserung der Trittschalldämmung leichter Treppen am Beispiel einer Holzwangentreppe, DAGA 2005, München

[2] L. Cremer, M. Heckl: '*Structure-borne Sound*', Springer Verlag Berlin, 1996.

[3] Mondot, Petersson: '*Characterisation of structure-borne sound sources: the source descriptor and the coupling function*', Journal of sound and vibration 114, pp. 507-518, 1987.

[4] S. H. Yap: '*The role of moments and forces in structure-borne sound emission from machines in buildings*', PhD Thesis at the University of Liverpool, 1988

[5] H.-M. Fischer et al.: *'Structure-borne sound excitation and transmission of lightweight stairs'*, Forum Acusticum 2002, Sevilla.

Approach for the Characterization of a Wooden Staircase as Structure-borne Sound Source

Jochen Scheck [1], Heinz-Martin Fischer [1], Barry Gibbs [2], Andreas Drechsler [1]

[1] *Fachhochschule Stuttgart – Hochschule für Technik, D-70174 Stuttgart, Email: jochen.scheck@hft-stuttgart.de*

[2] *University of Liverpool - Acoustics Research Unit, Liverpool L69 3BX*

Introduction

At present it is not possible to predict the sound transmission into adjacent rooms, from footfalls on lightweight stairs, which are connected to the separating wall. Especially at low frequencies excitation by human footfall and transmission is high and often causes annoyance to the inhabitants. To reduce problems in the future a characterization of lightweight stairs as structure-borne sound sources is required. In particular, a test method is required which will provide data, which will indicate the noisiness of the stair system when installed in a building. Concerning this matter investigations have been carried out on a wooden staircase with string board which is a common type of stair in Germany. In this paper the investigation of the vibration behaviour of the stair and an approach for the characterisation as structure-borne sound source is outlined.

Wooden Staircases with String Board

Structure-borne energy enters the building through the contact points which are shown in figure 1.

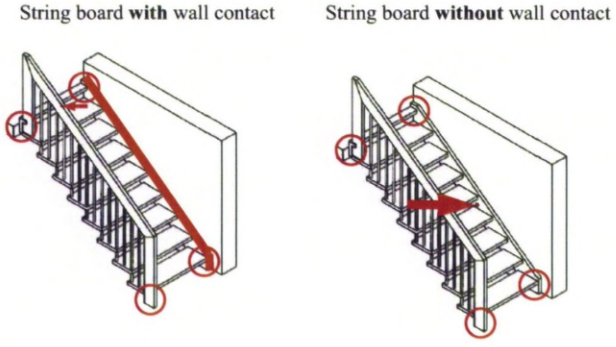

figure 1: contact points and dominant transmission paths

The stair is supported by the ceilings e.g. the floating floors. Up to now it is common practice to mount the string board directly at the wall using screws. In this case the transmission from the string board into the wall is significant. Experience shows that with the string board in contact with a common separating wall annoyance cannot be avoided. Even the normative requirements on the normalised impact sound pressure Level L'_n can hardly be met. The string board must be moved away from the wall as indicated in the right sketch of figure 1. However, the string board still has to be fixed at the wall, for safety reasons (stability when walking on the stair). This can be done through one connection [1]. Investigations show that in general transmission through this wall contact is the dominant transmission path. A detailed investigation of the structure-borne energy transmission through a single wall contact therefore is the topic of this current study.

Investigated System

The experimental investigation of a wooden staircase with string board was carried out in the staircase test facility. The string board was moved away from the wall and resiliently supported at both ends. The contact with the wall was through one rigid screwed connection, shown in figure 2. It was confirmed experimentally that, in this set-up, the dominant structure-borne sound transmission was through the screwed contact.

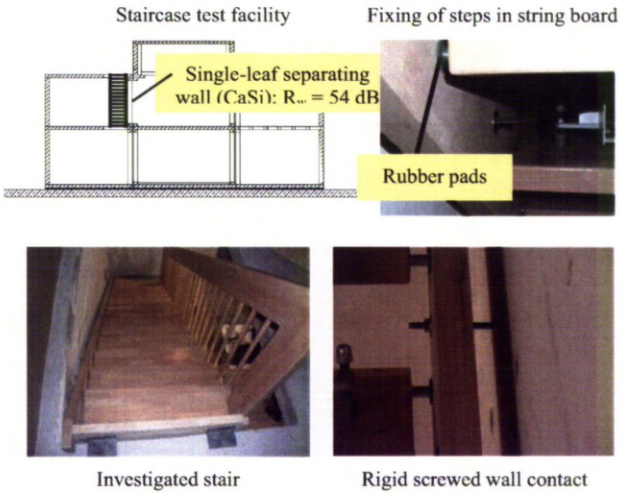

figure 2: investigated system

Experimental modal analysis of the stair

The vibration behaviour of the stair is a major influence regarding the excitation of the wall. To get an insight into the dynamic behaviour of the stair, an experimental modal analysis was conducted, using an instrumented hammer. Accelerometers were placed on a central step (the 8th step from the floor), near the contact point and also on the edge of the 5th step. Due to reciprocity, the measured operating deflection shapes, shown in figure 3, result from excitation at the accelerometer positions. In the frequency range below 100 Hz the vibration of the stair is determined by beam modes of the handrail (47 Hz, 77 Hz) and string board (67 Hz). The vibration strength at a particular frequency is therefore strongly dependant on the position of the excited step. The excitation of steps, situated at antinodes of the handrail / string board, causes significant vibration of the whole stair assembly. In contrast, excitation of steps at nodal positions, results in reduced vibration. For example the strong vibra-

tion of the stair at 77 Hz only occurs for excitation at step 5 since step 8 is situated at a nodal point of the corresponding handrail beam mode. In the frequency range above ≈ 100 Hz the vibration of the single steps is determined by plate modes (the first plate mode occurs at 106 Hz). The handrail acts as "deliverer" of vibration energy within the stair-system. At frequencies where step plate modes and handrail beam modes coincide, the vibration of the whole stair is strong (99 Hz). At frequencies where no handrail beam modes occur, the excitation energy is mainly contained in the directly excited step (e.g. 106 Hz). This is also the case if the handrail has a beam mode but the excited step is situated at a node. The beam modes of the string board determine the motion at the contact, perpendicular to the wall, and thus influence the excitation of the wall. Strong vertical motion at the wall contact follows if the wall contact and the excited step are situated at an antinode of the string board (67 Hz). On the other hand, in case of the excited step at a node of the string board, there can still be motion at the wall contact by energy transmission within the stair system due to handrail modes.

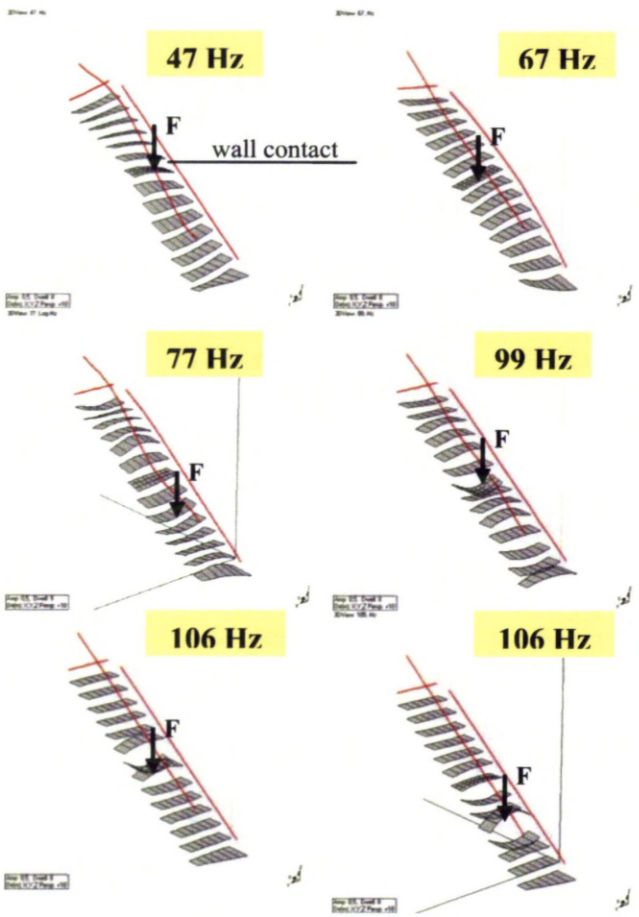

figure 3: measured operating deflection shapes at low frequencies

Stair as Structure-borne sound source

How can the stair be described as a structure-borne sound source? The stair assembly is a passive structure until it is excited on one or several of its steps. It then can be treated as an active source, which vibrates and transmits structure-borne power into the separating wall. The stair now can be treated in a similar manner to that used to predict the structure-borne power from vibrating machines in buildings and other structures. Accordingly the source descriptor concept [3] can be applied. It allows a characterisation of the stair as structure-borne sound source on a power basis. The source descriptor by definition is an inherent quantity of the source. The required quantities are the free velocity and mobility at the contact point formed by the rigid screw connection (figure 2). As shown the vibration behaviour of the stair strongly depends on the location of the external source. This effect can be considered e.g. by means of averaging the free velocities to be measured over all steps. From the receiver (wall) mobility the coupling function can be calculated and thus the power transmission of the stair in the installed condition can be predicted for a defined receiving wall.

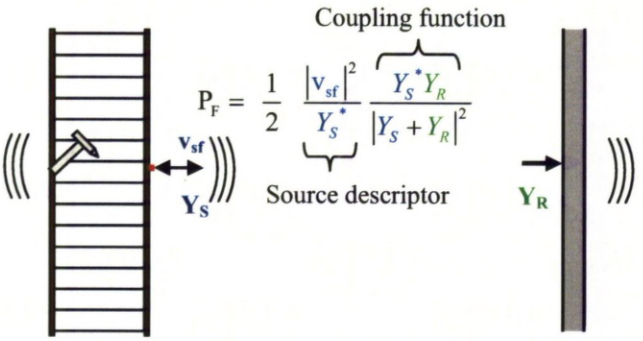

figure 4: stair as active component – source descriptor concept

Predominant components of excitation

For a single contact point, there are up to six degrees of freedom (3 translational; 3 rotational), which can contribute on the excitation of the wall. None can be neglected a priori. The structure-borne power imparted to the wall due to forces and moments is given by [2].

$$P_F = \frac{1}{2} F^* v \quad ; \quad P_M = \frac{1}{2} M^* w \tag{1}$$

In the next stage of this study, the components of excitation of the wall will be identified by means of reciprocal methods. This will allow the components to be identified which contribute to the structure-borne sound transmission into the wall and thence to the resultant sound pressure level in the adjacent room.

References

[1] Andreas Drechsler, 'Untersuchungen zur Verbesserung der Trittschalldämmung leichter Treppen am Beispiel einer Holzwangentreppe, DAGA 2005, München

[2] Cremer/Heckl, 'Structure-borne Sound', Springer Verlag Berlin Heidelberg New York, (1996)

[3] Mondot/ Petersson, 'Characterisation of structure-borne sound sources: the source descriptor and the coupling function', Journal of Sound and Vibration, 114, 507-518, (1987).